

# Fluorescent Polymeric Microbeads for Application as Solid State Multicolor Emitting Materials

Thesis Submitted to AcSIR For the Award of  
the Degree of  
**DOCTOR OF PHILOSOPHY**  
In Chemical Science



By  
Swapnil L. Sonawane  
Registration Number: 10CC11J26082

Under the guidance of  
Dr. Asha S. K.

CSIR-National Chemical Laboratory

***DEDICATED TO***

***My Family and Teachers***

***for their endless support and encouragement.....***

## DECLARATION

I hereby declare that the research work embodied in the thesis entitled “**Fluorescent Polymeric Microbeads for Application as Solid State Multicolor Emitting Materials**” has been carried out by me at Polymer Science and Engineering Division of CSIR-National Chemical Laboratory, Pune under the supervision of Dr. Asha S. K. I also affirm that this work is original and has not been submitted in part or full, for any other degree or diploma to this or any other University or Institution.

Date: **October 2016**

Polymer Science and Engineering Division

CSIR-National Chemical Laboratory,

Pune-411 008, India.



**Swapnil L. Sonawane**



राष्ट्रीय रासायनिक प्रयोगशाला  
(वैज्ञानिक तथा औद्योगिक अनुसंधान परिषद)  
डॉ. होमी भाभा रोड, पुणे - 411 008. भारत  
**NATIONAL CHEMICAL LABORATORY**  
(Council of Scientific & Industrial Research)  
Dr. Homi Bhabha Road, Pune - 411008. India




## Certificate

This is to certify that the work incorporated in this Ph.D. thesis entitled “**Fluorescent Polymeric Microbeads for Application as Solid State Multicolor Emitting Materials**” submitted by **Mr. Swapnil L. Sonawane** to **Academy of Scientific and Innovative Research (AcSIR)** in fulfillment of the requirements for the award of the Degree of Doctor of Philosophy, embodies original research work under my supervision. I further certify that this work has not been submitted to any other University or Institution in part or full for the award of any degree or diploma. Research material obtained from other sources has been duly acknowledged in the thesis. Any text, illustration, table etc., used in the thesis from other sources, have been duly cited and acknowledged.

Swapnil L. Sonawane  
(Student)

Dr. Asha S. K.  
(Supervisor)

Communications Channels  +91 20 25902000  
+91 20 25893300  
+91 20 25893400

Fax +91 20 25902601 (Director)  
+91 20 25902660 (Admin.)  
+91 20 25902639 (Business Development)

URL : [www.ncl-india.org](http://www.ncl-india.org)



## **ACKNOWLEDGEMENT**

*My journey in the CSIR-NCL has been travel with innumerable ups and downs, but as they say hard work, dedication, perseverance and will to learn new things end well. This journey would not have been accomplished without the constant support of my parents, teachers, friends, well-wishers and relatives. I wish to express my gratitude to many people who have been of crucial support to me.*

*First and foremost, my sincere thanks to my supervisor Dr. Asha S. K. She has been a mentor, a guide and a guardian to me whole through my PhD career. At all times, she has been open for discussions and I am grateful to her for sharing her scientific knowledge and experience. I deeply acknowledge the freedom provided by her to think and work independently for the pursuit of gaining knowledge and developing new ideas. Working with her was really a great pleasure and gave me a lot of valuable experience. I am very much appreciative for her unending support and encouragement towards me and also for showing confidence in this project and in my working abilities in conducting research and preparing this dissertation.*

*I sincerely thank the Council of Scientific and Industrial Research (CSIR), Delhi and CSIR-NCL Pune for their financial support and facilities. I am also thankful to Dr. Ashwini Kumar Nangia, Director and Dr. Sourav Pal, Former Director, CSIR-NCL for providing me the opportunity to work in this prestigious laboratory and giving all the facilities. I would also like to thank, Dr. A. K. Lele, HOD and Dr. A. J. Verma, Former HOD, PSE division, for providing all the facilities of the division.*

*I would also like to thank my Doctoral Advisory Committee (DAC) members Dr. N. P. Argade, Dr. P. P. Wadgaonkar and Dr. J. Nithyanandhan for their constructive discussion and thoughtful implication during the DAC meetings. Their valuable suggestions have immensely contributed in shaping up this thesis.*

*I admire and appreciate Student Academic Office (SAO) staff initially led by Dr. C. G. Suresh and now by Dr. M. S. Shashidhar for their kind help and co-operation, through this journey.*

*My special thanks goes to Prof. M. Jayakannan for his support and help during the initial stage of my research. His encouraging talks, valuable suggestions throughout my work has helped me lot to stand in all the situations. His friendly performance, understanding attitude and pleasing personality have always gave me the freedom to get his suggestions at any time.*

*I would also like to acknowledge Dr. S. Sivaram, Former Director, CSIR-NCL for teaching and suggesting new things in my research. His approachable attitude fascinated me and I always felt comfortable in sharing and discussing with him.*

*I extend my appreciation towards Dr. Sayam Sen Gupta, Dr. Banerjee, Dr. Ogale, Dr. S. P. Chavan, Dr. Nitin Patil, Dr. C. V. Rhode, Dr. Avadhani, Dr. Manjusha Shelke, Dr. Neelima, Dr. Badiger, Dr. Chikkali, Dr. B. Idage, Dr. S. B. Idage, Dr. Nilakshi, Dr. Shedge, Mr. Suresha Da, Mr. Arun for their valuable guidance and help.*

*I thank to Prof. A. A. Natu, IISER Pune, for his guideline and encouragement at the beginning and throughout my research career.*

*I also want to thank all my school and college teachers who have encouraged me to do well in life. Prof. J. N. Mali, Prof. S. J. Patil, Prof. R. M. Patil, (D. D. S. Patil College Erandol), Prof. B. V. Patil, Prof. R. N. Patil, Prof. N. M. Khose, Prof. C. D. Patil, Prof. A. P. Borse, Prof. J. T. Patil, Prof. Savita Patil, Prof. M. D. Suryawanshi, (S. S. V. P's Science College Dhule).*

*I will never forget the contribution of Prof. P. P. Mahulikar, Prof. D. H. More, Prof. D. G. Hundiwale, Dr. V. V. Gite and Prof. K. J. Patil (North Maharashtra University, Jalgaon) in my life. I also thank Dr. Bavane, Prof. Nemade, Dr. Narkhede, Dr. Waghulde, Dr. Sonar, for their help and support. Dr. S. S. Terdale, and Dr. P. D. Lokhande, (Savitribai Phule Pune University, Pune) always deserves a special mention in my life.*

*I would also take this opportunity to show my sincere thanks to those who have immensely helped me during my research. Menon Sir, Doble Mam, Ms. Poorvi, has helped me in GPC characterization. Mr. Gholap, Ketan and Harsha (SEM analysis), Ejaj, Sonal and Amar Yeware (Fluorescence Microscopic analysis), Shantakumari mam, and Shashikala mam for MALDI measurements. I also want to thank all members of PSE division and PAML for giving me all the superior times during my research.*

*I wish to thank my present and former labmates and friends both from NCL and IISER especially, Ghanashyam, Dr. Kaushalendra, Dr. Rekha, Dr. Nagesh, Dr. Chinmay, Dr. Nisha, Dr. Senthil, Shekhar, Saibal, Prajitha, Sandeep, Sarabjot, Shreekant, Momita, Bhavita, Jeena, Vinay, Alok, Akshata, Harish, Priyanka, Durga, Shreya, Dr. Mahima, Dr. Balamurugan, Dr. Smita, Dr. Pramod, Dr. Ananthraj, Dr. Bapu, Harpreet, Narsimha, Rajendra, Bhagyashree, Nilesh, Sonashri, Dhiraj, Anuj, Vivek, Uma, Abhishek for their help and complete support.*

*Any journey of life becomes hard, when we do not have the support of friends and well-wishers. Dr. Ajay, Dr. Yogesh, Dr. Nagle, Dr. Puja, Siddharth, Prakash, Jagannath, Nilam, Sandeep, Kushal, Milind, Bhagyasha, Roshan, Bhushan, Pramod, Yogesh, Bhausahab, Vishal, Vijay, Mayur, Ravi, Vikram, Nagnath, Rohit, Indrapal, Leena chechi, Kiran, Chitravel, Devraj for giving me the best time of life.*

*No words would express my gratitude and love to my family members for their continuous showering of boundless affection. Precious thanks to my mother (Asha Sonawane) and my father (late Laxman Sonawane), my brothers (Nitin dada, Dipak dada, Bhausahab and Vinod) sister-in-laws (Chaya, Savita and Deepali), my sisters (Neeta Tai and Sheela) for their sacrifices, adjustments and support throughout my PhD research work. Very warm thanks for their patience, love, support and for believing in my dreams. Heartfelt thanks to all kids of my family (Sakhina, Pappu, Bala, Pranali, Rinki, Vikram, Vishal, Shivam, Vikas, Vishakha) for making joyful environment during the visit of home.*

*I would like to express my love and gratitude to my wife Yogita, who has been always lovingly by my side through times of frustration and happiness.*

*I am glad to have very supportive family members, who have provided me all the best facilities at all time. I dedicate my thesis to all of them for their constant encouragement.*

*.....Swapnil*



## TABLE OF CONTENT

<b>Abbreviation</b>	<b>i-ii</b>
<b>Preface</b>	<b>iii-v</b>
<b><i>Chapter 1: Introduction and Literature survey</i></b>	<b><i>1-42</i></b>
1.1 Introduction to fluorescent materials.....	3
1.1.1 Solid state emitting materials.....	4
1.1.2 Solution state emitting materials.....	6
1.1.3 Gel state emitting materials.....	9
1.2 Development of fluorescent materials.....	10
1.2.1 Physical blending/mixing of dyes on polymer backbone.....	11
1.2.2 Covalent attachment of dyes to polymer backbone.....	13
1.2.2.1 Heterogeneous polymerization.....	14
1.2.2.1 Dispersion polymerization.....	16
1.3 Applications of fluorescent material.....	19
1.3.1 Multicolor emitting material.....	19
1.3.2 Bio-imaging and labelling.....	20
1.3.3 Sensors (oxygen, gas, explosive).....	23
1.4 Fluorescent dyes: Perylenebisimide, Oligo ( <i>p</i> -phenylenevinylene) and Pyrene.....	24
1.5 Molecularly Imprinted Polymers.....	26
1.5.1 Synthesis of Molecularly Imprinted Polymers.....	27
1.5.2 Applications of Molecularly Imprinted Polymers.....	29
1.6 Aim of the thesis.....	32

1.7 References.....	33
<b>Chapter 2:    <i>Development of Fluorescent Polystyrene Microbeads with Controlled Particle Size, Tunable Colors, and High Solid State Emission</i></b>	<b>43-76</b>
2.1 Abstract.....	45
2.2 Introduction.....	46
2.3 Experimental methods.....	48
2.3.1 Materials.....	48
2.3.2 Instrumentation.....	48
2.3.3 General procedures.....	49
2.4 Result and Discussions.....	53
2.4.1 Synthesis and structural characterization.....	53
2.4.2 Molecular weights determination and thermal properties of polymers.....	59
2.4.3 Microscopic characterization of polymers.....	60
2.4.4 Photophysical characterization.....	64
2.5 Conclusion.....	72
2.6 References.....	74
<b>Chapter 3:    <i>Blue, Green, and Orange-Red Emission from Polystyrene Microbeads for Solid-State White-Light and Multicolor Emission</i></b>	<b>77-104</b>
3.1 Abstract.....	79
3.2 Introduction.....	80
3.3 Experimental methods.....	81
3.3.1 Materials.....	81

3.3.2 Instrumentation.....	82
3.3.3 General procedures.....	82
3.4 Result and Discussions.....	83
3.4.1 Synthesis and structural characterization.....	83
3.4.2 Molecular weights determination and thermal properties of polymers.....	87
3.4.3 Microscopic characterization of polymers.....	89
3.4.4 Photophysical characterization.....	92
3.5 Conclusion.....	101
3.6 References.....	102
<b>Chapter 4: Fluorescent Polystyrene Microbeads as Invisible Security Ink and Optical Vapor Sensor for Nitro compounds</b>	<b>105-138</b>
4.1 Abstract.....	107
4.2 Introduction.....	108
4.3 Experimental methods.....	109
4.3.1 Materials.....	109
4.3.2 Instrumentation.....	111
4.3.3 General procedures.....	111
4.4 Result and Discussions.....	112
4.4.1 Synthesis and structural characterization.....	112
4.4.2 Molecular weights determination and thermal properties of polymers.....	116
4.4.3 Microscopic characterization of polymers.....	117
4.4.4 Photophysical characterization.....	119
4.5 Conclusion.....	135

4.6 References.....	136
<b>Chapter 5: Tailor Made Functional Beads by Dispersion Polymerization for Application in Fluorescence Molecular Imprinting Technology</b>	<b>139-161</b>
5.1 Abstract.....	141
5.2 Introduction.....	142
5.3 Experimental methods.....	143
5.3.1 Materials.....	143
5.3.2 Instrumentation.....	143
5.3.3 General procedures.....	144
5.4 Result and Discussions.....	145
5.4.1 Synthesis and structural characterization.....	145
5.4.2 Thermal properties and microscopic characterization of polymers.....	149
5.4.3 Photophysical characterization.....	151
5.4.4 Fluorescence microscopic characterization.....	157
5.5 Conclusion.....	159
5.6 References.....	160
<b>Chapter 6: Summary and Conclusions.....</b>	<b>162-166</b>
<b>Publications and Conferences.....</b>	<b>167-168</b>



## Abbreviations and Symbols

<b>Abbreviation</b>	<b>Expansion</b>
$\chi^2$	Chi-square
$\tau$	Decay time
$\bar{D}$	Polydispersity index
$\alpha$	Pre-exponential factor
$\Phi$	Quantum yield
$T_g$	Glass transition temperature
AIBN	Azobisisobutyronitrile
CIE	Commission Internationale de l'Eclairage (International Commission on Illumination)
$CDCl_3$	Deuterated chloroform
DAPI	4'-6-Diamidino-2-phenylindole
DCM	Dichloromethane
DEG	Di(ethylene glycol) diacrylate
DLS	Dynamic light scattering
DMAP	Dimethyl amino pyridine
DMF	N,N-Dimethyl formamide
EtN3	Triethylamine
FTIR	Fourier transform infrared
gm	Gram
GPC	Gel permeation chromatography
HCl	Hydrochloric acid
h	Hour
HPLC	High performance liquid chromatography
HR-TEM	High resolution transmission electron microscopy
KBr	Potassium bromide
K-t-OBu	Potassium tertiary butoxide
LED	Light emitting diode
MALDI-TOF	Matrix-assisted laser desorption ionization-time of flight
$M_n$	Number average molecular weight
$M_w$	Weight average molecular weight
mg	Milligram

mL	Millilitre
mol	Mole
mmol	Millimole
MMA	Methyl methacrylate
MIP	Molecularly Imprinted Polymers
NIP	Non-Imprinted Polymers
NMR	Nuclear magnetic resonance
nm	Nanometer
OLED	Organic light-emitting diode
OPV	Oligo ( <i>p</i> -phenylenevinylene)
OPVX	Oligo ( <i>p</i> -phenylenevinylene) cross-linker
PAA	Poly(acrylic acid)
PBI	Perylenebisimide
PBIX	Perylenebisimide cross-linker
PDP	3-Pentadecyl phenol
PDI	Polydispersity index
PEGMA	Poly(ethylene glycol) methacrylate
PMMA	Polymethyl methacrylate
ppm	parts per million
PS	Polystyrene
PTCDI	Perylenetetracarboxylicbisanhydride
PVA	Poly (vinyl alcohol)
PVP	Polyvinylpyrrolidone
Py	Pyrene
Rh B	Rhodamine-B
SEM	Scanning electron microscopy
TEM	Transmission electron microscopy
TGA	Thermogravimetric analysis
TFA	Trifluoroacetic acid
THF	Tetrahydrofuran
TMS	Tetramethylsilane
UV-vis	Ultraviolet-visible
WOLED	White Organic Light Emitting Diode
*	Solvent

## PREFACE

Fluorescent materials have attracted wide attention because of their potential application in different research areas in chemistry and biology, e.g. multicolor emission, bar-coding, photonic crystals, detection of explosives and as a standard in the fluorescence techniques like flow cytometry, cell sorting, and imaging etc. Polymerization techniques like suspension, emulsion, dispersion etc could be utilized to produce fluorescent narrow disperse polymer beads in size ranges varying from nanometer to micrometer depending on the size requirement for different applications. Among these methods, dispersion polymerization is a very attractive one for the large-scale preparation of monodisperse polymer beads in the 0.5-15 micrometer size range. Although the original dispersion polymerization method as developed in the early 1960 does not facilitate the incorporation of fluorophores, functional comonomers, cross-linkers etc, the polymerization procedure could be modified by delayed introduction of the cross-linker etc after the nucleation stage, to produce functional polymer beads with narrow size distribution using the dispersion polymerization.

Good solid state quantum yield is the key factor for developing efficient fluorescent materials. The important criteria for application of the fluorescent beads are monodispersity, non-leaching of the fluorophore, thermal and photo stability etc. Although fluorescent microspheres are commercially available their prohibitive cost, limited choice of the emission colors as well as leaching out of the encapsulated dye makes it important to design efficient fluorescent microspheres with narrow size distribution and wide range of emission color using easily adaptable procedure in the laboratory as well as in the industry. A polymerization methodology has to be adopted which would allow copolymerization of polymerizable fluorophore so as to covalently attach the fluorophore to the polymer chains, thereby preventing leakage while at the same time maintain particle size control.

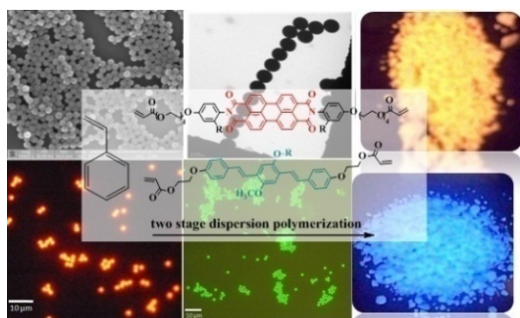
In this thesis work, the polymers were developed by dispersion polymerization methodology. The photophysical characteristics were studied using absorption and emission spectroscopy. The particle size of the PS beads was analyzed using Dynamic Light Scattering (DLS), Scanning Electron Microscopy (SEM) as well as fluorescence microscopic techniques.

The thesis work has been divided into five chapters. The first chapter gives a brief introduction of the fluorescent materials and various approaches for their synthesis and applications with detailed literature survey. It also gives a concise account on Molecularly Imprinted Polymers.

In the second working chapter a series of Polystyrene microbeads incorporating perylenebisimide and oligo (*p*-phenylenevinylene) fluorophores as the cross-linker were successfully developed by two stage dispersion polymerization strategy. The covalent attachment of the dye to the polymer backbone avoided dye leakage and also resulted in solid state emitting PS microbeads having an average diameter of 2-3  $\mu\text{m}$ . The PS beads incorporating PBI exhibited intense orange-red emission in the solid state with quantum yield  $\phi_{\text{Powder}} = 0.25$ , while the PS incorporating OPV as the cross-linker fluorophore exhibited intense green emission very high quantum yield of  $\phi_{\text{Powder}} = 0.71$ .

In chapter three single polymer based white light and multicolor emission in the solid state were demonstrated. Fluorescent polystyrene microbeads in the size range of 2-3  $\mu\text{m}$  were produced by incorporating orange-red emitting perylenebisimide and blue emitting oligo (*p*-phenylenevinylene) as cross-linkers into the polymer backbone during a two-stage dispersion polymerization. Pure white light emission in the powder form with CIE coordinates (0.33, 0.32) was achieved with one of the PS samples having appropriate amounts of both chromophores.

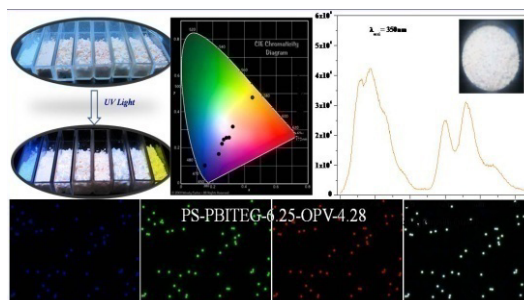
Fourth chapter describes the color-tunable solid state emitting polystyrene (PS) microbeads were developed by dispersion polymerization, which showed excellent fluorescent security ink characteristics along with sensitive detection of vapors of nitro aromatics like 4-nitro toluene (4-NT). The fluorophores pyrene and perylenebisimide were incorporated into the PS backbone as acrylate monomer and acrylate cross-linker



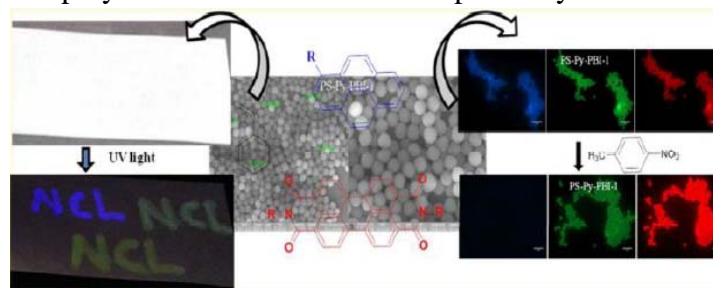
successfully developed by two stage dispersion polymerization strategy. The covalent attachment of the dye to the polymer backbone avoided dye leakage and also resulted in solid state emitting PS microbeads having an average diameter of 2-3  $\mu\text{m}$ . The PS beads

incorporating PBI exhibited intense orange-red emission in the solid state with quantum yield  $\phi_{\text{Powder}} = 0.25$ , while the PS incorporating OPV as the cross-linker fluorophore exhibited intense green emission very high quantum yield of  $\phi_{\text{Powder}} = 0.71$ .

In chapter three single polymer based white light and multicolor emission in the solid state were demonstrated. Fluorescent polystyrene microbeads in the size range of 2-3  $\mu\text{m}$  were produced by incorporating orange-red emitting perylenebisimide and blue emitting oligo (*p*-phenylenevinylene) as cross-linkers into the polymer backbone during a two-stage dispersion polymerization. Pure white light emission in the powder form with CIE coordinates (0.33, 0.32) was achieved with one of the PS samples having appropriate amounts of both chromophores.



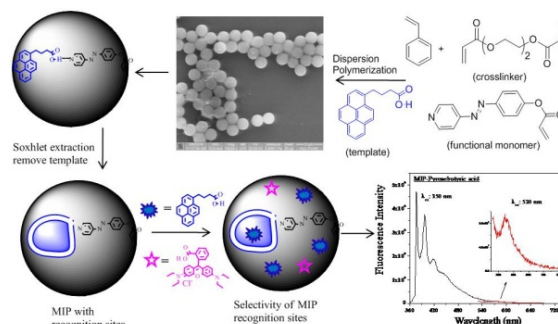
respectively, with solid state quantum yields of 94 % and 20 % observed for the pyrene and perylenebisimide based PS respectively. The ethanol dispersion of the polymer could



be used directly as a color tunable fluorescent security 'invisible' ink which became visible only under ultraviolet light. More than 80 %

quenching of pyrene emission was observed upon exposure of the polymer in the form of powder or as spin coated films to the vapors of 4-NT while the emission of perylenebisimide was unaffected. The limit of detection was estimated at  $10^{-5}$  moles (2.7ppm) of 4-NT vapors.

In the fifth chapter functional cross-linked microbeads were developed by dispersion polymerization as fluorescent Molecularly Imprinted Polymers (MIPs) having cavities with specific recognition sites. The functional molecule azobenzene was modified with pyridine and then self- assembled with dye molecules like Pyrenebutyric acid, which was then introduced during the second stage of dispersion polymerization. The synthesized MIPs exhibited blue fluorescence for Pyrenebutyric acid in acetonitrile suspension. The soxhlet technique was used to remove the assembled molecules in cross-linked beads by using acetonitrile as solvent. The loading and release of template from the functional cross-linked microbeads were followed by emission spectroscopy. The result showed that the developed MIPs exhibited selectivity of binding of the template.



The last chapter six summarizes the outcome of the research work carried out in this Ph.D. thesis.

**-:- Chapter 1 -:-**

---

---

***Introduction and Literature survey***

---

---



## 1.1 Introduction to Fluorescent Materials

Luminescence is a common phenomenon which is widely used in our day to day life. The materials exhibiting this phenomena are called as fluorescent materials. They absorb radiation of particular wavelength and emit it at a higher wavelength; however emission ceases as soon as the source is removed.<sup>1,2</sup> Fluorescent materials (organic, inorganic and polymeric) are the subject of intense research since last decades due to their huge demand in various field and for their development great effort has been undertaken by the research community as well as the industry.<sup>3,4</sup> Fluorescent materials showed wide applications in the fields of chemistry, biology and physics as optical brightener, security markers, road signage, memory chips, bio imaging, bio labeling, chemo and biosensors, forensics etc (figure 1.1).<sup>5-9</sup>



**Figure 1.1:** Role of fluorescent materials in day to day life.

Tunability in the color emission of fluorescent material is found to be very interesting and can be obtained by several phenomena like fluorescence resonance energy transfer (FRET),<sup>10</sup> electron transfer (ET) between donor and acceptor molecules,<sup>11</sup> aggregation induced emission (AIE),<sup>12</sup> isolated emission from individual molecules in the system etc.<sup>13,14</sup> Fine tuning of color from blue to green to orange-red results in the formation of white light emission.<sup>15,3,5</sup> Red and green light emitting diodes (LEDs) were already developed half a century ago as potential materials; however different groups were trying to develop 'blue LED' which is an essential component in white light emitting materials.<sup>16,17</sup> In 2014 *Hiroshi Amano, Isamu Akasaki* and *Shuji Nakamura* were awarded the Nobel Prize for the invention of Blue LED.<sup>18</sup> The fluorescent materials can emit in solid, solution as well as gel state and



can be developed as per required applications. The details are explained in the following sections.

### 1.1.1 Solid state emitting materials

Photoluminescent materials have gained much attention because of their potential applications in the next generation solid state lighting, panel displays and backlighting (figure 1.2). The ease of handling and possibility of coating on large surface area

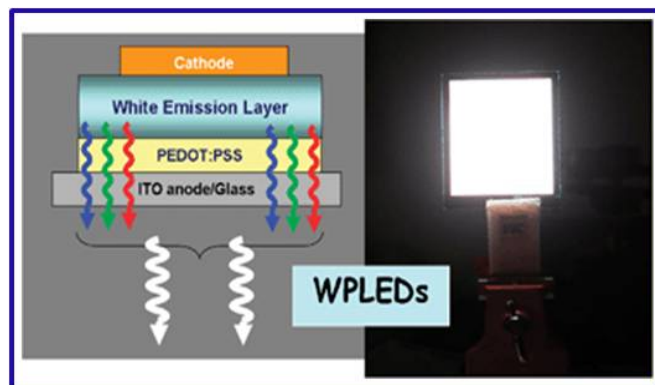


**Figure 1.2:** Solid state emission (Adapted from Chem. Soc. Rev., 2009, 38, 3391).

facilitates the applications of luminescent materials for technology improvement.<sup>19</sup> Various groups are working on the development of solid state emitting materials based on lanthanides and hybrid composites.<sup>20</sup> The group from Japan reported the fine powder of phosphorus containing composite materials for solid state lighting. By combination of  $(\text{La,Ca})_3\text{Si}_6\text{N}_{11}:\text{Ce}^{3+}$  phosphors with the 450 nm InGaN chip, the materials have proved its potential ability as a wavelength conversion phosphor for warm white LEDs.<sup>21</sup> Wang *et. al.* have shown that hybrid luminescent organoclay can be developed by mixing of lanthanides and aminoclay. Various emission color along with white light could be achieved from hybrid composite by changing the various parameters such as excitation wavelength, concentration of  $\text{Eu}^{+3}$ ,  $\text{Tu}^{+3}$  metals and the temperature (figure 1.3).<sup>22</sup> Solid state emission in the small organic molecules is a challenging task because of their aggregation tendency.<sup>23</sup> This problem can be addressed by substitution or functionalization of molecules. Li *et. al.* reported the solid state emission from synthetically modified anthracene derivatives. They showed that meta substitution of anthracene with tri-phenyl amine or tri-phenyl phosphine core gave



**Figure 1.3:** Images of luminescent materials with tunable emission colors under 254 nm UV lamp illumination (Adapted from ACS Appl. Mater. Interfaces 2014, 6, 12915).

enhanced solid state emission with high quantum yield.<sup>24</sup> Pati *et. al.* carried out the synthesis of a series of organic molecules with butadiyne spacer. The photophysical investigation of the molecules showed contrasting fluorescence in solid powder form which depended on the molecular arrangement of their crystal lattice.<sup>25</sup>

Apart from this, conjugated oligomers and polymers are also prominent as advanced materials for solid state emission.<sup>26,27</sup> The group of Richard Friend, developed copolymerization of PBI acrylate and polyfluorene where efficient energy transfer from donor to acceptor resulted in tunable solid state emission color in the polymer.<sup>28</sup> As a source of LED's, Tu *et. al.* described the synthesis of polyfluorene derivatives (donor) containing 1,8 naphthalene (acceptor) based single polymer which upon energy transfer from donor to acceptor gave solid state white light emission with tunable color.<sup>29</sup>

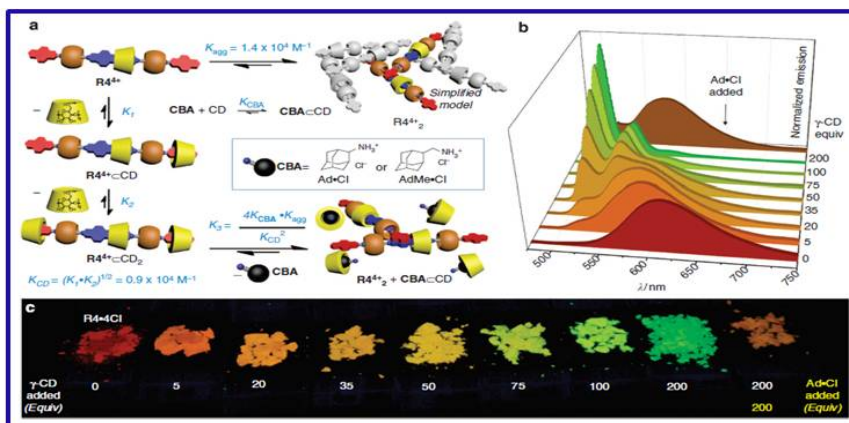


**Figure 1.4:** Equilibrium network and solid-state fluorescence studies (a) Graphical representation of the complex formation (b) Solid-state fluorescence spectra of complex (c)

Powders obtained from homogeneous mixtures of complex with varying amounts of  $\gamma$ -CD and Ad.Cl under UV light. (Adapted from Nat. Commun. 2015, 6, 6884).

By utilizing the supramolecular interaction, Hou *et. al.* demonstrated the synthesis of solid-state fluorescent materials by using heterorotaxane having pyrene and diazopyropyridinium for supramolecular encryption. After deposition of heterorotaxane on various papers the fine tuning of solid state emission from complex has been achieved which depends on the aggregation and de-aggregation process of selected units (figure 1.4).<sup>30</sup>  $\pi$ -conjugate materials are also found to be promising materials in various fields such as OLEDs and PLEDs development technology, whereas they aggregate in the solid state which affects their properties and quantum yield. This quenched emission of  $\pi$ -conjugate materials can be overcome to some extent by controlling the  $\pi$ -stacking interaction by attachment of suitable bulky anchoring groups to the polymer backbone.<sup>31,32</sup> The sequence of highly luminescent OPV and PPVs has been synthesized and their detailed photophysical study showed that by controlling their molecular interaction; high quantum yield near to unity could be achieved.<sup>33</sup> Deng *et. al.* developed the high solid state emitting amphiphilic copolymers of polyfluorene methacrylate by utilization of RAFT polymerization. They also showed that by simply changing the end group in copolymers high solid state multicolor emission could be achieved.<sup>34</sup> In order to achieve solid state emission, the metal was end-capped in the polymer backbone and by energy transfer process the tunable emission could be achieved. Basak *et. al.* designed the solid state emitting alternating co-polymer films in which europium metal was end-capped and color tuning of material from blue to white in the solid films was observed.<sup>35</sup> Isolation of more than two chromophores in the polymeric system is another way to obtain multicolor emission since the energy transfer from donor to acceptor is prohibited.<sup>36,37</sup>

### 1.1.2 Solution state emitting materials

Emission color from solution can be obtained by dissolving two or more chromophores in particular ratio.<sup>38,39</sup> In the past decades, it has been observed that most of the dyes known for their high quantum yield in the solution with tunable emission upon change in solvent polarity lose the emission in solid state due to  $\pi$ - $\pi$  stacking or aggregation

of dyes.<sup>40,41</sup> Wang *et. al.* studied fluorescence behaviour of pyrene and perylenebisimide connected to cholesterol moiety. They observed that supramolecular assembly afforded fluorescence resonance energy transfer from pyrene to perylenebisimide which showed different emission color.<sup>42</sup> Fluorescent materials in the solution state are generally used for optical sensing purposes. Most of the fluorescent materials are responsive to the external environment such as pH or metal binding which shows their potential as chemo or biosensors (for example; the emission of Rhodamine B is sensitive toward pH and metals solution as well).<sup>43,44</sup> The detailed survey of fluorescent materials and the mechanism of sensing has shown potential applications of fluorescent materials in the field of chemistry and biology.<sup>45,4</sup>

The research interest on the self assembly of dyes/conjugated polymer particles has been increasing now a days. Ni *et. al.* reported the host-guest interaction approach for the generation of color tunable material. They showed that simple addition of cucurbit[8]uril in to a solution of OPV derivatives resulted in the formation of supramolecular light emitting materials which could act as ratiometric fluorescence responsive candidates for achieving pure white light emission.<sup>46</sup> In another example water soluble perylenebisimide vesicles were prepared in which amphiphilic pyrene was encapsulated and FRET between both donor and acceptor molecules could be controlled simply by changing the pH of water (figure 1.5).<sup>47</sup>

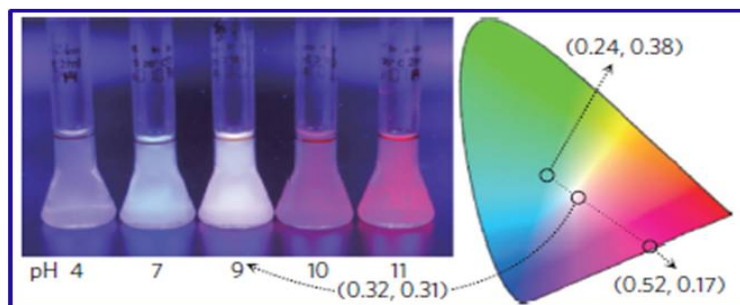


**Figure 1.5:** Photograph of donor-loaded vesicles in aqueous solution at different pH under an ultraviolet lamp. (Adapted from Nature Chemistry, 2009, 623).

Hybrid materials including organic molecules and metal complexes have been reported as luminescent materials in solution state. The hybrid molecular mixture of metal coordination complex of lanthanum europium and terbium was reported as white light emitting material with stimuli responsive properties (figure 1.6).

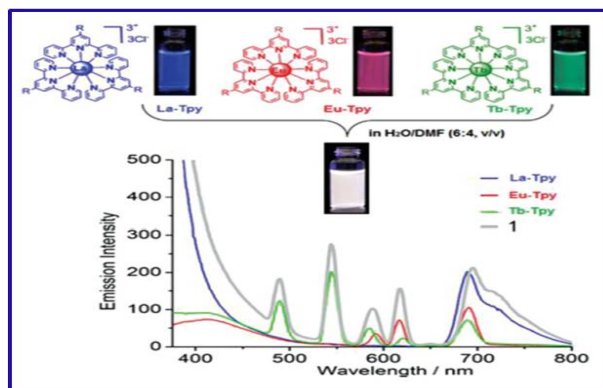


**Figure 1.6:** Hybrid material (La  $3+$  :Eu  $3+$  :Tb  $3+$  :Tpy in 1:1:1:9 molar ratio) molecular platform for white-light emission, photographs upon UV irradiation ( $\lambda_{exc} = 365$  nm) emission spectra. (Adapted from Adv. Optical Mater. 2015, 3, 1041).

The color of the solution was highly sensitive to pH, mechanical force and presence of chemical anions. However, the solubility issue of metals in solvents limited their applications.<sup>48</sup>

Conjugated polymers including polyfluorene, oligo (phenylenevinylene), polythiophenes are reported as potential materials because of their good quantum yield in solvent.<sup>49</sup> Muller *et. al.* demonstrated solution processable three color red-green-blue (RGB) emitting soluble conjugated polymer which upon curing photochemically gave a polymer network.<sup>50</sup> Photoresponsive conjugated nanospheres were synthesized by Bu *et. al.* by introducing dithienylethene moiety in to the polymer backbone. The fluorescence of nanospheres in the solution could be tuned by replacement of photoresponsive polymer with non photoresponsive polymer to obtain switching of color between white to RGB.<sup>51</sup>

Isolation of chromophores in the polymer backbone avoids FRET between the donor and acceptor molecules thereby enabling independent emission from the species which results in different emission color. White light emission from single polymer system was developed by a method called micelle-isolated-fluorescence.<sup>52,53</sup> Encapsulation of green and red light emitting dyes in separate micelle cores of di-block-co-polymer (poly(4-vinylpyridine) with blue light emitting polymer (polyfluorene) around their periphery has been reported which showed simultaneous emission of blue-green-red and careful combination of these three species by inhibiting the FRET gave pure white light emission in the solution (figure 1.7).<sup>54</sup>

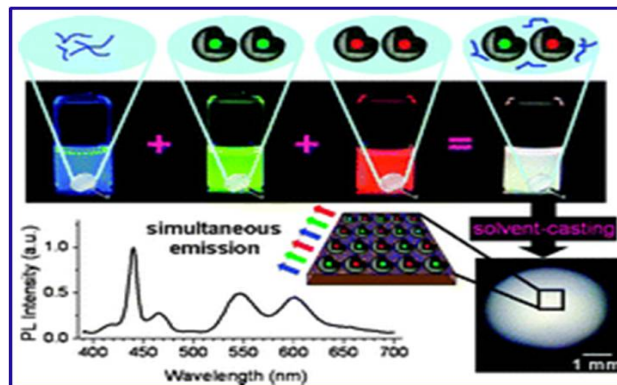


**Figure 1.7:** Schematic illustration to achieve white-light emission from a single layer of diblock copolymer micelles containing dyes in the separate cores and polyfluorene around the periphery of the micelles. (Adapted from Chem. Commun., 2009, 6723)

### 1.1.3 Gel state emitting materials

Gelation is an important phenomenon in which various types of dyes or inorganic complexes mixed in the solvent self assemble through weak interaction resulting in a network called gel.<sup>55,56</sup> Fluorescent gel is the new class of soft material which shows unique optical and electronic properties.<sup>57</sup> In general gel can be classified into two forms; the first class called as polymeric gel is formed by covalent interaction between monomers resulting in cross-linked network, which cannot be redissolved in any solvent. However the other class of gel called supramolecular gel is obtained by physical mixtures of functional molecules linked together by noncovalent interactions like H-bonding,  $\pi$ - $\pi$  stacking, Van der Waals interaction, ionic forces etc to form supramolecular network by self assembly approach.<sup>58,59</sup>

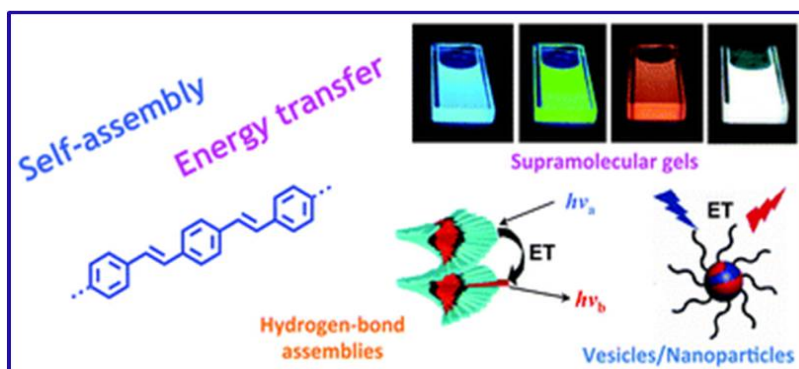


**Figure 1.8:** Supramolecular self assembly approach for the development of fluorescent gel (Adapted from Chem. Soc. Rev., 2014, 43, 4222).

Supramolecular gel or organogel are the best examples in which the process of energy transfer is facilitated. Nandi *et. al.* reported coassembled light harvesting fluorescent microgel by mixing melamine derivative with riboflavin and rhodamine which gave white light emission. The emission of different colors from the microgel is based on the energy transfer between the chromophores.<sup>60</sup> Functional organic molecules have also been studied for their supramolecular self assembly and energy transfer between them results in tunable emission color. Several examples of fluorescent polyaromatic compounds based organo gel have been explored in a recent review (figure 1.8).<sup>61</sup>

$\pi$ -conjugated material can be self assembled in a scaffold where in the presence of acceptor molecules, the phenomena of FRET occurs which results in change in emission color. Oligo (*p*-phenylenevinylene) (OPV) based derivatives have been reported as outstanding candidates for their self assembly property giving different functional architectures such as ribbons, fibers, rod and so on.<sup>62,61</sup> Recently cyano-substituted OPV was reported as fluorescent organogel where emission could be tuned depending on the position of cyano group. Various dyes and metal complexes give different types of gel which can be utilized for photon upconversion, sensing of nitro compounds, light emitting diode, color display or as light absorbing material.<sup>63</sup> Fluorescent gel based on coordination polymer are also reported where the interaction between metal and ligands leads to the enhancement of emission from the ligands after formation of coordination polymer gel.<sup>64</sup>

## 1.2 Development of fluorescent materials

Fluorescent materials with very high brightness and good photostability is an important criteria for fluorescence imaging and detection with respect to speed, resolution, and sensitivity.<sup>65,66</sup> Several strategies have been utilised for the development of fluorescent material which includes self assembly of the block-co-polymers to encapsulate dye molecules, post-polymerization method (Miniemulsion and Reprecipitation), non-covalent interaction (physical adsorption/blending) or covalent attachment of dyes to polymer backbone during the polymerization time. In principle the fluorescent polymeric particles can be developed by direct copolymerization of dyes via heterogeneous polymerization. A recent review from the group of Prof. O'Reilly summarizes the advanced strategies for obtaining fluorescent polymer particles (figure 1.9).<sup>67</sup>



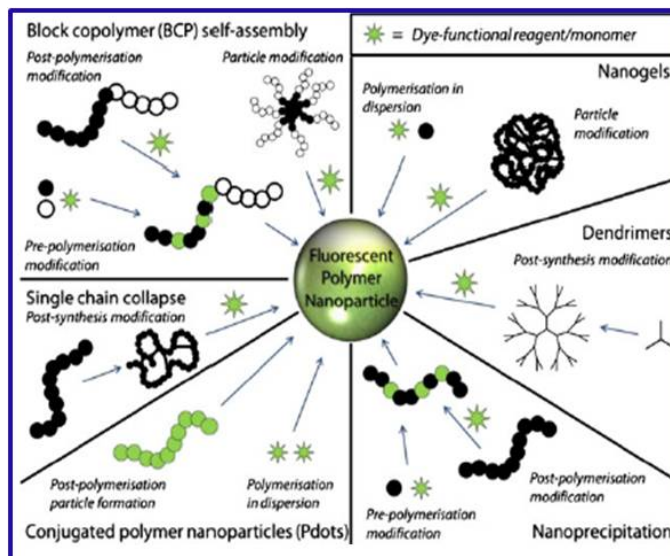


**Figure 1.9:** Various routes for synthesis of fluorescent polymer particles. (Adapted from PolymInt 2015, 64, 174).

In the following sections the strategies for the development of fluorescent polymers will be discussed in detail.

### 1.2.1 Physical blending/mixing of dyes on polymer backbone

These are the simple methods for development of fluorescent polymer particles with specific size and tunable emission.

Approach (1): Supramolecular interaction: Non-bonding interactions (like H-bonding, Van der Waal forces and  $\pi$ - $\pi$  interaction) have been extended for the attachment of fluorescent dyes to the functional polymer resulting in fluorescence from the polymeric material (figure 1.10).<sup>68</sup>

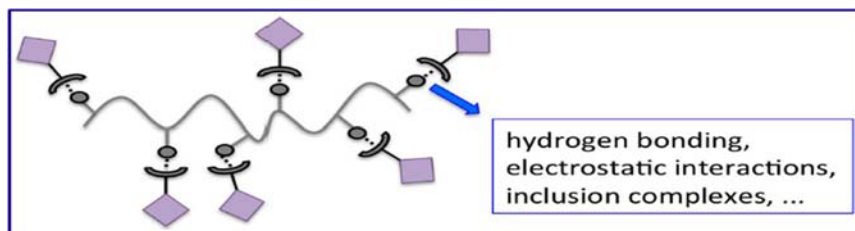


**Figure 1.10:** Schematic illustration of non-covalent interaction between dye and polymers (Adapted from Polymers 2015, 7, 717).



Linear fluorescent supramolecular polymer was reported by host guest interaction between crown ether and dye molecule. The resulting polymer showed high quantum yield in solution and solid state which could be tuned by the addition of metals.<sup>69</sup> In the recent example shown by Peng et. al., multicolor emitting nanoparticles of supramolecular polymer/copolymers were developed. The emission of color in the fluorescent polymers can be tuned by excitation energy transfer in the supramolecular architecture.<sup>70</sup>

Approach (2): Encapsulation of colored material: Recently fluorescent polymeric beads were developed by entrapment of fluorescent materials in the polymer matrix during the polymerization which avoids the aggregation of dyes there by avoiding the quenching of fluorescence.<sup>71</sup> Stable and water dispersible suspension of conjugated polymers have demand in biological applications for sensing and imaging. This strategy was explored for the development of fluorescent particles by encapsulating conjugated polymers in block copolymers and by controlling the number of light emitting species in the polymer backbone giving tunable emission wavelength in the resulting fluorescent particles.<sup>72</sup>

Approach (3): Postpolymerization method which includes a) Miniemulsion and b) Reprecipitation. Several groups have been working for the development of highly fluorescent polymeric particles using these methods.<sup>73,74</sup>

a) Miniemulsion:- It is the common method for the synthesis of fluorescent polymeric particles (figure 1.11). In this method (i) the conjugated polymer is dissolved in water immiscible solvent

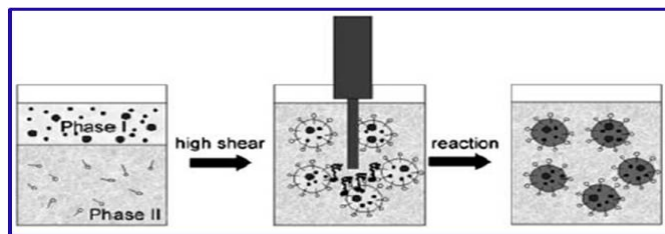


**Figure 1.11:** Preparation of nanoparticles by miniemulsion method (Adapted from Nanoscale, 2010, 2, 484).

(ii) the obtained solution is injected in water having appropriate amount of surfactant to prevent flocculation (iii) the resultant mixture is stirred with high speed ultrasonication to get

stable miniemulsion having small polymer droplets and later the organic solvent is allowed to evaporate to form stable dispersion of fluorescent polymer particles in the water.

b) Reprecipitation: - In this method (i) the fluorescent polymer is dissolved in good solvent (water miscible, e.g. THF, DMSO) (ii) the resulting solution is added to a bad solvent (water) with stirring and sonication to form the polymeric particles (iii) the organic solvent from the water dispersion is removed by evaporation to get the stable fluorescent polymeric particles (figure 1.12).<sup>75,76</sup>

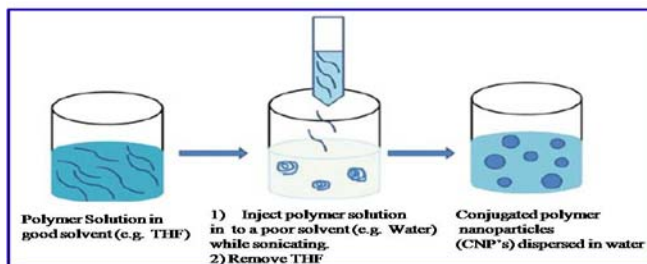


**Figure 1.12:** Preparation of nanoparticles by reprecipitation method (Adapted from Nanoscale, 2010, 2, 484).

Moon *et.al.* has shown the development of fluorescent polymeric particles by dissolving polyphenylenevinylene polymer in DMSO and subsequent addition of polymer solution to bad solvent to get the stable dispersion of fluorescent polymer particle. The stable fluorescent polymeric particles were studied for the applications in optoelectronics and cell imaging fields.<sup>77</sup> Although the strategies explained above are potential and simple, the disadvantage of dye leakage from polymer backbone and inability to obtain controlled particle size limits the utilization of these methods.<sup>78,79</sup>

### 1.2.1 Covalent attachment of dyes to polymer backbone

In order to prepare fluorescent polymer beads, direct polymerization or copolymerization of dye via radical polymerization path is another approach where the fluorescent polymers would be generated.<sup>80,65-66</sup> Usually the dyes having acrylate functionality are copolymerized with monomers of styrene or MMA via polymerization methodology or dyes could be directly attached to the preformed functional polymers resulting in the fluorescent polymeric materials.<sup>81,82</sup> On the other hand, fluorescent polymer particle have also been synthesized by heterogeneous polymerization. The advantage of the

covalent attachment of dyes to the polymer backbone is absence of dye leakage along with uniform distribution of dye along the polymer chains resulting in high quantum yield of emission.<sup>83,84</sup> For example polymerizable monomers like styrene, ethyl acrylate, phenyl acrylate was functionalized with different derivatives of fluorescent BODIPY dye (figure 1.13). The copolymerization of these derivatives with styrene in water by using RAFT

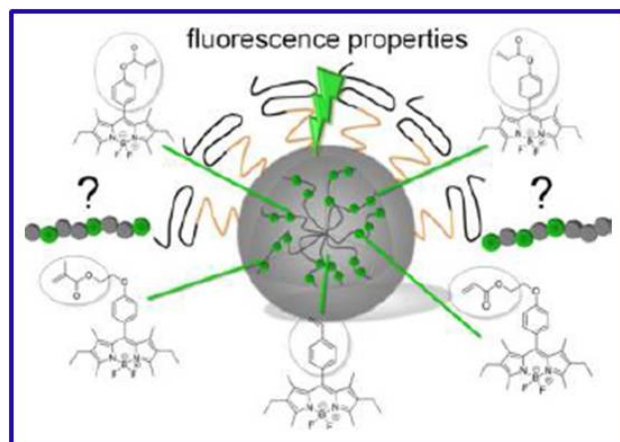


**Figure 1.13:** Schematic representation of BODIPY functionalized fluorescent polystyrene particles (Adapted from *Macromolecules* 2013, 46, 5167).

mini-emulsion polymerization method gave fluorescent polymer particles which showed high quantum yield compared to quantum dots.<sup>85</sup> In another example, Li and coworkers used emulsion polymerization to polymerize styrene, acrylamide and PDI acrylate for the development of highly fluorescent core shell nanoparticles.<sup>86</sup>

### 1.2.2.1 Heterogeneous (Free Radical) polymerization

Heterogeneous radical polymerization method is a promising method by which polymer beads having different size ranging from 0.01 to 1000  $\mu\text{m}$  can be obtained.<sup>87,88</sup> Polymer microbeads generally called as colloids which can be defined as the particles with dimension ranging from nanometer to micrometer size could be synthesized using above method (figure 1.14). Various polymerization techniques like suspension, emulsion, dispersion etc are utilized to obtain narrow disperse beads of polymer with varying size ranges from nanometer to micrometer depending on the size need for different applications.

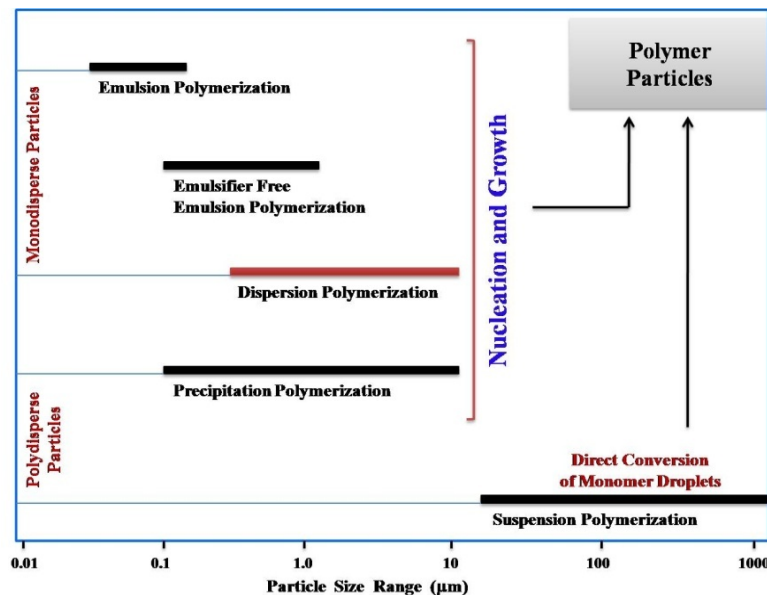


**Figure 1.14:** General kinetic features and particle size ranges of heterogeneous (particle forming) polymerization processes (Adapted from Colloid Polym., Sci. 1992, 270, 717).

According to the need of utilization, polymer particles should follow the criteria of (a) small size and volume, (b) large specific surface area, (c) stable dispersion, (d) ability to diffuse, (e) uniform size and morphology, etc.<sup>89</sup> The basic ingredients of emulsion polymerization are monomer, surfactant, initiator and medium (aqueous phase). In the conventional emulsion polymerization the low water soluble monomer is inserted in to aqueous phase with surfactant (above critical micelle concentration). The polymerization starts at ambient temperature (70 °C) with addition of water soluble initiators. Once the colloidal particles forms, the nucleation starts in the micelles (where monomer is present) and the process continues to form the growing polymer chain with the typical size range of 10 to 300 nm. Although the role of the surfactant is to prevent the coagulation of the formed polymer particles it is always problematic to remove all the surfactants from polymer matrix.<sup>90</sup> Zeng *et. al.* carried out the copolymerization of methyl methacrylate by emulsion polymerization in which two fluorescent dyes (donor-acceptor) were covalently incorporated into the polymer backbone to form a FRET pair.<sup>91</sup> Reilly *et. al.* reported the synthesis of fluorescent polymer beads by using high amount of surfactant in oil emulsion strategy as potential material for bioimaging applications.<sup>92</sup>

Microemulsion and miniemulsion are types of emulsion polymerization that differ from each other by their contents, droplet size and particle formation. These are the two heterophase polymerization methods which have been applied for the development of fluorescent polymers. Even though the mechanism of formation of polymer beads is different in both the cases the resultant polymer particle suspension can be stable for several months.<sup>93,94</sup> For example, Taniguchi *et. al.* reported the miniemulsion polymerization as a powerful method for the synthesis of fluorescent polymer particles by covalent attachment of dyes to the polymer backbone.<sup>95</sup> In another example submicrometer and isodisperse fluorescent latex was synthesized by emulsion polymerization of styrene in batch process where the polymer particle size could be tune by varying the amount of surfactant.<sup>96</sup>

In the suspension polymerization, monomer and initiator are water insoluble and are suspended in the aqueous phase with stabilizing agents. The high speed stirring of the reaction phase results in the formation of microdroplets which acts as suspension agents and the initiation of polymerization is achieved at desired temperature (20-100 °C). The monomer droplets are directly converted to polymer particles under suitable condition to get polymer microbeads 10-1000 µm in size as dispersed solid phase.<sup>97,98</sup>

Particle size control in polymers is a very important criteria for many applications such as separation media, fluorescent microscopic imaging, medical diagnosis, surface immobilization etc. Several methods have been reported for the synthesis of fluorescent polymer particles and the choice of suitable solvent and stability of dyes in required conditions also have been investigated.<sup>99,100</sup> Among these methods, dispersion polymerization is one of the attractive methods for the large-scale synthesis of monodisperse polymer beads in the size range of 0.5-15 µm. Submicron monodisperse polymer particles can be achieved by dispersion polymerization under certain conditions.<sup>101</sup> In this thesis dispersion polymerization was utilized for the development of fluorescent polymer beads, and the dispersion polymerization technique is explained in detail in the following section.

### **1.2.2.2 Dispersion Polymerization**

Dispersion polymerization is defined as a type of precipitation polymerization in which the monomer is polymerized in presence of suitable stabilizer; the solvent selected for this method is a good solvent for monomer and stabilizer while it is bad solvent for the resulting

polymer. By using partially hydrolyzed poly(vinyl alcohol) (PVA) as stabilizer and quaternary ammonium salt as costabilizer, Almog *et al.* synthesized the monodisperse polymer particles of polystyrene and studied the stability of dispersion.<sup>102</sup> Later in 1985 dispersion polymerization of styrene in ethanol as solvent and polyvinylpyrrolidone (PVP) as water soluble stabilizer was first carried out by Lok *et al.* which raised the interest about the methodology of dispersion polymerization.<sup>103</sup> In the initial stage the emulsion, suspension and precipitation polymerization are in the heterogeneous phase; however the dispersion polymerization is homogeneous and it becomes heterogeneous once the polymer chain grows.<sup>104</sup> The mechanism of dispersion polymerization process follows two steps, first is nucleation and second is particle formation. The nucleation step is very fast, complex and sensitive however the particle growth formation is robust and simple which is very well studied.<sup>105,106</sup>

Ober *et al.* discussed the preparation of monodisperse polymer particles by dispersion polymerization in which various solvent combinations have been utilized.<sup>107</sup> The requirement for the dispersion polymerization are monomer, initiator, stabilizer, costabilizer and solvent medium in which all the ingredients are soluble, however the product precipitates during the polymerization. After initiation of polymerization AIBN undergoes radical formation which reacts with monomer and by addition of several monomers it forms growing chain that remains soluble in the reaction media until it reaches a critical chain length after which it precipitates. The nanosized nuclei which forms by aggregation of precipitated chains are unstable and they try to attain stability by aggregating more chains to form larger particle. The overall procedure is called nucleation and it is very fast and complex. The larger particles adsorb to the steric stabilizers thereby avoiding coagulation and the whole process happens very fast with complexity.<sup>108-110</sup> The role of stabilizer during the chain growth stage is very important in dispersion polymerization. The size of the particle and size distribution is controlled by the stabilizer.<sup>111</sup> Various hydrophobic polymers such as Polyvinylpyrrolidone (PVP), Poly(acrylic acid) (PAA), cellulosic derivatives and Poly(vinyl alcohol) (PVA) have been utilized as stabilizer for the synthesis of monodisperse polymer particles by dispersion polymerization.<sup>112-113,103,109,108</sup>

Tseng *et al.* carried out the dispersion polymerization of styrene in alcohol with azobased initiator. In their experiment, they studied the role of stabilizer and costabilizer on

the particle size and proved that during the nucleation time the stabilizers and costabilizers are adsorbed onto the larger particles of preformed chains to avoid coalescence. Anionic and non-anionic costabilizers have been utilized for the dispersion polymerization.<sup>114</sup> Although the dispersion polymerization method is applied for development of uniform monodisperse particles; it is not suitable for monomers with functional groups. In such cases uncontrolled particle size with agglomerated mass resulted after the polymer formation.<sup>115,116</sup> Attempts to overcome this problem by adopting seeded dispersion polymerization also had not yielded much successes.<sup>117,118</sup>

The development of cross-linked monodisperse particle via dispersion polymerization is a challenging task. Even though dispersion polymerization method was reported in early 1985, it did not facilitate the addition of functional comonomers, fluorophores, cross-linkers.<sup>119</sup> It was proved that the presence of these functional moieties disturb the monodispersity of particle size and in particular, with cross-linkers which results in coagulation of the polymer.<sup>120</sup>

To overcome this problem, Prof. Winnik et. al. reported the synthesis of monodispersed cross-linked beads incorporating a cross-linker via polymerization method which they named as “two stage” dispersion polymerization. In this method, they were able to control the particle size by the delayed addition of the cross-linker after the nucleation stage. (figure 1.15).<sup>104</sup>

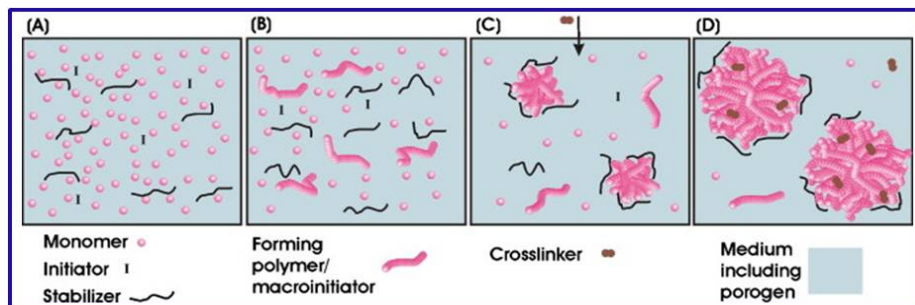


**Figure 1.15:** Schematic representation of the dispersion polymerization stages (A) Initially monomer, initiator and polymeric stabilizer are dissolved in the medium. (B) Formation of oligomers, which are soluble in the medium. (C) 1% monomer conversion i.e. nucleation stage (sensitive). (D) Particles grow by capturing monomers and oligomers from the medium. (Adapted from Progress in Polymer Science 2012, 37, 365).

Utilizing this strategy, they clearly showed the successful incorporation of the cross-linker divinyl benzene (DVB) into PS backbone and still obtained monodisperse particles (figure 1.16).<sup>121</sup>

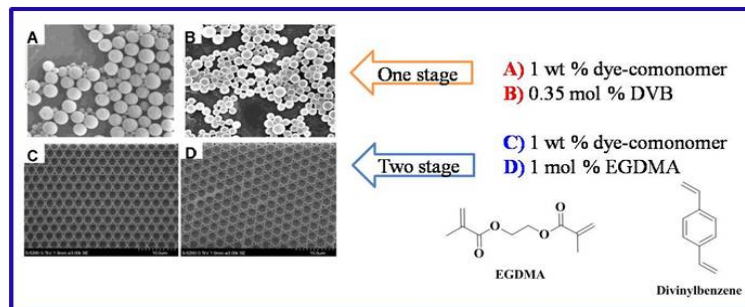


**Figure 1.16:** Polymer particles obtained via one stage and two stage dispersion polymerization by varying the crosslinkers. (Adapted from J. Am. Chem. Soc. 2004, 126, 6562).

Later, Peng *et al.* reported that fluorescent cross-linked core shell PMMA particles can be synthesized by dispersion polymerization and the particle size was controlled by varying the time of addition of cross-linker and dye during the nucleation process.<sup>122</sup>

### 1.3 Applications of fluorescent materials

Because of their brightness and high quantum yields, fluorescent polymers have been utilized for various applications. The following sections summarize the literature reports on the fluorescent materials where they find applications in several fields.

#### 1.3.1 Multicolor emitting material

Fluorescent material with multicolor emission have been widely applied in light emitting diodes (LEDs), dye lasers, data recording and storage, LCD and panel displays.<sup>123,124</sup> Single polymer having multicolor emission is a challenging task. Researchers are trying to address this issue by optimization of different color emitting materials included in single system.<sup>125,126</sup> Polyfluorene with naphthalimide based component were developed for white light emitting single polymeric system.<sup>127</sup> Subsequently various fluorescent material including small organic molecules, polymers have been utilized as potential light emitting materials.<sup>128</sup> It well established and studied that the phenomena like FRET, ET occurred in



designed materials, which upon treatment with external stimuli gave tunability in color emission.<sup>129</sup> Application of luminescent materials for storage of important data is an interesting research now a days.<sup>130,131</sup> Due to their response to external environment, the smart materials show reversible nature towards chemical changes which cause different emission color in the solid state.<sup>132</sup> Thirumalai *et. al.* developed reversible fluorescent ink by self assembly of hydrophilic-hydrophobic  $\pi$ -conjugated material in aqueous solution which was erasable by water (figure 1.17).<sup>133</sup>

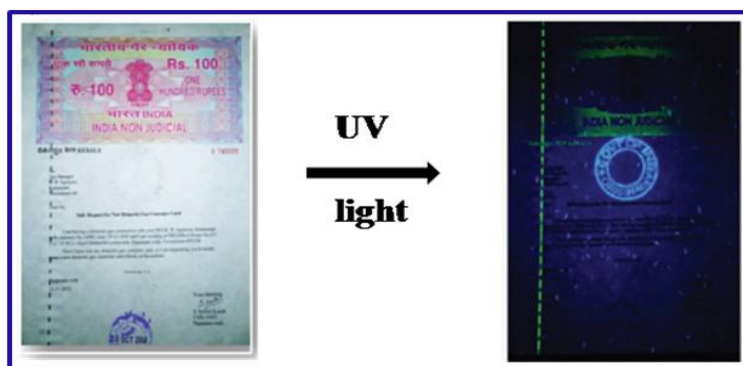


**Figure 1.17:** Applications of fluorescent gel as security purpose, document under normal light and after irradiation of UV light (Adapted from Sci. Rep., 2015, 5, 9842).

The photonic crystal based on soft polymer opal system has been also developed by selectively arranged nanospheres followed by cross-linking giving luminescent polymeric material. The rubbery nature of polymer after stretching and solvent treatment causes the change in color emission which can be used for image display, anticounterfeit material etc.<sup>134</sup> Chen *et. al.* developed cross-linked metallogel of lanthanide and terpyridyl end-capped four arm poly(ethylene glycol) polymer. The co-ordination complex was further utilized as white light with multicolor emitting material. The tunability of color was highly dependent on the amount of lanthanum present in the system.<sup>135</sup>

### 1.3.2 Bio-imaging, labeling and barcoding

Fluorescent polymeric material has great demand in the biological science for imaging and labeling applications.<sup>136</sup> They have also been applied to visualize the mode of interaction and pathway while entering the cell, for example in the drug delivery and uptake applications.<sup>137</sup> Polystyrene microbeads with multicolor emission have added advantage for

various types of bio applications.<sup>138,139</sup> Flow cytometric analysis is the important tool in biology which is used to count and sort the cell. (figure 1.18).

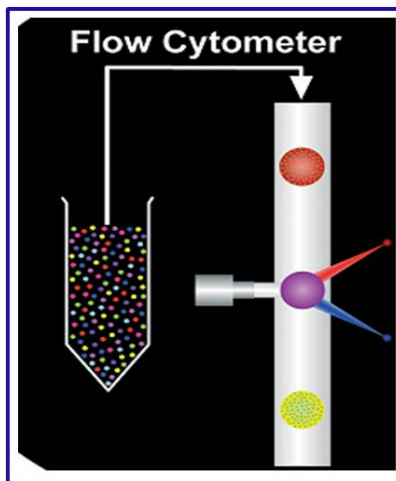


**Figure 1.18:** Fluorescent microbeads as standard in Flow Cytometric analysis (Adapted from *Angew. Chem. Int. Ed.* 2006, 45, 6104).

The controlled particle size of polymer beads with uniform emission are utilized as a standard in flow cytometric analysis. Barcoding is the emerging area in the biological science which helps to probe the cell.<sup>140</sup> Depending on specific applications encoding of colloidal suspension with particular tag has been developed to study the interaction between biological specimens.<sup>141</sup> Various quantum dots have been incorporated to the polystyrene microbeads; the spectral barcoding was investigated and showed that the ratiometric barcode could be developed.<sup>142</sup> Chemical encoding is the potential technique to understand the behaviour of molecules in the internal system, for that microsphere have been tagged with fluorescent dye, after that various functionalities such as secondary amines, nucleic acid has been attached to the surface.<sup>143,144</sup> For example Batersby *et. al.* studied the high throughput molecular screening with colloidal suspension of fluorescent microbeads and showed their applications in barcoding, drug discovery and proteomics. They carried out series of experiments to understand the coding of each reporting particles with the emission properties (figure 1.19).<sup>145</sup> Microbeads are also utilized for the immobilization of enzyme on the surface. By decoding the beads the identification of analyte can be possible. Several companies including Luminex has developed the system where the fluorescent beads have been used for the optical decoding to determine the protein binding.<sup>146</sup>

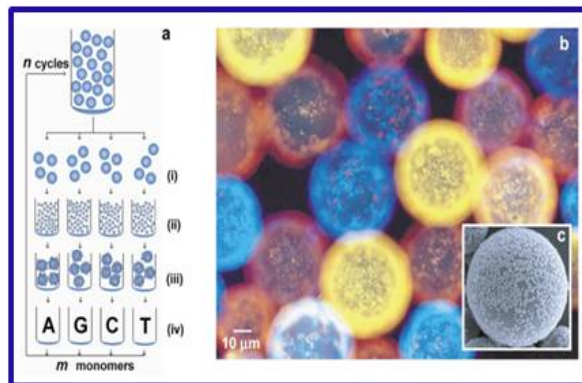


**Figure 1.19:** Active barcoding of combinatorial libraries: (a) schematic diagram of a split-and-mix DNA library synthesis on support beads (b) Fluorescence microscopic image of microbeads with several barcodes. (c) SEM of the 1 $\mu$ m reporters attached to a ceramic support bead (Adapted from Chem. Comm., 2002, 1435).

Single beads with multicolor emission can be applied in biology. Jonathan *et. al.* reported that the hydrophilic core and hydrophobic cavity of fluorescent cross-linked polystyrene microbeads are useful for the bioconjugation of green fluorescent proteins to study the invitro cellular imaging.<sup>147</sup> Due to their outstanding properties fluorescent polymer particles also serve as potential materials in the field of bioimaging.<sup>148</sup>

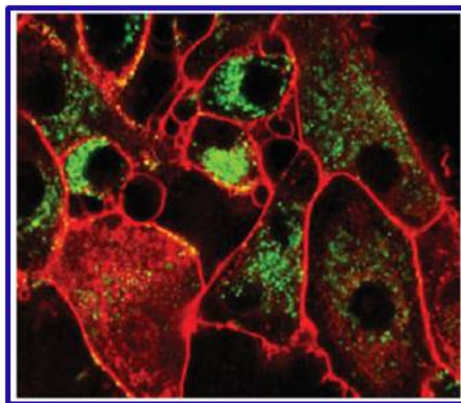


**Figure 1.20:** Fluorescence microscopic image of HeLa cell using the fluorescent latex beads (Adapted from Macromol. Chem. Phys. 2005, 206, 2440).

Hydrophobic fluorescent particles of polystyrene have been used for the labeling and imaging of cells due to their biocompatible nature. Landfester *et. al.* developed fluorescent

polymer latex by miniemulsion polymerization which were utilized as potential material for the imaging of Hela cell (figure 1.20).<sup>149,150</sup>

### 1.3.3 Sensors (oxygen, gas, explosive)

Fluorescent materials have the advantage of showing different signals in different environment. Owing to these properties and sensitive nature of the fluorescent polymeric material they have been extensively used in the sensing purpose in material science and engineering.<sup>151,152,43</sup> Various types of novel fluorescent materials based on small molecules to polymers have been reported as potential materials for the detection and sensing of analytes (figure 1.21).

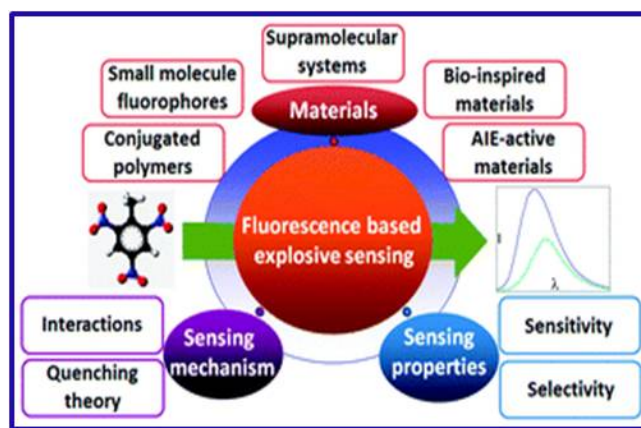


**Figure 1.21:** Fluorescent materials for sensing applications (Adapted from Chem. Soc. Rev., 2015, 44, 8019).

Fluorescence resonance energy transfer (FRET) one method of sensing, where the binding of analyte to the donor material results in reduction of the latter's emission. The quenching constant for this process can be determined by applying Stern-Volmer plot. The process of sensing mainly depends on the electron-transfer between donor and acceptor (sensor to quenchers). It has been proved that the selectivity and sensitivity of detection mainly depends on the electron-donating or accepting ability of the sensors.<sup>153</sup> To date various fluorescent materials have been constructed for detection of analytes that includes porphyrin based derivatives, polycyclic hydrocarbons, polysiloles, polycarbazoles etc.<sup>154</sup>

The sensing of the analyte has been reported in different form, it can be in the solution state or in solid state. In the solid state (films or fibers or particles) luminescent material has been utilized for the detection/sensing of analytes. The advantages of solid state fluorescent material are fabrication, easy handling, processability and so on.<sup>155</sup> Now a day's detection of chemical compounds like nitroaromatics is one of the most challenging problem for military operation, homeland security and environmental safety. Several groups have shown the potential use of fluorescent materials in the field of chemical sensing. The small size and polymeric nature of fluorescent microspheres make them suitable candidates for the generation of micro or nanosensors for analysis and device fabrication (figure 1.22).<sup>156</sup> The contributions from the group of Prof. Otto S. Wolfbeis has presented the applications of fluorescent microspheres for different types of protocol like, high density sensing and suspension array, barcoding etc.<sup>157,151</sup> Walt *et. al.* demonstrated the optical fibers as an artificial nose in which fluorescent dyes were immobilized on the optical fibers. They also showed the advantages of fluorescent micobeads as high density array sensor over the organic dyes.<sup>158</sup> Fluorescent materials based on industrial polymers like PS, PPV and copolymers of them have been explored and applied for the detection of explosives.<sup>159,160</sup>

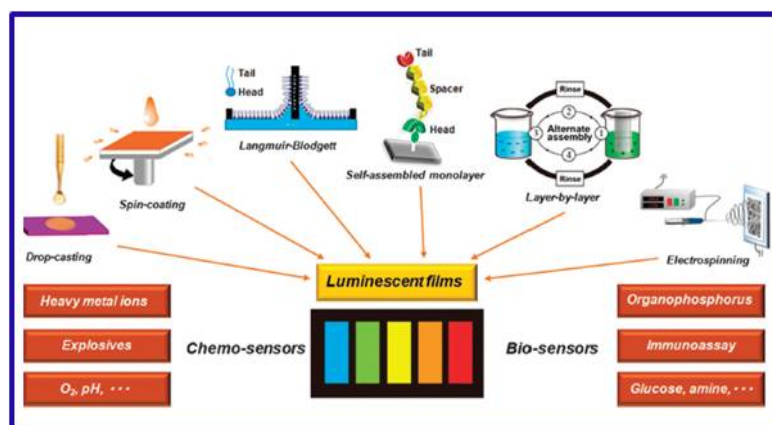
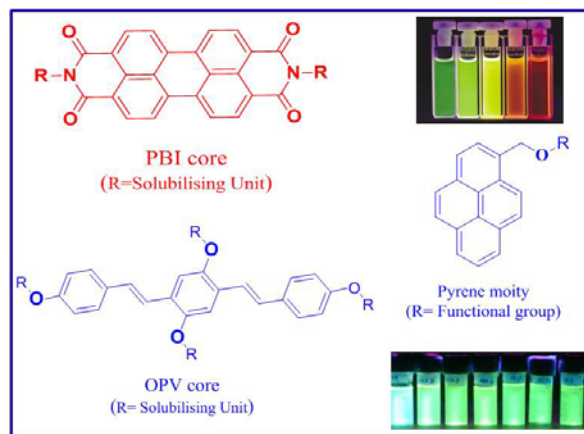


**Figure 1.22:** Representation and summary of luminescent films as chemo and biosensing applications (Adapted from Chem. Soc. Rev., 2015, 44, 6981).

#### 1.4 Fluorescent dyes: Perylenebisimide, Oligo (*p*-phenylenevinylene) and Pyrene

There are several dyes reported as fluorescent materials because of their high quantum yield. Among the various dyes, Perylenebisimide (**PBI**), Oligo (*p*-

phenylenevinylene) (**OPV**) and Pyrene are chromophores having absorption in the visible region and a high fluorescence quantum yield reaching nearly unity (scheme 1.1).



**Scheme 1.1:** Structure of fluorescent dyes.

They are thermally as well as photo chemically stable, both of which are essential criteria for application in luminescent polymers.<sup>161-163</sup> They have been explored widely as a light emitting and sensing material. PBI dye was used in the pigment industry for more than five decades as red vat dyes, due to their light and weather-fastness, favorable combination of insolubility and migrational stability, thermal and chemical inertness as well as high strength with shades ranging from orange, red, violet to even black.<sup>164,165</sup> PBI and Pyrene are the class of polyaromatic fused rings that have found application in different areas such as organic solar cells, sensitizers for photodynamic therapy, color tunable light emitting diodes, fluorescent labels, sensors, lasers etc.<sup>166,167</sup> OPV is also an equally explored challenging moiety having a good  $\pi$ -conjugated back bone especially useful as blue light emitting material and widely applied in various fields.<sup>168</sup> Furthermore, the color of OPV fluorophore can be fine tuned by varying the conjugation length as the absorption and emission wavelength fluctuate with variation in conjugation length.<sup>169</sup>

Pyrene as a fluorophore has been extensively investigated in sensor applications including detection of explosives based on 'nitroaromatics'. The electron deficient nature of the nitroaromatic molecules like trinitrotoluene (TNT), dinitrotoluene (DNT) and nitrotoluene (NT) enables donor-acceptor interactions with electron rich  $\pi$ -aromatic donors like pyrene leading to the quenching of fluorescence of the latter.<sup>170</sup> Both the monomeric

(300-450 nm) and excimeric (420-550 nm) emissions of pyrene are sensitive to the interaction with nitro aromatic molecules, although the sensitivity of the excimer emission is higher.<sup>171</sup> Several pyrene based small molecule sensors have been reported in the last 15 years which were designed specifically for detection of explosives.<sup>172</sup> Copolymerization of these dyes with polymer backbone like PS, PMMA, PVA for the development of fluorescent polymers in different shapes including beads, fibers and sheet are reported as high performance materials.<sup>173-175</sup>

### 1.5 Molecularly Imprinted Polymers (MIP)

Development of functional materials with unique properties is the focus of intense research during the few decades. The key reason of functional material is their selective recognition of analyte.<sup>176</sup> Various methodologies have been adopted for the development of functional materials. Molecular Imprinting Technology (MIT) was first proposed by Prof. M. V. Polyakov in 1931, where he prepared silica with specific solvent (benzene, toluene, xylene) and demonstrated the preferential binding of silica towards the solvent.<sup>177</sup> Later in 1972 a group from Japan introduced the cross-linked system based on organic polymer chain resulting in improvement in adsorption capacity. MIT is the best method which enables us to synthesize 'tailor-made' functional materials such as Molecularly Imprinted Polymers (MIPs).<sup>178</sup> Wulff *et. al.* in 1970 reported covalent approach for synthesis of MIPs.<sup>179</sup> However in 1981 the noncovalent approach was also presented by Arshedy *et. al.* for new development in the MIPs synthesis.<sup>180</sup> Recently there is increasing interest for development of MIPs, because of their specialized features such as ease of large-scale synthesis, high thermal and chemical stability, and ability to reorganize molecules selectively (figure 1.23).

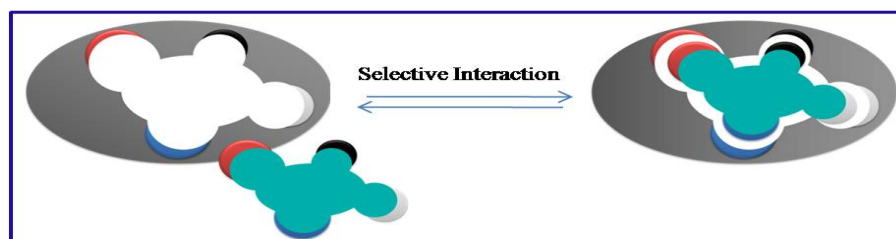


**Figure 1.23:** Representation of MIPs for selective interactions (Adapted from nanomyp, <http://nanomyp.com/en/page.cfm?id=39&>).



Several reviews have been presented for the general introduction and development of MIPs.<sup>181,182</sup> MIPs contain selective recognition sites in the backbone as a result of polymerization around a template molecule covalently or non-covalently bound to functional monomers. The polymers behave as an artificial receptor to identify the compounds from their mixture. Because of their outstanding properties, MIPs offer a broad range of application in analytical and biological science.<sup>183, 181</sup>

### 1.5.1 Synthesis of Molecularly Imprinted Polymers

Molecularly Imprinted Polymers are highly cross-linked systems with specific binding affinity towards the molecules. Radical polymerization is the suitable method for the synthesis of MIPs.<sup>184</sup> Various shape and size of MIPs are reported that includes films, bulk monolith and spherical beads.<sup>185</sup> However the ideal morphology of the MIPs that play a crucial role in availing the binding sites is the spherical form which can be obtained by heterogeneous polymerization.<sup>186</sup> The basic requirement for the synthesis of MIPs includes a functional monomer (analyte), the prototype (template), cross-linker and the porogen (solvent).

MIP synthesis follows three stages (figure 1.24)

- Complex formation:- organization of the template material with functional molecules via covalent bonding and non-covalent approach (supramolecular assembly) such as  $\pi$ - $\pi$  interactions, hydrogen bonding, ionic interactions.
- Polymerization:- to polymerize the template/monomer complex mixture in presence of cross-linker and solvent to generate material with specific recognition sites.

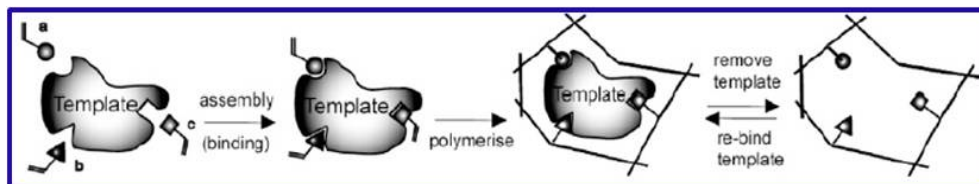
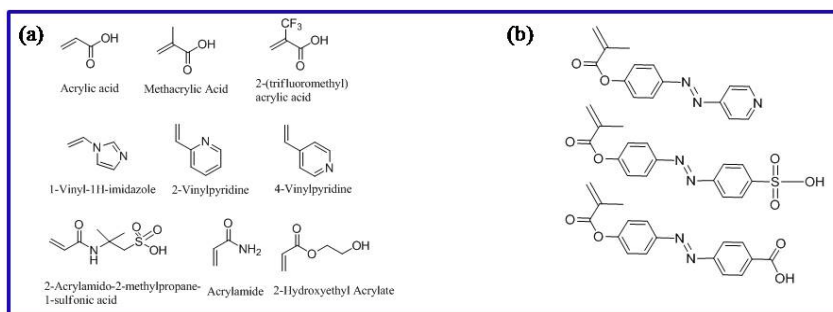


**Figure 1.24:** Schematic representation for the synthesis of MIPs (Adapted from Diane Carrera MacMillan Group Meeting Sept 14, 2005).



- c) Removal of the template:- the template is extracted by washing with organic solvent or via soxhlet extraction techniques which leaves the specific sites that are complimentary to the shape and size of template.

**(i) Functional monomers:** Functional monomers plays a vital role in the MIP synthesis. It acts as a backbone as well as linker to hold the template molecules after readsorption. Different functional molecules have been used for the binding of templates in the MIPs.<sup>176, 183</sup> There are several monomers presented in the literature (Scheme 1.2 a).

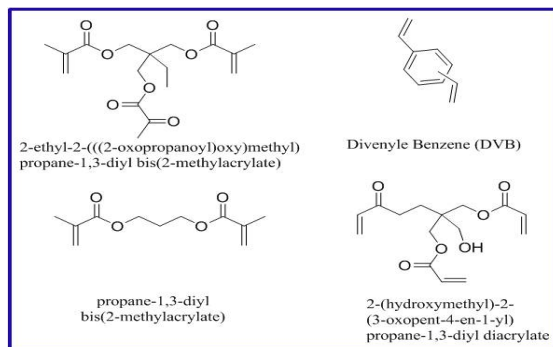


**Scheme 1.2:** (a) Structures of functional monomers (b) structures of responsive functional monomers. (Adapted from Chem. Soc. Rev., 2011, 40, 2922).

Few of them respond to the external stimuli such as light, heat, pH etc. For example hydroxyl, amino and pyridine functionalized monomers are highly desirable for responding to pH and heat as stimuli. MIPs having such functionalities were utilized for the interaction with template molecules.<sup>187</sup> Light responsive functional dyes such as azobenzene, spiropyran are known for their ability to switch from trans to cis. Taking the benefits of photoresponsive properties various MIPs were developed which showed the light triggering abilities towards analytes.<sup>188,189</sup> Few examples of responsive functional monomers are given above in scheme 1.2 b.

**(ii) Cross-linker:** The stability of MIPs is very important which depends on the cross-linker present in the backbone. The role of cross-linkers is to stabilize the binding sites in the MIPs for recognition of template molecules.<sup>190</sup> Various cross-linker with mono or bi acrylate

functionality were reported. (scheme 1.3). The rigidity of MIPs is directly proportional to the cross-linkers present in the backbone.<sup>176</sup>



**Scheme 1.3:** Structures of cross-linkers generally utilized for synthesis of MIPs (Adapted from Int. J. Mol. Sci. 2011, 12, 5908).

### 1.5.2 Applications of Molecularly Imprinted Polymers

The cross-linked 3D network of MIPs have specific sites for binding of analytes in MIP synthesis. MIPs have been utilized in material science and technology for various applications, which includes purification and separation of compounds, to mimic the analytes, as a chemical and biological sensor, in catalytic applications and in analytical areas (figure 1.25).<sup>191,192</sup>

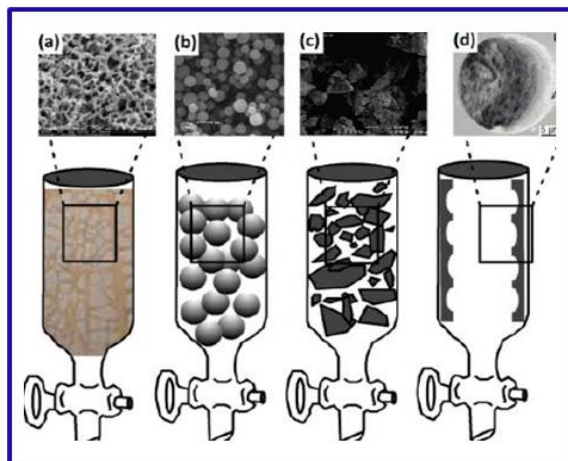


**Figure 1.25:** Applications of various MIP materials in separation media (a) the stationary phase is a highly porous polymer (b) spherical particles, (c) irregularly shaped particles, and (d) surface imprinting on the wall of the column (Adapted from Anal. Chem. 2014, 86, 250–261)

The removal and identification of material is a very challenging task in chromatography separation, where MIPs have served as potential material with good results.<sup>193</sup> Removal of contaminants from the personal care products by using MIPs has benefited environmental protection. In the sample preparation, solid phase extraction is the important step where MIPs have great potential as supportive material. Shirgel *et. al.* reviewed the application of MIPs in various fields such as sensors and drug delivery, biology and material science etc. Due to their advanced properties MIPs have been used as artificial antibodies. Direct replacement of antibody by MIPs has been achieved by several groups.<sup>194</sup> Mosbouch *et. al.* reported the molecular imprinting strategy which is highly desirable method for substitution of biological receptors and antibodies.<sup>195</sup> MIPs have also served as chemical sensor for the detection and removal of nitrocompounds. Sensitive and selective detection of chemical vapour of hazardous compounds in the aqueous phase using MIPs has been shown.<sup>196</sup> MIPs can act as stimuli responsive materials.<sup>197</sup> Polyacrylic acid-polyethersulphonate based pH sensitive MIPs were developed for the uptake of bisphenol-A where the change in pH of solution affects the uptake capacity of template molecule.<sup>198</sup>

Using Azodyes as functional monomers the photoresponsive MIPs were developed by several groups (figure 1.26). The trans-cis property of the azo MIPs towards light was applied for the release study of pesticide.<sup>199</sup> Optical sensors of MIPs has received much

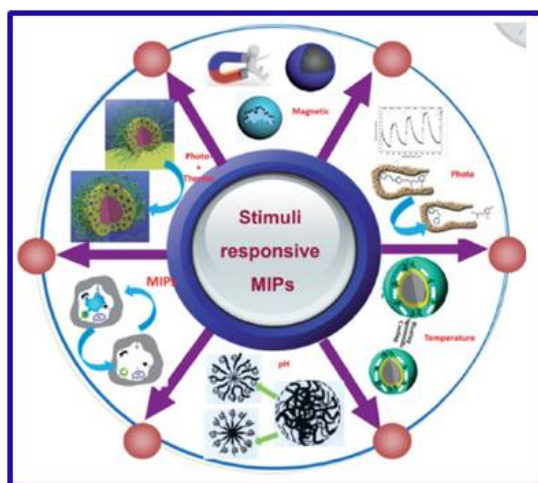


**Figure 1.26:** Applications of stimuli responsive MIPs (Adapted from J. Mater. Chem. C, 2013, 1, 4406).

attention because of its unique property and signalling ability towards the template molecule. Few reports are presented to show the advanced characteristics of MIPs as a fluorescent sensor.<sup>200-202</sup> It is reported that the phenomenon of FRET mainly depends on the distance between donor and acceptor molecules either physically entrapped or covalently attached to the backbone.<sup>203</sup> A recent report showed the development of fluorescent MIPs were covalently incorporated donor dye molecule interacted with acceptor drug molecule (analyte). The intensity of emission depended on the binding and removal of acceptor molecule. The change in fluorescence confirmed the potential applications of fluorescence.<sup>204</sup>

### 1.6 Aim of the thesis

The above discussion provides a detailed literature survey of fluorescent materials, their development using various methods and their applications in different fields. A study of the applied aspects of fluorescent materials by many researchers was also explored. Although surveyed widely, many challenges are there yet to be answered. It is important to design fluorescent polymeric materials with desired particle size and wide range of emission using simple polymerization methodology in the laboratory as well as in industry. For instance the current synthetic methodologies adopted for the preparation of fluorescent materials and the properties of resulting materials face many limitations. For example, development of fluorescent polymers with controlled particle size, non-leaching of fluorophore, thermal and photostability, multicolor emission from single polymer and high solid state quantum yield are lacking in the field. We have attempted to address some of the above mentioned problems by developing fluorescent polymer beads using dispersion polymerization methodology. Perylenebisimide (**PBI**), Oligo (*p*-phenylenevinylene) (**OPV**) and Pyrene (**Py**) based dyes were used as fluorescent molecules because of their strong absorption in the visible region and good quantum yield. The resulting polymer beads exhibited nearly monodisperse particle size, good thermal and photostability, multicolor emission and high solid state quantum yield. The covalent incorporation of fluorescent dyes resulted in the non-leaching of fluorophore from polymer backbone which in turn resulted in uniform emission.

The thesis is focused on the following major aspects:

- (i) Development of fluorescent polystyrene polymeric microbeads by dispersion polymerization method.
- (ii) Application of the polystyrene beads as solid state white light emitting material and as a fluorescent ink.
- (iii) Synthesis of functional multicolor emitting beads and their investigation for the detection of nitro compounds.
- (iv) Development of fluorescent molecularly imprinted polymers (**MIPs**) for selective recognition of the template molecules.

The new findings have been presented in the current thesis which has summarized and concluded in the last chapter six.

## 1.7 Reference

- (1) Lakowicz, J. R. 2nd ed. Kluwer *Academics/Plenum Publisher: New York*, **1999**.
- (2) Siraj, N. et. al. *Anal. Chem.* **2016**, 88, 170–202.
- (3) Reineke, S.; Thomschke, M.; Lüssem, B.; Leo, K. *Rev. Mod. Phys.* **2013**, 85, 1245–1293.
- (4) Thomas, S. W.; Joly, G. D.; Swager, T. M. *Chem. Rev.* **2007**, 107, 1339–1386.
- (5) Reineke, S. *Rev. Mod. Phys.*, **2013**, 85, 1247–1292.
- (6) Basabe-Desmonts, L.; Reinhoudt, D. N.; Crego-Calama, M. *Chem. Soc. Rev.* **2007**, 36, 993–1017.
- (7) Shang, M.; Chunxia, Li.; Lin, J. *Chem. Soc. Rev.*, **2014**, 43, 1372–1386.
- (8) Lavastre, O.; Illitchev, I.; Jegou, G.; Dixneuf P. H. *J. Am. Chem. Soc.* **2002**, 124, 5278–5279.
- (9) Sheng, L.; Li, M. J.; Zhu, S. Y.; Li, H.; Xi, G.; Li, Y. G.; Wang, Y.; Li, Q. S.; Liang, S. J.; Zhong, K.; Zhang, S. X. A. *Nat. Commun.* **2014**, 5.
- (10) Würthner, F.; Ahmed, S.; Thalacker, C.; Debaerdemaeker, T. *Chem. Eur. J.* **2002**, 8, 4742–4750.
- (11) Ward, M. D. *Chem. Soc Rev*, **1997**, 26, 366–375.
- (12) Mei, J.; Leung, N. L. C.; Kwok, R. T. K.; Lam, J. W. Y.; Tang, B. Z. *Chem. Rev.* **2015**, 115, 11718–11940.
- (13) Hecht, S.; Fréchet, J. M. J. *Angew. Chem., Int. Ed.* **2001**, 40, 74–91.
- (14) Peng, J.; Chen, M.; Qiu, F.; Yang, Y.; Sohn, B-H.; Kim, D. H. *App. Phys. Let.* **2008**, 93, 183303.
- (15) Trindade, F. J.; Triboni, E. R.; Castanheira, B.; Brochsztain, S. *J. Phys. Chem. C* **2015**, 119, 26989–26998.
- (16) Chin-Ti Chen, *Chem. Mater.* **2004**, 16, 4389–4400
- (17) Tang, C.; Xu-Dong Liu, X-D.; Liu, F.; Wang, X-L.; Xu, H.; Huang, W. *Macromol. Chem. Phys.* **2013**, 214, 314–342.
- (18) Akasaki, I.; Amano H.; Nakamura, S. *The Nobel Prize In Physics* **2014**, The Royal Swedish Academy of Sciences.
- (19) Wu, H.; Ying, L.; Yang W.; Cao, Y. *Chem. Soc. Rev.*, **2009**, 38, 3391–3400.
- (20) Shang, M.; Chunxia Li\* and Jun Lin, *Chem. Soc. Rev.*, **2014**, 43, 1372–1386.
- (21) Suehiro, T.; Hirosaki N.; R-J. *ACS Appl. Mater. Interfaces* **2011**, 3, 811–816.

- (22) Wang, T.; Li, P.; Li, H. *ACS Appl. Mater. Interfaces*, **2014**, *6*, 12915–12921.
- (23) Ma, X.; Sun, R.; Cheng, J.; Liu, J.; Gou, F.; Xiang, H.; Zhou, X. *J. Chem. Educ.* **2016**, *93*, 345–350.
- (24) Li, Z.; Ishizuka, H.; Sei, Y.; Akita, M.; Yoshizawa, M. *Chem. Asian J.* **2012**, *7*, 1789–1794.
- (25) Pati, A. K.; Gharpure, S. J.; Mishra, A. K. *J. Phys. Chem. A* **2015**, *119*, 10481–10493.
- (26) Wei, Y.; Chen, W.; Zhao, X.; Ding, S.; Han, S.; Chen, L. *Polym. Chem.*, **2016**, *7*, 3983–3988.
- (27) Vamvounis, G.; Holdcroft, S. *Adv Mat.* **2004**, *16*, 716–719.
- (28) Ego, C.; Marsitzky, D.; Becker, S.; Zhang, J.; Grimsdale, A.C.; Müllen, K.; MacKenzie, J. D.; Silva, C.; Friend, R. H. *J. Am. Chem. Soc.* **2003**, *125*, 437–443.
- (29) Guoli Tu, G. et al. *Adv. Funct. Mater.* **2006**, *16*, 101–106.
- (30) Hou, X.; Ke, C.; Bruns, C. J.; McGonigal, P. R.; Pettman, R. B.; Stoddart, J. F. *Nat. Commun.* **2015**, *6*, 6884.
- (31) AlSalhi, M. S.; Alam, J.; Dass, L. A.; Raja, M. *Int. J. Mol. Sci.* **2011**, *12*, 2036–2054.
- (32) Chou, C. H.; Hsu, S. L.; Dinakaran, K.; Chiu, M. Y.; Wei, K. H. *Macromolecules* **2005**, *38*, 745–751.
- (33) Amrutha S. R.; Jayakannan M. *Macromolecules* **2007**, *40*, 2380–2391.
- (34) Chao Deng, Jun Ling, *Macromol. Rapid Commun.* **2016**, *37*, 1352–1356.
- (35) Basak, S.; Narayana, Y. S. L. V.; Baumgarten, M.; Müllen, K.; Chandrasekar, R. *Macromolecules* **2013**, *46*, 362–369.
- (36) Zhou, Q.; Zhang, J.; Ren, Z.; Yan, S.; Xie, P.; Zhang, R. *Macromol. Rapid Commun.* **2008**, *29*, 1259–1263.
- (37) Luo, J.; Li, X.; Hou, Q.; Peng, J.; Yang, W.; Cao, Y. *Adv. Mater.* **2007**, *19*, 1113–1117.
- (38) Tang, C. W.; VanSlyke, S. A. *Appl. Phys. Lett.* **1987**, *51*, 913–915.
- (39) Wong, M. Y.; Hedley, G. J.; Xie, G.; Kölln, L. S.; Samuel, I. D. W.; Pertegás, A.; Bolink, H. J.; Zysman-Colman, E. *Chem. Mater.* **2015**, *27*, 6535–6542.
- (40) Würthner, F.; Chen, Z.; Hoeben, F.J.; Osswald, P.; You, C. C.; Jonkheijm, P.; Herrikhuyzen, J. V.; Schenning, A. P.; van der Schoot, P. P.; Meijer, E. W.; Beckers, E. H.; Meskers, S. C.; Janssen, R. A. *J. Am. Chem. Soc.* **2004**, *126*, 10611–10618.

- (41) Marchioni, F.; Chiechi, R.; Patil, S.; Wudl, F.; Chen, Y.; Shinar, J. *Appl. Phys. Lett.* **2006**, *89*, 61101.
- (42) Wang, G.; Chang, X.; Peng, J.; Liu, K.; Zhao, K.; Yu, C.; Fang, Y. *Phys. Chem. Chem. Phys.*, **2015**, *17*, 5441–5449.
- (43) Wolfbeis O. S. *J. Mater. Chem.*, **2005**, *15*, 2657–2669.
- (44) Han, J.; Burgess, K. *Chem. Rev.* **2010**, *110*, 2709–2728.
- (45) Li, X.; Gao, X.; Shi, W.; Ma, H.; *Chem. Rev.* **2014**, *114*, 590–659.
- (46) Ni, X.-L.; Chen, S.; Yang, Y.; Tao, Z.; *J. Am. Chem. Soc.* **2016**, *138*, 6177–6183.
- (47) Zhang, X.; Rehm, S.; Safont-Sempere, M. M.; Würthner, F. *Nat. Chem.* **2009**, *1*, 623–629.
- (48) Pangkuan Chen. P.; Holten-Andersen N. *Adv. Optical Mater.* **2015**, *3*, 1041-1046.
- (49) Grimsdale, A. C.; Leok Chan, K.; Martin, R. E.; Jokisz, P. G.; Holmes, A. B. *Chem. Rev.* **2009**, *109*, 897–1091.
- (50) Müller, C. D.; Falcou, A.; Reckefuss, N.; Rojahn, M.; Wiederhirn, V.; Rudati, P.; Frohne, H.; Nuyken, O.; Becker, H.; Meerholz, K. *Nature* **2003**, *421*, 829–833.
- (51) Bu, J.; Watanabe, K.; Hayasaka, H.; Akagi, K. *Nat. Commun.* **2014**, *5*, 3799.
- (52) Li, C. H.; Hu, J. M.; Liu, S. Y. *Soft Matter* **2012**, *8*, 7096–7102.
- (53) Bae, S. H.; Yoo, S.; Bae, W. K.; Lee, S.; Lee, J.-K.; Sohn, B.-H.; *Chem. Mater.* **2008**, *20*, 4185–4187.
- (54) Wang, R.; Peng, J.; Qiu, F.; Yang, Y.; Xie, Z. *Chem. Commun.* **2009**, *44*, 6723–6725.
- (55) Li, J.-L.; Liu, X.-Y. *Adv. Funct. Mater.* **2010**, *20*, 3196-3216.
- (56) A.; Shiraki, T.; Haraguchi, S.; Tamaru, S.-i.; Shinkai, S. *Chem.-Asian J.* **2011**, *6*, 266-282.
- (57) Terech, P.; Weiss, R. G.; *Chem. Rev.* **1997**, *97*, 3133–3160.
- (58) Hirst, A. R.; Escuder, B.; Miravet, J. F.; Smith, D. K. *Angew. Chem., Int. Ed.* **2008**, *47*, 8002-8018.
- (59) Du, X.; Zhou, J.; Shi, J.; Xu, B. *Chem. Rev.* **2015**, *115*, 13165–13307.
- (60) Bairi, P.; Roy, B.; Chakraborty, P.; Nandi, A. K. *ACS Appl. Mater. Interfaces* **2013**, *5*, 5478-5485.
- (61) Babu, S. S.; Praveen, V. K.; Ajayaghosh, A.; *Chem. Rev.*, **2014**, *114*, 1973–2129.



- (62) Sukul, P. K.; Asthana, D.; Mukhopadhyay, P.; Summa, D.; Muccioli, L.; Zannoni, C.; Beljonne, D.; Rowan, A. E.; Malik, S. *Chem. Commun.* **2011**, *47*, 11858–11860.
- (63) Aparicio, F.; Cherumukkil, S.; Ajayaghosh, A.; Sanchez, L. *Langmuir* **2016**, *32*, 284–289.
- (64) Zhang, J.; Su, C.-Y. *Coord. Chem. Rev.*, **2013**, *257*, 1373–1408.
- (65) Peng, H.-S.; Chiu, D. T. *Chem. Soc. Rev.* **2015**, *44*, 4699–4722.
- (66) Reisch, A.; Klymchenko, A. S. *Small*. **2016**, *12*, 1968–1992.
- (67) Robin M. P.; O'Reilly, R. K. *PolymInt* **2015**; *64*: 174–182.
- (68) Fleischmann, C.; Lievenbrück, M.; Ritter, H. *Polymers* **2015**, *7*, 717–746.
- (69) Chen, D.; Zhan, J.; Zhang, M.; Zhang, J.; Tao, J.; Tang, D.; Shen, A.; Qiu, H.; Yin, S. *Polym. Chem.* **2015**, *6*, 25–29.
- (70) Peng, H.-Q.; Sun, C.-L.; Niu, L.-Y.; Chen, Y.-Z.; Wu, L.Z.; Tung, C.-H.; Yang, Q.-Z. *Adv. Fun. Mat.* **2016**, *26*, 5483–5489.
- (71) Vaidya, S. V.; Couzis, A.; Maldarelli, C. *Langmuir* **2015**, *31*, 3167–3179.
- (72) Lia, K.; Liu, B. *Chem. Soc. Rev.* **2014**, *43*, 6570–6597.
- (73) K. Landfester, *Angew. Chem., Int. Ed.* **2009**, *48*, 4488–4507.
- (74) Reisch, A.; Didier, P.; Richert, L.; Oncul, S.; Arntz, Y.; Mely, Y.; Klymchenko, S. *Nat. Commun.* **2014**, *5*, 4089.
- (75) Tuncel, D.; Demir, H. V. *Nanoscale* **2010**, *2*, 484–494.
- (76) Wu, C.; McNeill, J. *Langmuir* **2008**, *24*, 5855–5861.
- (77) Moon, J. H.; Deans, R.; Krueger, E.; Hancock, L. F. *Chem. Commun.* **2003**, 104–105.
- (78) Robin, M. P.; O'Reilly, R. K. *Chem. Sci.* **2014**, *5*, 2717–2723.
- (79) Adronov, A.; Robello, D. R.; Frechet, J. M. J. *J. Polym. Sci. Part A Polym. Chem.* **2001**, *39*, 1366–1373.
- (80) Wang, S.; Kim, G.; Lee, Y. E. K.; Hah, H. J.; Ethirajan, M.; Pandey, R. K.; Kopelman, R. *ACS Nano* **2012**, *6*, 6843–6851.
- (81) Tronc, F.; Li, M.; Lu, J.; Winnik, M. A.; Kaul, B. L.; Graciet, J. C. *J. Polym. Sci. Part A Polym. Chem.* **2003**, *41*, 766–778.
- (82) Wang, B.; Lu, J.; Liang, H.; Feng, H.; Hub, L. *Poly Int.* **2015**, *64*, 942–947.
- (83) Elsabahy, M.; Wooley, K. L. *Chem Soc Rev.* **2012**, *41*, 2545–2561.

- (84) Grazon, C.; Rieger, J.; Méallet-Renault, R.; Clavier, G.; Charleux, B. *Macromol. Rapid Commun.* **2011**, *32*, 699–705.
- (85) Grazon, C.; Rieger, J.; Méallet-Renault, R.; Charleux, B.; Clavier, G. *Macromolecules* **2013**, *46*, 5167–5176.
- (86) Tian, Z.; Shaller, D.; Li, A. D. Q.; Shaller, A. D.; Li, A. D. Q. *Chem. Commun.* **2009**, *2*, 180–182.
- (87) Arshady, R. *Colloid Polym. Sci.* **1992**, *270*, 717–732.
- (88) Li, G. L.; Möhwald, H.; Shchukin, D. G. *Chem. Soc. Rev.* **2013**, *42*, 3628–3646.
- (89) Kawaguchi, H.; *Prog. Polym. Sci.* **2000**, *25*, 1171–1210.
- (90) Nomura, M.; Tobita, H.; Suzuki, K. *Adv Polym Sci* **2005**, *175* (Chapter 1), 1–128.
- (91) Chen, J.; Zhang, P.; Fang, G.; Yi, P.; Yu, X.; Li, X. *J. Phys. Chem. B* **2011**, *115*, 3354–3362.
- (92) Robin, M. P.; Raymond, J. E.; O'Reilly, R. K. *Mater. Horiz.* **2015**, *2*, 54–59.
- (93) Chow, P. Y.; Gan, L. M. *Adv. Polym. Sci.* **2005**, *175*, 257–298.
- (94) Schork, F. J.; Luo, Y.; Smulders, W.; Russum, J. P.; Butt, A.; Fontenot, K. *Adv. Polym. Sci.* **2005**, *175*, 129–255.
- (95) Taniguchi, T.; Takeuchi, N.; Kobaru, S.; Nakahira, T. *J. Colloid Interface Sci.* **2008**, *327*, 58–62.
- (96) Joumaa, N.; Lansalot, M.; Theretz, A.; Elaissari, A.; Sukhanova, A.; Artemyev, M.; Nabiev, I.; Cohen, J. H. M. *Langmuir* **2006**, *22*, 1810–1816.
- (97) Yuan, H. G.; Kalfas, G.; Ray, W. H. *J. Macromol Sci, Rev. Macromol. Chem. Phys.* **1991**, *31*, 215–299.
- (98) Yamashita, N.; Konishi, N.; Tanaka, T.; Okubo, M. *Langmuir* **2012**, *28*, 12886–12892.
- (99) Beija, M.; Charreyre, M.-T.; Martinho, J. M. G. *Prog. Polym. Sci.* **2011**, *36*, 568–602.
- (100) Liu, Q.-H.; Liu, J.; Guo, J.-C.; Yan, X.-L.; Wang, D.-H.; Chen, L.; Yan, F.-Y.; Chen, L.-G. *J. Mater. Chem.* **2009**, *19*, 2018–2025.
- (101) Kawaguchi, S.; Ito, K. *Adv. Polym. Sci.* **2005**, *175*, 299–328.
- (102) Almog, Y.; Levy, M. *J. Polym. Sci. Part A Polym. Chem.* **1981**, *19*, 115–126.
- (103) Ober, C. K.; Lok, K. P.; Hair, M. L.; *J. Polym. Sci. Part A Polym. Chem.* **1985**, *23*, 103–108.
- (104) Gokmen, M. T.; Du Prez, F. E. *Prog. Polym. Sci.* **2012**, *37*, 365–405.

- (105) Paine, A. J. *Macromolecules* **1990**, *23*, 3109–3117.
- (106) Jayachandran, K. N. N.; Chatterji, P. R. *J. Macromol. Sci. Part C*. **2006**, *41*, 79–94.
- (107) Ober, C. K.; van Grunsven, F.; McGrath, M.; Hair, M. L. *Colloids and Surfaces* **1986**, *21*, 347–354.
- (108) Shen, S.; Sudol, E. D.; El-Aasser, M. S. *J. Polym. Sci., Part A Polym. Chem.* **1994**, *32*, 1087–1100.
- (109) Bamnolker, H.; Margel, S. *J. Polym. Sci., Part A Polym. Chem.* **1996**, *34*, 1857–1871.
- (110) Deslandes, Y.; Mitchell, D. F.; Paine, A. J. *Langmuir* **1993**, *9*, 1468–1472.
- (111) Horak, D.; Svec, F.; Frechet, J. M. J.; *J. Polym. Sci., Part A Polym. Chem.* **1995**, *33*, 2329–2338.
- (112) Bosma, G.; Pathmamanoharan, C.; de Hoog, E. H.; Kegel, W. K.; van Blaaderen, A.; Lekkerkerker, H. N. W. *J. Colloid Interface Sci.* **2002**, *245*, 292–300.
- (113) Tuncel, A.; Kahraman, R.; Piskin, E.; *J. Appl. Polym. Sci.* **1993**, *50*, 303–319.
- (114) Tseng, C. M.; Lu, Y. Y.; El-Aasser, M. S.; Vanderhoff, J. W.; *J. Polym. Sci., Part A Polym. Chem.* **1986**, *24*, 2995–3007.
- (115) Yang, W. L.; Yang, D.; Hu, J. H.; Wang, C. C.; Fu, S. K. *J. Polym. Sci., Part A Polym. Chem.* **2001**, *39*, 555–561.
- (116) Yang, W. L.; Hu, J. H.; Tao, Z. H.; Li, L.; Wang, C. C.; Fu, S. K. *Colloid Polym. Sci.* **1999**, *277*, 446–451.
- (117) Wang, D. N.; Dimonie, V. L.; Sudol, E. D.; El-Aasser, M. S. *J. Appl. Polym. Sci.* **2002**, *84*, 2710–2720.
- (118) Yamamoto, Y.; Okubo, M.; Iwasaki, Y. *Colloid Polym. Sci.* **1991**, *269*, 1126–1132.
- (119) Lok, K. P.; Ober, C. K. *Can. J. Chem.* **1985**, *63*, 209–216.
- (120) Song, J. S.; Winnik, M. A. *Macromolecules* **2005**, *38*, 8300–8307.
- (121) Song, J. S.; Tronc, F.; Winnik, M. A. *J. Am. Chem. Soc.* **2004**, *126*, 6562–6563.
- (122) Peng, B.; Van Der Wee, E.; Imhof, A.; Van Blaaderen, A. *Langmuir* **2012**, *28*, 6776–6785.
- (123) Xu, J.; Chi, Z. *RSC Smart Material*, (Chapter-1) **2014**, 1-263.
- (124) Yu, T.; Liu, L.; Xie, Z.; Ma, Y. *Sci. China Chem.* **2015**, *58*, 907–915
- (125) Kim, J.; Park, J.; Jin, S.-H.; Lee, T. S. *Polym. Chem.* **2015**, *6*, 5062–5069.

- (126) Kusano, H.; Hosaka, S.; Shiraishi, N.; Kawakami, S.; Sugioka, K.; Kitagawa, M.; Ichino, K.; Kobayashi, H. *Synth. Met.* **1997**, *91*, 337–339.
- (127) Tu, G.; Mei, C.; Zhou, Q.; Cheng, Y.; Geng, Y.; Wang, L.; Ma, D.; Jing, X.; Wang, F. *Adv. Funct. Mater.* **2006**, *16*, 101–106.
- (128) Wang, Y. Z.; Sun, R. G.; Meghdadi, F.; Leising, G.; Swager, T. M.; Epstein, A. J. *Synth. Met.* **1999**, *102*, 889–892.
- (129) Peng, H.Q.; Niu, L.-Y.; Chen, Y.-Z.; Wu, L.-Z.; Tung, C.H.; Yang, Q-Z. *Chem. Rev.* **2015**, *115*, 7502–7542.
- (130) Ghosh, S.; Praveen, V. K.; Ajayaghosh, A. *Annu. Rev. Mater. Res.* **2016**, *46*, 235–262.
- (131) Yoon, B.; Lee, J.; Park, I. S.; Jeon, S.; Lee, J.; Kim, J.-M. *J. Mater. Chem. C* **2013**, *1*, 2388–2403.
- (132) Maggini, L.; Bonifazi, D. *Chem. Soc. Rev.*, **2012**, *41*, 211–241.
- (133) Thirumalai, R.; Mukhopadhyay, R. D.; Preveen V. K.; Ajayagosh, A. *Sci. Rep.*, **2015**, *5*, 9842.
- (134) Ding, T.; Cao, G.; Schäfer, C. G.; Zhao, Q.; Gallei, M.; Smoukov, S. K.; Baumberg, J. *J. ACS Appl. Mater. Interfaces* **2015**, *7*, 13497–13502.
- (135) Bünzli, J.-C. G.; Piguet, C. *Chem. Soc. Rev.* **2005**, *34*, 1048–1077.
- (136) Chinen, A. B.; Guan, C. M.; Ferrer, J. R.; Barnaby, S. N.; Merkel, T. J.; Mirkin, C. A. *Chem. Rev.*, **2015**, *115*, 10530–10574.
- (137) Reisch, A.; Didier, P.; Richert, L.; Oncul, S.; Arntz, Y.; Mely, Y.; Klymchenko, A. S. *Nat. Commun.* **2014**, *5*, 4089.
- (138) Sánchez-Martín, R. M.; Alexander, L.; Bradley, M. In *Annals of the New York Academy of Sciences*, **2008**, *1130*, 207–217.
- (139) Scarmagnani, S.; Walsh, Z.; Slater, C.; Alhashimy, N.; Paull, B.; Macka, M.; Diamond, D. *J. Mater. Chem.* **2008**, *18*, 5063–5071.
- (140) Heck, T.; Pham, P.-H.; Hammes, F.; Thony-Meyer, L.; Michael Richter, M. *Bioconjugate Chem.* **2014**, *25*, 1492–1500.
- (141) Wilson, R.; Cossins, A. R.; Spiller, D. G.; *Angew. Chem. Int. Ed.* **2006**, *45*, 6104–6117.
- (142) Vaidya, S. V.; Gilchrist, M. L.; Maldarelli, C.; Couzis, A. *Anal. Chem.* **2007**, *79*, 8520–8530.

- (143) Potyrailo, R.; Mirsky, V. K. *Chem. Rev.* **2008**, *108*, 770–813.
- (144) Sukhanova, A.; Nabiev, I. *Crit. Rev. Oncol./Hematol.* **2008**, *68*, 39–59.
- (145) Battersby, B. J.; Lawrie, G. A.; Johnston, A. P. R.; Trau, M. *Chem. Commun.* **2002**, *14*, 1435–1441.
- (146) Dunbar, S. A.; Vander Zee, C. A.; Oliver, K. G.; Karem, K. L.; Jacobson, J. W. *J. of Microbio. Meth.* **2003**, *53*, 245–252.
- (147) Behrendt, J. M.; Nagel, D.; Chundoo, E.; Alexander, L. M.; Dupin, D.; Hine, A. V.; Bradley, M.; Sutherland, A. J. *PLoS One* **2013**, *8* e50713.
- (148) Wolfbeis, O. S. *Chem. Soc. Rev.* **2015**, *44*, 4743–4768.
- (149) Mailänder, V.; Landfester, K. *Biomacromolecules* **2009**, *10*, 2379–2400.
- (150) Ramirez, L.; Landfester, K. *Macromol. Chem. Phys.* **2003**, *206*, 2440–2449.
- (151) Sun, X.; Wang Y.; Lei, Y. *Chem. Soc. Rev.* **2015**, *44*, 8019–8061.
- (152) McQuade, D. T.; Pullen, A. E.; Swager, T. M. *Chem. Rev.* **2000**, *100*, 2537–2574.
- (153) Germain, M. E.; Knapp, M. J. *Chem. Soc. Rev.* **2009**, *38*, 2543–2555.
- (154) Salinas, Y.; Martínez-Mañez, R.; Marcos, M. D.; Sancenón, F.; Costero, A. M.; Parra, M.; Gil, S. *Chem. Soc. Rev.* **2012**, *41*, 1261–1296.
- (155) Yang, J.-S.; Swager, T. M. *J. Am. Chem. Soc.* **1998**, *120*, 11864–11873.
- (156) Guan, W.; Zhou, W.; Lu, J.; Lu, C. *Chem. Soc. Rev.* **2015**, *44*, 6981–7009.
- (157) Wang, X.; Wolfbeis, O. S. *Chem. Soc. Rev.* **2014**, *43*, 3666–3761.
- (158) LaFratta, C. N.; Walt, D. R. *Chem. Rev.* **2008**, *108*, 614–637.
- (159) Xu, X.; Miao, K.; Chen, Y.; Fan, L. J. *ACS Appl. Mater. Interfaces* **2015**, *7*, 7759–7766.
- (160) Lobnik, A.; Turel, M.; Urek, Š. *Adv. Chem. Sensors* **2012**, 1–28.
- (161) Breul, A. M.; Hager, M. D.; Schubert, U. S. *Chem. Soc. Rev.* **2013**, *42*, 5366–5407.
- (162) Martínez-Huitle, C. A.; Brillas, E. *Applied Catalysis B: Environmental.* **2009**, *87*, 105–145.
- (163) Chern, C. S.; Chen, T. J.; Liou, Y. C. *Polymer* **1998**, *39*, 3767–3777.
- (164) Weiss, C. K.; Landfester, L. *Adv. Polym. Sci.* **2010**, *233*, 185–236.
- (165) Würthner, F. *Chem. Commun.* **2004**, 1564–1579.
- (166) Würthner, F.; Saha-Möller, C. R.; Fimmel, B.; Ogi, S.; Leowanawat, P.; Schmidt, D. *Chemical Reviews.* **2016**, *116*, 962–1052.

- (167) Figueira-Duarte, T. M.; Mullen, K. *Chem. Rev.* **2011**, 111, 7260–7314.
- (168) Kanibolotsky, A. L.; Perepichka, I. F.; Skabara, P. J. *Chem. Soc. Rev.* **2010**, 39, 2695–2728.
- (169) Chen, Y.; Chen, H.; Zhang, H.; Fan, Li.-J. *ACS Appl. Mater. Interfaces*, **2015**, 7, 26709–26715.
- (170) Shanmugaraju, S.; Mukherjee, P. S. *Chem. Commun.* **2015**, 51, 16014–16032.
- (171) Winnik, F. M. *Chem. Rev.* **1993**, 93, 587–614.
- (172) Venkatramaiah, N.; Firmino, A. D. G.; Almeida Paz, F. A.; Tome, J. P. C. *Chem. Commun.* **2014**, 50, 9683–9686.
- (173) Liu, Y. D.; Quan, X. M.; Choi, H. J. *Colloid Polym. Sci.* **2012**, 290, 1703–1706.
- (174) Nisha, S. K.; Asha, S. K. *ACS Appl. Mater. Interfaces* **2014**, 6, 12457–12466.
- (175) Leng, Y.; Sun, K.; Chen, X.; Li, W. *Chem. Soc. Rev.* **2015**, 44, 5552–5595.
- (176) Haupt, K.; Linares, A. V.; Bompart, M.; Bui, B. T. S. *Top. Curr. Chem.* **2012**, 325, 1–28.
- (177) Polyakov, M. V. *Zhurnal Fizieskoj Khimii*, **1931**, 2, 799–805.
- (178) Takagishi, T.; Klotz, I. M. *Biopolymers* **1972**, 11, 483–491.
- (179) Wulff, G.; Sarhan, A. *Angew. Chem., Int. Ed.* **1972**, 11, 341–344.
- (180) Arshady, R.; Mosbach, K. *Macromol. Chem. Phys.* **1981**, 182, 687–692.
- (181) Spivak, D. A. *Advanced Drug Delivery Reviews* **2005**, 57, (12), 1779–1794
- (182) Mayes, A. G.; Whitcombe, M. J. *Advanced Drug Delivery Reviews*. **2005**, 57, 1742–1778.
- (183) Chen, L.; Xu, S.; Li, J. *Chem Soc Rev* **2011**, 40, 2922–2942.
- (184) Niu, M.; Pham-Huy, C.; He, H. *Microchimica Acta*, **2016**, 1–19.
- (185) Biffis, A.; Drakova, D.; Falcimaigne-Cordin, A. *Top. Curr. Chem.* **2012**, 325, 29–82.
- (186) Wang, J.; Cormack, P. A. G.; Sherrington, D. C.; Khoshdel, E. *Angew. Chemie Int. Ed.* **2003**, 42, 5336–5338.
- (187) Chen, W.; Ma, Y.; Pan, J.; Meng, Z.; Pan, G.; Sellergren, B. *Polymers*. **2015**, 7, 1689–1715.
- (188) Fang, L.; Chen, S.; Guo, X.; Zhang, Y.; Zhang, H. *Langmuir* **2012**, 28, 9767–9777.
- (189) Renkecz, T.; Mistlberger, G.; Pawlak, M.; Horváth, V.; Bakker, E. *ACS Appl. Mater. Interfaces* **2013**, 5, 8537–8545.

- (190) Vasapollo, G.; Sole, R. D.; Mergola, L.; Lazzoi, M. R.; Scardino, A.; Scorrano, S.; Mele, G. *Int. J. Mol. Sci.* **2011**, *12*, 5908–594.
- (191) Ye, L.; Yilmaz, E.; Yan, M.; Eds.; R. O.; Dekker, M. New York, 2005, Chapter 17, 435–454.
- (192) Piletsky, S.; Turner, A. P. F. *Optical Biosensors Present and Future* **2002**, 397–425.
- (193) Kandimalla, V. B.; Ju, H. *Analytical and Bioanalytical Chemistry*. **2004**, *380*, 587–605.
- (194) Schirhagl, R. *Anal. Chem.* **2014**, *86*, 250–261.
- (195) Ye, L.; Mosbach, K. *Chem. Mater.* **2008**, *20*, 859–868.
- (196) Jenkins, A. L.; Ellzy, M. W.; Buettner, L. C. *J. Mol. Recognit.* **2012**, *25*, 330–335.
- (197) Ge, Y.; Butler, B.; Mirza, F.; Habib-Ullah, S.; Fei, D. *Macromol. Rapid Commun.* **2013**, *34*, 903–915.
- (198) Zhao, W. F.; Fang, B. H.; Li, N.; Nie, S. Q.; Wei, Q.; Zhao, C. S. *J. Appl. Polym. Sci.* **2009**, *113*, 916–921.
- (199) Xu, S.; Lu, H.; Zheng, X.; Chen, L. *J. Mater. Chem. C* **2013**, *1*, 4406–4422.
- (200) Suriyanarayanan, S.; Cywinski, P. J.; Moro, A. J.; Mohr, G. J.; Kutner, W. *Top. Curr. Chem.* **2012**, *325*, 165–265.
- (201) Chen, L.; Wang, X.; Lu, W.; Wu, W.; Li, J. *Chem. Soc. Rev.*, **2016**, *45*, 2137–2211.
- (202) Lim, G. W.; Lim, J. K.; Ahmad, A. L.; Chan, D. J. C. *Anal. Bio. Chem.* **2016**, *408*, 2083–2093.
- (203) Wan, W.; Wagner, S.; Rurack, K. *Anal. Bioanal. Chem.* **2016**, *408*, 1753–1771.
- (204) Wan, W.; Biyikal, M.; Wagner, R.; Sellergren, B.; Rurack, K. *Angew. Chem. Int. Ed.* **2013**, *52*, 7023–7027.

-:- **Chapter 2** -:-

---

---

*Development of Fluorescent Polystyrene Microbeads with Controlled Particle Size, Tunable Colors, and High Solid State Emission*

---

---

**This chapter has been adapted from the following paper:**

“Sonawane, S. L.; Asha S. K. *ACS Appl. Mater. Interfaces*, **2013**, 5, 12205–12214

**DOI:** 10.1021/am404354q.





## 2.1 Abstract

A series of fluorescent Polystyrene (PS) microbeads with narrow size distribution and intense solid state emission was developed. Fluorophores based on perylenebisimide (**PBI**) and oligo (*p*-phenylenevinylene) (**OPV**) designed as acrylic cross-linkers were introduced into the polymerization recipe in a two-stage dispersion polymerization, carried out in ethanol in presence of polyvinylpyrrolidone (PVP) as stabilizer. The structural design permitted introduction of upto  $10^{-5}$  moles of the fluorophores into the polymerization medium without fouling of the dispersion. The particle size measured using dynamic light scattering (DLS) indicated that they were nearly monodisperse with size in the range 2-3  $\mu\text{m}$  depending on the amount of fluorophore incorporated. Fluorescence microscope images of ethanol dispersion of the sample exhibited intense orange red emission for **PS-PBI-X** series and green emission for **PS-OPV-X** series. A PS incorporated with both **OPVX** and **PBIX** exhibited dual emission upon exciting at the OPV wavelength of 350 nm and PBI wavelength of 490 nm respectively. The low incorporation of fluorophore resulted in almost complete absence of aggregation induced reduction in fluorescence as well as red shifted aggregate emission. The solid state emission quantum yield measured using integrating-sphere setup indicated very high quantum yield of  $\phi_{\text{powder}} = 0.71$  for **PS-OPV-X** and  $\phi_{\text{powder}} = 0.25$  for **PS-PBI-X** series. The PS microbeads incorporating both OPV and PBI chromophores had a  $\phi_{\text{powder}} = 0.33$  for PBI emission and  $\phi_{\text{powder}} = 0.20$  for OPV emission. This strategy of introducing fluorophore as cross-linkers into the PS backbone is very versatile and amenable to simultaneous addition of different suitably designed fluorophores emitting at different wavelengths.

## 2.2 Introduction

Fluorescent polymer beads find application in myriad areas like multicolor emission,<sup>1</sup> bar-coding,<sup>2</sup> photonic crystals,<sup>3</sup> self assembly study<sup>4</sup> and as a standard in the fluorescence techniques like flow cytometry,<sup>5</sup> cell sorting,<sup>6</sup> sensing and imaging etc.<sup>7-9</sup> Some of the important criteria for application of the fluorescent beads are monodispersity, non-leaching of the fluorophore, thermal and photo stability etc.<sup>10,11</sup> Although fluorescent microspheres are commercially available their prohibitive cost as well as limited choice of the emission colors makes it important to design efficient fluorescent microspheres with narrow size distribution and wide range of emission color using easily adaptable procedure in the laboratory as well as in the industry. Fluorescent polymer particles are generally synthesized by incorporation of the dye with the polymer composite, physical adsorption,<sup>12</sup> encapsulation of the dye in block copolymers by hydrophobic-hydrophilic interaction,<sup>13-15</sup> gradual solvent evaporation, controlled mixing<sup>17</sup> and so on.<sup>18,19</sup> However these methods often face the problem of the dye leakage causing background fluorescence interference. The fluorescent polymer particles can also be synthesized by post polymerization dispersion techniques. However, these systems require additional steps after polymerization and control over uniform emission and monodispersity of the polymer particle is also difficult. To overcome these problems, copolymerization with polymerizable fluorophore and covalently attaching the fluorophore to the polymer chains is a good means to prevent leakage and obtain strongly fluorescent polymer particle with uniform distribution of the fluorophore in the polymer backbone.<sup>20-22</sup> A polymerization methodology has also to be adopted which would allow for narrow size distribution of the fluorophore incorporated polymer.

Various polymerization techniques like suspension,<sup>23</sup> emulsion,<sup>24</sup> dispersion<sup>25,26</sup> etc are utilized to obtain narrow disperse polymer beads in size ranges varying from nanometer to micrometer depending on the size requirement for different applications. Among these methods, dispersion polymerization is a very attractive one for the large-scale preparation of monodisperse polymer beads in the 0.5-15 micrometer size range. The original dispersion polymerization method as developed in the early 1960 did not facilitate the incorporation of fluorophores, functional comonomers, cross-linkers etc.<sup>25</sup> In presence of these “extra” reagents the polymerization would lose control over particle size and especially with cross-linkers result in coagulation of the polymer. In the early 2000s, M. A. Winnik et. al. showed

that polymer beads with narrow size distribution could be achieved in the dispersion polymerization method by delayed introduction of the cross-linker after the nucleation stage, which they named as the “two-stage” dispersion polymerization.<sup>27,28</sup> Using this procedure they demonstrated the successful incorporation of upto 3 mol % of the cross-linker divinyl benzene (DVB) into PS and still obtained nearly monodisperse particles.

In this chapter we present the incorporation of fluorescent cross-linkers into commercially available polymer like that of polystyrene (PS), adopting a two-stage dispersion polymerization route to produce highly fluorescent monodisperse PS beads. Among various commercially available polymers, polystyrene affords good control over the particle size and fluorescently labeled PS beads are compatible as cell markers for tracing both in vivo and in vitro.<sup>8</sup> Among stable organic fluorophores which have high quantum efficiency, perylene 3,4,9,10-tetracarboxylic diimide (**PBI**) and oligo (*p*-phenylenevinylene) (**OPV**) are some of the most preferred due to their strong absorption and fluorescence quantum yield combined with outstanding chemical, thermal and photochemical stability.<sup>29-32</sup> We report new cross-linkers based on perylene 3, 4, 9, 10-tetracarboxylic diimide (**PBI**) and oligo (*p*-phenylenevinylene) (**OPV**) known for their high quantum efficiency, which were made more compatible with the dispersion polymerization recipe by the introduction of flexible groups like tetraethylene glycol or branched alkoxy units. The fluorescent polystyrene beads were analyzed using microscopic techniques like fluorescence microscopy, scanning electron microscopy (SEM) and transmission electron microscopy (TEM). Photophysical characterization was carried out using absorption and fluorescence spectroscopic techniques. Using this methodology of fluorophore as the cross-linker it was observed that as less as  $10^{-7}$  moles of the fluorophore was sufficient to obtain highly fluorescent polystyrene beads which retained their high emission in the solid powder state ( $\phi_{\text{powder}} = 0.71\%$ ) also. The specific issues that are highlighted in this work are,

- (a) An easy and scalable route towards thermally stable Fluorescent Monodisperse Polymer beads, where the fluorophore is covalently incorporated in the polymer backbone, thereby avoiding fluorophore leakage.
- (b) These polymer beads are strongly emitting in the solid state also and have tunable emission colors.

- (c) The tunability of the emission colors with more than one color from the same polymer particle makes it very convenient to use for labeling studies where one can access different emission regions just by exciting at the appropriate wavelength without having to label with different fluorophores.
- (d) The versatility of the method allows for extending the approach to other commercially important polymers like PMMA also.

## 2.3 Experimental methods

**2.3.1 Materials:** Perylene-3, 4, 9, 10-tetracarboxylic dianhydride (PTCDA), 3-pentadecyl phenol, zinc acetate, imidazole, polyvinylpyrrolidone (PVP, Mw 360,000 g/mol), acrylic acid, 4-methoxyphenol, 2-ethylhexylbromide, triethylphosphite, 4-hydroxy benzaldehyde and potassium-tert-butoxide were purchased from Aldrich and used without further purifications. Styrene (Aldrich) was washed with sodium hydroxide followed by water, dried overnight using calcium chloride and vacuum distilled before use. HBr in glacial acetic acid, para-formaldehyde, potassium carbonate, potassium iodide, dimethyl sulfoxide, dimethyl formamide (DMF), tetrahydrofuran (THF), dichloromethane (DCM), and 2-chloroethanol were purchased from Merck and purified using standard procedures. Triton X-100 (70% solution in water) and 2, 2'-azobis-(isobutyronitrile) (AIBN) were purchased from Merck and the latter was recrystallised from Methanol.

### 2.3.2 Instrumentation

$^1\text{H}$  and  $^{13}\text{C}$  NMR spectra were recorded in  $\text{CDCl}_3$  using Bruker AVENS 200 MHz spectrophotometer. Chemical shifts ( $\delta$ ) are reported in ppm at 298 K, with trace amount of tetramethylsilane (TMS) as internal standard. MALDI-TOF analysis was carried out on a Voyager-De-STR MALDI-TOF (Applied Biosystems, Framingham, MA, USA) instrument equipped with 337 nm pulsed nitrogen laser used for desorption and ionization. The mode of operation was in a reflector mode with an accelerating voltage of 25 kV. Micromolar solutions of the compounds in THF were mixed with Dithranol matrix and spotted on stainless steel MALDI plate and dried well. Size exclusion chromatography (SEC) in chloroform was done using polystyrene standards for calibration using a polymer lab PL-220 GPC instrument. The flow rate of the chloroform was maintained as 1 mL throughout the

experiments, and 2-3 mg in 1 mL of the samples were filtered and injected for recording the chromatograms at 30 °C. Thermogravimetric analysis (TGA) was performed using a PerkinElmer STA 6000 thermogravimetric analyser. Samples were run from 40 to 800 °C with a heating rate of 10 °C/min under nitrogen. Absorption spectra were recorded using Perkin-Elmer Lambda 35 UV-spectrophotometer. Steady-state fluorescence studies were performed using Horiba Jobin Yvon Fluorolog 3 spectrophotometer having a 450 W xenon lamp. The emission and excitation slit width was maintained at 1 nm throughout the experiments, and the data was obtained in “S1/R1” mode (to account for the variations in lamp intensity). The solid state quantum yield was measured using a Model F-3029, Quanta-Phi 6" Integrating Sphere connected with a Horiba Jobin Yvon Fluorolog 3 spectrophotometer. FEI, QUANTA 200 3D Scanning Electron Microscope with tungsten filament as electron source was used for recording SEM images. 1 mg of polymer dispersed in 2 mL of ethanol was drop cast on silicon wafers and the solvent was allowed to evaporate at room temperature in air for 12 hours. Before recording the morphology, films were coated by 5 nm thick gold film by sputtering method. Transmission Electron microscopy (TEM) was done using an FEI-Tecnai™-F20 electron microscope operating at 200 kV. 0.5 mg of polymer dispersed in 2 mL of ethanol was deposited directly on carbon coated copper grid and the solvent was allowed to evaporate at room temperature in air for 12 hours. DLS measurements were carried out on Zetasizer ZS 90 apparatus, utilizing 633 nm red laser (at 90 ° angle) from Malvern instruments. The reproducibility of the data was checked at least three times using freshly prepared independent polymer solutions. The fluorescence microscopic images were taken by Epi-fluorescence microscope Leitz Labor Lux, Germany and images were observed by a cannon power shot S-80 camera. (Excitation wavelength: 488–520 nm, green filter for OPV, and 550-550 nm, red filter for PBI). For sample preparation, very dilute dispersion of polymers in ethanol was drop cast on to glass plate, covered with cover slip and directly observed under fluorescence microscope.

### 2.3.3 General procedures

#### (i) Synthesis of PBI-PDP-Diol:

The symmetric PDP substituted perylenebismide derivative (PBI-PDP-diol) was synthesized by earlier report.<sup>33</sup> In detail, single neck round bottom flask having perylenetetracarboxylic

dianhydride 4.1 gm (0.0104 mol; 1 equiv) was heated with 4-amino-3-pentadecylphenol 7.2 gm, (0.023 mol, 2.15 equiv) and Zn (OAc)<sub>2</sub>, 0.15 gm in imidazole 60 gm, at 160 °C under nitrogen atmosphere for 6 h. The reaction mixture was then cooled to room temperature and precipitated by adding 2 N HCl and washed with deionized water (1 L). The crude product was purified by dissolving in a minimum amount of THF and precipitating into methanol. The methanol washing was continued until the washings were clear and finally washed with hexane. The purified dark red solid was dried in a vacuum oven at 80 °C for 10 h. Yield = 8.4 gm (74.3 %); m.p.>400 °C; <sup>1</sup>H NMR (CDCl<sub>3</sub>+TFA): δ=8.91 (s, 8 H; perylene), 6.89–7.16 (m, 6 H; Ar-H-PDP), 2.39 (t, 4 H; Ar-CH<sub>2</sub>), 1.53 (t, 4 H; Ar-CH<sub>2</sub>-CH<sub>2</sub>), 1.0–1.4 (br, 48 H; aliphatic CH<sub>2</sub>), 0.84 ppm (t, 6 H; terminal CH<sub>3</sub>); <sup>13</sup>C NMR: δ=166.27, 163.21, 162.65, 160.62, 155.86, 143.08, 136.66, 134.16, 130.32, 127.00, 126.14, 124.92, 123.12, 122.59, 115.03, 111.82, 106.19, 32.17, 31.28, 29.92, 29.60, 22.85, 13.81 ppm; FTIR: ν =3359 (ν(OH<sub>stretch</sub>)), 2922, 2853, 1698 (ν(C=O<sub>imide</sub>)), 1656, 1592, 1498, 1403, 1360, 1348, 1300, 1250, 1231, 1198, 1176, 967, 862, 813, 796, 750 cm<sup>-1</sup>; MALDI-TOF (dithranol matrix): *m/z* calcd for C<sub>66</sub>H<sub>78</sub>N<sub>2</sub>O<sub>6</sub>: 995.34; found: 996.65 [M+1], 1018.58 [M+Na].

### (ii) Synthesis of PBI-PDP-TEG Diol:

In a two necked round bottom flask attached with reflux condenser, PBI-PDP-Diol 3.5 gm, (0.0035 mol), KI (0.02 gm) and 4.88 gm, (0.035 mol) K<sub>2</sub>CO<sub>3</sub> were taken along with 150 mL of dry DMF under N<sub>2</sub> atmosphere. The reaction mixture was refluxed for one hour and then brought to room temperature (25 °C). 2.8 gm (0.0073 mol) of TEG-monotosylate in DMF was added over a period of thirty minutes at 0 °C to the above reaction mixture. The reaction mixture was stirred for 1.5 hours at 0-5 °C, following which it was refluxed for 48 hrs at 85-90 °C. The reaction was monitored by TLC. For workup, the reaction mixture was cooled to 25 °C and poured into 20 % HCl solution. The precipitate was filtered, washed with water and dried under vacuum at 75 °C for 12 hours. The compound was purified by column chromatography in DCM/methanol (5 %) as solvent. Yield = 3.7 gm (58 %). <sup>1</sup>H NMR (200 MHz, CDCl<sub>3</sub>, δ ppm): 8.8-8.7 (m, 8H, perylene ring), 7.13 (dd, 2H, Ar-PDP), 6.96 (m, 4H, Ar-PDP), 4.55 (t, 4H, Ar-OCH<sub>2</sub>), 4.21 (t, 4H, Ar-OCH<sub>2</sub>), 3.92-3.75 (bm, 24H), 2.37 (t, 4H), 1.51 (m, 4H), 1.08-1.19 (m, 48H, alkyl chain), 0.84 (t, 6H). MALDI-TOF MS (Dithranol

matrix):  $m/z$  calcd for  $C_{82}H_{110}N_2O_{14}$  : 1346.80; found 1346.60+23  $[M+Na^+]$  1346.60  $[M+K^+]$ .

### (iii) Synthesis of PBIX:

In a 250 mL two necked round bottom flask, 1.00 gm (0.00075 mol) of PBI-PDP-TEG diol,  $Et_3N$  (0.4 ml; 0.0037 mol), and dry DCM (80 ml) were taken under nitrogen atmosphere and stirred well at 0 °C for half hour. Acryloyl chloride (0.3 ml, (0.037 mol) in DCM was added to the reaction mixture over a period of 15-20 minutes at 0 °C. Reaction was carried out for 24 hours at room temperature and monitored by TLC. For workup, the organic layer was washed with water and brine and extracted into DCM. The compound was purified by column chromatography in DCM/methanol (5%) as solvent. Yield = 0.7 gm (70%).  $^1H$  NMR (200 MHz,  $CDCl_3$ ,  $\delta$ ppm ): 8.72 (m, 8H, Perylene ring), 7.11 (dd, 2H, Ar-PDP), 6.98 (m, 4H, Ar-PDP), 6.38 (dd, 2H, acrylic double bond), 6.17 (q, 2H, acrylic double bond), 5.85 (dd, 2H, acrylic double bond), 4.33 (t, 4H, Ar-OCH<sub>2</sub>), 4.20 (t, 4H, Ar-OCH<sub>2</sub>), 3.89-3.74 (bm, 24H), 2.4 (t, 4H), 1.51 (m, 4H), 1.08-1.19 (m, 48H, alkyl chain), 0.84 (t, 6H).  $^{13}C$  NMR (400 MHz,  $CDCl_3$ ) 166.1, 163.58, 159.1, 141.5, 134.8, 131.8, 131.0, 129.6, 128.2, 126.5, 123.4, 123.2, 116.0, 112.6, 70.8, 70.6, 69.1 67.4, 63.7, 31.8, 29.6, 29.5, 29.3, 27.2, 22.6, 14.1. MALDI-TOF MS (Dithranol matrix):  $m/z$  calcd for  $C_{40}H_{42}N_2O_4$ : 1456.8; found 1479+23  $[M+Na^+]$ , 1479+23+39  $[M+Na^+ K^+]$ , 1478+39+39  $[M+2K^+]$ .

### (iv) Synthesis of OPV cross-linker:

The symmetric OPV diol was synthesized as reported in literature.<sup>34</sup> In a 250 mL two necked round bottom flask, 1.1 gm (0.00196 mol) of OPV Diol was taken along with  $Et_3N$  (1 ml; 0.0078 mol) and dry DCM (80 ml) under nitrogen atmosphere and stirred well at 0 °C for half an hour. Acryloyl chloride (0.64 ml; 0.078 mol) in DCM was added to the reaction mixture for a period of 15-20 min at 0 °C. The reaction was carried out for 24 hours at room temperature and monitored by TLC. For workup, the organic layer was evaporated and the compound was purified by column chromatography in 20 % ethyl acetate /pet ether solvent combination. Yield = 0.45 gm (41%)  $^1H$  NMR (200 MHz,  $CDCl_3$ ,  $\delta$ ppm): 7.46-6.92 (3m, 14H, Ar-H, and vinylic H), 6.41 (dd, 2H, acrylic double bond), 6.18 (m, 2H, acrylic double bond), 5.89 (dd, 2H, acrylic double bond), 4.52 (m, 2H, ArOCH<sub>2</sub>), 4.23 (m, 2H, C(O)OCH<sub>2</sub>), 3.90 (s, 3H, ArOCH<sub>3</sub>) 3.90 (d, 2H, ArOCH<sub>2</sub>), 1.70-1.37 (m, 9H, alkyl protons), 0.97-0.90 (t,



6H).  $^{13}\text{C}$  NMR (400 MHz,  $\text{CDCl}_3$ ) 165.8, 157.7, 151.0, 150.9, 131.0, 127.8, 127.5, 127.4, 126.4, 121.2, 114.6, 109.9, 108.7, 71.5, 65.7, 62.6, 56.1, 39.5, 30.6, 29.0, 23.9, 22.8, 13.8, 11.0 MALDI-TOF MS (Dithranol matrix): m/z calcd for  $\text{C}_{41}\text{H}_{48}\text{O}_8$ : 668.8; found 668.5 [ $\text{M}^+$ ].

**(v) Two stage Dispersion Polymerization procedure to prepare PS-PBI/OPV-X:**

The stabilizer (PVP), costabilizer (Triton X-305), initiator (AIBN) and half of the styrene monomer and ethanol were added to a 250 mL three necked reaction flask equipped with a gas inlet, overhead stirrer and rubber septum. After a homogeneous solution formed at room temperature, the solution was deoxygenated by bubbling nitrogen gas at room temperature for at least 30 minutes. Then the flask was placed in a 70 °C oil bath and stirred mechanically at 120 rpm. The cross-linker (**PBIX/OPVX**) was dissolved in the remaining styrene and ethanol at 60 °C under nitrogen. After the cross-linker had dissolved and the polymerization reaction had run for 1 hour, the hot Styrene- cross-linker solution was added into the reaction flask over a period of 3 hours (drop by drop addition). The reaction was continued for 4 hours under continuous flow of nitrogen with overhead stirring. The precipitated polymer in the reaction medium was washed with 200 ml x 4 times of methanol and separated by centrifuge. The polymer was dried under vacuum at 50 °C for 6 hours. The polymerization content is given in table 2.1.

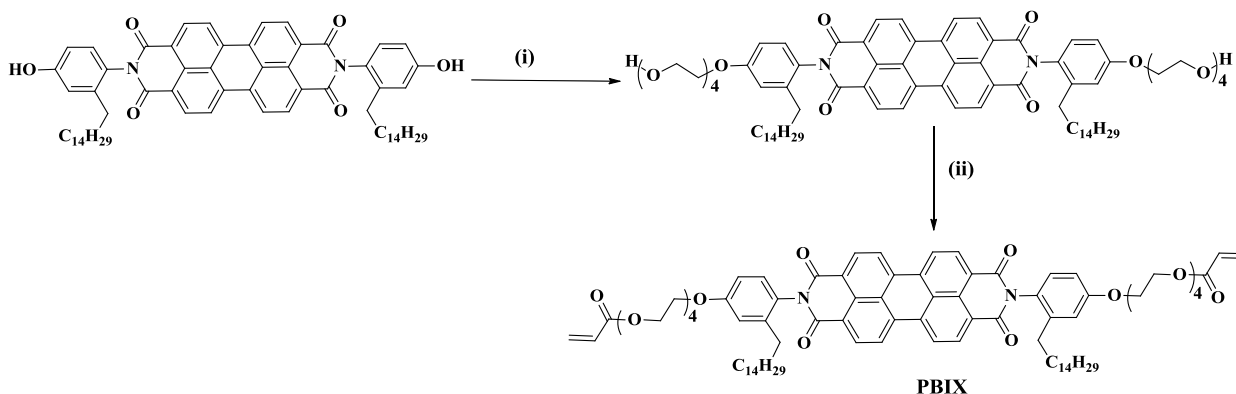
**(vi) Two stage Dispersion Polymerization for the preparation of PMMA-PBI-X-OPV-X:**

In a 250 mL three necked reaction flask equipped with a gas inlet, overhead stirrer and rubber septum, stabilizer (PVP), costabilizer (Triton X-305), initiator (AIBN) and half of the methyl methacrylate (MMA) monomer and ethanol were added. After a homogeneous solution formed at room temperature, the solution was deoxygenated by bubbling nitrogen gas at room temperature for at least 30 minutes. Then the flask was placed in a 70 °C oil bath and stirred mechanically at 120 rpm. The cross-linker (PBI-X/OPV-X) was dissolved in the remaining methyl methacrylate and ethanol at 60 °C under nitrogen. After the cross-linker had dissolved and the polymerization reaction had run for 1 hour, the hot MMA and cross-linker solution was added into the reaction flask over a period of 3 hours (drop by drop addition). The reaction was continued for 4 hours under continuous flow of nitrogen with overhead stirring. The precipitated polymer in the reaction medium was washed with 200 ml x 4 times of methanol and separated by centrifuge. The polymer was dried under vacuum at 50 °C for 6 hours.

## 2.4 Results and Discussion

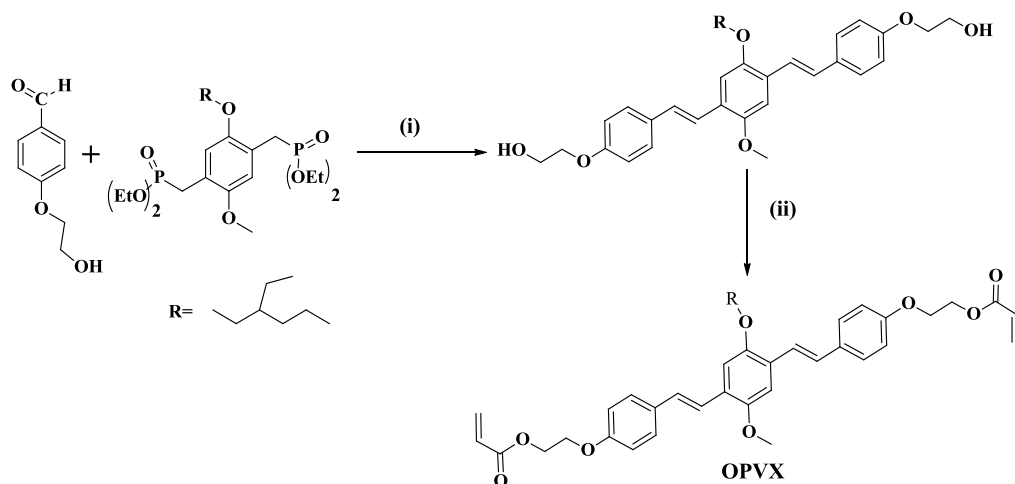
### 2.4.1 Synthesis and characterization

The synthesis of the fluorescent cross-linkers based on perylenebisimide (**PBIX**) and oligo (*p*-phenylenevinylene) (**OPVX**) is shown in **scheme 2.1** and **2.2** respectively. **PBIX** was synthesized starting with the imidization of perylenetetracarboxylic anhydride with 4-amino-3-pentadecyl phenol. The details of the synthesis to obtain the final acryloyl functionalized cross-linker is given in the experimental section. In a similar manner the hydroxyl functionalized OPV molecule was coupled with acryloyl chloride to obtain the **OPVX** cross-linker.



**Scheme 2.1:** Synthesis of Perylenebisimide based cross-linker (**PBIX**).

**Reagents:** (i) TEG-Monotosylate,  $K_2CO_3$ , DMF, 0–25–90 °C, 48 hours,  $N_2$ . (ii) Acryloyl Chloride, DCM,  $Et_3N$ , 0–25 °C, 24 hours,  $N_2$ .



**Scheme 2.2:** Synthesis of Oligo (*p*-phenylenevinylene) based cross-linker (**OPVX**).

Reagents (i) K-t-OBu, THF, 0-25 °C, 24 hours (ii) Acryloyl Chloride, DCM, Et<sub>3</sub>N, 25 °C, 24 hours, N<sub>2</sub>.

The structure and purity of the cross-linkers were confirmed by <sup>1</sup>H NMR (figure 2.1 for PBI-Diol, figure-2.2 for PBIX and figure 2.3 for OPVX), MALDI (figure 2.4, a and b) and also by the single peak in the SEC chromatogram (figure 2.5, a and b).

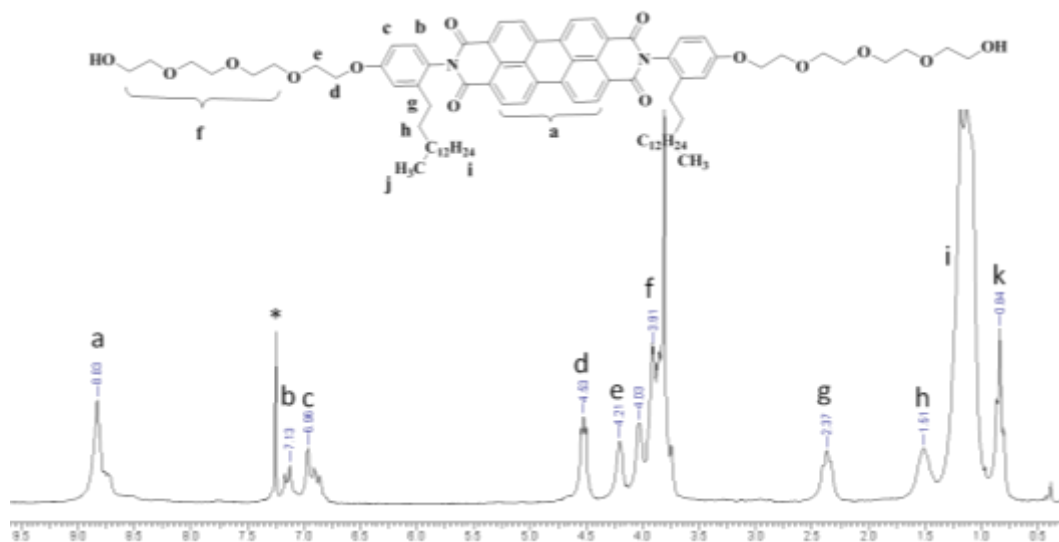


**Figure 2.1:** <sup>1</sup>H NMR spectrum of **PBI-PDP-TEG-Diol** recorded in CDCl<sub>3</sub>

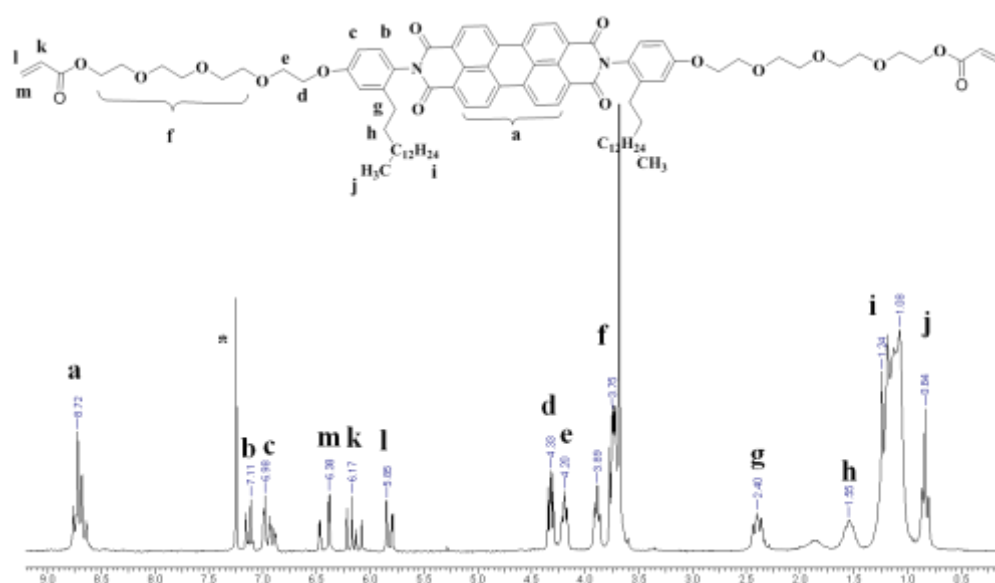


**Figure 2.2:** <sup>1</sup>H NMR spectrum of **PBI** cross-linker recorded in CDCl<sub>3</sub>

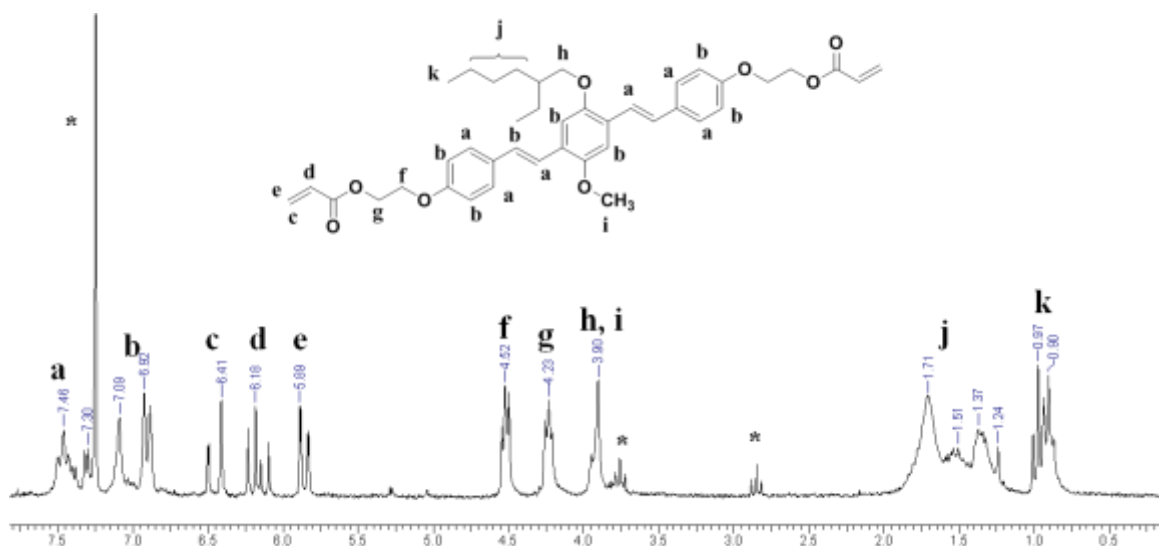


Figure 2.3:  $^1\text{H}$  NMR spectrum of OPV cross-linker recorded in  $\text{CDCl}_3$ .

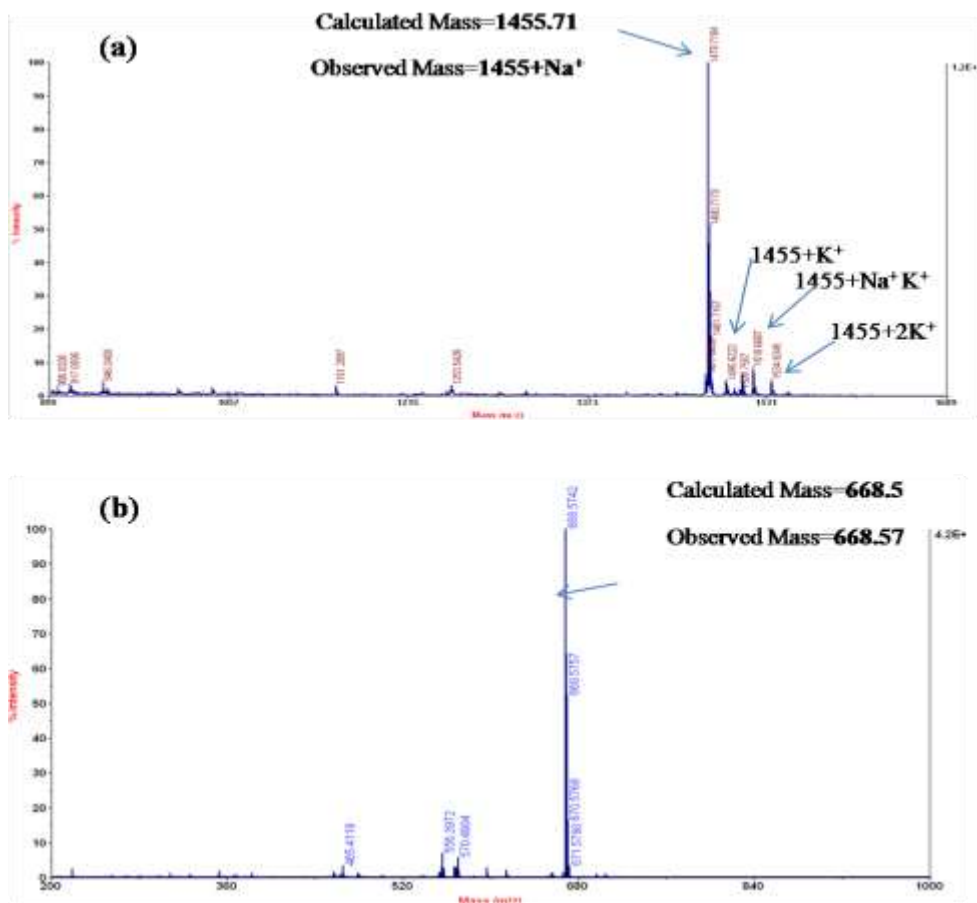
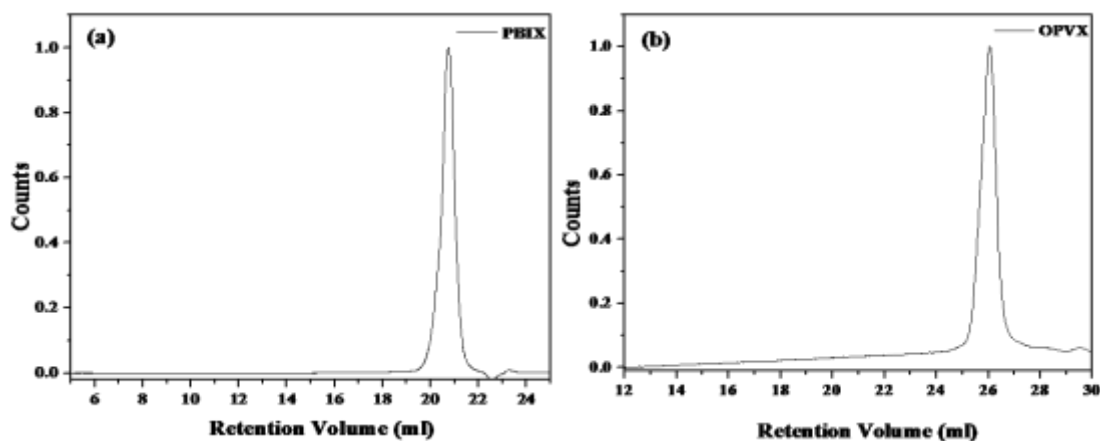


Figure 2.4: MALDI-TOF spectra of (a) PBIX and (b) OPVX.



**Figure 2.5:** Size exclusion chromatography of cross-linker (a) **PBIX** and (b) **OPVX**.

The MALDI spectra of **PBIX** showed peaks at higher mass corresponding to single as well as multiple sodium and potassium adducts which could be attributed to the alkali metal ion coordination with the ethylene glycol segments on the **PBIX** backbone. The two-stage dispersion polymerization recipe to incorporate the fluorescent cross-linkers **PBIX** and **OPVX** into PS backbone is given in table below.

**Table 2.1:** Dispersion polymerization method.

Component	Material	Amount (gm)	
		1 <sup>st</sup> Stage	2 <sup>nd</sup> Stage
Monomer	Styrene	1.89	1.89
Cross-linker	PBI/OPV	No	2.5 to 20
Medium	Ethanol	7.4	7.4
Stabilizer	PVP	0.25	No
Costabilizer	Triton X-100	0.08	No
Initiator	AIBN	0.060	No
Reaction time	8 hours	-	-
Rotation Speed	120 rpm	-	-

Varying amounts of the cross-linker (5 – 20 mg; 3.4 to 14  $\mu\text{M}$ ) (0.13 to 0.51 wt % w.r.t. styrene) were taken in the feed to obtain a series of lightly cross-linked polystyrene. One PS was synthesized using both **PBIX** and **OPVX**  $\sim 3.0 \times 10^{-6}$  mols each. The highest amount of the cross-linker that could be added in the feed during the second stage without the dispersion crashing out was 14  $\mu\text{M}$ . The actual incorporation of the PBI as well as OPV

based cross-linker into the PS backbone was determined using Beer-Lamberts Law using the molar extinction coefficient of the respective cross-linker (**PBIX** = 62082 L. M<sup>-1</sup>. cm<sup>-1</sup>, **OPVX** = 36315 L. M<sup>-1</sup>. cm<sup>-1</sup>).<sup>35,36</sup> The PS with **PBIX** and **OPVX** were named as the **PS-PBI-X** and **PS-OPV-X** series respectively, where 'x' indicated the amount (in μM) of the respective cross-linker incorporated. **Table-1** gives the fluorophore incorporation determined from UV-Vis studies.

**Table 2.2:** Sample designation, number and weight average molar mass, polydispersity indices (PDI), yield and 5 Wt % loss temperature of the **PS/PBI/OPV** based polymers.

Sr No	Sample Name	Moles in feed	Moles of Cross-linker <sup>a</sup>	Yield (%)	M <sub>n</sub> <sup>b</sup>	M <sub>w</sub> <sup>b</sup>	PDI	TGA <sup>c</sup> (T <sub>d</sub> =5%)
1	PS-PBI-0.16	3.4x10 <sup>-6</sup>	1.6x10 <sup>-7</sup>	80	40,000	99,900	2.5	345
2	PS-PBI-1.0	6.8x10 <sup>-6</sup>	1x10 <sup>-6</sup>	78	24,800	91,600	3.7	345
3	PS-PBI-2.7	1x10 <sup>-5</sup>	2.7x10 <sup>-6</sup>	76	37,900	154,000	4.0	345
4	PS-PBI-3.8	1.4x10 <sup>-5</sup>	3.8x10 <sup>-6</sup>	75	32,400	149,000	4.6	345
5	PS-OPV-0.38	3.7x10 <sup>-6</sup>	3.8x10 <sup>-7</sup>	80	24,900	99,000	4.0	340
6	PS-OPV-1.8	7.5x10 <sup>-6</sup>	1.8x10 <sup>-6</sup>	82	34,700	18,0000	5.1	340
7	PS-OPV-2.9	1.5x10 <sup>-5</sup>	2.9x10 <sup>-6</sup>	86	17,600	670,000	4.4	340
8	PS-OPV-5.12	2.2x10 <sup>-5</sup>	5.12x10 <sup>-6</sup>	85	19,400	63,000	3.5	340
9	PS-PBI-0.82- OPV-0.88	3.4x10 <sup>-6</sup> 3.7x10 <sup>-6</sup>	8.2x10 <sup>-7</sup> 8.8x10 <sup>-7</sup>	80	21,000	78,300	3.7	340
10	PS	-	-	90	40,200	1,24,800	3.1	320
11	PS-DVB (Insoluble)	-	-	78	-	-	-	340

- Incorporation from UV and measured in chloroform
- Measured by size exclusion chromatography (SEC) in chloroform (CHCl<sub>3</sub>), calibrated with linear, narrow molecular weight distribution polystyrene standards.
- TGA measurements at heating rate of 10 °C/ min under nitrogen.

The PS remained completely soluble for the highest cross-linker incorporation also (~5 μM).

The complete solubility of these polystyrene samples in common organic solvents enabled

the structural characterization using proton NMR spectroscopy, UV-Vis absorption spectroscopy as well as molecular weight determination using size exclusion chromatogram (SEC).

**Figure 2.6** shows the labeled proton NMR spectra of the perylenebisimide cross-linker **PBIX** along with the polystyrene with 3.8  $\mu\text{M}$  PBI incorporation **PS-PBI-3.8**. The eight aromatic protons of the perylene ring at 8.72 ppm matched very well in intensity with the six protons of the acrylic double bond in the region 5.8 to 6.48 ppm for **PBIX**. The inset in the top spectra shows the perylene aromatic protons which had become broad after incorporation in the polystyrene.

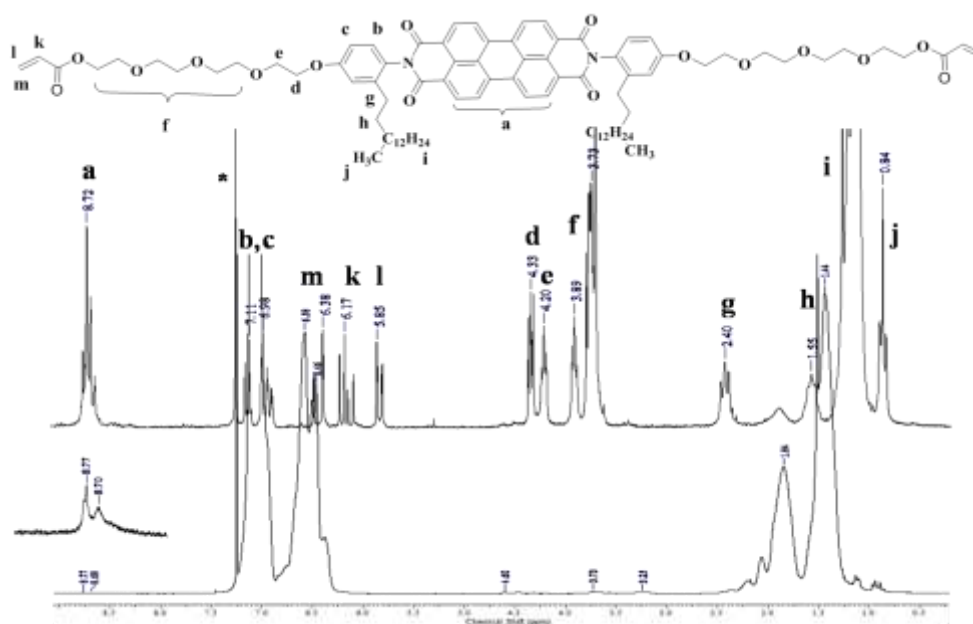


**Figure 2.6:** Comparison of the  $^1\text{H}$  NMR spectra of **PS-PBI-3.8** polymer with **PBIX** recorded in  $\text{CDCl}_3$ .

The aromatic protons of the PDP ring were merged with the aromatic peaks of PS. In the case of the **PS-OPV-X**, the aromatic protons of the OPV were completely overlapped by the aromatic protons of PS thereby making it difficult to observe the peaks corresponding to the **OPVX** in the polymer. The proton NMR spectra of **PS-PBI-0.82-OPV-0.88** having both perylenebisimide and oligo (*p*-phenylenevinylene) incorporation is given above in **Figure 2.7**.

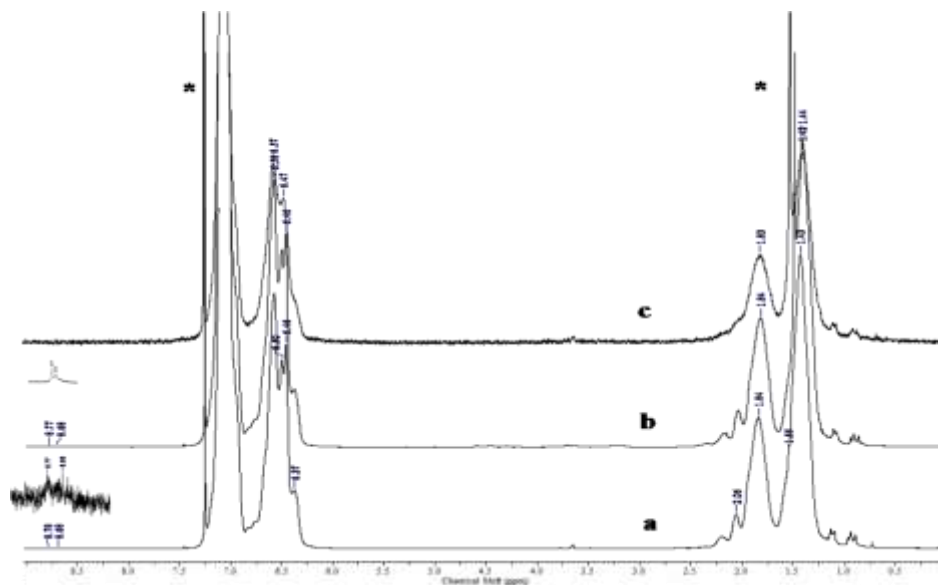


**Figure 2.7:**  $^1\text{H}$  NMR spectra of (a) PS-PBI-0.82-OPV-0.88 (b) PS-PBI-0.16 and (c) PS-OPV-0.38 recorded in  $\text{CDCl}_3$ .

#### 2.4.2 Molecular weight determination and Thermal properties of polymers

The molecular weight of the cross-linked PS was determined by SEC using chloroform as the eluent. The GPC chromatogram is given in the **figure 2.8**.

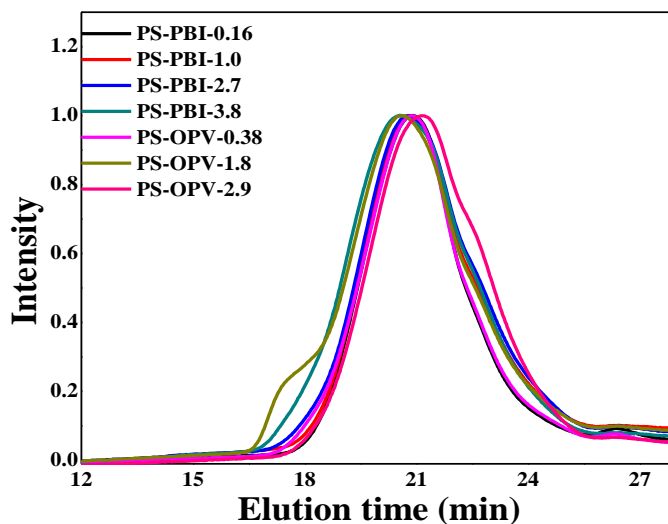


**Figure 2.8:** The size exclusion chromatography of polymers.



Higher incorporation of the rigid cross-linker resulted in considerable reduction in the  $M_w$  values especially in the case of **PS-OPV-X** polymers. **Table-2** gives the molecular weight determined by SEC along with that of PS alone prepared under identical conditions. The **PS-PBI/OPV-X** series of polymers had higher thermal stability compared to PS as determined by the thermogravimetric analysis. PS had a 5 weight % loss at 320 °C, while the **PS-PBI/OPV-X** polymers exhibited 5 weight % loss at a much higher temperature of 340-345 °C. A 3 mol % divinylbenzene (DVB) cross-linked PS prepared by the two stage dispersion polymerization under identical conditions also exhibited a 5 weight % loss temperature of 340 °C. The light cross-linking brought in by the rigid fluorescent cross-linker increased the thermal stability of the polymers.<sup>37</sup> Table 2 lists the 5 weight % loss temperature and below **Figure 2.9** gives the TGA plot.

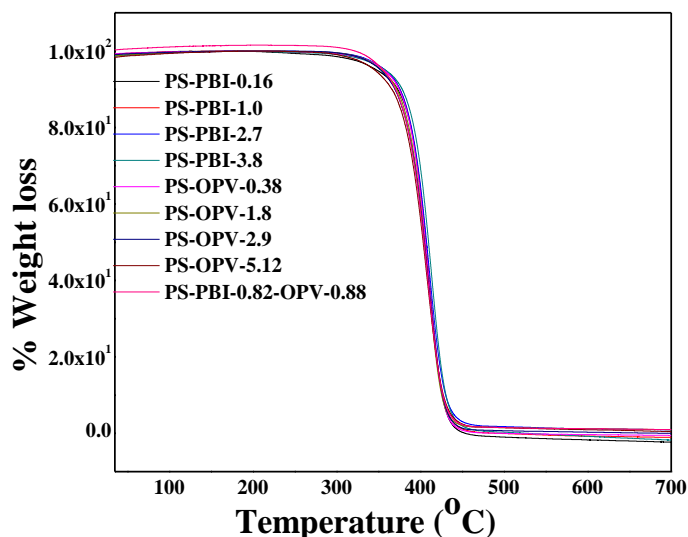


**Figure 2.9:** Thermo gravimetric Analysis (TGA) of all PS samples.

### 2.4.3 Microscopic characterization

The dispersity of the PS particles was determined using dynamic light scattering (DLS) studies carried out in ethanol dispersion. The samples showed an average particle size of 2-3  $\mu\text{m}$  with increasing size for higher cross-linker incorporation. **Figure 2.10** shows the DLS curves for **PS-PBI-X** and **PS-OPV-X** series which clearly indicated narrower particle size distribution for low incorporation of cross-linker.

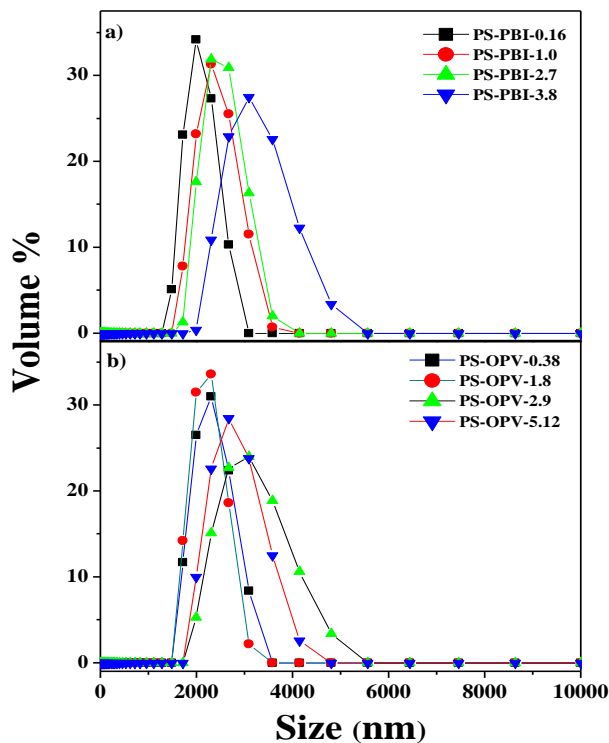


**Figure 2.10:** Volume – average size distribution of (a) **PS-PBI-X** and (b) **PS-OPV-X** series in ethanol dispersion obtained by dynamic light scattering (DLS) analysis.

The SEM images also supported the narrow particle size distribution. **Figure 2.11** and **2.12** shows the SEM images for **PS-PBI-X** and **PS-OPV-X** polymers respectively, showing the monodisperse nature of particle with average size  $\sim 2.6 \mu\text{m}$ .

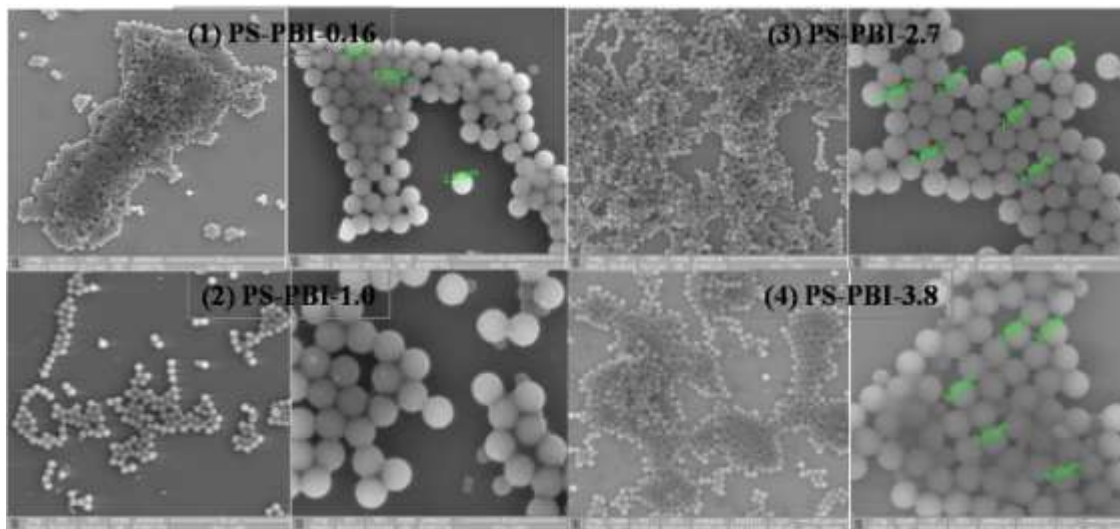


**Figure 2.11:** SEM images of **PS-PBI-X** series drop cast on silicon wafer (1 mg/2 ml ethanol dispersion).

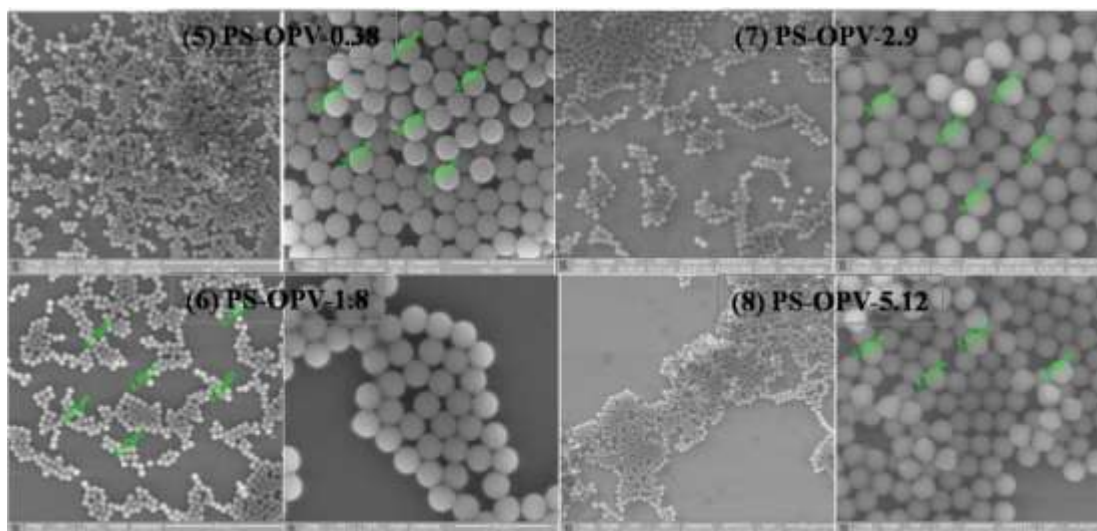


**Figure 2.12:** SEM images of **PS-OPV-X** series drop cast on silicon wafer (1 mg/2 ml ethanol dispersion).

To confirm the monodispersity of microbeads TEM analysis for **PS-PBI-0.16** (top) and **PS-OPV-0.38** (bottom) sample was carried out. In both cases the spherical particles were monodisperse with an average diameter of 2.0  $\mu\text{m}$  shown below in **figure 2.13**.

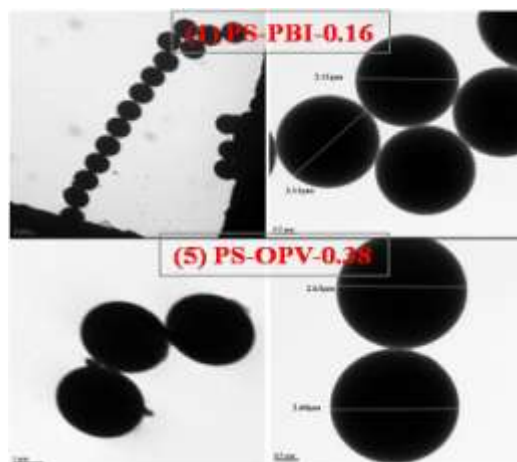


**Figure 2.13:** TEM images of **PS-PBI-0.16** (top) and **PS-OPV-0.38** (bottom) (0.5 mg / 2 ml ethanol dispersion) drop cast on carbon coated copper grids.

Fluorescence microscope images of ethanol dispersion of samples drop cast on glass substrate demonstrated the emission from the fluorescent PS. **Figure 2.14** show the emission of **PS-PBI-X** beads while the images from **Figure 2.15** correspond to those for **PS-OPV-X** polymers.

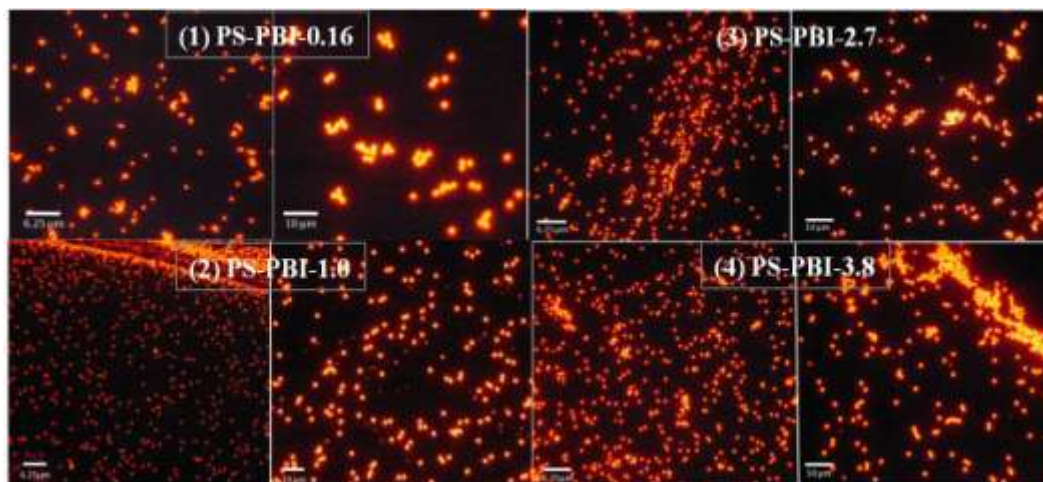


**Figure 2.14:** Fluorescence optical microscopy images of **PS-PBI-X** series of polymers, (1) **PS-PBI-0.16** (2) **PS-PBI-1.0** (3) **PS-PBI-2.7** and (4) **PS-PBI-3.8** using 500-550 nm, red filter.

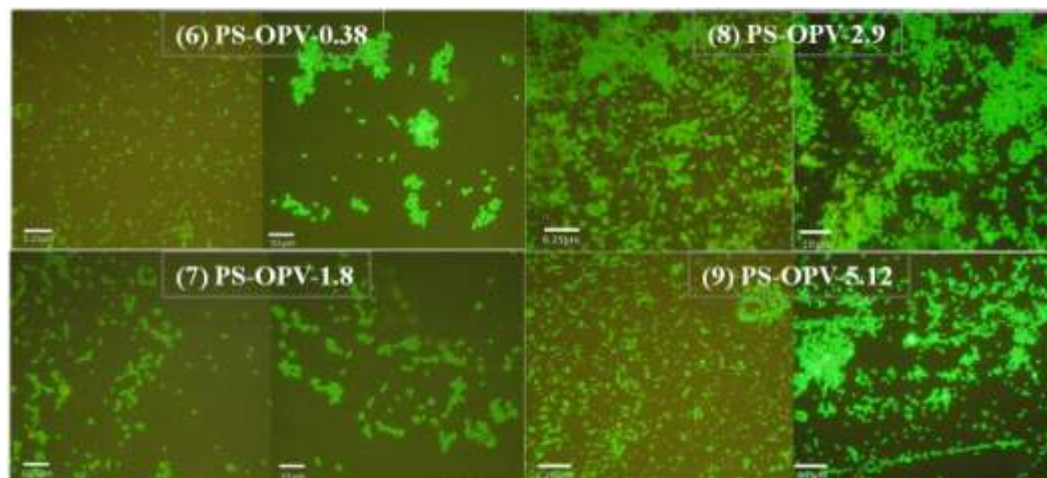


**Figure 2.15:** Fluorescence optical microscopy images of **PS-OPV-X** series of polymers, (6) **PS-OPV-0.38** (7) **PS-OPV-1.8** (8) **PS-OPV-2.9** and (9) **PS-OPV-5.12** using 488-520 nm, blue filter.

The average particle size observed from the fluorescence images were  $\sim 1.7 \mu\text{m}$  for **PS-PBI-X** and  $\sim 1.4 \mu\text{m}$  for **PS-OPV-X** respectively. This was in accordance with the sizes

observed from SEM and TEM images of the samples indicating their monodispersity. **Figure 2.16-a** shows the SEM (top) and fluorescence microscope images (bottom) for the **PS-PBI-0.82-OPV-0.88** sample. The particle size obtained from SEM images was slightly higher ( $\sim 4 \mu\text{m}$ ) than that of the PS particles incorporating either PBI or OPV alone. However, the fluorescence microscope image indicated an average particle size of  $2.5 \mu\text{m}$ , whereas DLS data of the ethanol dispersion of **PS-PBI-0.82-OPV-0.88** showed a much smaller particle size  $\sim 1.5 \mu\text{m}$  (figure 2.16-b ). The dual emission from the sample was clearly observable from the fluorescence images (figure 6 bottom) upon using the green and red filter for OPV and PBI emission respectively. The green filter (transparent in the range 488–520 nm) allowed for some of the PBI emission also to filter through, resulting in the yellow-green emission of the particles in contrast to the green emission from the **PS-OPV-0.38** sample.

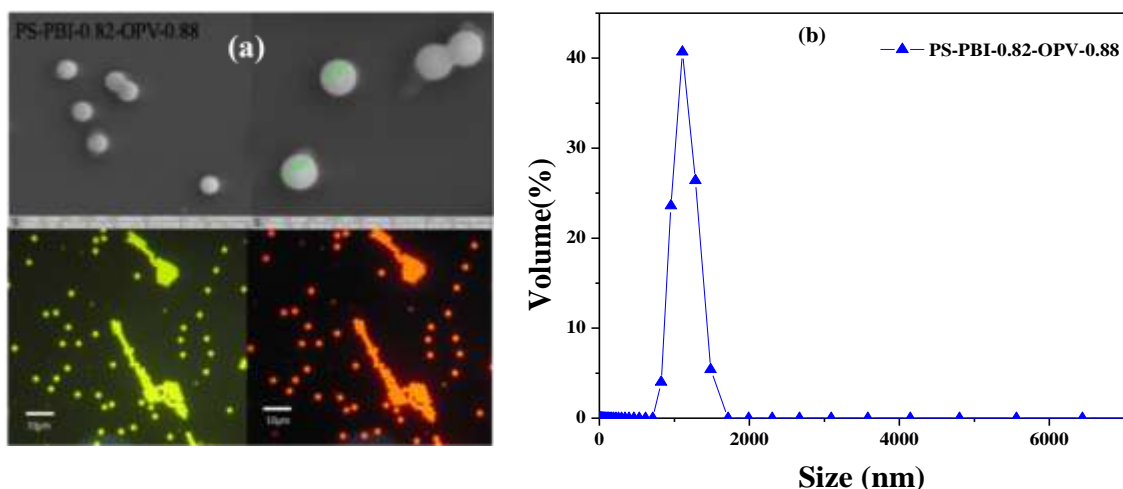


**Figure 2.16:** (a) (top) SEM images of **PS-PBI-0.82-OPV-0.88** drop cast on silicon wafer (1 mg/2 ml ethanol dispersion) and (bottom) Fluorescence optical microscopy images using 500-550 nm, red filter for PBI and using 360-488–520 nm, green filter for OPV imaging. (b) Volume-average size distribution of **PS-PBI-0.82-OPV-0.88** in ethanol dispersion obtained by Dynamic Light Scattering (DLS) analysis.

#### 2.4.4 Photophysical characterization

The photophysical characteristics of the fluorescent PS beads were determined by recording the absorption and emission spectra of 0.1 OD (at the absorption wavelength maxima) solution in chloroform. **Figure 2.17** compares the normalized (at peak maxima) absorption and emission spectra of the cross-linkers **PBIX** and **OPVX** respectively. The absorption



spectra of **PBIX** exhibited peaks in the range of 400-530 nm, corresponding to the  $S_0-S_1$  transition with well resolved vibronic structure from 0-0, 0-1, 0-2, and 0-3 transitions respectively.

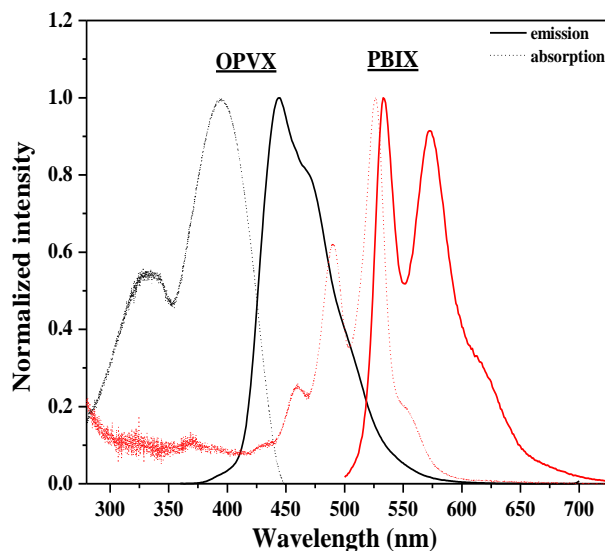


**Figure 2.17:** Normalized absorption and emission spectra of **PBIX** and **OPVX** in  $\text{CHCl}_3$  (0.1 OD at 370 nm;  $\lambda_{\text{ex}} = 370$  nm for **OPVX** and 0.1 OD at 527 nm;  $\lambda_{\text{ex}} = 490$  nm for **PBIX**).

The emission spectrum had emission wavelength maxima at 535 nm. The **OPVX** had absorption maxima at 390 nm and emission wavelength maxima at 430 nm.

The fluorescence quantum yields of the two cross-linkers were determined by the relative method using rhodamine-6G in ethanol as a standard for PBI ( $\lambda_{\text{ex}}$ : 490 nm) and quinine sulphate solution in 0.5 M  $\text{H}_2\text{SO}_4$  solution as the standard for OPV ( $\lambda_{\text{ex}}$ : 370 nm).

**Table 2.3:** Photoluminescence quantum yield measured as powder and in  $\text{CHCl}_3$  solution.

Sr No	Polymer	$\text{CHCl}_3$		Powder	
		$\lambda_{\text{em}}$ (nm)	$\phi$	$\lambda_{\text{ex}}$ (nm)	$\phi$
1	PBIX	490	0.27	490	0.055
2	OPVX	350	0.88	350	0.037
3	PS-PBI-0.16	490	0.33	490	0.25
4	PS-OPV-0.38	350	0.66	350	0.71
5	PS-PBI-0.82- OPV-0.88	490	0.34	490	0.33 (PBI)
		350	0.57	350	0.20 (OPV)

The values were  $\phi_{\text{PBI}} = 0.27$  and  $\phi_{\text{OPV}} = 0.88$  for **PBIX** and **OPVX** respectively shown in table 2.3. The absorption and emission spectra were recorded for the **PS-PBI-X** and **PS-OPV-X** series in chloroform. **Figure 2.18a** shows the absorption and emission (dotted line) spectra of **PS-OPV-0.38**; the corresponding spectra for **OPVX** is also given for sake of comparison. Upon incorporation in the PS backbone a blue shift of  $\sim 40$  nm was observed in the absorption spectra of **PS-OPV-2.5** (390 nm for **OPVX** to 350 nm for **PS-OPV-0.38**). A similar blue shift of 37 nm was observed in the emission spectra of the polymer also and the emission had two peaks at 407 and 413 nm. A probable reason for this blue shift is the stacking of the aromatic units of PS surrounding the OPV chromophores. To investigate this, the **OPVX** was incorporated into PMMA backbone by a two stage dispersion polymerization route. **Figure 2.18b** compares the absorption and emission spectra of **PMMA-OPVX** along with **OPVX** recorded in chloroform. The **PMMA-OPVX** did not exhibit any shift in absorption or emission and was exactly identical to that of the **OPVX**, validating the reasoning that the blue shift observed in the case of the **PS-OPV-X** was due to the presence of the aromatic PS units enveloping the OPV chromophore. **Figure 2.18c** shows the absorption and emission (dotted line) spectra of **PS-PBI-0.16** along with that of the cross-linker **PBIX**. **PBIX** did not show any changes or shift in wavelength upon incorporation in the PS backbone and had similar absorption and emission wavelength maxima. **Figure 18d** shows the absorption and emission spectra of **PS-PBI-0.16-OPV-0.38**, which had both OPV and PBI incorporated. Its absorption spectra had contribution from both the chromophores with a broad OPV absorption in the 350 nm region and a vibrationally fine structured absorption corresponding to PBI in the range 400-530 nm. Upon excitation at the perylene absorption of 490 nm, emission corresponding to PBI was observed at 533 nm. Upon excitation at the OPV wavelength of 350 nm, intense emission corresponding to OPV with peak maxima at 407 and 413 nm were observed along with small emission corresponding to PBI. A possible energy transfer from OPV to PBI was ruled out since PBI also has absorption in the range  $\sim 350$  nm making selective excitation of OPV impossible. In fact, excitation of the PBI alone polymer – **PS-PBI-0.16** (0.1 OD at 350 nm) at 350 nm also showed emission similar in intensity to that of the **PS-PBI-0.82-OPV-0.88** indicating that the observed emission from perylene upon excitation at the OPV wavelength could probably be due to direct excitation of PBI.

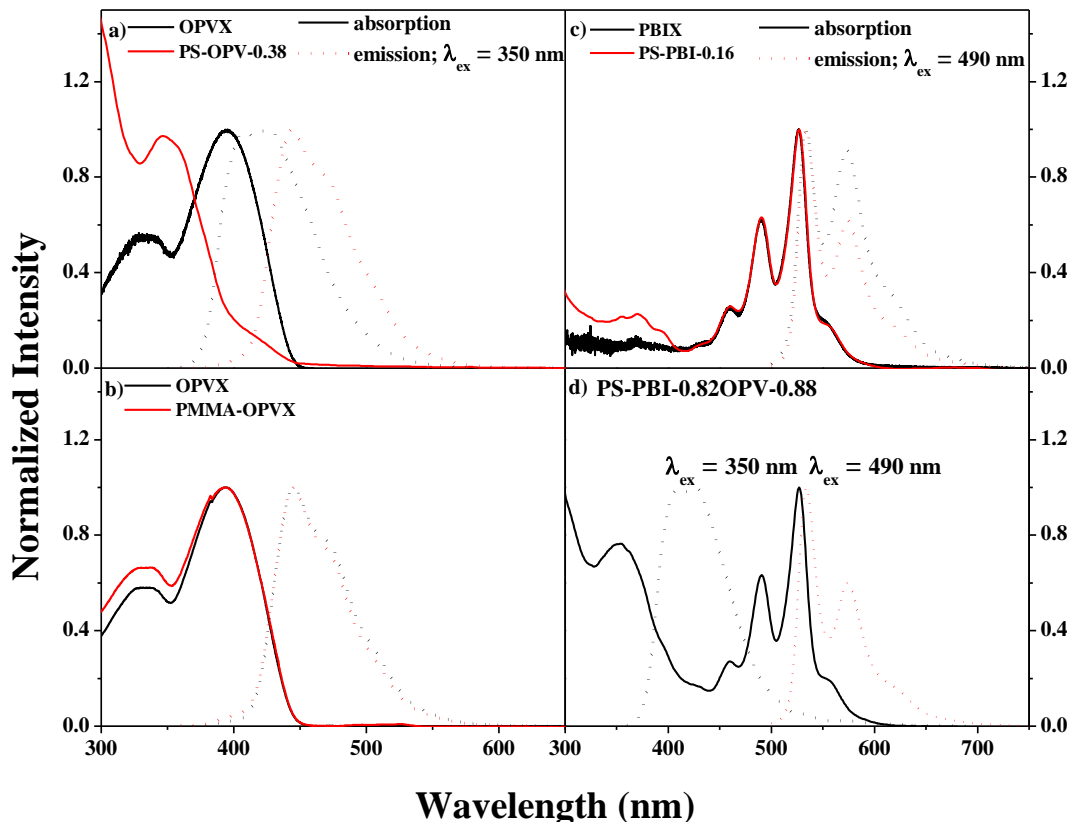


**Figure 2.18:** Absorption and emission spectra (dotted line) of (a) **OPVX** (0.1 OD at 370 nm;  $\lambda_{\text{ex}} = 350$  nm) and **PS-OPV-0.38** (0.1 OD at 350 nm,  $\lambda_{\text{ex}} = 350$  nm) (b) **OPVX** (0.1 OD at 370 nm;  $\lambda_{\text{ex}} = 350$  nm) and **PMMA-OPVX** (c) **PBIX**, **PS-PBI-0.16** (0.1 OD at 527 nm;  $\lambda_{\text{ex}} = 490$  nm) along with (d) **PS-PBI-0.82-OPV-0.88** (0.1 OD at 350 nm,  $\lambda_{\text{ex}} = 350$  nm and 0.1 OD at 527 nm;  $\lambda_{\text{ex}} = 490$  nm) in  $\text{CHCl}_3$ .

The highlight of the present work was the solid state monomeric (non-aggregated) emission from the monodispersed, thermally stable PS beads. The very pale pink colored **PS-PBI-X** and colorless **PS-OPV-X** samples upon observation under hand-held UV lamp emitted intense orange and blue fluorescence respectively. **Figure 2.19a** shows the images of the powdered PS samples both under normal and UV light. **Figure 2.19b** compares the solid state absorption spectra (recorded in the reflectance mode) of the **PS-PBI-0.16**, **PS-OPV-0.38** and **PS-PBI-0.82-OPV-0.88** powders.



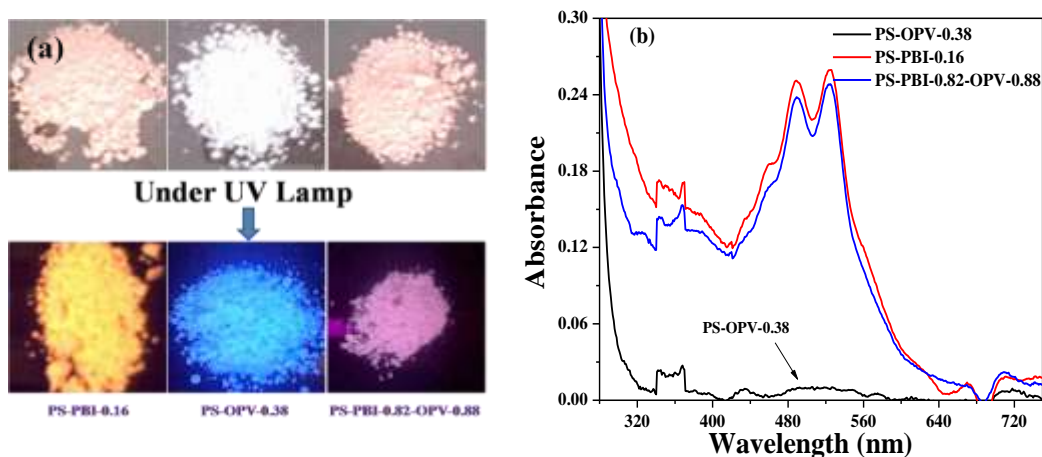


**Figure 2.19:** (a) The images of the powdered **PS-PBI-0.16**, **PS-OPV-0.38** and **PS-PBI-0.82-OPV-0.88** samples both under (top) normal and (bottom) UV light. (b) The solid state absorption spectra (recorded in the reflectance mode) of the **PS-PBI-0.16**, **PS-OPV-0.38** and **PS-PBI-0.82-OPV-0.88** samples.

The absorption corresponding to the OPV was so weak that it was not observable in the powder state. The PBI chromophore has a higher molar absorption coefficient compared to OPV chromophore; therefore, peaks corresponding to the perylene absorption were visible in the solid powder form. Comparing the absorption spectra of **PS-PBI-0.16** recorded as a solid powder with that in chloroform, the (0,1) vibronic transition had higher intensity in the former compared to the latter as shown in figure 2.20.

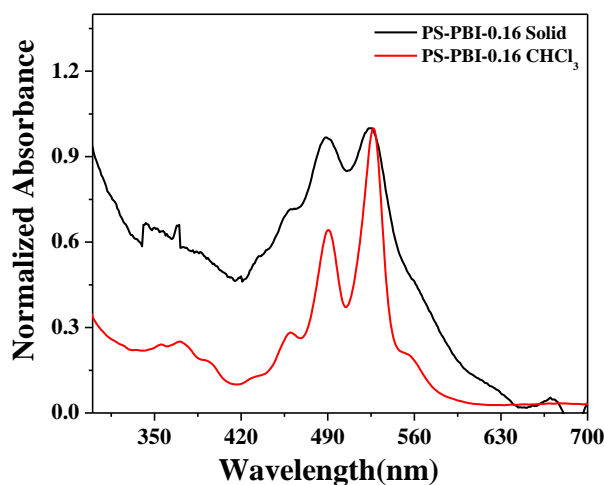


**Figure 2.20:** Comparison of the solid state absorption spectra (recorded in the reflectance mode) of the **PS-PBI-0.16**, with that recorded in solution in chloroform.

However no red shifting of the absorption maxima characteristic of aggregation was observed in the solid state absorption spectra.

**Figure 2.21** compares the normalized emission spectra of the cross-linkers and polymers recorded in the powder form with the corresponding spectra recorded in chloroform solution. The cross-linkers exhibited very weak emission in the solid state. **Figure 2.21a** compares the spectra for the cross-linker **OPVX** upon excitation at 350 nm.

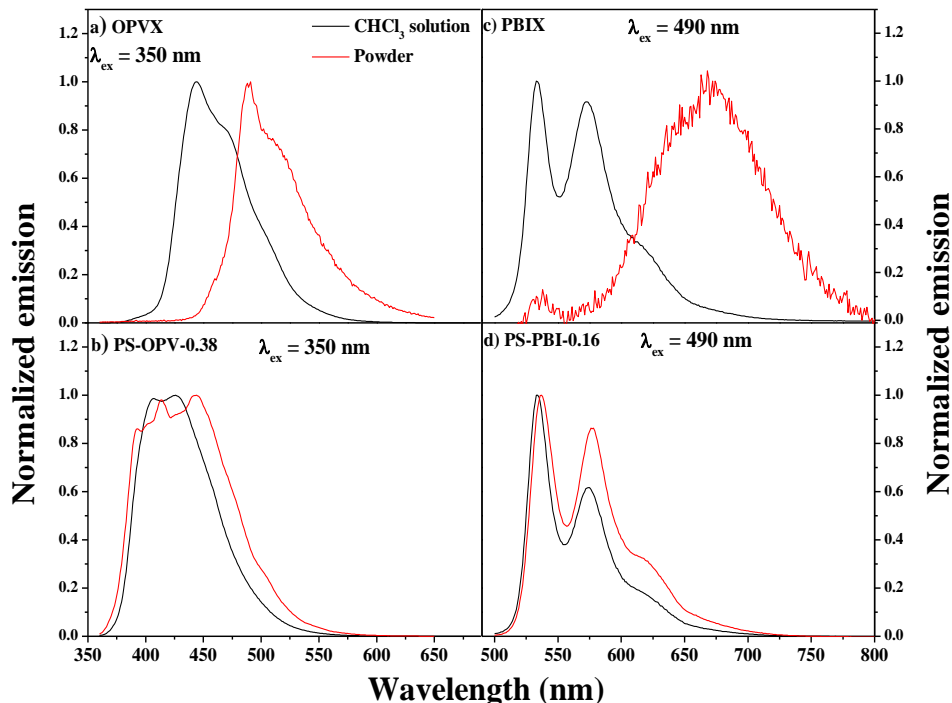


**Figure 2.21:** Comparison of the emission spectra in the solution state in chloroform and solid state for the cross-linkers and polymer. (a) **OPVX** in  $\text{CHCl}_3$  and as powder upon excitation at 350 nm (b) **PS-OPV-0.38** in  $\text{CHCl}_3$  and as powder upon excitation at 350 nm (c) **PBIX** in  $\text{CHCl}_3$  and as powder upon excitation at 490 nm (d) **PS-PBI-0.16** in  $\text{CHCl}_3$  and as powder upon excitation at 490 nm.

The spectra in the solid state was red shifted by 46 nm (peak maxima at 490 nm) compared to that in solution indicating aggregation in the solid state. **Figure 2.21b** compares the emission spectra of **PS-OPV-0.38** recorded in powder form and in solution. In contrast to the red shift observed for the cross-linker, no red shift was observed for the emission of **PS-OPV-0.38** in the solid compared to that in solution. The emission in the solid state had a maxima centered  $\sim 400$  nm with vibrational fine structure. The vibronic structure indicated absence of

pronounced molecular interactions among the OPV chromophores distributed in the PS backbone in the solid state. As observed in the solution state, a blue shift of 45 nm was observed in the solid state emission spectra of the **PS-OPV-0.38** compared to **OPVX**. **Figure 2.21c** compares the solid and solution state emission spectra for **PBIX**. The solid state emission from **PBIX** was characterized by red shifted emission from aggregates  $\sim 660$  nm, which was absent in the solution state of the same sample. In the case of the cross-linked PS containing PBI i.e **PS-PBI-0.16** (**figure 2.21d**), the emission in the solid state was characterized by the higher intensity of the (0,1) vibrational transition compared to the (0,0) transition and a complete absence of aggregate emission  $> 600$  nm. The solid state fluorescence quantum yield  $\phi_{\text{powder}}$  was determined using an integrating-sphere Quanta  $\phi$  Horiba attachment under excitation at 490 nm for PBI and 350 nm for OPV respectively. **PBIX** had low solid state quantum yield  $\phi_{\text{powder}}$  of  $\sim 0.055$ ; whereas **PS-PBI-0.16** had a high quantum yield  $\phi_{\text{powder}}$  of  $\sim 0.25$ . The  $\phi_{\text{powder}}$  of **OPVX** was very low  $\sim 0.037$  compared to that of **PS-OPV-0.38**, which had a  $\phi_{\text{powder}} \sim 0.71$  (table 2.3). **Figure 2.22** compares the emission spectra of the cross-linked PS series of polymers in the powder form.

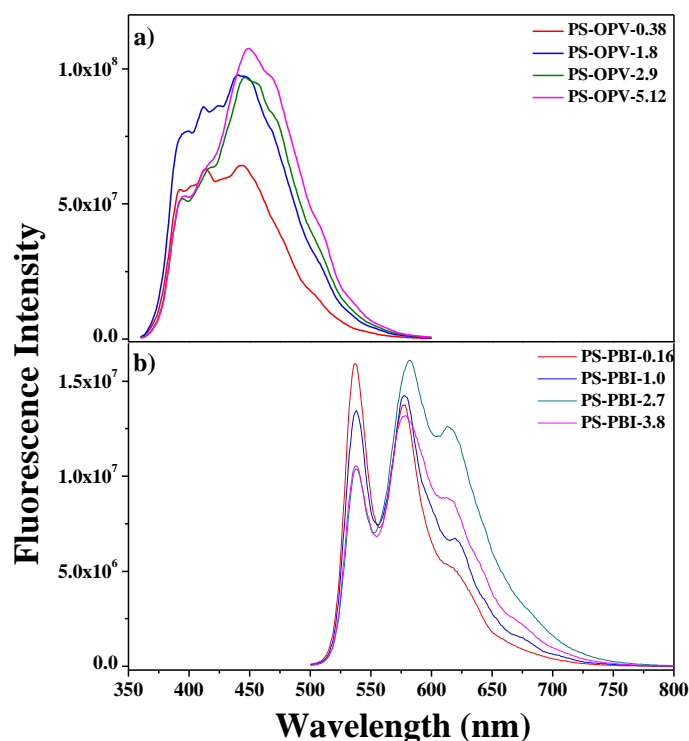


**Figure 2.22:** Solid state (powder) emission spectra of the cross-linked PS polymers upon excitation at 350 nm for (a) **PS-OPV-X** series and (b) at 490 nm for **PS-PBI-X** series.

The PS with higher incorporation of OPV; namely **PS-OPV-1.8**, **PS-OPV-2.9** and **PS-OPV-5.12** exhibited fluorescence with the PL intensity increasing with gradual red shift of peak maxima. In the case of the cross-linked PS containing PBI, no aggregate emission beyond 600 nm was observed.

**Figure 2.23** compares the emission spectra of the PS bead containing both PBI and OPV, viz; **PS-PBI-0.82-OPV-0.88**. It exhibited reduced emission intensity for OPV upon excitation at the OPV absorption wavelength maxima of 350 nm. Emission from the PBI in the range  $> 500$  nm was also observed upon excitation at 350 nm. Since molecular interactions among the chromophores were expected to be absent or negligibly low in the solid state, energy transfer from the OPV to PBI chromophore was not expected. **Figure 2.23** also shows the emission from the PBI alone polymer i.e **PS-PBI-0.16** upon excitation at 350 nm. **PBI** had reasonable absorption at 350 nm resulting in direct excitation of perylene upon excitation at 350 nm suggesting that selective excitation of **OPV** was not possible in the **PS-PBI-0.82-OPV-0.88** polymer. Excitation at 490 nm resulted in strong emission from PBI in the case of **PS-PBI-0.82-OPV-0.88**. The quantum yield for the **PBI** emission in **PS-PBI-0.82-OPV-0.88** was quite high at 0.33 compared to that for **OPV** which was 0.20.

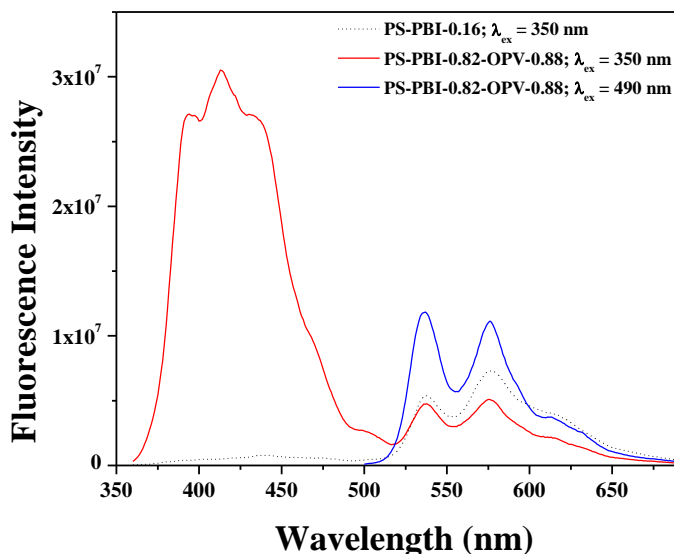


**Figure 2.23:** Solid state emission spectra of **PS-PBI-0.82-OPV-0.88** upon excitation at 350 nm and 490 nm. The emission from **PS-PBI-0.16** upon excitation at 350 nm is also given for comparison (dotted line).

**PBI** as well as **OPV** are chromophores well-known for their tendency to aggregate and lead to quenching of fluorescence in concentrated solution and solid state.<sup>38-40</sup> Sometimes strategies like introduction of bulky substitutes that can reduce aggregation induced fluorescence quenching or positive effects of aggregate emission based on some J-type aggregates have been reported in literature especially for perylenebisimides to exhibit fluorescence in the solid state.<sup>41-44</sup> Some bay substituted perylenebisimides have been shown to exhibit intense fluorescence emission in the solid state.<sup>45,46</sup> The solid state emissions in most of these cases are aggregate emission in the ~600 nm range.<sup>47,48</sup> Our current report is one of the few reports where these highly emitting fluorophores have been successfully incorporated into a polymer scaffold in the form of cross-linker and achieved fluorescent polymer beads with intense emission from the non-aggregated chromophore in the solid state.<sup>19, 42,49,50</sup> The absolute quantum yield of the powder sample determined using the integrating sphere set up and the fluorescence microscopic images was proof for this. The fact that this approach allows the incorporation of simultaneous addition of multiple fluorophores emitting in different colors makes it very convenient to use for labeling studies where one can access different emission regions just by exciting at the appropriate wavelength without having to label with different fluorophores.

## 2.5 Conclusion

A series of polystyrene microbeads incorporating fluorophores like perylenebisimide (**PBI**) and oligo (*p*-phenylenevinylene) (**OPV**) as the cross-linker were successfully developed by two stage dispersion polymerization strategy. Dispersion polymerization was adopted as the method of choice since it was more tolerant to rigid aromatic molecules with poor solubility, and allowed their incorporation into the polymer backbone and still maintained control over the particle size distribution. The advantage of adapting the fluorophore itself as the cross-linker was two-fold. One, fluorescent cross-linked polymer particles could be obtained in one shot without having to add two ingredients – the fluorophore and the cross-linker separately in the reaction medium and the covalent attachment of the dye to the polymer backbone avoided dye leakage. The second and most appealing reason was the ability of maximum emission from very low fluorophore incorporation as larger incorporation of fluorophores like **PBI** and **OPV** are known to result

in aggregation induced quenching. Thus, using this strategy upto  $\sim 5 \times 10^{-6}$  moles of the rigid fluorophores could be incorporated into PS backbone. The fluorescent spherical PS beads had an average diameter of 2-3  $\mu\text{m}$ . The PS beads incorporating PBI exhibited intense orange red emission in the solid state with quantum yield  $\phi_{\text{Powder}} = 0.25$ , while the PS incorporating OPV as the cross-linker fluorophore exhibited intense green emission with very high quantum yield of  $\phi_{\text{Powder}} = 0.71$ . This is the first time that successful monomer emission (no emission from aggregate) with high quantum efficiency has been achieved from fluorophores based on **PBI** and **OPV**, which are known to undergo  $\pi$ - $\pi$  stacking interaction of their aromatic core in the solid state and even in highly concentrated form in solution resulting in quenching of their emission. An added advantage of this strategy of fluorophore as cross-linker was the ability to incorporate more than one tailor-made fluorophore into the PS backbone enabling fine-tuning of the emission colors. Fluorescent microbeads with stable intense emission find application in various areas and the approach introduced here is expected to be a viable route towards their easy and reproducible development.

## 2.6 Reference

- (1) Peng, B.; Wee, E.; Imhof, A.; Blaaderen, A. *Langmuir* **2012**, *28*, 6776–6785.
- (2) Han, M.; Gao, X.; Su, J. Z.; Nie, S. *Nat. Biotechnol.* **2001**, *19*, 631–635.
- (3) Diacon, A.; Rusen, E.; Mocanu, A.; Hudhomme, P.; Cincu, C. *Langmuir* **2011**, *27*, 7464–7470.
- (4) Wu, S.-K.; Tang, T.-P.; Tseng, W. J. *J. Mater. Sci.* **2008**, *43*, 6453–6458.
- (5) Tung, Y. C.; Zhang, M.; Lin, C. T.; Kurabayashi, K.; Skerlos, S. J. *Sens. Actuators, B* **2004**, *98*, 356–367.
- (6) Sanchez-Martin, R. M.; Alexander, L.; Muzerelle, M.; Cardenas-Maestre, J. M.; Tsakiridis, A.; Brickman, J. M.; Bradley, M. *ChemBioChem.* **2009**, *10*, 1453–1456.
- (7) Sukhanova, A.; Nabiev, I. *Crit. Rev. Oncol./Hematol.* **2008**, *68*, 39–59.
- (8) Holzapfel, V.; Musyanovych, A.; Landfester, K.; Lorenz, M. R.; Mailander, V. *Macromol. Chem. Phys.* **2005**, *206*, 2440–2449.
- (9) Medintz, I. L.; Uyeda, H. T.; Goldman, E. R.; Mattoussi, H. *Nat. Mater.* **2005**, *4*, 435–446.
- (10) Chan, Y.; Zimmer, J. P.; Stroh, M.; Steckel, J. S.; Jain, R. K.; Bawendi, M. G. *Adv. Mater.* **2004**, *16*, 2092–2097.
- (11) Martín-Banderas, L.; Rodríguez-Gil, A.; Cebolla, Á.; Chávez, S.; Berdún-Álvarez, T.; Garcia, J. M. F.; Flores-Mosquera, M.; Gañán-Calvo, A. M. *Adv. Mater.* **2006**, *18*, 559–564
- (12) Ribeiro, T.; Baleizao, C.; Farinha, J. P. S. *J. Phys. Chem. C* **2009**, *113*, 18082–18090.
- (13) Yang, Z.; Wang, Z.; Yao, X.; Wang, Y. *Langmuir* **2012**, *28*, 3011–3017.
- (14) Sadovoy, A. V.; Lomova, M. V.; Antipina, M. N.; Braun, N. A.; Sukhorukov, G. B.; Kiryukhin, M. V. *ACS Appl. Mater. Interfaces* **2013**, *5*, 8948–8954.
- (15) Jung, Y.; Hickey, R. J.; Park, S. J. *Langmuir* **2010**, *26*, 7540–43.
- (16) Yabu, H.; Tajima, A.; Higuchic, T.; Shimomura, M. *Chem. Commun.* **2008**, 4588–4589.
- (17) Schu"tze, F.; Stempfle, B.; Ju"ngst, C.; Wo"ll, D.; Zumbusch, A.; Mecking, S. *Chem. Commun.* **2012**, 2104–2106.
- (18) Dullens, R. P. A.; Claesson, E. M.; Kegel, W. K. *Langmuir* **2004**, *20*, 658–664.
- (19) Baier, M. C.; Huber, J.; Mecking, S. *J. Am. Chem. Soc.* **2009**, *131*, 14267–14273.

- (20) Tuncel, D.; Demir, H. V. *Nanoscale* **2010**, *2*, 484–494.
- (21) Shelton, A. H.; Price, R. S.; Brokmann, L.; Dettlaff, B.; Schanze, K. S. *ACS Appl. Mater. Interfaces* **2013**, *5*, 7867–7874.
- (22) Thielbeer, F.; Chankeshwara, S. V.; Bradley, M. *Biomacromolecules* **2011**, *12*, 4386–4391.
- (23) Arshady, R. *Colloid Polym. Sci.* **1992**, *270*, 717–732.
- (24) Sosnowski, S.; Feng, J.; Winnik, M. A. *J. Poly. Sci., Part A: Polym. Chem.* **1994**, *32*, 1497–1505.
- (25) Sudol, S. S. E. D.; EL-Aasser, M. S. *J. Polym. Sci., Part A: Polym. Chem.* **1993**, *31*, 1393–1402.
- (26) Horak, D. *Acta Polym.* **1996**, *47*, 20–28.
- (27) Song, J. S.; Tronc, F.; Winnik, M. A. *J. Am. Chem. Soc.* **2004**, *126*, 6562–6563.
- (28) Song, J. S.; Winnik, M. A. *Macromolecules* **2005**, *38*, 8300–8307.
- (29) Würthner, F. *Chem. Commun.* **2004**, *14*, 1564–1579.
- (30) Hains, A. W.; Chen, H.-Y.; Reilly, T. H., III; Gregg, B. A. *ACS Appl. Mater. Interfaces* **2011**, *3*, 4381–4347.
- (31) Singh, H.; Balamurugan, A.; Jayakannan, M. *ACS Appl. Mater. Interfaces* **2013**, *5*, 5578–5591.
- (32) Kim, I.; Haverinen, H. M.; Li, J.; Jabbour, G. E. *ACS Appl. Mater. Interfaces* **2010**, *2*, 1390–1394.
- (33) Bhavsar, G. A.; Asha, S. K. *Chem. Eur. J.* **2011**, *17*, 12646–12658.
- (34) Deepa, P.; Jayakannan, M. *J. Polym. Sci., Part A: Polym. Chem.* **2008**, *46*, 5897–5915.
- (35) Avlasevich, Y.; Li, C.; Mullen, K. *J. Mater. Chem.* **2010**, *20*, 3814–3826.
- (36) Peeters, E.; Ramos, A. M.; Meskers, S. C. J.; Janssen, R. A. J. *J. Chem. Phys.* **2000**, *112*, 9445–9454.
- (37) Shim, S. E.; Yang, S.; Choi, H. H.; Choe, S. *J. Polym. Sci., Part A: Polym. Chem.* **2004**, *42*, 835–845.
- (38) Goel, M.; Jayakannan, M. *J. Phys. Chem. B* **2010**, *114*, 12508–12519.



- (39) Chen, Z.; Lohr, A.; Saha-Mo"ller, C. R.; Wu"rthner, F. *Chem. Soc. Rev.* **2009**, *38*, 564–584.
- (40) Rodr"iguez-Abreu, C.; Aubery-Torres, C.; Solans, C.; L"opez- Quintela, A.; Tiddy, G. J. *T. ACS Appl. Mater. Interfaces* **2011**, *3*, 4133–4141.
- (41) Langhals, H.; Ismael, R.; Yuruk, O. *Tetrahedron* **2000**, *56*, 5435–5441.
- (42) Langhals, H.; Krotz, O.; Polborn, K.; Mayer, P. *Angew. Chem., Int. Ed.* **2005**, *44*, 2427–2428.
- (43) W"urthner, F.; Kaiser, T. E.; Saha-M"oller, C. R. *Angew. Chem., Int. Ed.* **2011**, *50*, 3376–3410.
- (44) Qu, J.; Zhang, J.; Grimsdale, A. C.; M"ullen, K.; Jaiser, F.; Yang, X.; Neher, D. *Macromolecules* **2004**, *37*, 8297–8306.
- (45) Zhao, Q.; Zhang, S.; Liu, Y.; Mei, J.; Chen, S.; Lu, P.; Qin, A.; Ma, Y.; Sun, J. Z.; Tang, B. *Z. J. Mater. Chem.* **2012**, *22*, 7387–7394.
- (46) Che, Y.; Yang, X.; Balakrishnan, K.; Zuo, J.; Zang, L. *Chem. Mater.* **2009**, *21*, 2930–2934.
- (47) Ford, W. E.; Kamat, P. V. *J. Phys. Chem.* **1987**, *91*, 6373–6380.
- (48) Neuteboom, E. E.; Meskers, S. C. J.; Meijer, E. W.; Janssen, R. A. *J. Macromol. Chem. Phys.* **2004**, *205*, 217–222.
- (49) Mizoshita, N.; Tani, T.; Inagaki, S. *Adv. Mater.* **2012**, *24*, 3350–3355.
- (50) Sch"utze, F.; Stempfle, B.; J"ungst, C.; W"oll, D.; Zumbusch, A.; Mecking, S. *Chem. Commun.* **2012**, *48*, 2104–2106.

-:- Chapter 3 -:-

---

*Blue, Green, and Orange-Red Emission from Polystyrene Microbeads for Solid-State White-Light and Multicolor Emission*

---

**This chapter has been adapted from the following paper:**

“Sonawane, S. L.; Asha S. K. *J. Phys. Chem. B.* **2014**, *118*, 9467–9475.

DOI: 10.1021/jp504718m.



### 3.1 Abstract

Solid state white light emission was achieved from Polystyrene (PS) microbeads incorporated with fluorophores based on perylenebisimide (**PBITEG**) and oligo (*p*-phenylenevinylene) (**OPV**) as acrylic cross-linkers. The PS beads incorporated with only **PBITEG** gave intense orange red emission; PS incorporated with OPV exhibited green emission, whereas a series of polymers incorporating both cross-linkers exhibited varying shades of white light emission. One of the PS sample - **PS-PBITEG-6.25-OPV-4.28**, exhibited pure white light emission in the powder form with CIE coordinates (0.33, 0.32). The rigid aromatic cross-linkers were incorporated into PS backbone in a two-stage dispersion polymerization to afford PS beads in the size range 2-3  $\mu\text{m}$ . The incorporation of fluorophores as cross-linkers enabled covalent attachment of the dye to the polymer backbone avoiding dye leakage, besides avoiding aggregation induced fluorescence quenching.

### 3.2 Introduction

Fluorescent materials have attracted wide attention because of their potential application in different research areas in chemistry and biology.<sup>1-4</sup> White light emitting luminescent materials (organic, inorganic and polymeric) are the subject of intense research since the last decade due to their application in LEDs,<sup>5-6</sup> panel displays,<sup>7-8</sup> color tuning materials<sup>9-10</sup> and solid state lighting.<sup>7, 11-12</sup> The basic requirement for white light emission is the combination of emission of the three primary colors i.e. blue, green and red in a particular intensity that covers the visible wavelength range from 400 to 700 nm. According to the Commission Internationale d'Éclairage (CIE) chromaticity diagram,<sup>13</sup> white light can be achieved by careful tuning of contribution of each color and by varying the distance between the different dye components leading to Forster resonance energy transfer (FRET) in the required systems.<sup>5, 14-17</sup> Many researchers have developed fully organic/polymeric materials emitting white light mostly in the solution state.<sup>18-20</sup> A few reports are available for solid state based white light emitting thin films and powder based on small molecules,<sup>21-22</sup> quantum dots,<sup>23-24</sup> organogels,<sup>25-26</sup> metal organic frameworks,<sup>27</sup> nanofibers,<sup>28</sup> micro<sup>29</sup> and nanoparticles,<sup>30</sup> lanthanides,<sup>31-32</sup> and crystals.<sup>9, 33</sup> Conjugated polymers based on poly(*p*-phenylene vinylenes) (PPV) and oligo (*p*-phenylene vinylene) (OPV), perylenebisimide (PBI), polythiophenes (PTh), polyfluorenes (PF), benzthiadiazoles also have contributed towards light harvesting systems because of their potential ability as donor and acceptor materials.<sup>10, 29, 34-35</sup> Supramolecular self assembly of the donor and acceptor to achieve FRET based white light emission is a widely studied area in the field of material chemistry.<sup>5, 36-37</sup> Achieving white light emission from a single polymer is quite a challenging task.<sup>38</sup> Utilizing a combination of blue emitting oligo (fluorene), green emitting oligo (*p*-phenylenevinylene) and red emitting perylene, Albertus P. H. J. Schenning and co-workers presented the white-light emitting hydrogen-bonded supramolecular copolymers.<sup>36, 39</sup> Reports show that tunable luminescence can be obtained from silicon linked polystyrene hybrid materials by quantum confinement effects.<sup>40-42</sup> Fluorescence quenching due to aggregation of chromophores is one of the biggest challenges plaguing the device application of most of the organic light emitting materials. Several strategies have been reported to overcome this problem in literature.<sup>43-44</sup> Controlling emission by encapsulating the

dye/quantum dots in block copolymers, thereby inhibiting energy transfer also has been a strategy for obtaining emission from pure non-aggregated species.<sup>45-46</sup>

In the previous chapter, we had shown the solid state emission from polystyrene (PS) beads incorporated with PBI and OPV based cross-linkers in a two stage dispersion polymerization strategy.<sup>47</sup> The chromophores were isolated in the polymer matrix thereby inhibiting aggregation induced fluorescence quenching or FRET based emission color tuning. Here we report tunable emission colors as well as solid state white light emission with high quantum yield from PS beads containing both blue emitting **OPV** and red emitting **PBITEG** which were covalently incorporated as cross-linkers. Single polymer based solid state white light (CIE coordinates; X = 0.33, Y = 0.32) as well as multicolor emission is reported. The isolated blue emitting **OPV** and new orange-red emitting **PBITEG**, were covalently incorporated into PS beads as cross-linkers. By changing the feed ratio of both the **OPV** and **PBITEG** chromophores we could tune the color in the solid state from blue to white and orange-red. To the best of our knowledge, this is the first example of solid state white light emission from a single polymer system, where chromophore isolation was used as the strategy to obtain multiple emission from different RGB components.

### 3.3 Experimental methods

#### 3.3.1 Materials:

Perylene-3,4,9,10-tetracarboxylic dianhydride (PTCDA), zinc acetate, imidazole, polyvinylpyrrolidone (PVP, Mw 360,000 g/mol), acrylic acid, 4-methoxyphenol, 2-ethylhexylbromide, triethylphosphite, 4-hydroxy benzaldehyde, and potassium *tert*-butoxide were purchased from Aldrich and used without further purifications. Styrene (Aldrich) was washed with sodium hydroxide followed by water, dried overnight using calcium chloride, and vacuum distilled before use. HBr in glacial acetic acid, *para*-formaldehyde, potassium carbonate, potassium iodide, dimethyl sulfoxide, N, N-dimethylformamide (DMF), tetrahydrofuran (THF), dichloromethane (DCM), and 2-chloroethanol were purchased from Merck and purified using standard procedures. Triton X-100 (70% solution in water) and 2,2'-azobisisobutyronitrile (AIBN) were purchased from Merck and the latter was recrystallised from Methanol.

### 3.3.2 Instrumentation:

$^1\text{H}$  and  $^{13}\text{C}$  NMR, GPC, MALDI, DLS, TGA, SEM, UV-Vis and steady-state fluorescence based characterization were carried out exactly as described in previous chapter. The fluorescence microscopic images were taken by Carl Zeiss inverted fluorescence microscope Model AXIO OBSERVER.ZI using DAPI (350-430 nm blue), Alexa (488-520 green) and Rhodamine (480-580 nm red) filters. Polymer solutions were prepared as very dilute dispersion in ethanol, which were drop cast on glass plate, covered with cover slip and directly observed under fluorescence microscope.

### 3.3.3 General procedures

#### (i) Synthesis of perylenebisimide cross-linker (PBITEG):

PBITEG was synthesized starting from PBI-TEG diol, which was synthesized as per literature procedure.<sup>48</sup> 650 mg ( $8.7 \times 10^{-4}$  mols) of PBI-TEG diol and 0.58 mL ( $4.3 \times 10^{-3}$  mol) of  $\text{Et}_3\text{N}$  was dissolved in 100 mL of dry dichloromethane (DCM) in a 250 mL two necked round bottom flask. A slow addition of acryloyl chloride (0.35 ml,  $4.3 \times 10^{-3}$  mol) in DCM was performed over a period of 15-20 minutes into the 250 mL two necked round bottom flask at  $0^\circ\text{C}$ . The reaction mixture was slowly brought to room temperature ( $25^\circ\text{C}$ ) and allowed to stir for 24 hours. The progress of the reaction was monitored using TLC. The workup of the reaction mixture was carried out by washing the organic layer with water and brine, followed by evaporation of the solvent. The compound was purified by column chromatography in DCM/methanol (1%) as solvent. Yield = 250 mg (38%).  $^1\text{H}$  NMR (200 MHz,  $\text{CDCl}_3$ ,  $\delta$  ppm): 8.64 (m, 8H, perylene ring), 6.35 (dd, 2H, acrylic double bond), 6.13 (q, 2H, acrylic double bond), 5.82 (dd, 2H, acrylic double bond), 4.46 (t, 4H,  $-\text{OCH}_2$ ), 4.24 (t, 4H,  $-\text{NCH}_2$ ), 3.86 (t, 4H), 3.60-3.71 (m, 20H),  $^{13}\text{C}$  NMR (500 MHz,  $\text{CDCl}_3$ ,  $\delta$  ppm) 165.88, 162.95, 134.01, 130.93, 13.75, 128.85, 127.97, 125.78, 122.81, 122.68, 70.41, 70.30, 69.83, 68.80, 63.39, 39.03. MALDI-TOF MS (Dithranol matrix):  $m/z$  calcd for  $\text{C}_{46}\text{H}_{46}\text{N}_2\text{O}_{14}$ : 850.29; found 850.29+23  $[\text{M}+\text{Na}^+]$  850.29  $[\text{M}+\text{K}^+]$ .

#### (ii) Two stage Dispersion Polymerization for the preparation of PS-PBITEG-X-OPV-X:

Procedure same as explained in chapter 2 section 2.3.3 (v). The polymerization content is given in table 3.1.

**(iii) Two stage Dispersion Polymerization for the preparation of PMMA-PAA-PBITEG-X-OPV-X:**

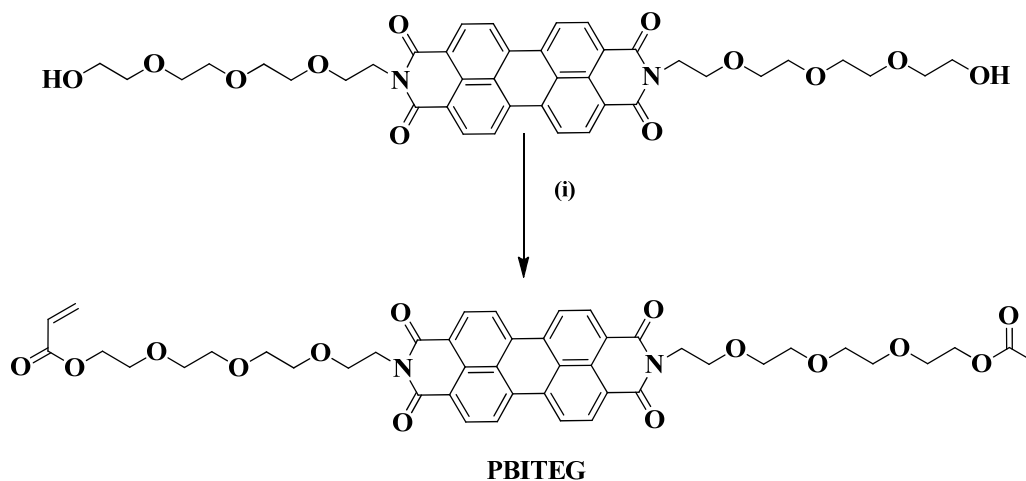
Procedure same as explained in chapter 2 section 2.3.3 (v) and (vi).

**PBITEG** and **OPV** cross-linkers had low solubility in the methyl methacrylate (**MAA**), therefore acrylic acid (**AA**) (0.5 gm) was added for the solubility purpose in the **MMA-PBITEG-OPV** mixture and the solution were added during the second stage of dispersion polymerization.

### 3.4 Result and Discussion

#### 3.4.1 Synthesis and characterization

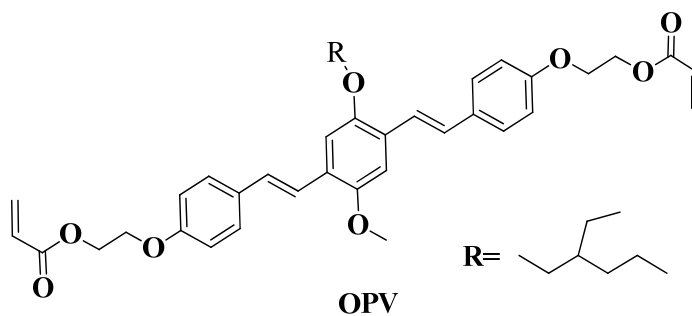
The structure of the cross-linkers used in the study and the synthesis of the fluorescent cross-linker based on perylenebisimide (**PBITEG**) is shown in **scheme 3.1a**. The details of the synthesis to obtain the final acryloyl functionalized **PBITEG** cross-linker is given in the experimental section. The synthesis of oligo (*p*-phenylenevinylene) (**OPV**) was reported in chapter 2 section 2.3.3.(iv) and the structure is shown in **scheme 3.1b**.



**Scheme 3.1a:** Synthesis of perylenebisimide based cross-linker (**PBITEG**)

**Reagents:** (i) Acryloyl Chloride, DCM, Et<sub>3</sub>N, 0-25 °C, 24 hours, N<sub>2</sub>.





**Scheme 3.1b:** Structure of oligo (*p*-phenylenevinylene) based cross-linker (**OPV**).

The details of the complete structural characterization of the **PBITEG** cross-linker is provided in the **figures 3.1a to c**.

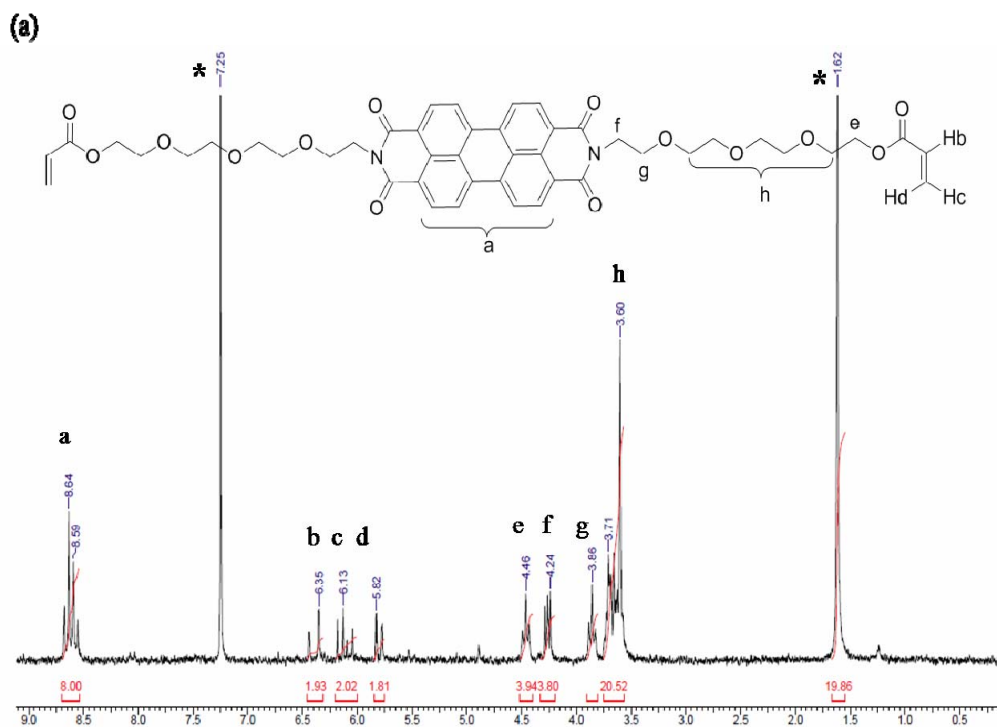
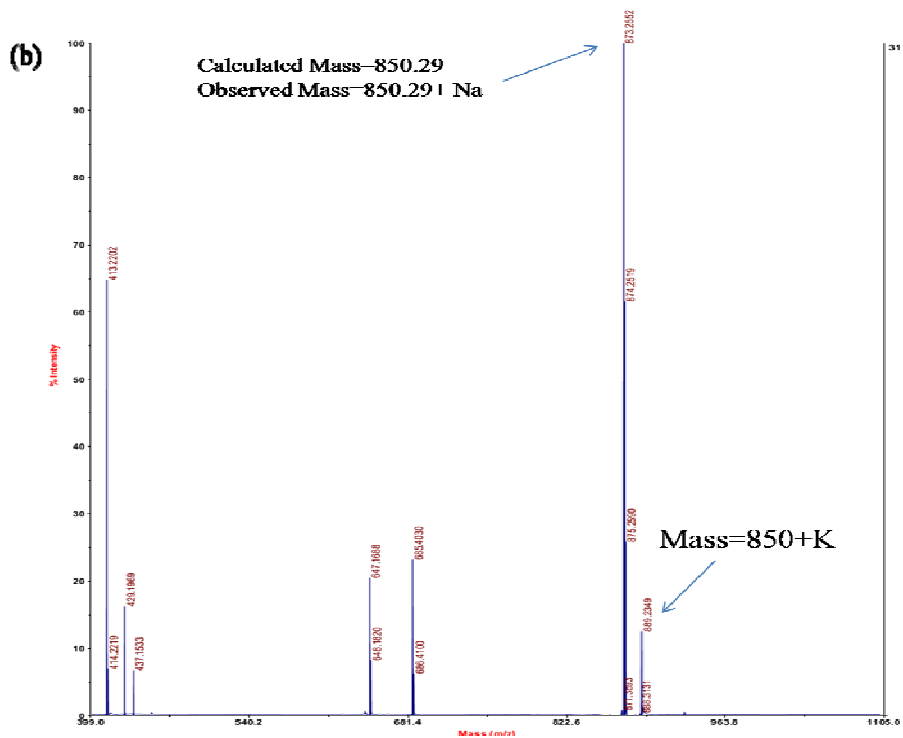


**Figure 3.1a:**  $^1\text{H}$  NMR spectrum of **PBITEG** cross-linker recorded in  $\text{CDCl}_3$ .

The single peak in MALDI spectra corresponds to the **PBITEG** cross-linker in **figure 3.1b**.



The two stage dispersion polymerization procedure that we followed was described in experimental section chapter 2. 3.3. The amounts of cross-linker was varied from 4.9 mM to 6.25 mM for **PBITEG** and 3.13 mM to 4.2 mM for **OPV** (0.13 to 0.51 wt % w.r.t. styrene) in the feed during the second stage of the polymerization. The content for the two stage dispersion polymerization are given below in the **Table 3.1**.

**Table 3.1: Two stage Dispersion Polymerization contents.**

Component	Material	Amount (gm)	Amount (gm)
		1 <sup>st</sup> Stage	2 <sup>nd</sup> Stage
Monomer	Styrene	1.89	1.89
Cross-linker	PBITEG/OPV	No	0.0024 to 0.0036 / 0.0021 to 0.0029
Medium	Ethanol	7.4	7.4
Stabilizer	PVP	0.25	No
Costabilizer	Triton X-100	0.08	No
Initiator	AIBN	0.060	No
Reaction time	8 hours	-	-
Rotation Speed	120 rpm	-	-

Two PS samples with single chromophore incorporation (either **OPV** or **PBITEG**) were also developed. The PS with **PBITEG** and **OPV** were named as the **PS-PBITEG-X-OPV-X**, where 'X' indicated the amount (in mM) of the respective cross-linker incorporated. The incorporation of the fluorophores were too low to be detected using NMR spectroscopic techniques; therefore, absorption spectroscopy was used to estimate their incorporation based on the molar extinction coefficient of the respective cross-linker (**PBITEG** = 80,600 LM<sup>-1</sup>cm<sup>-1</sup>, **OPV** = 36315 LM<sup>-1</sup>cm<sup>-1</sup>).<sup>47</sup> The extremely low incorporation (~10<sup>-7</sup> moles) of the cross-linkers enabled complete solubilization of the resulting lightly cross-linked polymers.<sup>49</sup> **Table 3.2** compares the moles of fluorophore taken in feed with their actual incorporation.

**Table 3.2:** Sample designation, number and weight average molar mass, polydispersity indices (PDI), yield and 5 wt % loss temperature of the **PS-PBITEG-X-OPV-X** based polymers.

Sample Name	Moles in feed ( $10^{-6}$ )	Moles Incorporated <sup>a</sup> ( $10^{-7}$ )	Yield (%)	$M_n^b$	$M_w^b$	PDI <sup>b</sup>	TGA <sup>c</sup> ( $T_d=5\%$ )
PS-PBITEG-6.25	3.7	6.25	93	45,900	96,800	2.1	345
PS-PBITEG-6.25- OPV-4.28	3.7 3.7	6.25 4.28	81	34,600	123,200	3.5	345
PS-PBITEG-4.98- OPV-3.6	3.7 4.3	4.98 3.6	90	28,500	101,700	3.5	345
PS-PBITEG-5.4- OPV-3.13	3.7 3.14	5.45 3.13	92	23,000	64,400	2.8	345
PS-PBITEG-7.4- OPV-3.71	4.3 3.7	7.4 3.71	81	27,300	115,900	4.2	345
PS-PBITEG-4.93- OPV-4.15	3.3 3.7	4.93 4.15	92	20,200	64,700	3.2	345
PS-PBITEG-3.84- OPV-4.15	2.8 3.7	3.84 4.15	86	27,900	94,800	3.4	345
PS-OPV-3.88	3.7	3.88	80	24,900	99,000	4	340
PS	-	-	90	40,200	1,24,800	3.1	320

- a) Measured in chloroform  
 b) Measured by size exclusion chromatography (SEC) in chloroform ( $\text{CHCl}_3$ ), calibrated with linear, narrow molecular weight distribution polystyrene standards.  
 c) TGA measurements at heating rate of  $10^\circ\text{C}/\text{min}$  under nitrogen.

### 3.4.2 Molecular weight determination and thermal properties of polymers

The molecular weight of the polymers was determined by SEC using chloroform as the eluent and the values are given in **Table 3.2**. For comparison the molecular weight details of PS alone prepared under identical conditions is also included in table 3.2. The GPC chromatogram is given in the **Figure 3.2**. It could be seen from the table that higher incorporation of the rigid cross-linker resulted in reduction in the  $M_w$  values. The thermal stability of the cross-linked polymers was determined by thermogravimetric analysis (TGA) carried out under nitrogen atmosphere. **Figure 3.3** gives the TGA plot and **table 3.2** lists the 5 weight % loss temperature which was observed at 324-345  $^\circ\text{C}$ .

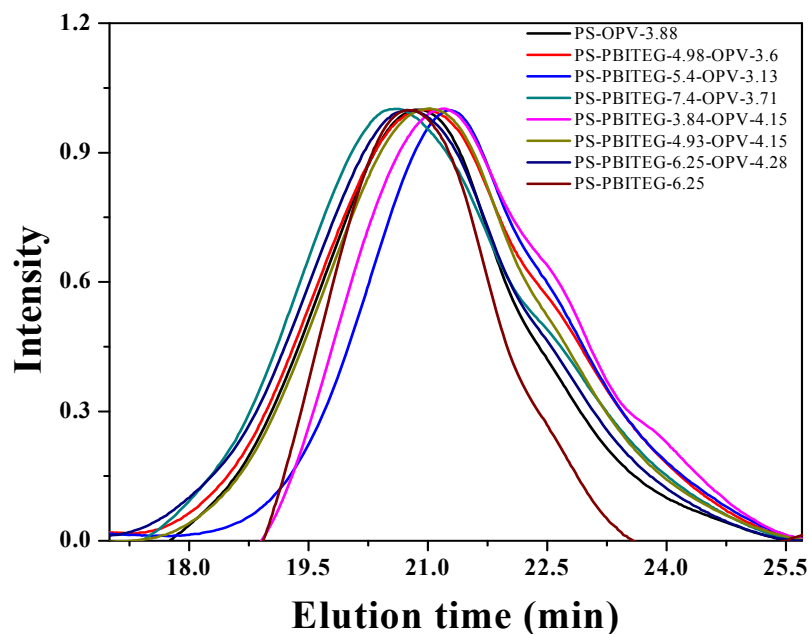


**Figure 3.2:** The size exclusion chromatography of all **PS-PBITEG-X-OPV-X** polymers.

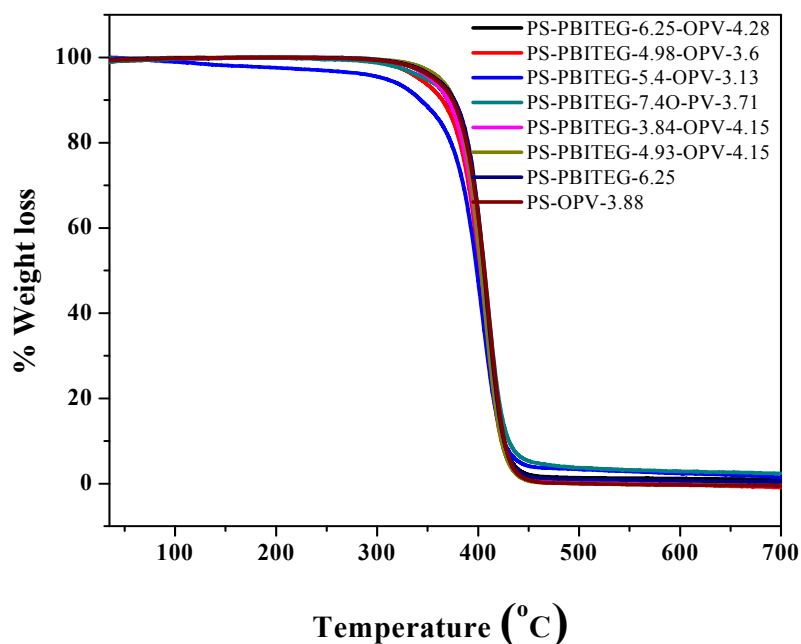


**Figure 3.3:** Thermogravimetric Analysis (TGA) of all **PS-PBITEG-X-OPV-X** samples.

### 3.4.3 Microscopic characterization of polymers

Dynamic light scattering (DLS) was used to estimate the particle size dispersity of the cross-linked PS beads, which were examined as ethanol dispersions.

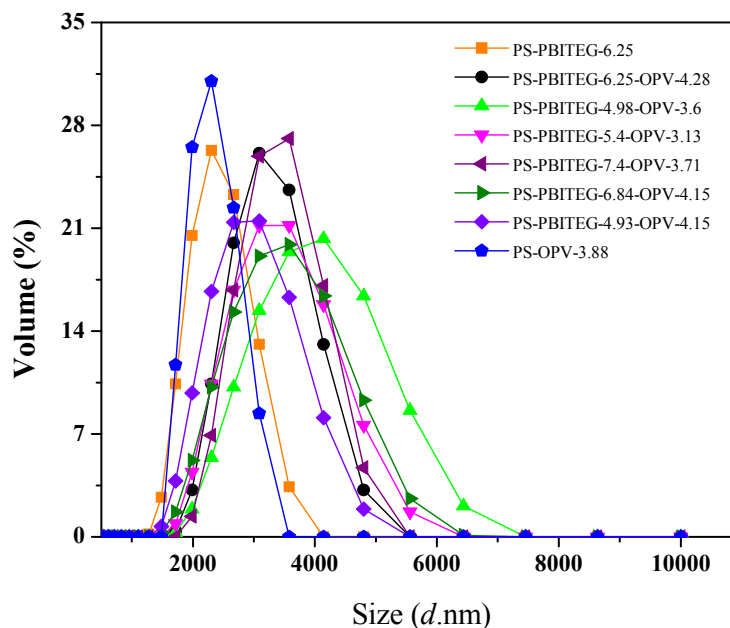


**Figure 3.4:** Volume - average size distribution of PS-PBITEG-X-OPV-X series in ethanol dispersion obtained by dynamic light scattering (DLS) analysis.

The single chromophore incorporated PS-OPV-3.88 and PS-PBITEG-6.25 samples showed similar average particle size of 2.3  $\mu\text{m}$ , while the PS beads with both chromophores exhibited slightly higher size distribution of 3.0 to 4.0  $\mu\text{m}$ . **Figure 3.4** shows the DLS plots for all the polymers.

SEM images of ethanol dispersed samples of **PS-PBITEG-X-OPV-X** on glass substrate is given in **Figure 3.5**.

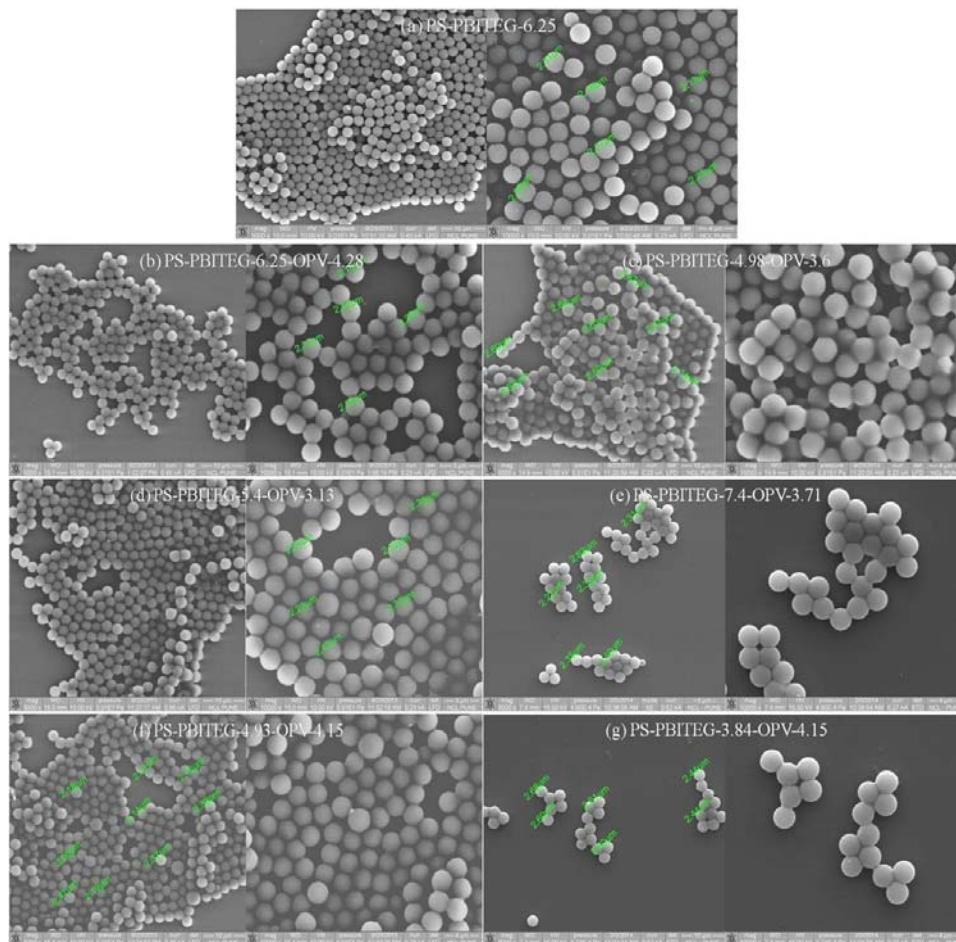


**Figure 3.5:** SEM image of **PS-PBITEG-X-OPV-X** series drop cast on silicon wafer (1 mg/2 ml ethanol dispersion).

It was clear that the particle size distribution observed in the SEM images was approximately similar to that obtained from DLS.

**Figure 3.6** shows the fluorescence microscope images of ethanol dispersed samples of **PS-PBITEGA-X-OPVA-X** series on glass substrate using DAPI (350-430 nm Blue), Alexa (488-520 Green) and Rhodamine (500-550 nm Red) filters. The merged image shows white light emission from the PS beads.

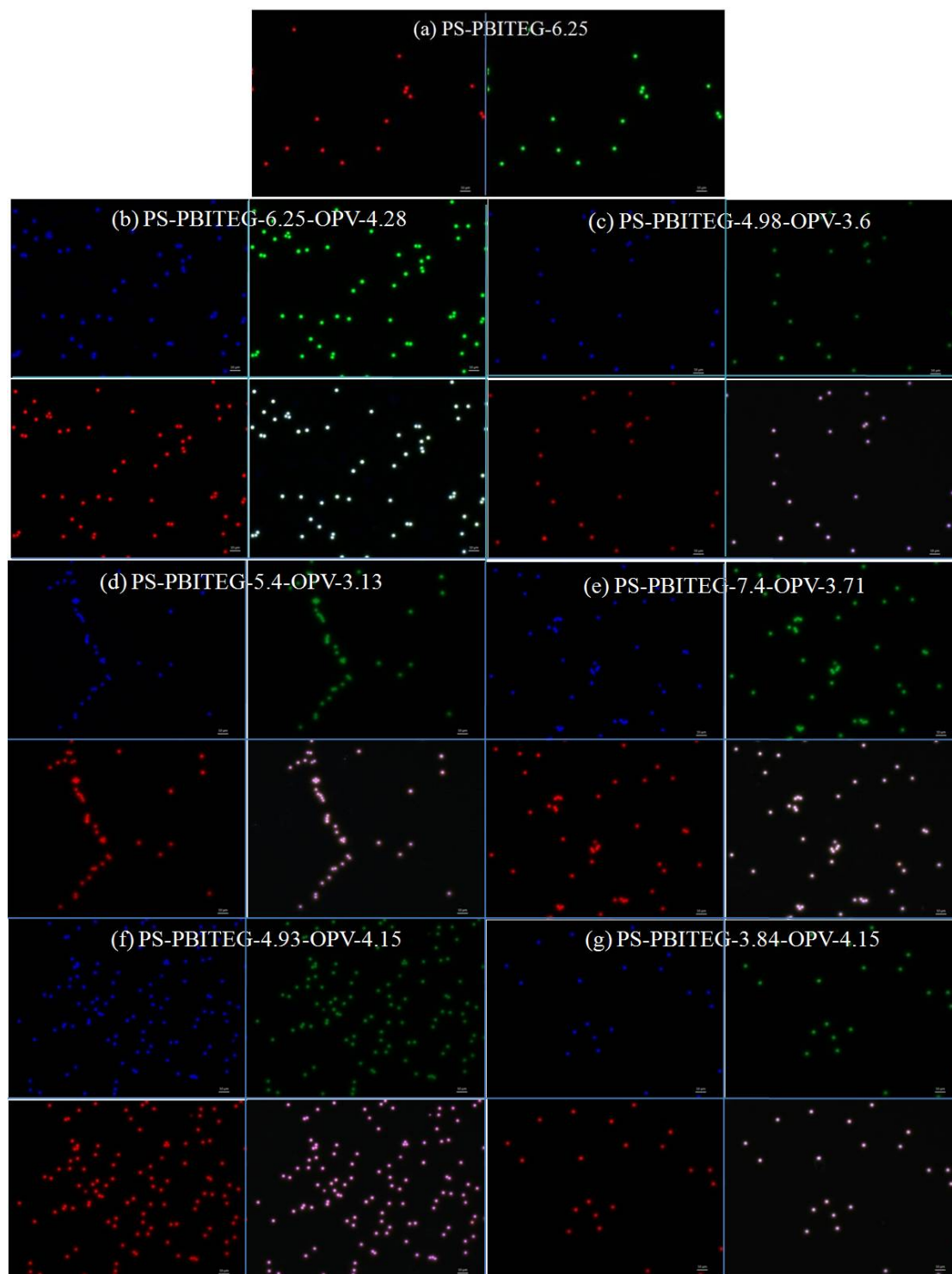


**Figure 3.6:** Fluorescence optical microscopy images of (a) PS-PBITEG-6.2 (b) PS-PBITEG-6.25-OPV-4.28 (c) PS-PBITEG-4.98-OPV-3.6 (d) PS-PBITEG-5.4-OPV-3.13 (e) PS-PBITEG-7.4-OPV-3.71 (f) PS-PBITEG-4.93-OPV-4.15 (g) PS-PBITEG-3.84-OPV-4.15 using



DAPI (350-430 nm Blue) Alexa (488-520 Green) and Rhodamine (480-580 nm Red) filters along with merged image.

The fluorescence microscope images also confirmed the size of the PS beads to be  $\sim 2.6 \mu\text{m}$ , consistent with the DLS and SEM observation.

### 3.4.4 Photophysical characterization

The absorption and emission spectra were recorded in the solid state in powder form for the polymers. **Figure 3.7** shows images taken of the polymers under a hand-held UV lamp **(a)** and the absorption spectrum of all the polymers in the powder form recorded in the reflectant mode **(b)**.

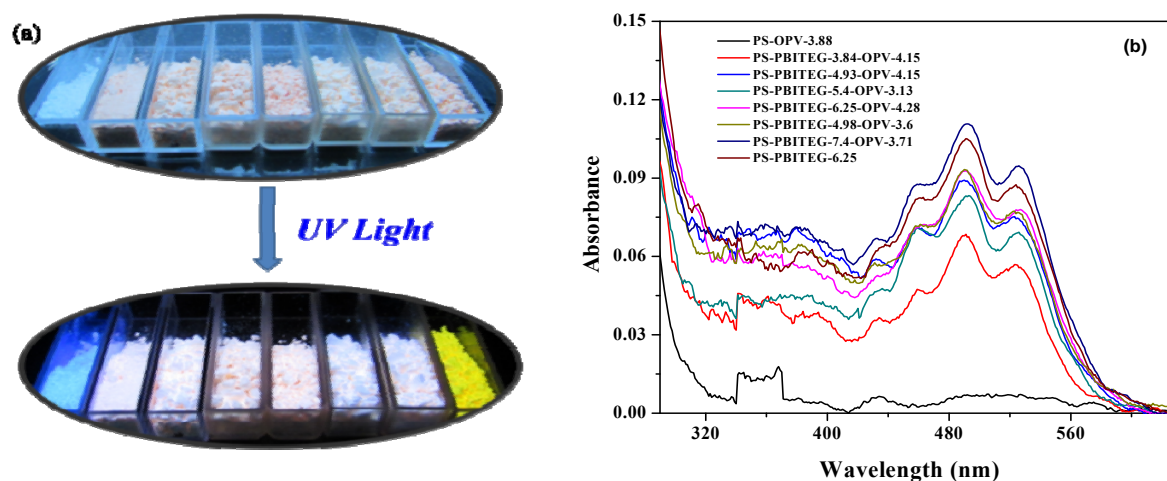


**Figure 3.7:** (a) The images of the powdered samples of all polymers **PS-PBITEG-X-OPV-X** under (top) normal and (bottom) UV light. (b) The solid state absorption spectra (recorded in the reflectance mode) of the **PS-PBITEG-X-OPV-X** samples with **PS-OPV-3.88** and **PS-PBITEG-6.25** also included for comparison.

**PS-OPV-3.88** exhibited blue light emission; **PS-PBITEG-6.25** had yellowish orange emission whereas the other polymers incorporating varying amounts of both fluorophore exhibited white light emission with varying shades of whiteness intensity. Both the measurements (a and b) supported the solid state emission from **PS-PBITEGA-X-OPV-X** series of polymers. **Figure 3.8a** shows the solid state (powder form) emission spectra of the

polymer **PS-PBITEG-6.25-OPV-4.28** upon excitation at 350 nm. It showed peaks corresponding to **OPV** as well as **PBITEG** emission in the range 350 to 500 nm and 520 to 675 nm respectively. The inset in the figure shows the photograph of the white light emission from the powder sample as observed under a hand-held UV lamp.

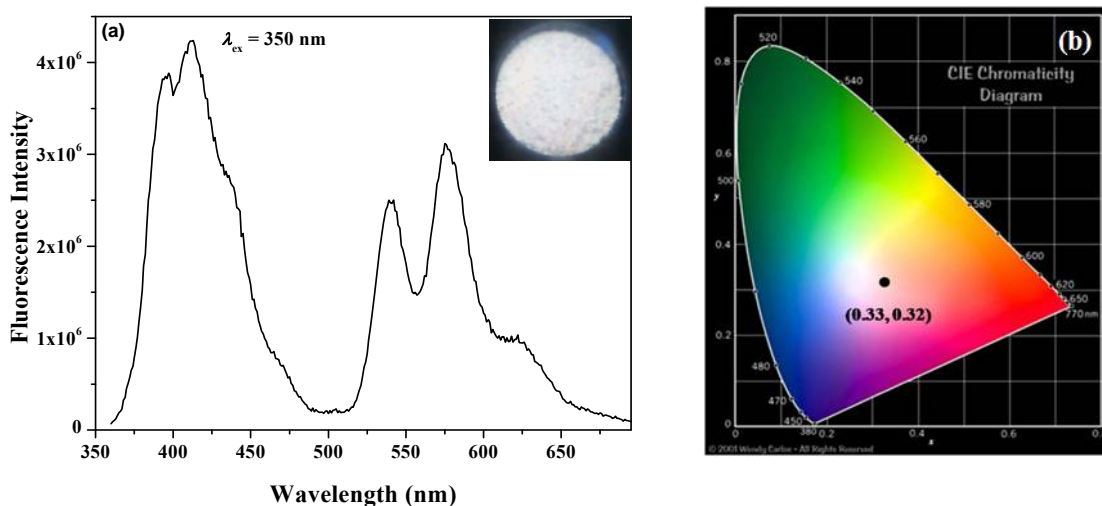


**Figure 3.8:** (a) Solid state (powder) emission spectra of the cross-linked **PS-PBITEG-X-OPV-X** series upon excitation at 350 nm and (b) the corresponding CIE coordinate diagram.

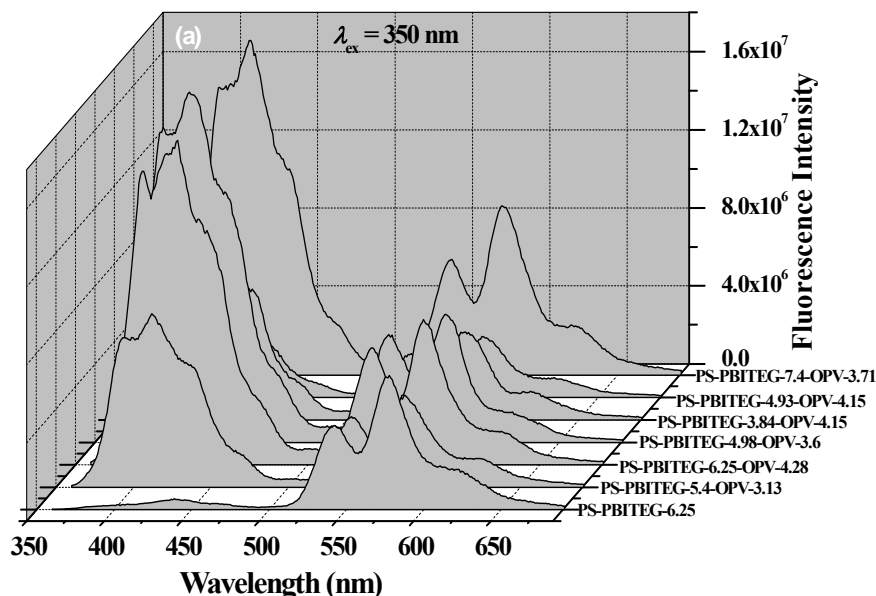


**Figure 3.9:** Solid state (powder) emission spectra of the cross-linked **PS-PBITEG-X-OPV-X** series upon excitation at 350 nm.

The purity of the white light emission was assigned in photochromic terms, as standardized by Commission Internationale d'Eclairage, and the CIE coordinates was obtained as (0.33, 0.32 : **figure 3.8b**), which was quite close to that of pure white light emission (0.33, 0.33). The emission in the powder form of all the PS samples upon excitation at 350 nm is given in **figure 3.9**.

The CIE color coordinates of all polymer from emission were also calculated and added in CIE chromaticity diagram which is given in **figure 3.10**.

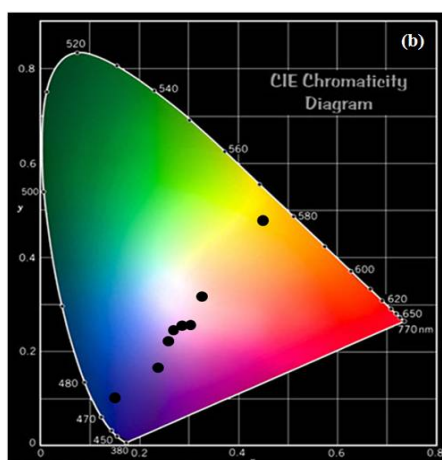


**Figure 3.10:** The CIE coordinate diagram for all the **PS-PBITEG-X-OPV-X** polymers.

The quantum yield for solid state emission  $\phi_{\text{powder}}$  was measured using an integrating-sphere Quanta  $\phi$  Horiba attachment with 490 nm excitation for **PBITEG** and 350 nm for **OPV** respectively and the values are given in **Table 3.4**. **PS-OPV-3.88** exhibited the quantum yield value of 0.72 ( $\lambda_{\text{exc}} = 350$  nm), while **PS-PBITEG-6.25** had a  $\phi_{\text{powder}}$  of 0.21 ( $\lambda_{\text{exc}} = 490$  nm). The polymers with varying incorporation of both fluorophores exhibited  $\phi_{\text{powder}}$  values ranging from 0.28 to 0.13 for blue **OPV** emission ( $\lambda_{\text{exc}} = 350$  nm; range 360-510 nm) and 0.26 to 0.21 for **PBITEG** emission in the range 500 to 700 nm ( $\lambda_{\text{exc}} = 490$  nm). It can be seen from **table 3.4** that the quantum yield for **PBITEG** emission was not much affected by the presence of the **OPV** chromophore, whereas considerable reduction was observed in the **OPV** emission when **PBITEG** was also incorporated into the PS backbone.

**Table 3.4:** Photoluminescence quantum yield in powder form and corresponding CIE Coordinates.

Sample Name	Solid State Quantum Yield ( $\phi$ )		CIE Color Coordinate	
	$\lambda_{\text{ex}} = 350 \text{ nm}$	$\lambda_{\text{ex}} = 490 \text{ nm}$	X	Y
OPV-Cross-linker	0.02	-	-	-
PBITEG-Cross-linker		0.06	-	-
PS-OPV-3.88	0.72	-	0.15	0.1
PS-PBITEG-6.25		0.21	0.45	0.48
PS-PBITEG-5.4-OPV-3.13	0.22 <sup>a</sup>	0.23 <sup>b</sup>	0.30	0.26
PS-PBITEG-6.25-OPV-4.28	0.13 <sup>a</sup>	0.23 <sup>b</sup>	0.33	0.32
PS-PBITEG-4.98-OPV-3.6	0.27 <sup>a</sup>	0.25 <sup>b</sup>	0.29	0.24
PS-PBITEG-3.84-OPV-4.15	0.28 <sup>a</sup>	0.26 <sup>b</sup>	0.26	0.22
PS-PBITEG-4.93-OPV-4.15	0.26 <sup>a</sup>	0.25 <sup>b</sup>	0.28	0.24
PS-PBITEG-7.4-OPV-3.71	0.18 <sup>a</sup>	0.21 <sup>b</sup>	0.30	0.26
PS-PBITEG-6.25+PS-OPV-3.88 (Physical Mix)	-	-	0.24	0.18

(a) Selected wavelength range : 360- 510 nm

(b) Selected wavelength range : 500- 700 nm

In order to understand the reason for the reduction in the **OPV** emission quantum yield, a physical mixture of the two PS polymers having single chromophore incorporation was studied. Thus, a 1:1 (w/w) physical mixture of the two polymers **PS-OPV-3.88** and **PS-PBITEG-6.25** was made and its solid state emission spectra was compared with that of the polymer having similar molar (covalent) incorporation of both the chromophores i.e **PS-PBITEG-6.25-OPV-4.28**. In **figure 3.11** the emission spectra of **PS-OPV-3.88**, **PS-PBITEG-6.25-OPV-4.28** and the physical mixture of **PS-OPV-3.88** and **PS-PBITEG-6.25** are compared. The same spectrum after normalization at the **OPV** emission maxima ~430 nm is also included in the figure. It could be clearly observed that a reduction in **OPV** emission intensity with a change in peak shape occurred in both the physical mixture (black line) and **PS-PBITEG-6.25-OPV-4.28** (magenta line) compared to the **OPV** alone polymer **PS-OPV-**

**3.88.** The figure also shows the emission from the **PBITEG** alone polymer i.e **PS-PBITEG-6.25** upon excitation at 350 nm (blue line) as well as 490 nm (green line). Excitation at 350 nm corresponding to the **OPV** absorption maxima also resulted in excitation of **PBITEG**; selective excitation of **OPV** was not possible in the system.

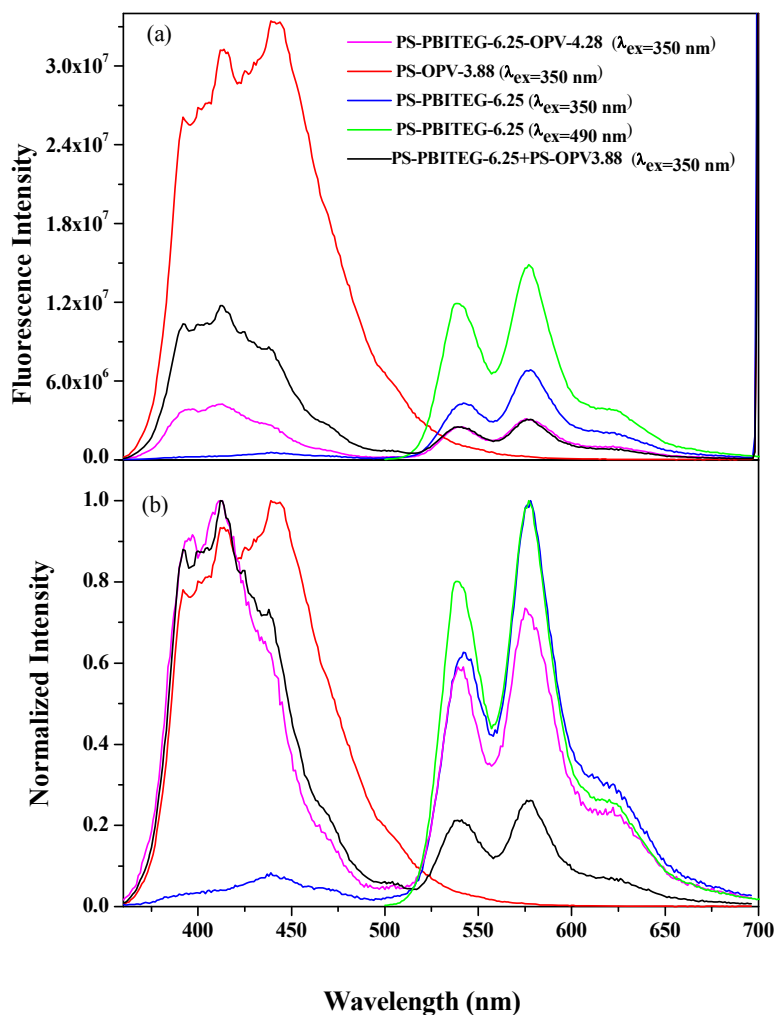


**Figure 3.11:** (a) Solid state emission spectra upon excitation at 350 nm for **PS-OPV-3.88**, **PS-PBITEG-6.25-OPV-4.28**, physical mixture of **PS-PBITEG-6.25+PS-OPV-3.88** along with that of **PS-PBITEG-3.2** (excitation at 490 nm) and (b) the same spectra after normalization at the OPV emission maxima of  $\sim 430$  nm.

**Figure 3.12a** (top) shows the excitation spectra of **PS-PBITEG-6.25-OPV-4.28**, **PS-PBITEG-6.25**, the physical mixture of **PS-OPV-3.88** and **PS-PBITEG-6.25+PS-OPV-3.88**, collected at 576 nm. With the excitation spectra collected for **PS-OPV-3.88** at 433 nm. The absence of **OPV** absorption from the **PS-PBITEG-6.25-OPV-4.28** as well as the physical mixture of **PS-OPV-3.88** and **PS-PBITEG-6.25** demonstrated the absence of energy transfer between the **OPV** and **PBITEG** chromophores. And it was clear from the comparison of excitation spectrum of all the polymers with **PS-OPV-3.88** and **PS-PBITEG-6.25+PS-OPV-4.28** that is given in the **figure 3.12.b** (bottom).

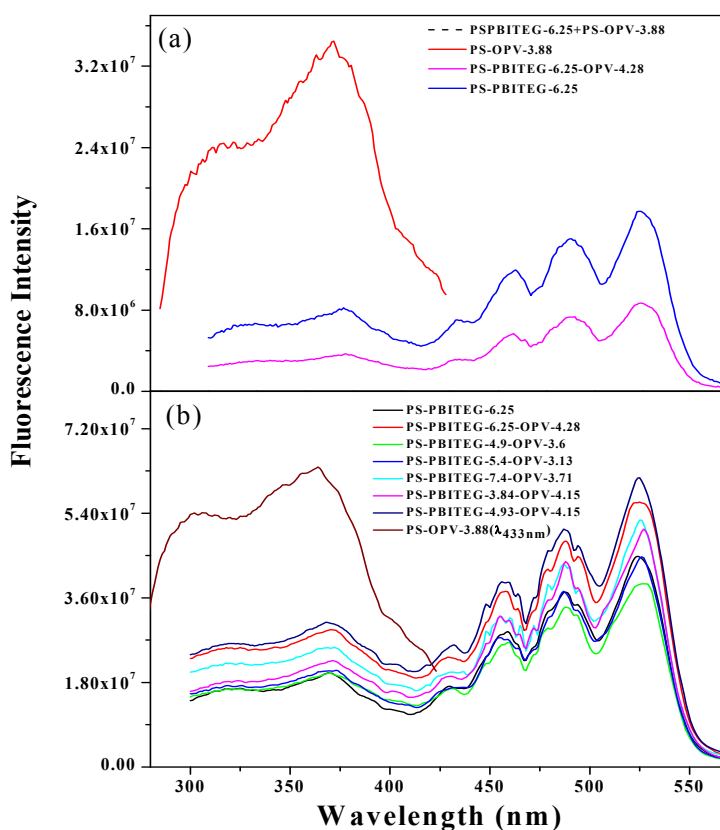


**Figure 3.12:** (a) Solid state excitation spectra collected at 433 nm for **PS-OPV-3.88** and at 576 nm for **PS-PBITEG-6.25-OPV-4.28**, **PS-PBITEG-6.25** with the physical mixture of **PS-PBITEG-6.25+PS-OPV-3.88** is also given for comparison (top). (b) The excitation spectrum of all **PS-PBITEG-X-OPV-X** polymes in solid state with excitation spectra of **PS-OPV-3.88** collected at 433 nm (bottom).

These facts suggested that energy transfer from **OPV** to **PBITEG** could not have been the reason for the observed change of shape of the OPV emission spectra as well as the observation of **PBITEG** emission upon excitation of the **OPV** chromophore. Fluorescence emission life time decay studies were undertaken by excitation using a LED of 340 nm and collecting the data at 412 nm.

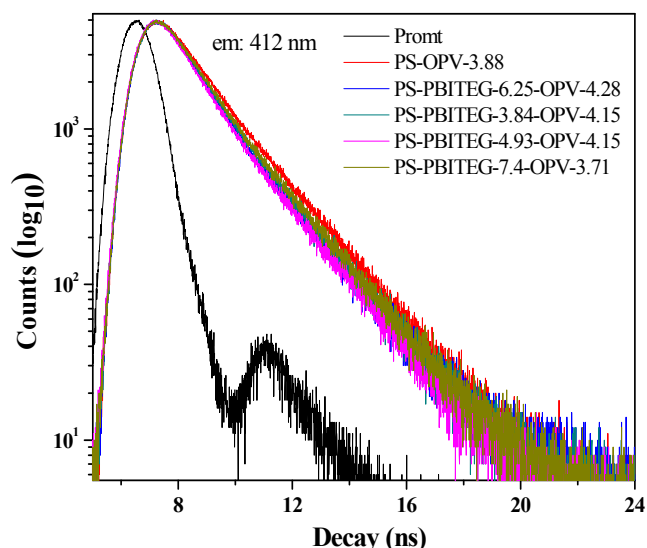


**Figure 3.13:** Fluorescence decay profiles (LED 340 nm, em: 412 nm) of **PS-OPV-3.88**, **PS-PBITEG-3.84-OPV-4.15**, **PS-PBITEG-4.93-OPV-4.15**, **PS-PBITEG-7.4-OPV-3.71** in the powder state.

Lifetime decay profiles of four polymers **PS-OPV-3.88**, **PS-PBITEG-3.84-OPV-4.15**, **PS-PBITEG-4.93-OPV-4.15**, **PS-PBITEG-7.4-OPV-3.71** in the powder state are shown in the above **Figure 3.13** and the fit values are given in **table 3.5**. Although the decay of all the polymers were best fitted using a triexponential fit, the most prominent species ( $\alpha_3 = 0.98$ ) in the **OPV** alone polymer – **PS-OPV-3.88** had a life time of 0.1 ns. The lifetime decay of the polymers with both **OPV** and **PBITEG** incorporation were complicated by more than two species which decayed with different lifetimes. The fact that selective excitation of **OPV** chromophore alone was not possible using excitation source near 340 nm could be the reason for the presence of multiple emitting species.

**Table 3.5:** Parameters ( $\tau$ : decay time,  $\alpha$ : pre-exponential factor,  $\chi^2$ : chi-squared value) retrieved from the tri-exponential fit for **PS-PBITEG-X-OPV-X** based polymers in the powder form obtained by using nano LED 340 nm for excitation and 412 nm for observation.

Polymer	$\tau_1 (\alpha_1)$ ns	$\tau_2 (\alpha_2)$ ns	$\tau_3 (\alpha_3)$ ns	$\chi^2$
PS-OPV-3.88	1.02 (0.01)	1.97 (0.01)	0.1 (0.98)	1.12
PS-PBITEG-6.25-OPV-4.28	0.98 (0.32)	1.98 (0.17)	0.10 (0.51)	1.15
PS-PBITEG-3.84-OPV-4.15	3.49 (0.00)	1.64 (0.05)	0.02 (0.95)	1.29
PS-PBITEG-4.93-OPV-4.15	1.05 (0.26)	1.84 (0.24)	0.16 (0.50)	1.04
PS-PBITEG-7.4-OPV-3.71	0.97 (0.28)	1.81 (0.21)	0.18 (0.50)	1.12

Thus, the fluorescence life time decay data could not give a conclusive evidence for absence of energy transfer. However, one more indirect evidence for absence of energy transfer to be the cause of the reduction in fluorescence emission intensity and change in shape of emission from **OPV** was obtained by comparing the emission spectra of the **OPV** alone polymer in the form of thin drop cast film as well as in powder. **Figure 3.14** compares the normalized (at 412 nm) emission spectra of the **OPV** alone polymer **PS-OPV-3.88** collected both in the powder form as well as drop cast from chloroform. A change in peak shape as well as reduction in fluorescence intensity was observed for the chloroform drop cast film similar to that observed for the **PS-OPV-PBITEG** polymers. This data indicated that the **OPV** chromophore was extremely sensitive to the surrounding and some changes in the packing might be the cause of this change in the shape of the emission spectra collected in the film compared to that in powder.<sup>50</sup> The influence of the aromatic styrene rings of the PS backbone affecting the packing of the OPV rings also cannot be ruled out. We had demonstrated previously that incorporation of the OPV cross-linker into a non-aromatic polymer backbone like that of Poly(methylmethacrylate) (PMMA) did not exhibit any shift or change of shape of the OPV chromophore absorption or emission in solution.<sup>47</sup> However, when **PBITEG** was also introduced into the backbone of PMMA along with **OPV** (details of synthesis is given in



experimental section), drastic changes in the emission of the **OPV** chromophore was observed in powder form.

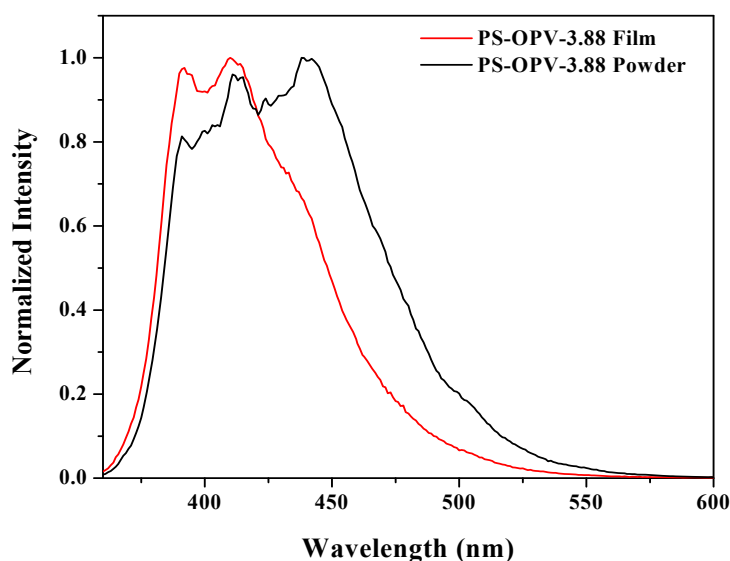


**Figure 3.14:** Comparison of solid state emission spectra of **PS-OPV-3.88** in the powder form and as drop cast film from  $\text{CHCl}_3$  upon excitation at 350 nm.

**Figure 3.15** compares the emission spectra recorded in the powder form for **PMMA-OPV** and **PMMA-PBITEG-OPV** polymers upon excitation at 350 nm.

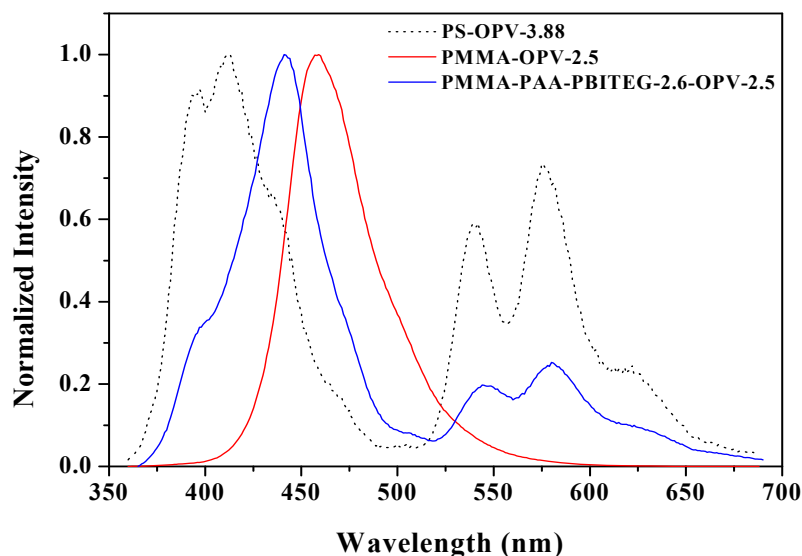


**Figure 3.15:** Comparison of solid state (powder) emission spectra of **PS-OPV-3.88** with that of **PMMA-OPV-2.5** and **PMMA-PAA-PBITEG-2.6-OPV-2.5** upon excitation at 350 nm.

The spectrum of **PS-OPV-3.88** is also given for comparison. Nearly ~15 nm blue shift was observed for the OPV emission in presence of PBITEG (458 nm for PMMA-OPV vs 440 nm for PMMA-PBITEG-OPV), although no shift was observed for the PBI emission. It was thus evident that OPV as a chromophore was extremely sensitive to its environment as well as packing, whether it was stacked tightly along with similar aromatic core like PS or packing influenced by the nature of the solvent from which it was drop cast to form film or by the presence of other chromophores like PBI in the vicinity. This change in the environment or packing was reflected as a change in the extent of aggregation leading to fluorescence quenching and change in spectral pattern in the powder form in the **PS-PBITEG-X-OPV-X** polymers.

### 3.5 Conclusion

In summary, we have demonstrated single polymer based white light and multicolor emission in the solid state. Fluorescent polystyrene microbeads in the size range of 2-3  $\mu\text{m}$  were produced by incorporating orange-red emitting perylenebisimide and blue emitting oligo (*p*-phenylenevinylene) as cross-linkers into the polymer backbone. Pure white light emission in the powder form with CIE coordinates (0.33, 0.32) was achieved with one of the PS samples having appropriate amounts of **OPV** and **PBITEG (PS-PBITEG-6.25-OPV-4.28)**. The two-stage dispersion polymerization method along with the concept of fluorophore as covalent cross-linker for chromophore isolation affords an easy and scalable method to produce fluorescently labeled polymer particles with controlled size from commercial polymers like PS.

### 3.6 Reference

- (1) Schubert, E. F.; Kim, J. K. *Science*, **2005**, *308*, 1274–1278.
- (2) Han, M.; Gao, X.; Su, J. Z.; Nie, S. *Nat. Biotechnol.* **2001**, *19*, 631–635.
- (3) Hudson, Z. M.; Lunn D. J.; Winnik, M. A.; Manners, I. *Nat. Commun.* **2014**, 1–8.
- (4) Sukhanova, A.; Nabiev, I. *Crit. Rev. Oncol./Hematol.* **2008**, *68*, 39–59.
- (5) Huang, C-H.; Chiu, Yi-Chen.; Yeh, Y. T.; Chan, T-S.; Chen, T-M. *ACS Appl. Mater. Interfaces* **2012**, *4*, 6661–6668.
- (6) Babu, S. S.; Praveen, V. K.; Ajayaghosh, A. *Chem. Rev.* **2014**, *114*, 1973–2129.
- (7) Wu, H.; Ying, L.; Wei, Y.; Cao, Y. *Chem. Soc. Rev.* **2009**, *38*, 3391–3400.
- (8) D’Andrade B. W.; Forrest, S. R. *Adv. Mater.* **2004**, *16*, 1585–1595.
- (9) Fang, X.; Roushan, M.; Zhang, R.; Peng, J.; Zeng, H.; Li, J. *Chem. Mater.* **2012**, *24*, 1710–1717.
- (10) Yan, D.; Lu, J.; Ma, J.; Wei, M.; Evans, D. G.; Duan, X. *Angew.Chem. Int. Ed.* **2011**, *50*, 720–723.
- (11) Farinola, G. M.; Ragni, R. *Chem. Soc. Rev.* **2011**, *40*, 3467–3482.
- (12) Kamtekar, K. T.; Monkman, A. P.; Bryce, M. R.; *Adv. Mater.* **2010**, *22*, 572–582.
- (13) <http://hyperphysics.phy-astr.gsu.edu/hbase/vision/cie.html#c2> (accessed on June 12, 2010).
- (14) Chen, Z.; Grumstrup, E. M.; Gilligan, A. T.; Papanikolas, J. M.; Schanze, K. S. *J. Phys. Chem. B* **2014**, *118*, 372–378.
- (15) Ajayaghosh, A.; Praveen, V. K.; Vijayakumar C. *Chem. Soc. Rev.*, **2008**, *37*, 109–122.
- (16) Maiti, D. K.; Bhattacharjee, R.; Datta, A.; Banerjee, A. *J. Phys. Chem. C* **2013**, *117*, 23178–23189.
- (17) Wang, T.; Chirmanov, V.; Chiu, W. H. M.; Radovanovic, P. V. *J. Am. Chem. Soc.* **2013**, *135*, 14520–14523.
- (18) Zhang, X.; Görl D.; Würthner F. *Chem. Commun.* **2013**, *49*, 8178–8180.
- (19) Vijayakumar, C.; Sugiyasu, K.; Takeuchi, M. *Chem. Sci.* **2011**, *2*, 291–294.
- (20) Roushan, M.; Zhang, X.; Li, J. *Angew. Chem. Int. Ed.* **2012**, *51*, 436–439.
- (21) Chang, Y-T.; Chang, J-K.; Lee, Yi-T.; Wang, Po-S.; Wu, J-L.; Hsu, Che-C.; Wu, I-W.; Tseng, Wei-H.; Pi, T-W.; Chen, C-T.; et al. *ACS Appl. Mater. Interfaces* **2013**, *5*, 10614–10622.

- (22) Wang, X.; Chang, Yi-Lu.; Lu, J-S.; Zhang T.; Lu, Z-H.; Wang, S. *Adv. Funct. Mater.* **2014**, *24*, 1911–1927.
- (23) Liang, R.; Yan, D.; Tian, R.; Yu, X.; Shi, W.; Li, C.; Wei, M.; Evans, D. G.; Duan, X. *Chem. Mater.* **2014**, *26*, 2595–2600.
- (24) Sohn, I. S.; Unithrattil, S.; Im, W. B. *ACS Appl. Mater. Interfaces* **2014**, *6*, 5744–5748.
- (25) Bairi, P.; Roy, B.; Chakraborty, P.; Nandi, A. K. *ACS Appl. Mater. Interfaces* **2013**, *5*, 5478–5485.
- (26) Chen, Q.; Zhang, D.; Zhang, G.; Yang, X.; Feng, Y.; Fan, Q.; Zhu, D. *Adv. Funct. Mater.* **2010**, *20*, 3244–3251.
- (27) Sun C-Y.; Wang, X-L.; Zhang, Xi.; Qin, C.; Li, P.; Su, Z-M.; Zhu, D-X.; Shan, G-G.; Shao, K-Z.; Wu, H.; Li, J. *Nat. Commun.* **2013**, 1–8.
- (28) Giansante, C.; Raffy, G.; Schäfer, C.; Rahma, H.; Kao, M-T.; Olive, A. G. L.; Guerzo, A. D. *J. Am. Chem. Soc.* **2011**, *133*, 316–325.
- (29) Narayana, Y. S. L. V.; Basak, S.; Baumgarten, M.; Müllen, K.; Chandrasekar, R. *Adv. Funct. Mater.* **2013**, *23*, 5875–5880.
- (30) Tseng, K-P.; Fang, F-C.; Shyue, J-J.; Wong, K-T.; Raffy, G.; Guerzo, A. D.; Bassani, D. M. *Angew. Chem. Int. Ed.* **2011**, *50*, 7032–7036.
- (31) Balamurugan, A.; Reddy, M. L. P.; Jayakannan, M. *J. Phys. Chem. B* **2009**, *113*, 14128–12138.
- (32) Huang, C-H.; Liu, Wei-R.; Chen, T-M.; *J. Phys. Chem. C* **2010**, *114*, 18698–18701.
- (33) Dukes, A. D.; Samson, P. C.; Keene, J. D.; Davis, L. M.; Wikswo, J. P.; Rosenthal, S. J. *J. Phys. Chem. A* **2011**, *115*, 4076–4081.
- (34) Ego, C.; Marsitzky, D.; Becker, S.; Zhang, J.; Grimsdale, A. C.; Mullen, K.; MacKenzie, J. D.; Silva, C.; Friend, R. H. *J. Am. Chem. Soc.* **2003**, *125*, 437–443.
- (35) Liu, J.; Guo, X.; Bu, L.; Xie, Z.; Cheng, Y.; Geng, Y.; Wang, L.; Jing, X.; Wang, F. *Adv. Funct. Mater.* **2007**, *17*, 1917–1925.
- (36) Abbel, R.; Weegen, van der Weegen, R.; Pisula, W.; Surin, M.; Leclre, P.; Lazzaroni, R.; Meijer, E. W.; Schenning, A. P. H. *J. Chem. Eur. J.* **2009**, *15*, 9737–9746.
- (37) Praveen, V. K.; Ranjith, C.; Bandini, E.; Ajayaghosh A.; Armaroli, N. *Chem. Soc. Rev.* **2014**, *43*, 4222–4242.

- (38) Tu, G.; Mei, C.; Zhou, Q.; Cheng, Y.; Geng, Y.; Wang, L.; Ma, D.; Jing, X.; Wang, F. *Adv. Funct. Mater.* **2006**, *16*, 101–106.
- (39) Abbel, R.; Grenier, C.; Pouderoijen, M. J.; Stouwdam, J. W.; Leclère, P. E. L. G.; Sijbesma, R. P.; Meijer, E. W.; Schenning, A. P. H. J. *J. Am. Chem. Soc.* **2009**, *131*, 833–843.
- (40) Yang, Z.; Dasog, M.; Dobbie, A. R.; Lockwood, R.; Zhi, Y.; Meldrum, A.; Veinot, J. G. C. *Adv. Funct. Mater.* **2014**, *24*, 1345–1353.
- (41) Harun, N. A.; Benning, M. J.; Horrocks, B. R.; Fulton, D. A.; *Nanoscale*, **2013**, *5*, 3817–3827.
- (42) Wu, X. L.; Fan, J. Y.; Qui, T.; Yang, X.; Siu, G. G.; K. C.; Chu, P. K. *Phy. Rev. Lett.* **2005**, *94*, 026102.
- (43) Lee, H. M.; Kim, Y. N.; Kim, B. H.; Kim, S. O.; Cho, S. O. *Adv. Mater.* **2008**, *20*, 2094–2098.
- (44) Wang, R.; Peng, J.; Qiu, F.; Yang, Y. *Chem. Commun.* **2011**, *47*, 2787–2789.
- (45) Yoo, S.; An, S. J.; Choi, G. H.; Kim, K. S.; Yi, G.-C.; Zin, W.-C.; Jung, J. C.; Sohn, B.-H. *Adv. Mater.* **2007**, *19*, 1594–1596.
- (46) Park, S.; Kwon, J. E.; Kim, S. H.; Seo, J.; Chung, K.; Park, S.-Y.; Jang, Du.-J.; Medina, B. M.; Gierschner, J.; Park, S. Y. *J. Am. Chem. Soc.* **2009**, *131*, 14043–14049.
- (47) Sonawane, S. L.; and Asha, S. K. *ACS Appl. Mater. Interfaces* **2013**, *5*, 12205–12214.
- (48) Wang, W.; Li, L.-S.; Helms, G.; Zhou, H.-H.; Li, A. D. Q. *J. Am. Chem. Soc.*, **2003**, *125*, 1120–1121.
- (49) Amjad, Z. *Kluwer Academic Publishers* **2002**.
- (50) Amrutha, S. R.; Jayakannan, M. *Macromolecules* **2007**, *40*, 2380–2391.

**-:- Chapter 4 -:-**

---

---

***Fluorescent Polystyrene Microbeads as Invisible Security Ink and Optical Vapor Sensor for Nitro compounds***

---

---

**This chapter has been adapted from the following paper:**

“Sonawane, S. L.; Asha S. K. *ACS Appl. Mater. Interfaces*, **2016**, 8, 10590-10599.

**DOI:** 10.1021/acsami.5b12325.



#### 4.1 Abstract

Color-tunable solid state emitting polystyrene (PS) microbeads were developed by dispersion polymerization, which showed excellent fluorescent security ink characteristics along with sensitive detection of vapors of nitro aromatics like 4-nitro toluene (4-NT). The fluorophores pyrene and perylenebisimide (**PBI**) were incorporated into the PS backbone as acrylate monomer and acrylate cross-linker respectively. Solid state quantum yields of 94 % and 20 % were observed for the pyrene and perylenebisimide respectively in the **PS/Py** and **PS/PBI** polymers. The morphology and solid state fluorescence was measured by SEM, fluorescence microscopy, absorbance and fluorescence spectroscopy techniques. The ethanol dispersion of the polymer could be used directly as a fluorescent security ‘invisible’ ink which became visible only under ultraviolet light. The color of the ink could be tuned depending on the amounts of the pyrene and perylenebisimide incorporated with blue and orange-green for pyrene alone or perylenebisimide alone beads respectively and various shades in between including pure white for beads incorporating both the fluorophores. More than 80 % quenching of pyrene emission was observed upon exposure of the polymer in the form of powder or as spin coated films to the vapors of 4-NT while the emission of perylenebisimide was unaffected. The limit of detection was estimated at  $10^{-5}$  moles (2.7 ppm) of 4-NT vapors. The ease of synthesis of the material along with its invisible ink characteristics and nitro aromatic vapor detection opens up new opportunities for exploring the application of these PS based materials as optical sensors and fluorescent ink for security purposes.



## 4.2 Introduction

Solid state luminescent materials (organic, inorganic and polymers) have tremendous demand in the field of material science because of their high impact in applications like solid state light emitters, bio and chemosensor, security and color tuning material for optical recording etc.<sup>1-3</sup> Functional materials including  $\pi$ -conjugated electron rich small molecules<sup>4</sup> polyelectrolyte,<sup>5</sup> quantum dots,<sup>6</sup> microporous metal-organic frameworks (MOFs),<sup>7</sup> polyrotaxane co-ordination polymers<sup>8</sup> conjugated polymers based on polyfluorenes, poly (phenylenevinylene)s (PPV) and oligo (*p*-phenylenevinylene) (OPV),<sup>9-10</sup> molecularly imprinted polymers (MIPs),<sup>11</sup> etc have been developed as high-performance fluorescence sensing materials. Although these are promising materials, the effort involved in their synthesis makes them less favorable. Fluorescent polymeric microspheres with controlled particle size, high photostability, tunable emission properties and thermal stability make them suitable as micro or nano sensors for analysis and device fabrication.<sup>12-13</sup> For instance, M. A. Winnik et. al. reported lanthanide metal encoded polystyrene microbeads where the post-functionalization of fluorescent microbeads with analyte was applied for highly multiplexed bioassay.<sup>14</sup> Fluorescent microbeads are usually synthesized by physical entrapment of dye in a polymer matrix such as poly (methyl methacrylate),<sup>15</sup> polysilane,<sup>16</sup> polyvinyl chloride, polystyrene,<sup>17</sup> and cellulose acetate.<sup>18</sup> Research from the group of D. R. Walt et.al. and O. S. Wolfbeis et.al. have demonstrated the applications of fluorescent microspheres for different types of sensors like high density sensing and suspension array, bar-coding, and in optical fiber sensors as an artificial nose.<sup>19-21</sup> However, dye leakage and low photostability limits the utility of the fluorophore entrapped polymer in applications involving long time fluorescence monitoring.<sup>22-23</sup>

Pyrene and Perylenebisimide are well-studied fluorophores due to their outstanding properties such as intrinsic high fluorescence quantum yield and good photostability. They have been explored widely as a light emitting and sensing material.<sup>24-25</sup> Pyrene as a fluorophore has been extensively investigated in sensor applications including detection of explosives based on 'nitroaromatics'.<sup>26-27</sup> The electron deficient nature of the nitroaromatic molecules like trinitrotoluene (TNT), dinitrotoluene (DNT) and nitrotoluene (NT) enables donor-acceptor interactions with electron rich  $\pi$ -aromatic donors like pyrene leading to the quenching of fluorescence of the latter.<sup>28-29</sup> Several pyrene based small molecule sensors

have been reported in the last 15 years which were designed specifically for detection of explosives.<sup>30</sup> Vapor based sensing of explosives is highly desirable as it avoids leakage as well as evaporation of volatile solvents that can occur while handling solutions. The vapors of the explosives can diffuse into the polymer film where it comes in contact with the sensor moiety which will convey the signal as a variation in its emission characteristics. A good solid-state quantum yield is a key factor for an efficient chemosensor for vapor analytes.<sup>31-32</sup> There are several reports where pyrene was doped in a polymer matrix and the excimeric emission was utilized for the detection of vapors of nitroaromatics. For instance, a recent literature report explained solid state sensing of nitro explosive where the film was prepared by electro spinning pyrene with polystyrene in the presence of tetrabutylammonium hexafluorophosphate.<sup>33</sup> Yu Lei et. al. reported self-assembled fluorescent three dimensional nanostructured films of polystyrene and pyrene by dip-coating process for explosives detection.<sup>34</sup> Another recent report described highly fluorescent pyrene functionalized polystyrene nanofibers that were used for the detection of TNT, where a significant color change was observed upon 30 minutes exposure to vapors of TNT.<sup>35</sup> Bayindir et. al. reported pyrene doped mesoporous ormosil films for the detection of nitro explosives.<sup>36</sup>

The last two chapters reported an efficient approach for incorporation of fluorophores into the back bone of polymers like polystyrene by a two stage dispersion polymerization methodology.<sup>37-38</sup> In the present chapter, varying amounts of pyrene acrylate (**Py**) was introduced into the dispersion polymerization medium in the second stage followed by **PBI** cross-linker during the third stage. The polymers were applied for vapor phase sensing of nitroaromatics and as ‘invisible security ink’, which was invisible under natural lighting but became visible in different hues under UV lighting.

### 4.3 Experimental methods

**4.3.1 Materials:** Perylene-3, 4, 9, 10-tetracarboxylic dianhydride (PTCDA), zinc acetate, imidazole, polyvinylpyrrolidone (PVP, Mw 360,000 g/mol), acrylic acid, 1-Pyrenemethanol, DMAP (dimethyl amino pyridine), 1,3 dinitrobenzene (1,3-DNB), 2,4-Dinitrophenol (2,4-DNP), 2,4-Dinitrotoluene (2,4-DNT), 2,6-Dinitrotoluene (2,6-DNT), 4-Nitrophenol (4-NP) and 4-Nitrotoluene (4-NT) were purchased from Aldrich and used without further purifications. Styrene purchased from Aldrich was washed with sodium hydroxide and then

with water, after which it was dried overnight over calcium chloride and vacuum distilled before use. Tetrahydrofuran (THF), dichloromethane (DCM), and triethyl amine were purchased from Merck and purified using standard procedures. Triton X-100 (70% solution in water) and 2, 2'-azobis-(isobutyronitrile) (AIBN) were purchased from Merck. AIBN was recrystallized from Methanol before use.

#### **(a) Preparation of Sample for vapor Sensing**

2-3 mg of the polymer powder sample was pasted on a transparent cello tape mounted on a small piece of cardboard sheet (1.25 cm to 2.5 cm) with a hole in the centre. For the preparation of films the polymer sample was dispersed/dissolved in ethanol/chloroform and spin coated on quartz plate using spin coater.

#### **(b) Fluorescence lifetime decay experiments**

The **Py** fluorescence lifetime was collected by excitation using 340 nm LED source and decay was collected at 395 nm. The **PBI** fluorescence lifetime was collected using an LED source of 460 nm and the collection wavelength was 530 nm.

#### **(c) Fluorescence quenching experiments**

The fluorescence quenching experiments was conducted using a similar method reported in literature.<sup>36</sup> The saturated vapor of the required nitro compound was generated by placing powder samples of the respective nitro aromatic compound inside a sealed chamber for 48 h. For the sensing experiment, the polymer sample in the form of film (quartz plate) or powder (sample on cello tape) was inserted into the chamber in such a way as to avoid direct contact with the nitro compound. The powder sample holder was then exposed to vapor of 4-NT and time dependent emission spectra were measured. The sample was taken out and fluorescence spectra recorded at different time intervals. Fluorescence emission spectra were recorded in the range of 353–690 nm using  $\lambda_{\text{excitation}} = 343$  nm for **Py** and 500–700 nm using  $\lambda_{\text{excitation}} = 490$  nm for **PBI**. The quenching efficiency was defined as  $(I_0 - I)/I_0 \times 100$ , where ( $I_0$ ) was the initial fluorescence intensity at 397 nm (for pyrene) or 532 nm (for perylenebisimide) before exposure of sample to the nitro aromatic vapor and ( $I$ ) was the corresponding fluorescence intensity at different exposure times.

### 4.3.2 Instrumentation:

$^1\text{H}$  and  $^{13}\text{C}$  NMR, GPC, MALDI, DLS, TGA, SEM, UV-Vis and steady-state fluorescence based characterization were carried out exactly as described in chapter two. The fluorescence optical microscopy images were recorded using EVOS fluorescence microscope (excitation wavelength: blue filter (transparent in the range 350–450 nm, for pyrene) green and red filter (transparent in the range 488–580 nm, for PBI). The samples were prepared by drop casting dilute dispersion of polymers in ethanol on glass plate and covering with cover slip.

### 4.3.3 General procedures

#### (i) Synthesis of Pyrene Acrylate (Py):

In a 100 mL round-bottom flask, pyrene methanol (200 mg, 0.00085 mol) and  $\text{Et}_3\text{N}$  (0.77 mL, 0.0055 mole) along with catalytic amount of DMAP (dimethyl amino pyridine) was dissolved in dry THF (17 mL) under nitrogen atmosphere and stirred well at 0 °C for 15 minute. Acryloyl chloride (0.19 mL, 0.0023 mol) was taken in THF (3 mL) and added to the reaction mixture for a period of 15–20 min at 0 °C. The reaction was carried out for 4 hour at room temperature and monitored by TLC. The organic layer was evaporated and the compound was purified by column chromatography in 20% ethyl acetate/pet ether solvent combination. Yield = 185 mg (78%).  $^1\text{H}$  NMR (200 MHz,  $\text{CDCl}_3$ ,  $\delta$ ppm): 8.19-8.08 (m, 9H, Ar-H) 6.43 (dd, 2H, acrylic double bond), 6.19 (m, 2H, acrylic double bond), 5.87 (dd, 2H, acrylic double bond), 5.92 (s, 2H, Ar- $\text{CH}_2$ -O).  $^{13}\text{C}$  NMR (200 MHz,  $\text{CDCl}_3$ ) 166.3, 131.7, 131.1, 130.1, 130.6, 129.5, 128.6, 128.2, 127.8, 127.7, 127.3, 126, 125.5, 125.4, 124.6, 122.8, 64.9. MALDI-TOF-MS (Dithranol matrix):  $m/z$  calcd for  $\text{C}_{20}\text{H}_{14}\text{O}_2$ : 286.30; found 286.15 [ $\text{M}^+$ ].

#### (ii) Dispersion Polymerization procedure for the preparation of PS-Py-PBI-x:

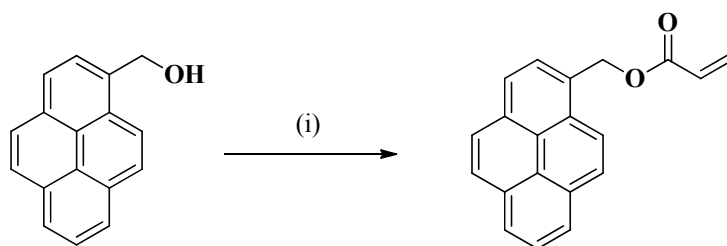
The stabilizer PVP (polyvinylpyrrolidone-360,000) (0.25 gm), costabilizer (Triton X-305) (0.086 gm), initiator (AIBN, 0.060 gm), styrene monomer (1.65 gm) and ethanol (7.4 gm) were added to a 100 mL three necked reaction flask equipped with a gas inlet, overhead stirrer and rubber septum. After a homogeneous solution formed at room temperature, the solution was deoxygenated by bubbling nitrogen gas at room temperature for at least 30 minutes. Then the flask was placed in a 70 °C oil bath and stirred mechanically at 120 rpm.

The pyrene acrylate (**Py**) was dissolved in styrene (1.43 gm) and ethanol (5.59 gm) and, added to the reaction mixture. In the third stage the cross-linker (**PBI**) was dissolved in the Styrene (0.666 gm) and ethanol (1.86 gm) at 60 °C under nitrogen. After the cross-linker had dissolved and the polymerization reaction had run for 15 minute, the hot styrene-cross-linker-ethanol solution was added into the reaction flask over a period of one hour (drop by drop addition) and polymerization was continued for 6 hours under continuous flow of nitrogen with overhead stirring. The precipitated polymer in the reaction medium was washed with 200 mL x 4 times of methanol and separated by centrifuge. The polymer was dried under vacuum at 50 °C for 6 hours.

## 4.4 Result and Discussion

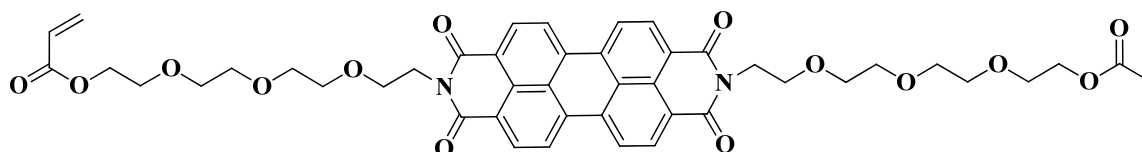
### 4.4.1 Synthesis and characterization

**Scheme 4.1a** shows the synthesis of blue emitting functional pyrene acrylate (**Py**) and the procedure is given in experimental section. The structure of orange-green emitting perylenebisimide (**PBI**) cross-linker is shown in scheme **4.1b**. The synthesis of **PBI** is reported in chapter three.<sup>38</sup>



**Scheme 4.1a:** Synthesis of Pyrene acrylate monomer (**Py**).

**Reagents:** (i) Acryloyl Chloride, DMAP, THF, Et<sub>3</sub>N, 0-25 °C, 5 hours, N<sub>2</sub>.



**Scheme 4.1b:** Structure of perylenebisimide based cross-linker (**PBI**).

The structural characterization details of **Py** is given in the figure 4.1a and b.

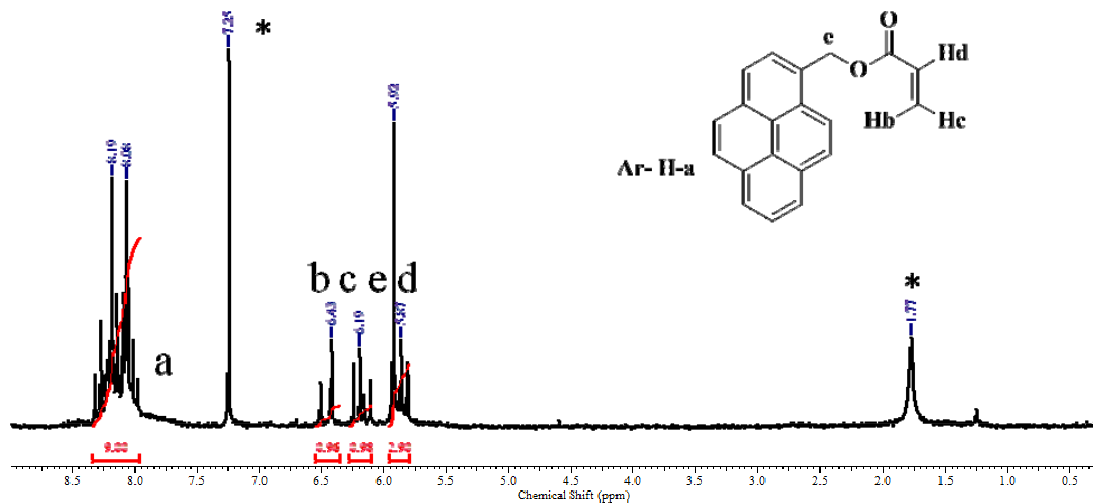


**Figure 4.1a:**  $^1\text{H}$  NMR spectrum of Pyrene acrylate (**Py**) recorded in  $\text{CDCl}_3$ .

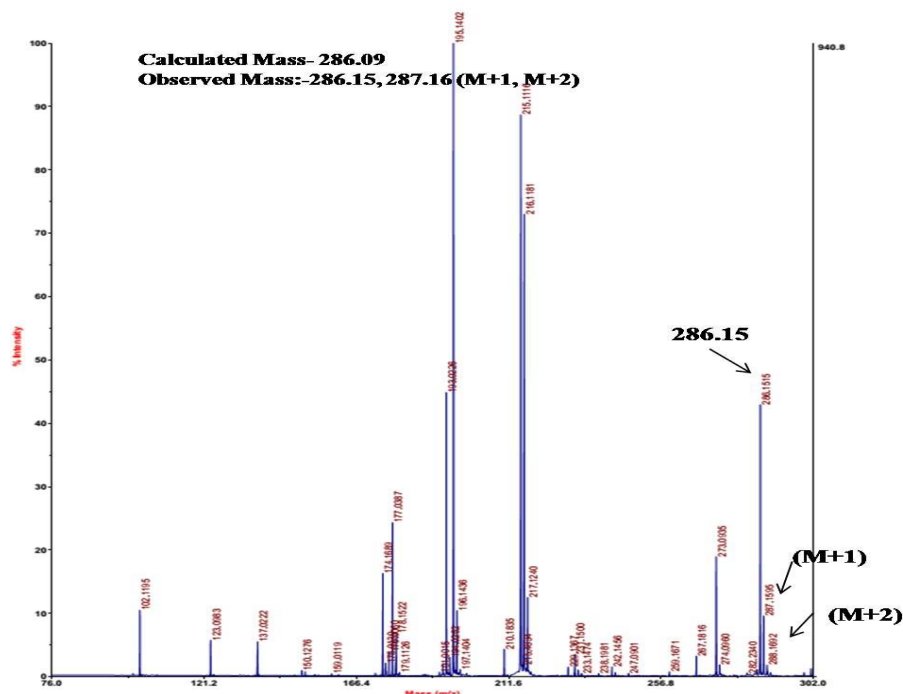


**Figure 4.1b:** MALDI-TOF spectrum of Pyrene acrylate (**Py**).

Solid state emitting PS microbeads were synthesized by three-stage dispersion polymerization, where the pyrene acrylate was added in the second stage after particle

nucleation and the **PBI** cross-linker was added in the third stage. The procedure and amounts of fluorophores used is given in **table 4.1**.

**Table 4.1:** Dispersion Polymerization contents

Component	Material	Amount (gm)	Amount (gm)	Amount (gm)
		1 <sup>st</sup> Stage	2 <sup>nd</sup> Stage	3 <sup>rd</sup> Stage
Monomer	Styrene	1.65	1.43	0.666
Co-monomer	Pyrene Acrylate	No	0.001 to 0.100	-
Cross-linker	PBI/DEG	No	-	0.0024 to 0.0032 /0.001
Medium	Ethanol	7.4	5.59	1.86
Stabilizer	PVP (360,000)	0.25	No	No
Costabilizer	Triton X-100	0.08	No	No
Initiator	AIBN	0.060	No	No
Reaction time	8 hours	-	-	-
Rotation Speed	120 rpm	-	-	-

The amount of the **PBI** cross-linker was kept approximately fixed around  $2.8$  to  $3.7 \times 10^{-6}$  moles, while that of the pyrene acrylate (**Py**) monomer was varied from  $0.35$  to  $17.5 \times 10^{-5}$  moles in the feed to obtain a series of solid state emitting polystyrene microbeads. PS sample with single chromophore incorporation, either **Py** (**PS-Py-DEG-4**) or **PBI** (**PS-PBI-5**)<sup>38</sup> (the synthesis of **PS-PBI-5** described in chapter 3, as named PS-PBITEG-6.25 used there) was also developed. In the pyrene alone sample di(ethyleneglycol) diacrylate (**DEG**) was used as the cross-linker in place of **PBI** cross-linker. The PS beads with **Py**, **PBI** and **DEG** were named as the **PS-Py-PBI-1**, **PS-Py-PBI-2**, **PS-Py-PBI-3** and **PS-Py-DEG-4** where increasing numbers represented the increasing amount of **Py** chromophore in the PS backbone. The proton signals of **Py** chromophore could be detected in the NMR spectrum of only one sample with the highest amount of pyrene incorporation i.e., **PS-Py-DEG-4** where <sup>1</sup>H NMR spectra recorded in CDCl<sub>3</sub> is given in **Figure 4.2**.

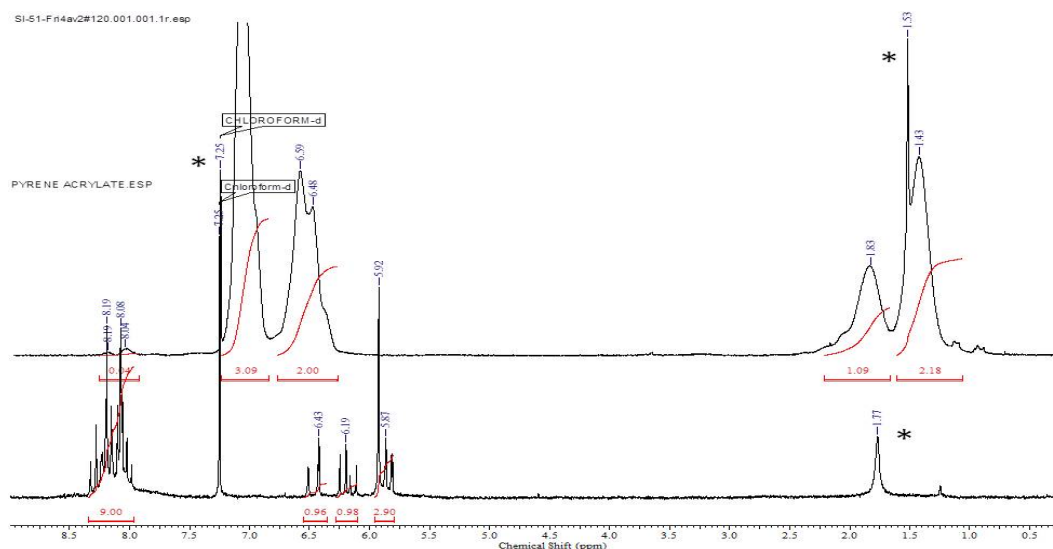


**Figure 4.2:** Comparative  $^1\text{H}$  NMR spectra of PS-Py-DEG-4 and Pyrene acrylate (Py) recorded in  $\text{CDCl}_3$ .

In other polymers the amount of the chromophore was extremely low to be observed in the NMR spectrum. Therefore the incorporation of the chromophore in the polystyrene backbone was calculated for all polymer samples from their absorption spectra using the Beer-Lamberts law and is indicated in **Table 4.2**.

**Table 4.2:** Sample designation, number and weight average molar mass, polydispersity indices ( $\mathfrak{D}$ ) and 5 Wt % loss temperature of the PS-Py-PBI/DEG based polymers.

Sample Name	Pyrene in feed (mole) ( $10^{-5}$ )	Incorporation (mole) ( $10^{-7}$ ) <sup>a</sup>	PBI in feed (mole) ( $10^{-6}$ )	Incorporation (mole) ( $10^{-7}$ ) <sup>a</sup>	$M_n^b$	$M_w^b$	$\mathfrak{D}^b$	TGA ( $T_d = 5\%$ ) <sup>c</sup>
PS-Py-PBI-1	0.35	1.5	3.4	7.2	21 300	72 200	3.3	340
PS-Py-PBI-2	3.1	8.3	2.8	5.0	32 000	88 600	2.7	340
PS-Py-PBI-3	3.1	10.0	3.7	7.8	27 700	97 000	3.4	340
PS-Py-DEG-4	17.5	49.0	-	-	50 000	173 600	3.4	350
PS-PBI-5	-	-	3.7	6.3	45 900	96 800	2.1	345

a=Incorporation of chromophore calculated by absorption studies in  $\text{CHCl}_3$ .

b=Measured by size exclusion chromatography (SEC) in tetrahydrofuran (THF), calibrated with linear, narrow molecular weight distribution polystyrene standards.

c=TGA measurements at heating rate of  $10^\circ\text{C}/\text{min}$  under nitrogen ( $T_d=5\%$ ).

The molar extinction coefficient for PBI= $80,600 \text{ L M}^{-1}\text{cm}^{-1}$  and Py= $34,096 \text{ L M}^{-1}\text{cm}^{-1}$  respectively.



#### 4.4.2 Molecular weight determination and thermal properties of polymers

The molecular weight of the polymers were determine by size exclusion chromatography (SEC). **Figure 4.3** represents the chromatogram and the details of molecular weight data are given in the table 4.2.

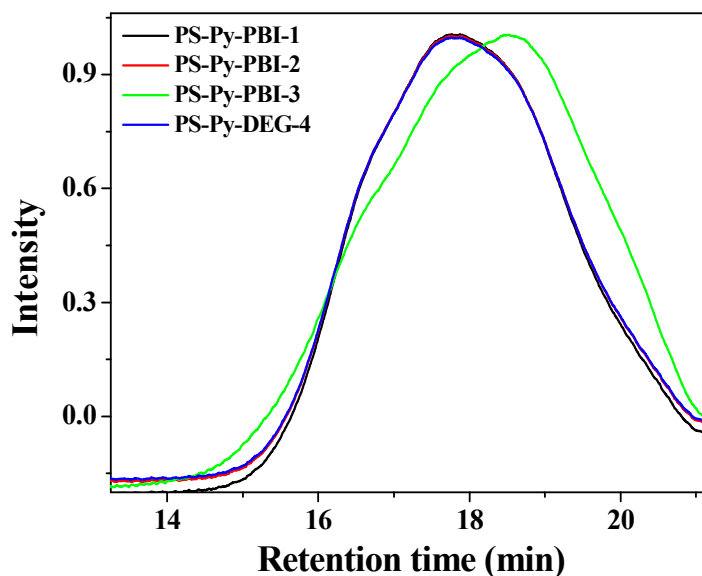


**Figure 4.3:** The size exclusion chromatography of all PS-Py-PBI/DEG polymers.

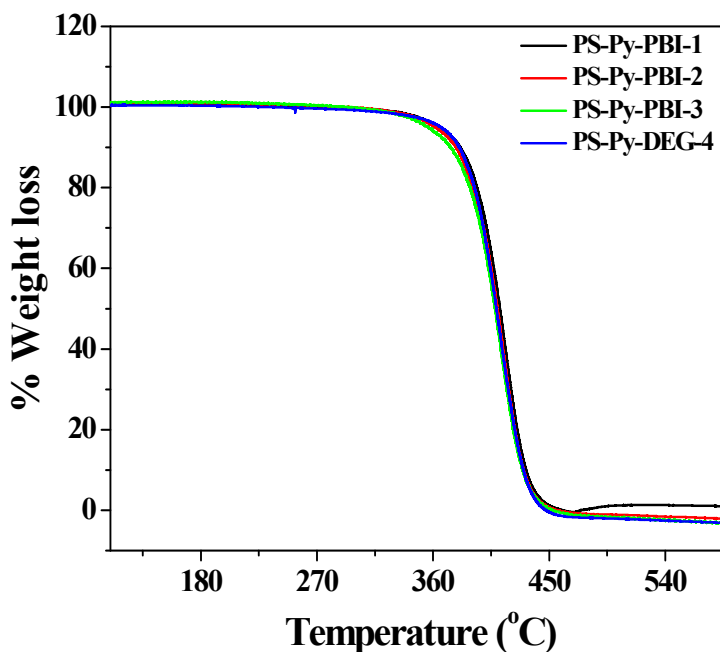


**Figure 4.4:** Thermogravimetric analysis (TGA) of all PS-Py-PBI/DEG samples.

**Table 4.2** lists the 5 weight % loss temperature and the corresponding TGA plot is given in the **figure 4.4**. The thermal stability of the **PS-Py-PBI-x** series was determined by thermogravimetric analysis carried out under nitrogen atmosphere where the 5 wt% loss was observed around 340-345 °C.

#### 4.4.3 Microscopic characterization of polymers

The particle size and morphology of PS beads were confirmed by Dynamic Light Scattering (DLS; polymer powder dispersed in ethanol) and Scanning Electron Microscope (SEM). **Figure 4.5** corresponds to DLS curves for all the polymers.

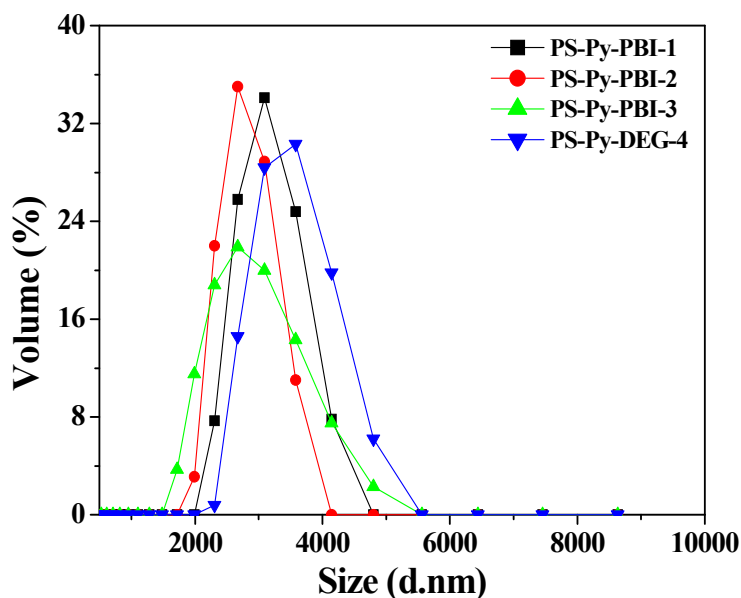


**Figure 4.5:** Volume - average size distribution of **PS-Py-PBI** samples in ethanol dispersion obtained by dynamic light scattering (DLS) analysis.

**Figure 4.6** shows the SEM images of the nearly monodisperse (2.4 to 2.5  $\mu\text{m}$ ) spherical beads for all the polymers.

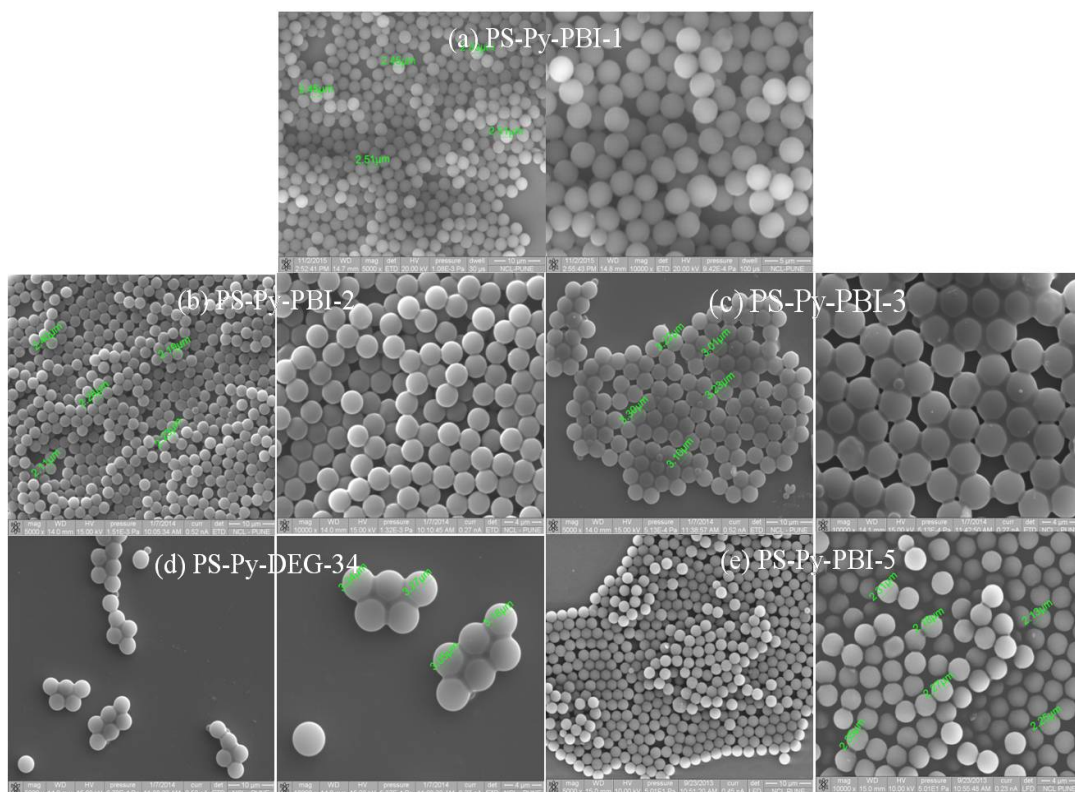


**Figure 4.6:** SEM images of (a) **PS-Py-PBI-1** (b) **PS-Py-PBI-2** (c) **PS-Py-PBI-3** (d) **PS-Py-DEG-4** and (e) **PS-PBI-5** drop cast on silicon wafer (1 mg/2 mL ethanol dispersion).

The uniform distribution of dyes in the PS beads and multicolor emission from the PS beads were seen by fluorescence microscope images. **Figure 4.7** shows the fluorescence microscope images of **PS-Py-PBI/DEG** series recorded using (a) DAPI (350-450 nm Blue), (b) Alexa (488-520 Green) and (c) Rhodamine (480-580 nm Red) filters showing emission at different wavelengths indicating presence of both pyrene and perylenebisimide fluorophores. Blue fluorescence was observed from PS having **Py** chromophore, PS having **PBI** showed green-orange fluorescence whereas multicolor fluorescence was observed from PS having both the **Py** and **PBI** chromophores. The particle size of the PS beads obtained from DLS, SEM and fluorescence microscopy were approximately similar.

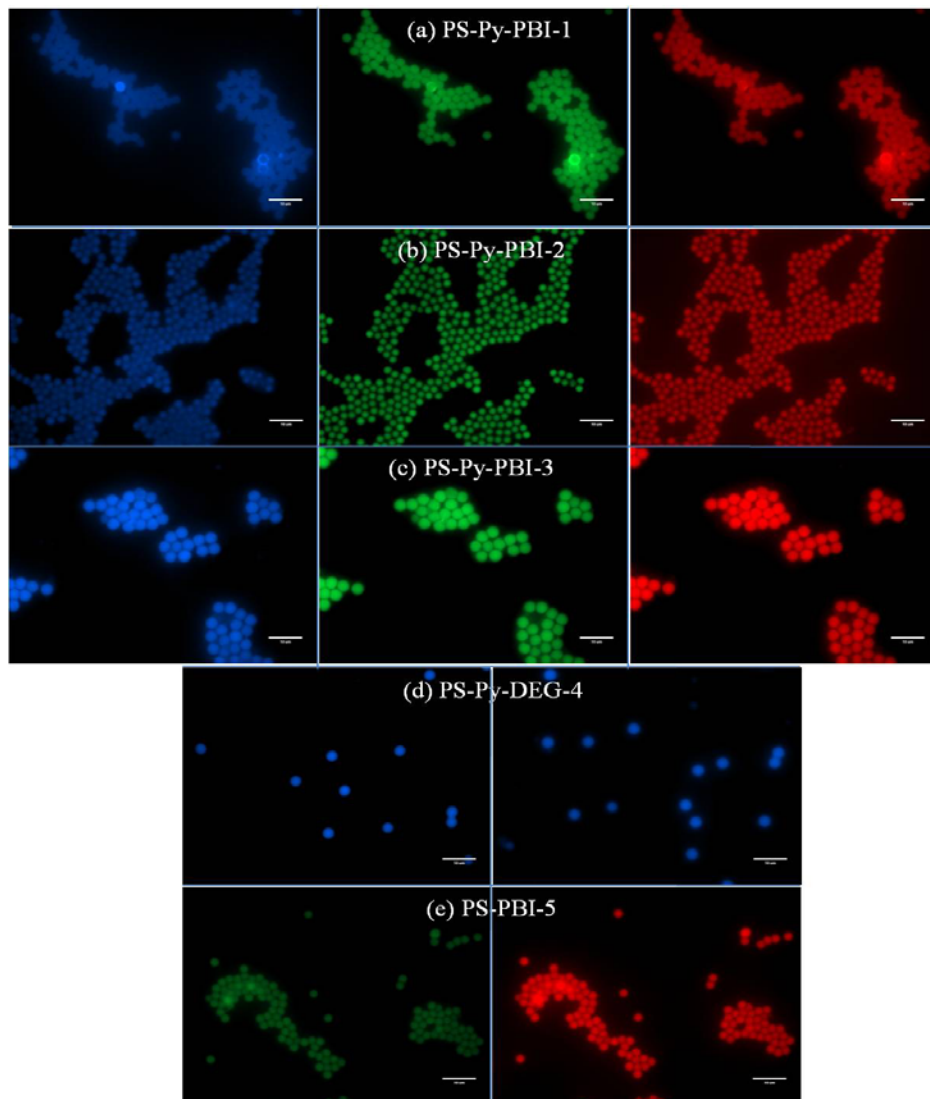


**Figure 4.7:** Fluorescence optical microscopy images of (a) **PS-Py-PBI-1** (b) **PS-Py-PBI-2** (c) **PS-Py-PBI-3** using DAPI (350-450 nm Blue), Alexa (488-520 Green) and Rhodamine (480-580 nm Red) filters and (d) **PS-Py-DEG-4** using DAPI (350-450 nm Blue) (e) **PS-PBI-5** using Alexa (488-520 Green) and Rhodamine (480-580 nm Red).

#### 4.4.4 Photophysical characterization

The normalized absorption and emission spectra of the **PBI** cross-linker and the Pyrene acrylate (**Py**) small molecule recorded in chloroform is given in **figure 4.8**, from which it could be seen that they exhibited the characteristic absorption and emission of perylenebisimide and pyrene chromophore respectively.<sup>39, 40</sup>

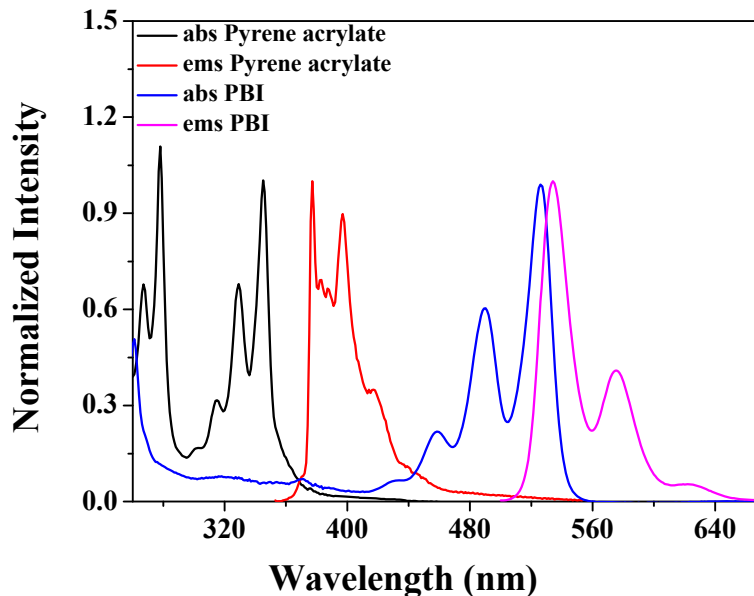


**Figure 4.8:** Normalized absorption and emission spectra of Pyrene acrylate (**Py**) and **PBI** respectively in  $\text{CHCl}_3$ . (0.1 OD at 343 nm;  $\lambda_{\text{ex}} = 343$  nm for Pyrene acrylate (**Py**) and 0.1 OD at 527 nm;  $\lambda_{\text{ex}} = 490$  nm for **PBI**).

The absorption and emission of the fluorescent PS beads were studied in chloroform solution (0.1 OD at the absorption wavelength maxima of pyrene i.e 343 nm) and in the solid state as a powder form. **Figure 4.9a** shows the absorption spectra of all **PS-Py-PBI** polymers in the chloroform solution. It could be seen that no variations in terms of peak position or shape was observed for the pyrene and perylenebisimide absorption upon incorporation in the polymer backbone. **Figure 4.9b** corresponds to the absorption spectra of all **PS-Py-PBI** polymers in the powder form recorded in the reflectant mode. **Figure 4.9c** and **4.9d** shows the respective emission spectra upon excitation at the pyrene absorption wavelength maximum of 343 nm. The most notable difference between the emission spectra in solution and powder form was the absence of pyrene excimeric emission in the solid state even for the **PS-Py-DEG-4** (**Py** alone sample) having high amounts of pyrene incorporation. In solution this sample exhibited a distinct broad emission in the 480 nm which was typical of diffusion controlled pyrene excimeric emission.<sup>41</sup>

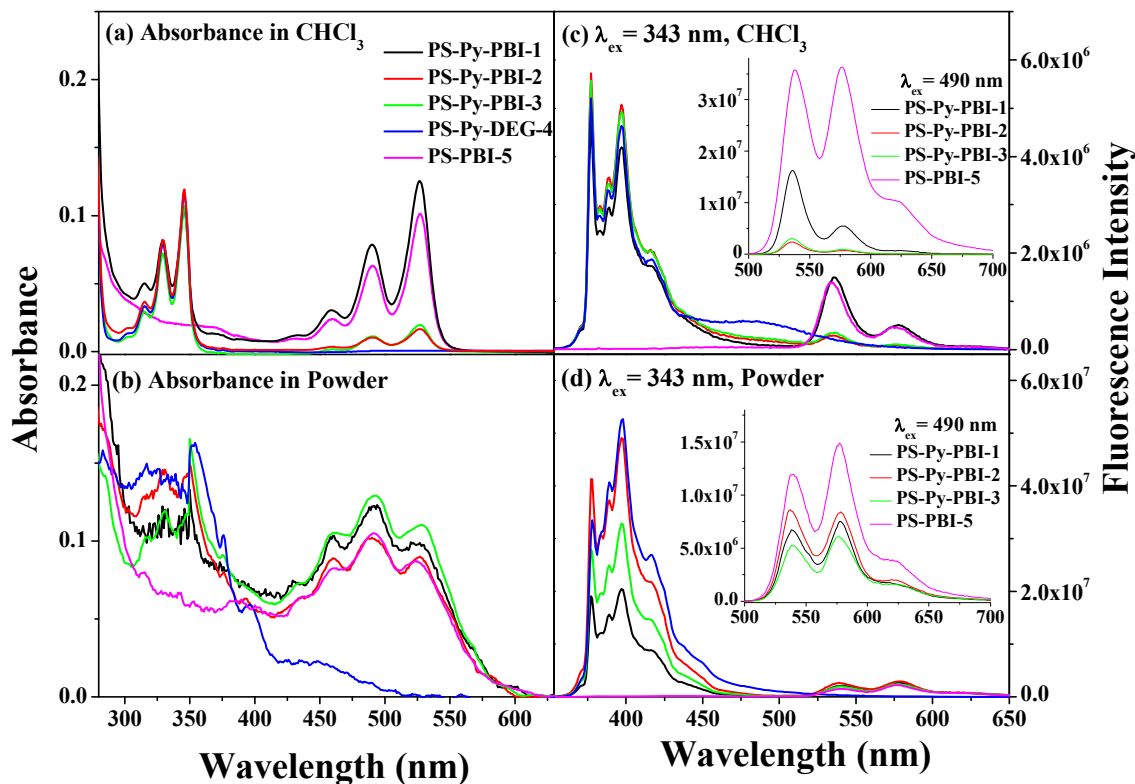


**Figure 4.9:** Solution and solid state absorption-emission for **PS-Py-PBI** upon excitation at 343 nm for **Py** and 490 for **PBI**. (a) Absorbance in CHCl<sub>3</sub> (b) absorbance in powder form collected in reflectant mode (c) emission in CHCl<sub>3</sub>, 0.1 OD at 343 nm;  $\lambda_{\text{ex}} = 343$  nm (d) emission in powder,  $\lambda_{\text{ex}} = 343$  nm. Inset in (c) emission in CHCl<sub>3</sub>,  $\lambda_{\text{ex}} = 490$  nm; Inset in (d) emission in powder,  $\lambda_{\text{ex}} = 490$  nm.

The reason for the absence of pyrene excimeric emission in the solid state was the isolation of the fluorophore afforded by the rigid aromatic **PS** units, which inhibited the  $\pi$ - $\pi$  stacking of the pyrene units. It could be seen that excitation of the perylenebisimide alone polymer **PS-PBI-5** at the pyrene absorption wavelength of 343 nm also resulted in emission from perylenebisimide beyond 520 nm, indicating that direct excitation of perylenebisimide also occurred upon excitation at 343 nm. The inset in **figure 2c** and **2d** corresponds to the emission spectra in chloroform solution and powder form respectively upon excitation at the perylenebisimide absorption wavelength of 490 nm.

**Table 4.3:** Photoluminescence quantum yield and average fluorescence lifetime determined for powder samples.

Sample Name	Solid State Q. Y. ( $\phi$ )		Av. Fluorescence life time (Powder) <b>Py</b> (ns) $\lambda_{\text{ex}}$ : 340 nm; $\lambda_{\text{obs}}$ : 395nm	Av. fluorescence life time (Powder) <b>PBI</b> (ns) $\lambda_{\text{ex}}$ : 460 nm; $\lambda_{\text{obs}}$ : 530 nm
	$\lambda_{\text{ex}} = 343 \text{ nm}$	$\lambda_{\text{ex}} = 490 \text{ nm}$		
PS-Py-PBI-1	0.41 <sup>a</sup>	0.25 <sup>b</sup>	2.75	3.80
PS-Py-PBI-2	0.68 <sup>a</sup>	0.25 <sup>b</sup>	-	-
PS-Py-PBI-3	0.61 <sup>a</sup>	0.22 <sup>b</sup>	2.26	3.64
PS-Py-DEG-4	0.94 <sup>a</sup>	-	2.20	-
PS-PBI-5	-	0.21 <sup>b</sup>	-	3.34

<sup>a</sup>=Selected wavelength range: 340- 510 nm.

<sup>b</sup>=Selected wavelength range: 500- 700 nm.

The solid state quantum yield  $\phi_{\text{powder}}$  was measured using an integrating-sphere Quanta  $\phi$  Horiba attachment with 490 nm excitation for **PBI** and 343 nm for **Py** respectively in the **PS-Py-PBI** polymers and the values are given in the **Table 4.3**. **PS-Py-DEG-4** (pyrene alone polymer) exhibited a quantum yield value of 0.94 ( $\lambda_{\text{exc}} = 343 \text{ nm}$ ) while **PS-PBI-5** (perylenebisimide alone polymer) had a  $\phi_{\text{powder}}$  of 0.21 ( $\lambda_{\text{exc}} = 490 \text{ nm}$ ). The polymers incorporating both fluorophores exhibited  $\phi_{\text{powder}}$  values ranging from 0.52 to 0.41 for blue **Py** emission and 0.21 to 0.25 for **PBI** emission. The solid state quantum yield of **PBI** was more or less similar for the polymers reflecting their nearly similar incorporation of perylenebisimide. On the other hand, the solid state quantum yield of pyrene reflected increasing  $\phi_{\text{powder}}$  values for increased incorporation of pyrene. Fluorescence lifetime decay studies were conducted to probe existence of energy transfer between the **Py/PBI** pair of fluorophores. The fluorescence lifetime measurements were carried out for powder samples of the pyrene alone (**PS-Py-DEG-4**), perylenebisimide alone (**PS-PBI-5**) and two of the **PS-Py-PBI** samples with high and low **Py** incorporation (**PS-Py-PBI-1** and **PS-Py-PBI-3** respectively).

The lifetime decay profiles of the polymers and details of the fit are given in **Figure 4.10** and **Tables 4.4** and **4.5** respectively.

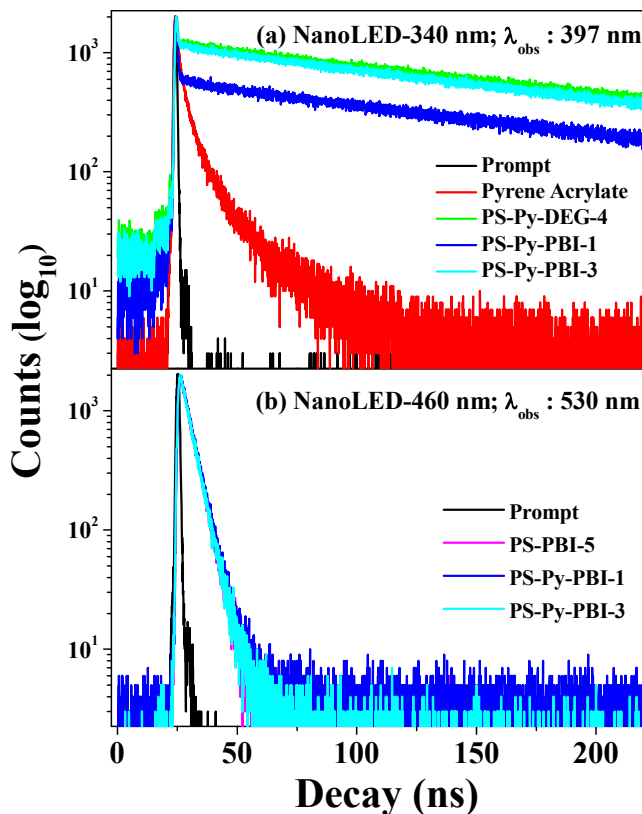


**Figure 4.10:** Fluorescence decay profiles (LED 340 nm, em: 397 nm and LED 460 nm, em: 530 nm) of **Py**, **PS-Py-DEG-4**, **PS-Py-PBI-1**, **PS-Py-PBI-3** and **PS-PBI-5** in the powder state.

The compiled data of the average lifetime decay values for the **Py** and **PBI** emission is given in **table 2**. From the table it could be seen that the average **PBI** fluorescence lifetime value for the polymer with only **PBI** incorporation (**PS-PBI-5**) was 3.34 ns.

**Table 4.4:** Parameters ( $\tau$ : Decay Time,  $\alpha$ : Pre-exponential Factor,  $\chi^2$ : Chi-Squared Value) retrieved from the triexponential fit for samples in powder form. The decay time was collected at 395 nm by using nano LED 340 nm for excitation of **Py**.



Sample	$\tau_1$ ( $\alpha_1$ )	$\tau_2$ ( $\alpha_2$ )	$\tau_3$ ( $\alpha_3$ )	Chi <sup>2</sup> ( $\chi^2$ )	Av. $\tau$ (sec)
Py	2.8x10 <sup>-9</sup> (0.03)	6.17x10 <sup>-11</sup> (0.97)	1.2x10 <sup>-8</sup> (0.01)	1.04	2.19x10 <sup>-10</sup>
PS-Py-DEG-4	1.96x10 <sup>-8</sup> (0.00)	3.92x10 <sup>-11</sup> (0.99)	1.69x10 <sup>-7</sup> (0.01)	0.97	2.21 x10 <sup>-9</sup>
PS-Py-PBI-1	7.7x10 <sup>-8</sup> (0.00)	9.5x10 <sup>-11</sup> (0.98)	1.57x10 <sup>-7</sup> (0.02)	1.02	2.75x10 <sup>-9</sup>
PS-Py-PBI-3	1.54x10 <sup>-8</sup> (0.00)	4.33x10 <sup>-11</sup> (0.99)	1.60x10 <sup>-7</sup> (0.01)	0.93	2.26x10 <sup>-9</sup>

**Table 4.5:** Parameters ( $\tau$ : Decay Time,  $\alpha$ : Pre-exponential Factor,  $\chi^2$ : Chi-Squared Value) retrieved from the triexponential fit for samples in powder form. The decay time was collected at 530 nm by using nano LED 460 nm for excitation of **PBI**.

Sample	$\tau_1$ ( $\alpha_1$ )	$\tau_2$ ( $\alpha_2$ )	$\tau_3$ ( $\alpha_3$ )	Chi <sup>2</sup> ( $\chi^2$ )	Av. $\tau$ (sec)
PS-PBI-5	2.7x10 <sup>-9</sup> (0.04)	4.46x10 <sup>-9</sup> (0.71)	2.8x10 <sup>-10</sup> (0.25)	1.21	3.34 x10 <sup>-9</sup>
PS-Py-PBI-1	2.15x10 <sup>-9</sup> (0.03)	4.52x10 <sup>-9</sup> (0.81)	4.4x10 <sup>-10</sup> (0.16)	0.98	3.8x10 <sup>-9</sup>
PS-Py-PBI-3	2.93x10 <sup>-9</sup> (0.10)	4.49x10 <sup>-9</sup> (0.72)	5.6x10 <sup>-10</sup> (0.18)	1.12	3.64 x10 <sup>-9</sup>

The average fluorescence lifetime value for the **PBI** emission did not decrease upon incorporation of **Py** also into the PS backbone. The polymers with both **Py** and **PBI** incorporation did not register any decrease in the **PBI** fluorescence decay lifetime; rather a marginal increase was observed. The average fluorescence lifetime value for **Py** emission in the **Py** alone polymer **PS-Py-DEG-4** was obtained as 2.2 ns. The average fluorescence lifetime values for **Py** emission from the two polymers **PS-Py-PBI-1** and **PS-Py-PBI-3** were obtained as 2.75 and 2.26 ns respectively, which was not very different from that of the **Py** alone polymer. Thus, the fluorescence life time decay data did not seem to suggest energy transfer occurring from **Py** to **PBI** in these PS polymers.

**(i) PS beads as fluorescent ink and Nitro aromatic sensor**

**Figure 4.11 (top)** shows the photograph of the polymers in the powder form taken under a hand-held UV lamp showing multicolor emission from the polymers having varying incorporation of **Py** and **PBI** fluorophores. Ethanol dispersion of the polymer beads could be used directly as ink to write on substrates like paper, glass slide etc which were invisible under normal lighting, but became visible under ultraviolet light. **Figure 4.11 (bottom)** shows the pattern (NCL: National Chemical Laboratory) written on filter paper from an ethanol dispersion of the polymer beads under normal lighting and under a hand-held UV lamp. The different polymer beads became visible in different colors under the UV light depending on the chromophore incorporation.

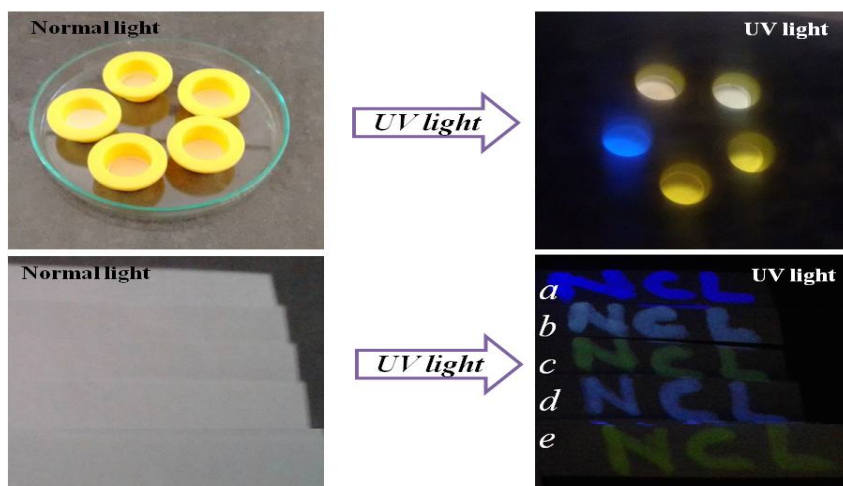


**Figure 4.11:** (Top) The images of the powdered samples of all polymers **PS-Py-PBI** under normal and UV light. (Bottom) Images of filter paper where ethanol dispersion of polymers were used as ‘invisible’ ink for writing in visible light and under hand-held UV light (a) **PS-Py-DEG-4** (b) **PS-Py-PBI-1** (c) **PS-Py-PBI-2** (d) **PS-Py-PBI-3** and (e) **PS-PBI-5**.

The pyrene alone polymer **PS-Py-DEG-4** gave a bright blue hue, while the perylenebisimide alone polymer **PS-PBI-5** became visible in orange yellow shade. The polymers with both pyrene and perylenebisimide exhibited various in- between hues with **PS-Py-PBI-1** exhibiting white shade.

Pyrene as a fluorophore has been shown to be sensitive towards nitro aromatic compounds like the nitro toluene, di nitro toluene, tri nitro toluene, tri nitro phenol etc, which

are reported military explosives.<sup>19</sup> The PS incorporating pyrene alone i.e. **PS-Py-DEG-4** was taken as a probable candidate for sensing nitro aromatic compounds (the structures of all the nitroaromatics used in the study are given in **figure- 4.12(b)**). An ethanol dispersion of the polymer was spin coated (~thickness-2 $\mu$ m) on quartz substrates and exposed to saturated vapors of the various nitro aromatic compounds in a sealed chamber for varying periods of time and the fluorescence was monitored.

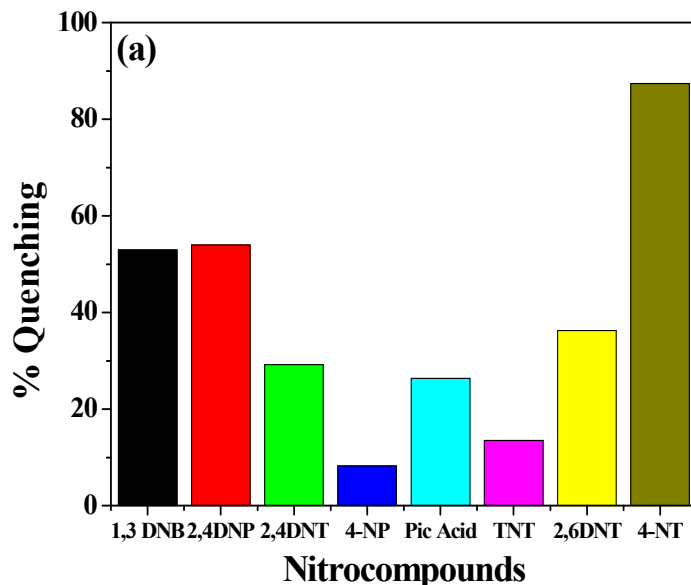


**Figure 4.12a:** Percent quenching of fluorescence at 397 nm for **PS-Py-DEG-4** upon exposure to vapors of various nitro aromatic compounds ( $\lambda_{\text{ex}} = 343$  nm).

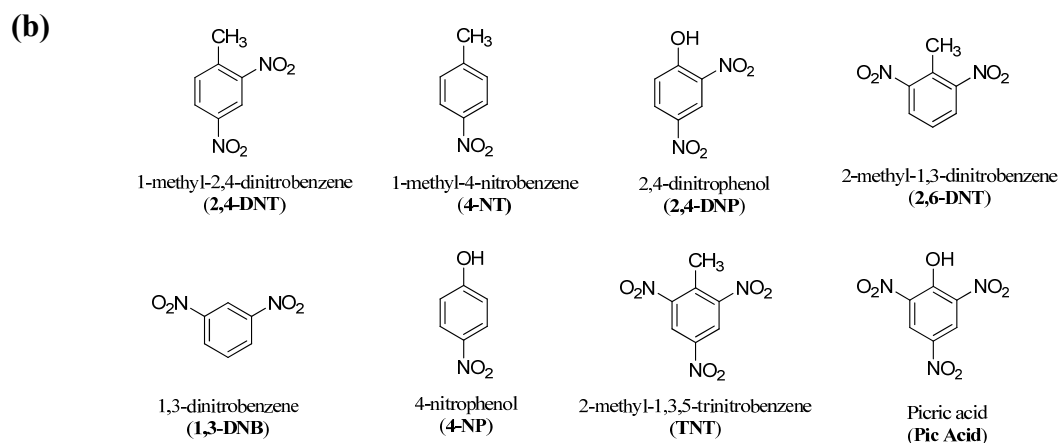


**Figure 4.12b:** Structure of nitroaromatic compounds used for sensing.

**Figure 4.12a** shows the percentage quenching of the emission maximum at 397 nm upon excitation at 343 nm for **PS-Py-DEG-4** after exposure to vapors of the nitroaromatics for a period of 60 minutes. A consistent trend of quenching of pyrene fluorescence was observed only towards 4-NT vapors. Consequently, only 4-NT was taken up for further sensing studies.

**Figure 4.13a** shows the emission spectra of spin coated sample of **PS-Py-DEG-4** from ethanol dispersion upon exposure to saturated vapors of 4-NT for various intervals of time.

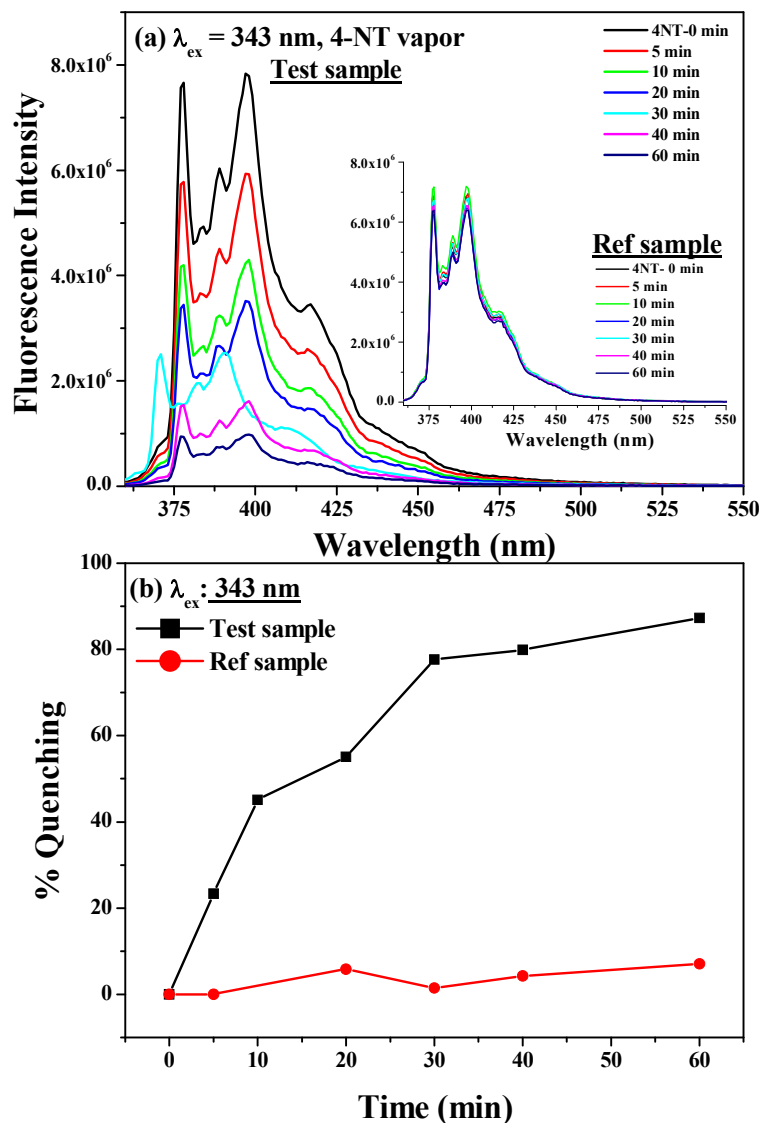


**Figure 4.13:** (a) Emission spectra of spin coated films of **PS-Py-DEG-4** from ethanol dispersion after exposure to 4-NT vapors for different intervals of time ( $\lambda_{ex} = 343$  nm). Inset:

emission from a reference film of **PS-Py-DEG-4** prepared under identical conditions, but not exposed to 4-NT vapor (b) Comparative plot showing percent quenching of emission of **PS-Py-DEG-4** reference and test samples over a period of one hour.

A 20 % quenching of the pyrene emission was observed in the first five minutes of exposure of the film to the vapors of 4-NT, which increased to more than 85 % quenching in an hours' time. A reference film of **PS-Py-DEG-4** (spin coated from ethanol dispersion under identical conditions as that of the test sample) was left exposed to air in a petridish and its emission was also monitored at various time intervals over a period of one hour. The inset in **figure 5a** shows the emission from the reference sample, which did not undergo any measurable variation in its fluorescence. **Figure 4.13b** compares the percentage quenching of fluorescence for both the reference and test films of **PS-Py-DEG-4** recorded over a period of one hour. The absence of a measurable quenching of fluorescence in the reference film established the air stability of the pyrene emission in the PS bead during the duration of the vapor sensing experiment.

**Figure 4.14.** shows the emission spectra from spin coated films of the perylenebisimide alone polymer i.e. **PS-PBI-5** after exposure to saturated vapors of 4-NT for different intervals of time (the wavelength of excitation was 490 nm).

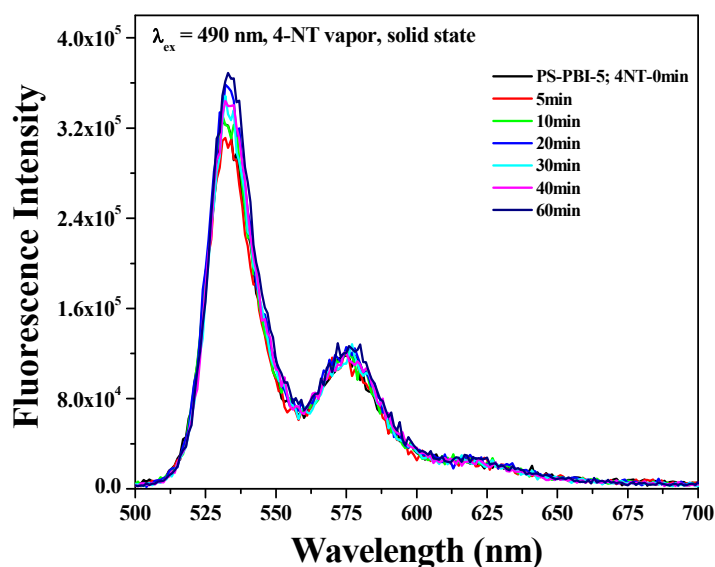


**Figure 4.14:** Emission spectra of spin coated films of **PS-PBI-5** from ethanol dispersion after exposure to 4-NT vapors for different intervals of time ( $\lambda_{\text{ex}} = 490 \text{ nm}$ ).

It could be seen from the figure that the **PBI** emission was almost unaffected by the presence of the 4-NT vapors.

The PS sample incorporating both the fluorophores pyrene and perylenebisimide **PS-Py-PBI-1** was exposed to saturated vapors of 4-NT. Powder sample as such was also used for the sensing studies along with films spin coated from ethanol dispersion and chloroform solution onto quartz plates. The time dependant fluorescence quenching of **PS-Py-PBI-1** in powder form, spin coated films from ethanol dispersion and chloroform solution upon exposure to 4-nitrotoluene vapors was carried out. **Figure 4.15** shows the emission spectra of **PS-Py-PBI-1** for excitation at 343 nm for **Py** as well as at 490 for **PBI** in powder and spin coated film forms.

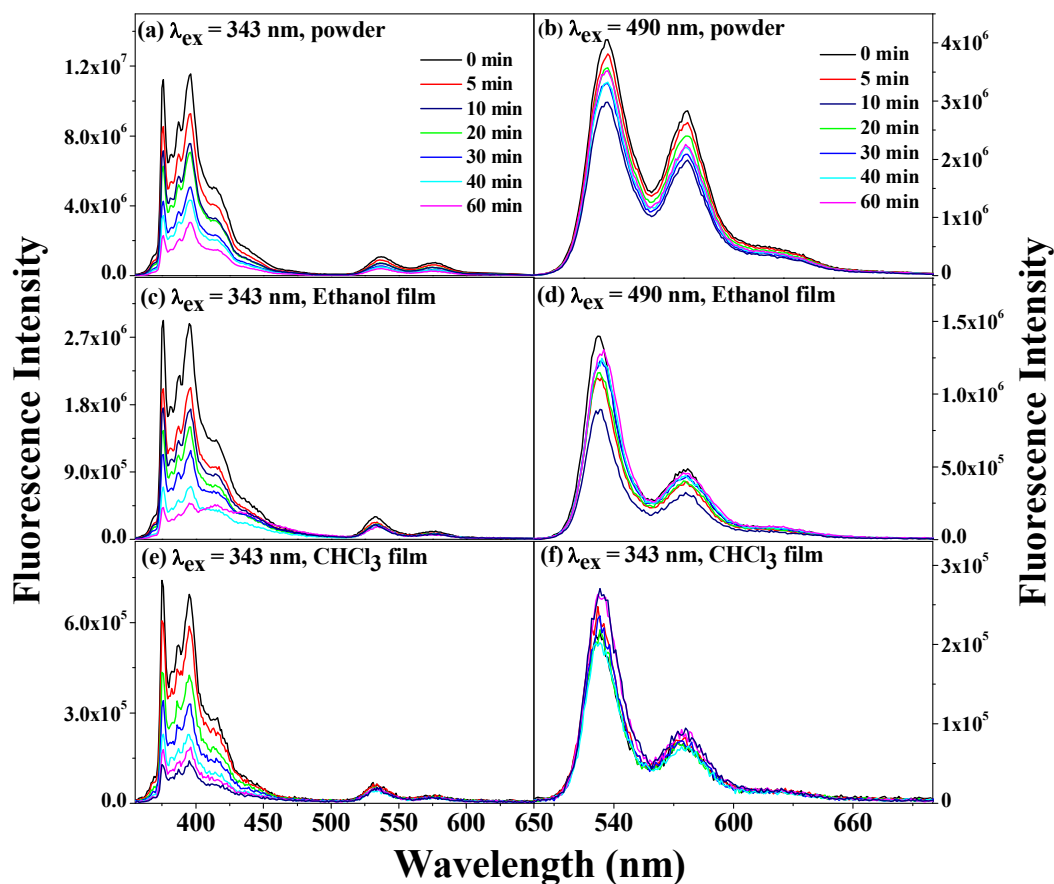


**Figure 4.15:** Time dependant fluorescence quenching of **PS-Py-PBI-1** (excitation at 343 nm for **Py** and excitation at 490 nm for **PBI**) in (a, b) powder form, spincoated films from (c, d) ethanol dispersion and (e, f) chloroform upon exposure to 4-nitrotoluene vapors.

**Figure 4.16.** presents the comparative plot of percent quenching of **Py** and **PBI** emission upon exposure to vapor of 4-NT for varying time intervals. It can be observed from **figure 4.16** that polymer films showed more than 80 % quenching of **Py** emission while the powder sample showed around 70 % quenching for the pyrene emission. In the first five minutes of exposure to the vapors of 4-NT, 20 to 30 % quenching of the **Py** emission was observed in the powder and film samples.

On the other hand, only less than 20 % quenching of **PBI** emission was observed even after an hour of exposure to the vapor. It clearly indicated that **Py** interacted much better with 4-NT compared to **PBI**, which was also confirmed by the excitation spectrum of **PS-Py-PBI-1** shown in the **figure 4.16**.

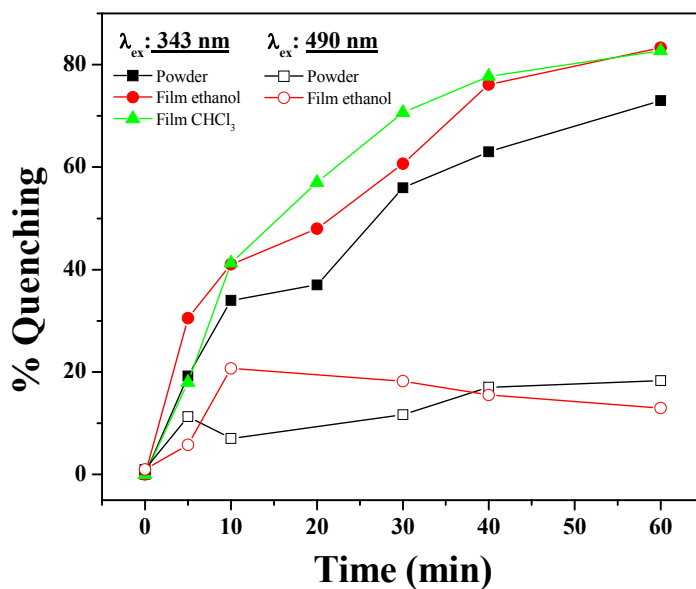


**Figure 4.16:** Comparative plot showing percent quenching of emission for **PS-Py-PBI-1** in powder state and in film form spin coated on quartz plate from ethanol dispersion and chloroform solution.

The **figure 4.17** corresponds to the comparative excitation spectra of **PS-Py-PBI-1** in powder form (a), spin coated films from ethanol dispersion (b) and chloroform (c) upon exposure to 4-nitrotoluene vapors for 60. The excitation spectra of **Py** exhibited sharp

reduction with exposure to the 4-nitro toluene vapors while the perylenebisimide excitation spectra remained more or less unaffected indicating that the emitting species was intact.

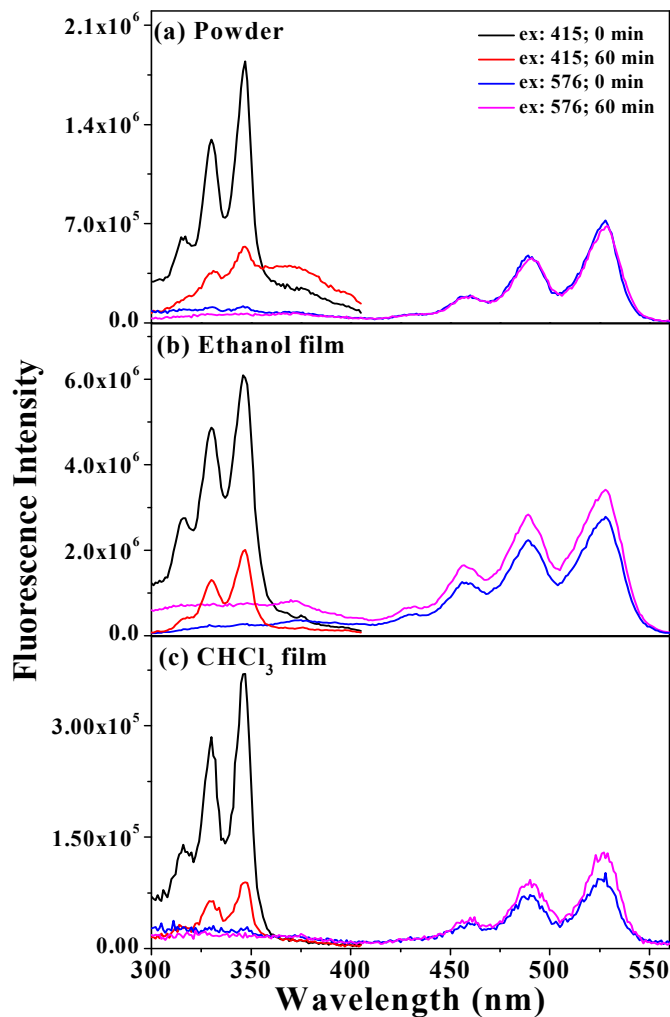


**Figure 4.17:** Excitation spectra of PS-Py-PBI-1 (excitation at 415 nm for Py and 576 nm for PBI respectively) in (a) powder form, spincoated from (b) ethanol dispersion and (c) chloroform upon exposure to 4-nitrotoluene vapors for 60 minutes.

Quantitative estimation of the sensing efficiency of the polymer beads for vapors of 4-NT would give a perspective of its performance in comparison with other materials reported in literature. However, quantification of analyte diffusion into a sensing material and correlating the vapor diffusion with the extent of PL quenching is not a trivial task.<sup>42, 43</sup> Although reports are available for the limit of detection (LOD) values for vapors of TNT, not many reports are available for 4-NT vapor in the literature. X. Xu et.al. reported 3-16 ng



LOD for 4-NT on the column of a high performance liquid chromatography atmospheric pressure ionization mass spectrometer (HPLC-API-MS).<sup>43</sup> Y. Li et. al. observed a LOD of 0.2 ppm for 4-NT using a zinc based coordination polymer. This was higher compared to the LOD for DNT (dinitrotoluene; 0.6 ppm), which was attributed to a static quenching mechanism arising from the higher adsorption of 4NT.<sup>44</sup> The estimation of LOD of **PS-Py-DEG-4** polymer for subsaturated vapor of 4-NT was carried out based on the observed extent of fluorescence quenching. Various known concentrations of the analyte 4-NT was dropcast on glass slides and kept inside a closed glass chamber. Thin films of the polymer **PS-Py-DEG-4** (20 mg/mL) spin coated from ethanol on quartz plates were introduced into the chamber for a period of 10 minutes. The emission from the quartz plates were recorded before and after the 10 minute exposure from which the percent of fluorescence quenching for the different analyte concentration was extracted.

The plot of percentage quenching of emission at 395 nm as a function of log of concentration expressed in moles is given in **Figure 4.18**.

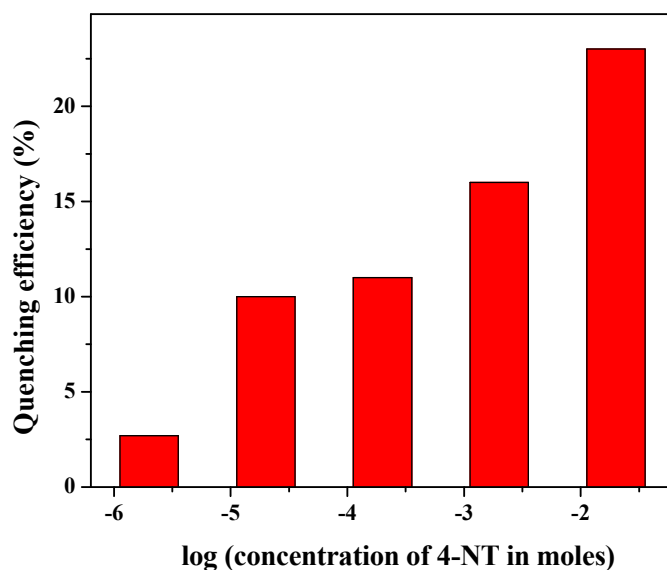


**Figure 4.18:** Limit of detection of 4-NT vapor by film of **PS-Py-DEG-4** spin coated from ethanol on quartz plates. Concentration of polymer = 20 mg/mL.

Literature reports states that a 5 % quenching of fluorescence is sufficient to detect an analyte.<sup>45</sup> Higher quenching efficiency was observed with increase in concentration of 4-NT and less than 5 % quenching of fluorescence was observed for  $2 \times 10^{-6}$  moles of 4-NT. Therefore, the LOD was determined as  $10^{-5}$  moles (2.7 ppm) of 4-NT vapors with a 10 % quenching of the polymer fluorescence.

For the simple demonstration of the applicability of these materials, the filter paper strip with pattern written using the ethanol dispersion of the polymers was exposed to the vapor of 4-NT for 30 minutes.

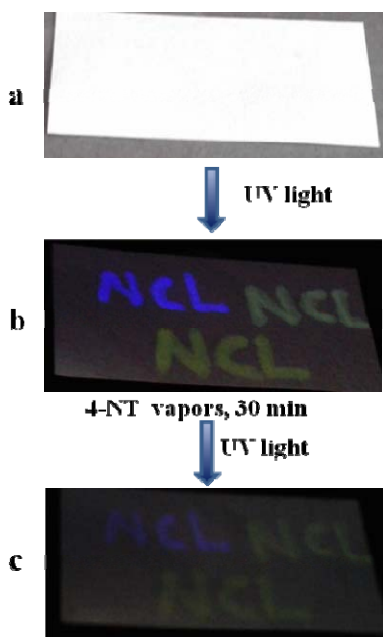


**Figure 4.19:** Visual detection of 4-NT by paper strip. (a) image showing writing on filter paper strip using different polymers under normal lighting (b) image showing the writing under a hand held UV lamp (365 nm) (c) quenched fluorescence after exposure to 4-NT vapors for 30 minutes.

**Figure 4.19** shows the selective change in intensity of blue **Py** emission compared to that of yellow **PBI** emission, which could be observed visually under a hand-held UV light. A better visualization of the selective fluorescence response of **PS** beads towards 4-NT vapors was achieved using fluorescence microscopy images.

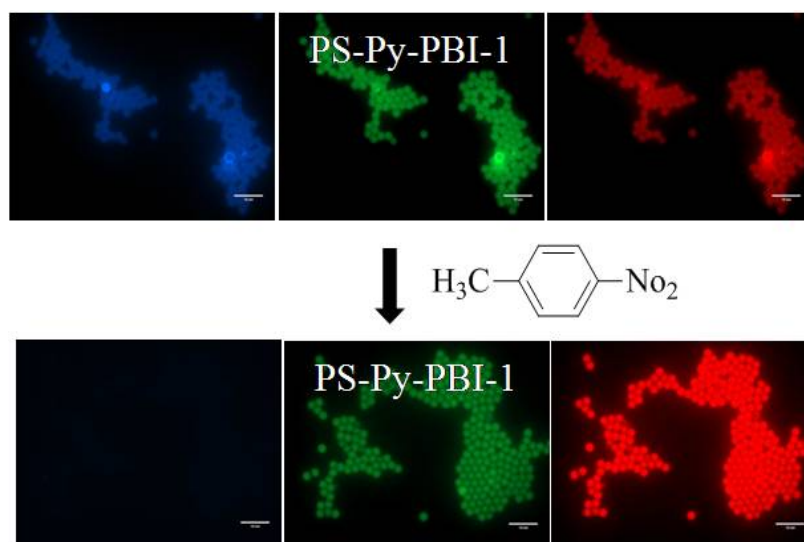


**Figure 4.20:** Fluorescence microscope images of PS beads before and after exposure to 4-NT vapor.

**Figure 4.20** shows the fluorescence microscopy images of **PS-Py-PBI-1** sample drop cast from ethanol dispersion on glass slides before and after exposure to 4-NT. Almost total quenching of the blue fluorescence could be observed from the polymer microbeads upon 20 minutes exposure to saturated 4-NT vapors while the green and red emission of perylenebisimide was intact in the beads. The selectivity of the polymer towards 4-NT compared to the other nitroaromatic molecules could be attributed to the high vapor pressure of 4-NT which leads to its strong physical adsorption onto the large surface area of the polymer bead or powder. Photoinduced electron transfer from electron rich Pyrene to LUMO of 4-NT is attributed to the observed quenching of pyrene emission. The electron deficient nature of perylenebisimide limits its interaction with 4-NT.

#### 4.4 Conclusion

In conclusion, polystyrene microbeads with air stable, color tunable solid state emission properties were developed in a three stage dispersion polymerization method whereby multiple fluorophores (pyrene and perylenebisimide) emitting in different wavelength could be covalently incorporated into the polymer backbone. The pyrene monomeric emission in the 340-500 nm region was sensitive to vapors of 4-nitrotoluene, while the emission of perylenebisimide beyond 500 nm was unaffected. The limit of detection (LOD) of pyrene

emission for vapors of 4-NT was observed to be  $10^{-5}$  moles (2.7 ppm). The selectivity is attributed to the electron rich nature of pyrene, which makes it sensitive towards electron deficient nitroaromatic compounds. The easy dispersibility of the PS microbeads in ethanol also afforded fluorescent ink solution to write on various substrates like glass or paper, which were invisible under normal lighting but became visible in various color shades upon observation under a hand-held UV lamp.

#### 4.5 Reference

- (1) Guan, W.; Zhou, W.; Lu, J.; Lu, C. *Chem. Soc. Rev.* **2015**, *44*, 6981–7009.
- (2) Hou, X.; Ke, C.; Bruns, C. J.; McGonigal, P. R.; Pettman, R. B.; Stoddart, J. F. *Nat. Commun.* **2015**, *6*, 6884.
- (3) Yoon, S.-J.; Chung, J. W.; Gierschner, J.; Kim, K. S.; Choi, M.-G.; Kim, D.; Park, S.Y. *J. Am. Chem. Soc.* **2010**, *132*, 13675–13683.
- (4) Mosca, L.; Behzad, S. K.; Anzenbacher Jr, P. *J. Am. Chem. Soc.* **2015**, *137*, 7967–7969.
- (5) Jinag, H.; Taranekar, P.; Reynolds, J. R.; Schanze, K. S. *Angew. Chem., Int. Ed.* **2009**, *48*, 4300–4316.
- (6) Freeman, R.; Willner, I. *Chem. Soc. Rev.* **2012**, *41*, 4067–4085.
- (7) Pramanik, S.; Zheng, C.; Zhang, X.; Emge, T. J.; Li, J. *J. Am. Chem. Soc.* **2011**, *133*, 4153–4155.
- (8) Park, In-H.; Medishetty, R.; Kim, Ja-Y.; Lee, S. S.; Vittal, J. J. *Angew. Chem. Int. Ed.* **2014**, *53*, 5591–5595.
- (9) McQuade, D. T.; Pullen, A. E.; Swager, T. M. *Chem. Rev.* **2000**, *100*, 2537–2574.
- (10) Babu, S. S.; Praveen, V. K.; Ajayaghosh, A. *Chem. Rev.* **2014**, *114*, 1973–2129.
- (11) Stringer, R. C.; Gangopadhyay, S.; Grant, S. A. *Anal. Chem.* **2010**, *82*, 4015–4019.
- (12) Robin, M. P.; O'Reilly, R. K. *Polym. Int.* **2015**, *64*, 174–182.
- (13) Sánchez-Martín, R. M.; Cuttle, M.; Mittoo, S.; Bradley, M. *Angew. Chem. Int. Ed.* **2006**, *45*, 5472–5474.
- (14) Abdelrahman, A. I.; Dai, S.; Thickett, S. C.; Ornatsky, O.; Bandura, D.; Baranov, V.; Winnik, M. A. *J. Am. Chem. Soc.* **2009**, *131*, 15276–15283.
- (15) Charles, P. T.; Adams, A. A.; Howell Jr, P. B.; Trammell, S. A.; Deschamps, J. R.; Kusterbeck, A. W. *Sensors* **2010**, *10*, 876–889.
- (16) Saxena, A.; Fujiki, M.; Rai, R.; Kwak, G. *Chem. Mater.* **2005**, *17*, 2181–2185.
- (17) Panawong, C.; Pandhumas, T.; Youngme, S.; Martwiset, S. *J. Appl. Polym. Sci.* **2015**, *132*, 41759.
- (18) Yang, Y.; Fan, X.; Long, Y.; Su, K.; Zou, D.; Li, N.; Zhou, J.; Li, K.; Liu, F. *J. Mater. Chem.* **2009**, *19*, 7290–7295.
- (19) LaFratta, C. N.; Walt, D. R. *Chem. Rev.* **2008**, *108*, 614–637.
- (20) Wang, Xu-D.; Wolfbeis, O. S. *Anal. Chem.* **2016**, *88*, 203–227.

- (21) Wang, X.-D.; Wolfbeis, O. S.; Meier R. *J. Chem. Soc. Rev.* **2013**, *42*, 7834–7869.
- (22) Dullens R. P. A.; Claesson, E. M.; Kegel, W. K. *Langmuir* **2004**, *20*, 658–664.
- (23) Sadovoy, A. V.; Lomova, M. V.; Antipina, M. N.; Braun, N. A.; Sukhorukov, G. B.; Kiryukhin, M. V. *ACS Appl. Mater. Interfaces* **2013**, *5*, 8948–8954.
- (24) Figueira-Duarte, T. M.; Del Rosso, P. G.; Trattnig, R.; Sax, S.; List, E. J. W.; Müllen, K. *Adv. Mater.* **2010**, *22*, 990–993.
- (25) Spenst, P.; Würthner, F. *Angew. Chem. Int. Ed.* **2015**, *54*, 10165–10168.
- (26) Liu, K.; Liu, T.; Chen, X.; Sun, X.; Fang, Y. *ACS Appl. Mater. Interfaces* **2013**, *5*, 9830–9836.
- (27) Shanmugaraju, S.; Mukherjee, P. S. *Chem. Commun.* **2015**, *51*, 16014–16032.
- (28) Venkatramaiah, N.; Firmino, A. D. G.; Almeida Paz, F. A.; Tomé, J. P. C. *Fast Chem. Commun.* **2014**, *50*, 9683–9686.
- (29) Basabe-Desmonts, L.; Reinhoudt, D. N.; Crego-Calama, M. *Chem. Soc. Rev.* **2007**, *36*, 993–1017.
- (30) Salinas, Y.; Martínez-Míñez, R.; Marcos, M. D.; Sancenón, F.; Costero, A. M.; Parra, M.; Gil, S. *Chem. Soc. Rev.* **2012**, *41*, 1261–1296.
- (31) Yang, J.-S.; Swager, T. M. *J. Am. Chem. Soc.* **1998**, *120*, 5321–5322.
- (32) Yang, J.-S.; Swager, T. M. *J. Am. Chem. Soc.* **1998**, *120*, 11864–11873.
- (33) Wang, Y.; La, A.; Ding, Y.; Liu, Y.; Lei, Y. *Adv. Funct. Mater.* **2012**, *22*, 3547–3555.
- (34) Sun, X.; Brückner, C.; Nieh, M.-P.; Lei, Y. *J. Mater. Chem. A* **2014**, *2*, 14613–14621.
- (35) Senthamizhan, A.; Celebioglu, A.; Bayir, S.; Gorur, M.; Doganci, E.; Yilmaz, F.; Uyar, T. *ACS Appl. Mater. Interfaces* **2015**, *7*, 21038–21046.
- (36) Beyazkilic, P.; Yildirim, A.; Bayindir, M. *ACS Appl. Mater. Interfaces* **2014**, *6*, 4997–5004.
- (37) Sonawane, S. L.; Asha, S. K. *ACS Appl. Mater. Interfaces* **2013**, *5*, 12205–12214.
- (38) Sonawane, S. L.; Asha, S. K. *J. Phys. Chem. B* **2014**, *118*, 9467–9475.
- (39) Winnik, F. M. *Chem. Rev.* **1993**, *93*, 587–614.
- (40) Würthner, F. *Chem. Commun.* **2004**, 1564–1579.
- (41) Jang, H.-S.; Wang, Y.; Lei, Y.; Nieh, M. -P. *J. Phys. Chem. C* **2013**, *117*, 1428–1435.
- (42) Ali, M. A.; Geng, Y.; Cavaye, H.; Burn, P. L.; Gentle, I R.; Meredith, P.; Shaw, P. E.; *Chem. Commun.*, **2015**, *51*, 17406–17409.

(43) Xu, X.; van de Craats, A. M.; de Bruyn, P. C. *J. Forensic Sci* **2004**, *49*, 1171–1180.

(44) Li, Y.; Liu, K.; Li, W-J.; Guo, A.; Zhao, F-Y.; Liu, H.; Ruan, W-J. *J. Phys. Chem. C* **2015**, *119*, 28544–28550.

(45) Kartha, K. K.; Babu. S. S.; Srinivasan, S.; Ajayaghosh, A. *J. Am. Chem. Soc.* **2012**, *134*, 4834–4841.

-:- **Chapter 5** -:-

---

*Tailor Made Functional Beads by Dispersion Polymerization for Application in Fluorescence Molecular Imprinting Technology*

---





### 5.1 Abstract

Functional Polystyrene (PS) cross-linked microbeads were developed by dispersion polymerization as fluorescent Molecularly Imprinted Polymers (**MIPs**) having cavities with specific recognition sites. The functional molecule **Azobenzene** was modified with pyridine and then self- assembled with **Pyrenebutyric acid** (template molecule), which was then introduced during the second stage of dispersion polymerization of polystyrene. The soxhlet technique was used to remove the assembled template molecules in the cross-linked PS beads by using acetonitrile as solvent. Non imprinted polymer (**NIP**) having no template was also synthesized for comparative study. Fluorescence spectroscopy could be used as a tool to derive insight into the location of the template molecules on the **MIP** or **NIP**. The template molecule **Pyrenebutyric acid** was adsorbed on the surface of the **NIPs** during binding studies as they lacked a selective cavity for the templates. This could be evidenced from the pyrene excimeric emission observed at 440 nm, which is usually attributed to emission from pyrene molecules in close proximity under a constrained environment like a surface. The template binding efficiency of the **NIPs** were much lower compared to **MIPs**. Pyrene emission from **MIP** upon rebinding showed typical monomeric emission in the 375 to 395 nm range, confirming its location in isolated cavities.

## 5.2 Introduction

Molecularly Imprinted Polymers (**MIPs**) are functional materials that have attracted a lot of interest due to their broad range of applications like for purification and separation,<sup>1-3</sup> chromatography,<sup>4</sup> catalysis,<sup>5</sup> sensors<sup>6</sup> and drug delivery etc.<sup>7-8</sup> Although different methods have been employed for developing the **MIPs** the general process involves the polymerization of functional monomers and cross-linkers in presence of a template. Removal of the template – usually by soxhlet extraction, results in binding sites which are specific for the template.<sup>9-10</sup> Cross-linked spherical beads is the most effective physical structure for the molecularly imprinted polymers,<sup>11-12</sup> which can be conveniently achieved using free radical polymerization in the aqueous media using polymerization techniques like the dispersion, precipitation, suspension etc.<sup>13-15</sup> These polymerization techniques have the added advantage of producing monodisperse beads in the size range of 0.1 to 10 micron for dispersion or 10 to 100 micron for suspension polymerization.<sup>16-17</sup> Quantification and characterization of template rebinding by the MIP is challenging due to the cross-linked nature of the material.<sup>18</sup> The analytical tools that are generally used for characterization are HPLC, GCMS, potentiometer etc.<sup>19-20</sup> Other techniques which could be used for detection and quantification of a template in MIP are surface plasmon resonance or quartz crystal microbalance,<sup>21-22</sup> surface acoustic wave technique<sup>23</sup> Infrared or Raman microspectroscopy.<sup>24-26</sup> Although these methods have been reported, their sensitivity in handling and time consuming process limits their applications. For instance, it is challenging to determine very low concentrations of analyte binding to the MIP as in the cases with herbicides and pesticides which are hazardous even in low concentrations.<sup>27</sup>

Among the sensitive methods of characterization, emission techniques like Fluorescence, Phosphorescence and Chemiluminescence are interesting areas of research that is being pursued world wide.<sup>28-30</sup> Fluorescent probes have the ability to exhibit different photophysical characteristics under different environments, which can be effectively made use of in rebinding studies in MIPs.<sup>31</sup> MIPs incorporated with fluorescent dyes in the backbone has been reported for application as sensors.<sup>32</sup> The phenomenon of forster resonance energy transfer (FRET), which involves a distance dependent energy transfer between suitable fluorescent donor and acceptor molecules has also been explored for MIP binding studies.<sup>33-34</sup> Rurack et. al. developed fluorescent molecularly imprinted

microparticles in which covalent attachment of dye to the MIPs gave enhancement in the fluorescence after rebinding of drug.<sup>35</sup>

In this chapter we describe the preparation of fluorescent **MIP** microspheres that were developed by dispersion polymerization technique using photoresponsive Azopyridine (**Azopy**) as a functional co monomer along with styrene. Pyrene dye is known for its high quantum yields; and is also known to be sensitive to its environment.<sup>36</sup> Pyrenebutyric acid (**Py**) was used as template molecules, which was pre assembled with **Azopy** and introduced during the second stage of the dispersion polymerization. A non imprinted polymer (**NIP**) was also made under identical condition but in the absence of the template dyes. The **MIP** and **NIP** were characterized using SEM and fluorescence microscopy imaging. Fluorescence spectroscopy was used to characterize the photophysical properties of the **NIP** and **MIP**. The detailed studies conducted in this work clearly establishes the unique ability of fluorescence to detect very low amounts of template molecules remaining trapped within the **MIP** scaffold even after prolonged periods of soxhlet extraction. The appropriate choice of pyrene as the fluorescent template also helped to get insight into the specific location of the template on the **MIP** or **NIP** – inside the selective cavity or on the surface.

### **5.3 Experimental methods**

**5.3.1 Materials:** Pyrenebutyric acid and Di (ethyleneglycol) diacrylate (DEGA) were purchased from Aldrich and used without further purifications. Other chemicals detail are same as given in chapter 2 section 2.3.1 (i).

#### **5.3.2 Instrumentation:**

The details of the instrumentation used for structural, morphology and photophysical characterization like the NMR, MALDI-TOF, TGA, SEM, UV-Vis and steady-state fluorescence etc were as previously described in chapter 2. The dispersion of polymers in acetonitrile was drop cast on to glass plate, covered with cover slip and directly observed under EVOS fluorescence microscope (excitation wavelength: blue filter transparent in the range 350–450 nm, for pyrene).

### 5.3.3 General procedures

#### (i) Synthesis of Azopyridine acrylate (**Azopy**):

In a 100 mL round bottom flask under N<sub>2</sub> atmosphere 4-(4-hydroxyphenylazo)pyridine (1.4 gm, 0.007 mole), triethylamine (1.12 mL, 0.008 mole) in dry THF (35 mL) were dissolved and stirred at 0 °C for the period of 1 hour. A solution of acryloyl chloride (0.66 mL, 0.008 mole) in dry THF (10 mL) was added to the mixture drop by drop over a period of 20-30 minutes at 0 °C under N<sub>2</sub> atmosphere. Reaction was continued at room temperature for overnight. For workup, the organic layer was washed with water and brine and extracted into DCM. The compound was purified by column chromatography in Ethyl acetate/Pet ether (30%) as solvent. Yield = 1.4 gm (crude), after purification = 0.6 gm (47%). <sup>1</sup>H NMR (200 MHz, CDCl<sub>3</sub>, δ ppm): 8.93 (d, 2H), 8.2 (d, 2H), 8.08 (d, 2H) 7.43 (d, 2H), 6.53 (dd, 1H, acrylic double bond), 6.37 (t, 1H, acrylic double bond), 6.13 (dd, 1H, acrylic double bond) MALDI-TOF MS (DHB matrix): m/z calculated for C<sub>14</sub>H<sub>11</sub>N<sub>3</sub>O<sub>2</sub>: 253; found 254 [M+1].

#### (ii) Complex preparation:

In a 25 mL round bottom flask under dark Azopyridine acrylate (**Azopy**) (0.030 gm, 1.18x10<sup>-4</sup> mole) were dissolved in dry THF (4.4 mL) and stirred for 10 minute at room temperature. A solution of Pyrenebutyric acid (**Py**) (0.034 gm, 1.18x10<sup>-4</sup> mole) in THF (3 mL) was added to the **Azopy** solution under N<sub>2</sub> atmosphere. The complex formation was continued by stirring the mixture in dark for six hours followed by removal of solvent.

#### (iii) Dispersion Polymerization procedure for the preparation of PS-Azo based MIP/NIP:

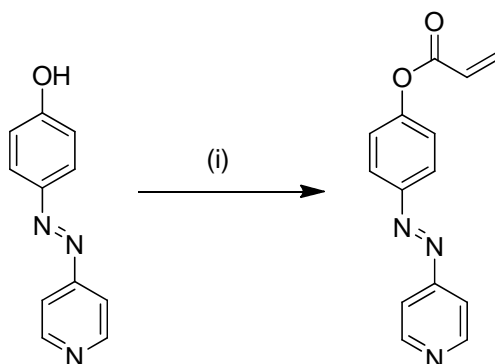
Procedure same as explained in chapter 2 section 2.3.3 (v).

The polymerization content is given in table 5.1.

## 5.4 Result and Discussion

### 5.4.1 Synthesis and characterization

The functional monomer Azopyridine acrylate (**Azopy**) used in the study was synthesized by following literature procedure<sup>37</sup> and the synthetic scheme is given below in **scheme 5.1**.



**Scheme 5.1:** Synthesis of Azopyridine acrylate (**Azopy**).

**Reagents:** (i) Acryloyl Chloride, THF, Et<sub>3</sub>N, 0-25 °C, 24 hours, N<sub>2</sub>.

The complete structural characterization details like NMR and MALDI of the **Azopy** is presented in the **figure 5.1(i)** and **(ii)**.

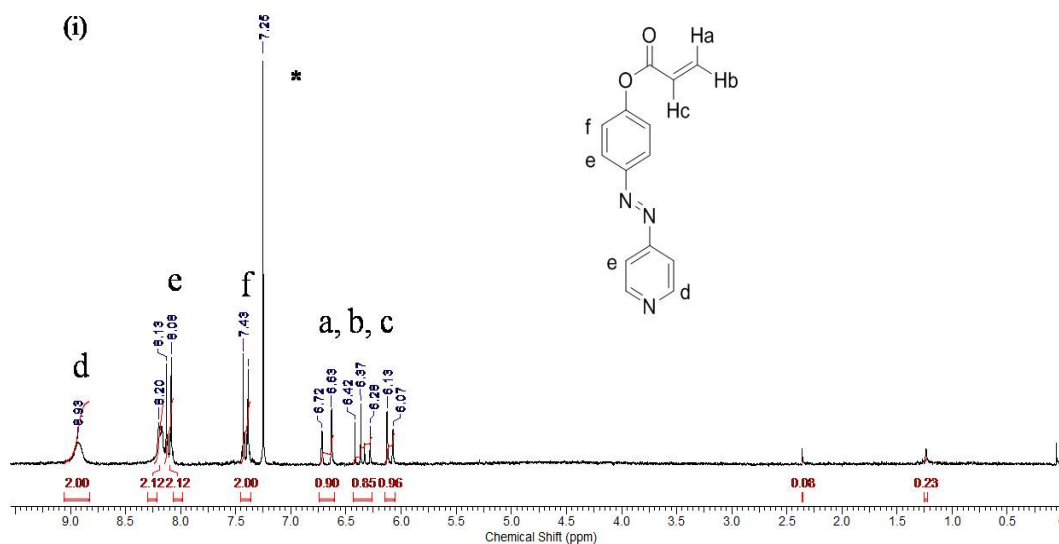


**Figure 5.1(i):** <sup>1</sup>H NMR spectrum of **Azopy** in CDCl<sub>3</sub>.

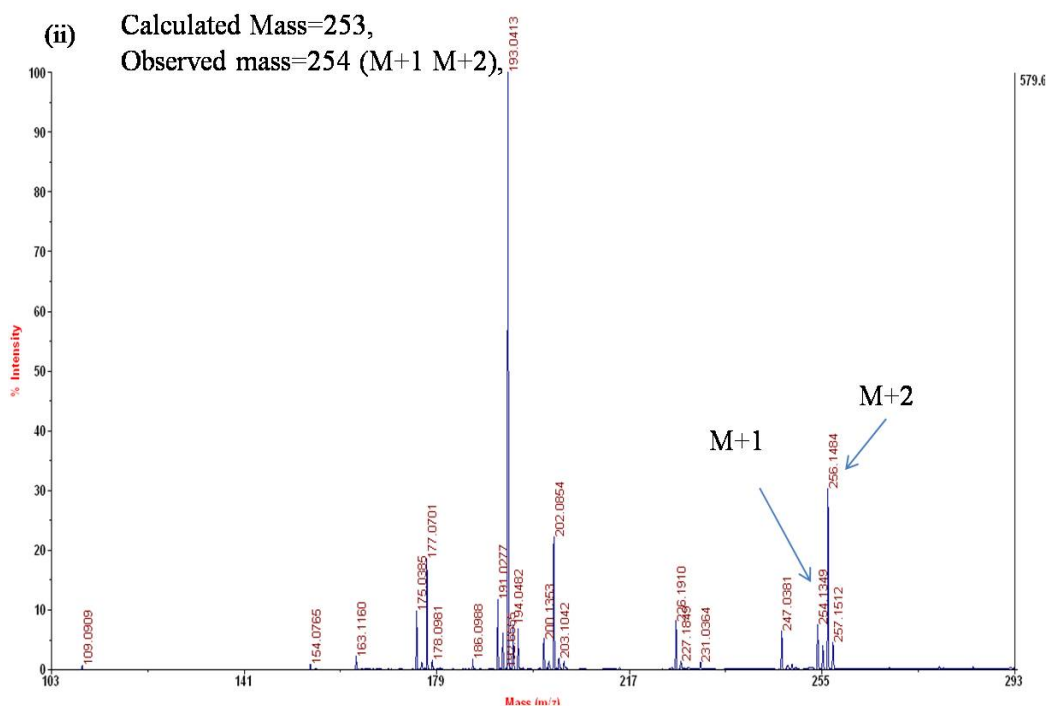
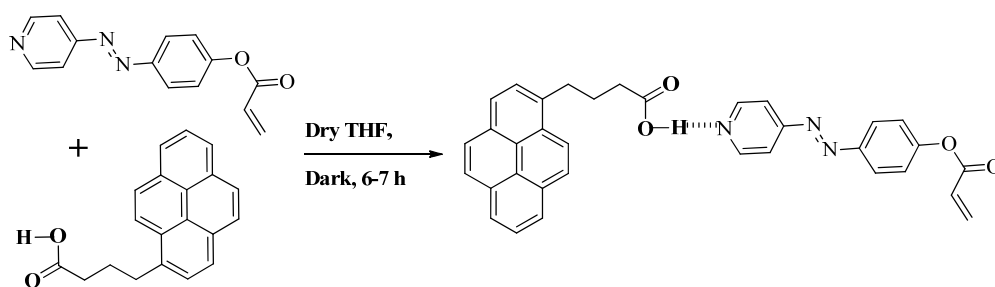


**Figure 5.1(ii):** MALDI-TOF spectrum of **Azopy**.

The pyridine unit on **Azopy** can form hydrogen bonds with carboxyl or hydroxyl moieties. Pyrenebutyric acid (**Py**) was selected as the template molecules. Separate studies were conducted to establish the complex formation between **Azopy** and pyrenebutyric acid, the details of which are given in the experimental section and **scheme 5.2**.



**Scheme 5.2:** Complex formation between Azopyridine acrylate and Pyrenebutyric acid (**Azopy-Py**).

The complex between template and functional monomer was characterized using FT-IR spectroscopy by mixing the complex on KBr pellets. The typical signals of C=N stretching of **Azopy** ring appears at  $1588\text{ cm}^{-1}$ .<sup>38</sup> However, it was difficult to trace the shifting of C=N stretching upon complexation since a broadening of peaks in the FT-IR bands was observed upon complexation. The corresponding FT-IR spectra for **Azopy-Py** complex is given in **Figure 5.2**.

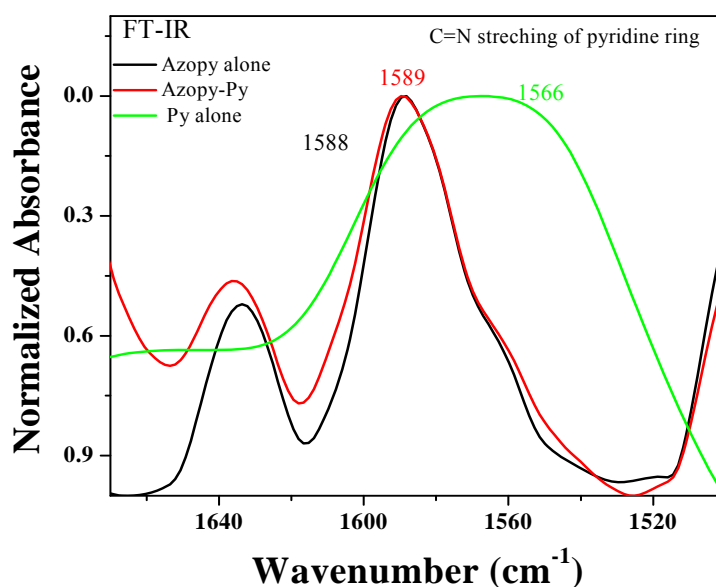


**Figure 5.2:** FTIR spectra for **Azopy-Py** complex (KBr mode).

Fluorescent MIPs were synthesized by polymerizing styrene and Azopy-template complex (**Azopy-Py**) in presence of di (ethylene glycol) diacrylate as the cross-linker in a two stage dispersion polymerization procedure. The total styrene content was divided into two halves and the first equivalent was allowed to polymerize using AIBN as the initiator in an ethanol medium. The cross-linker (**DEGA**) and the functional monomer-fluorescent template complex (**Azopy-Py**) were introduced into the polymerization medium after one hour along with the remaining styrene. The detailed procedure of the two stage dispersion

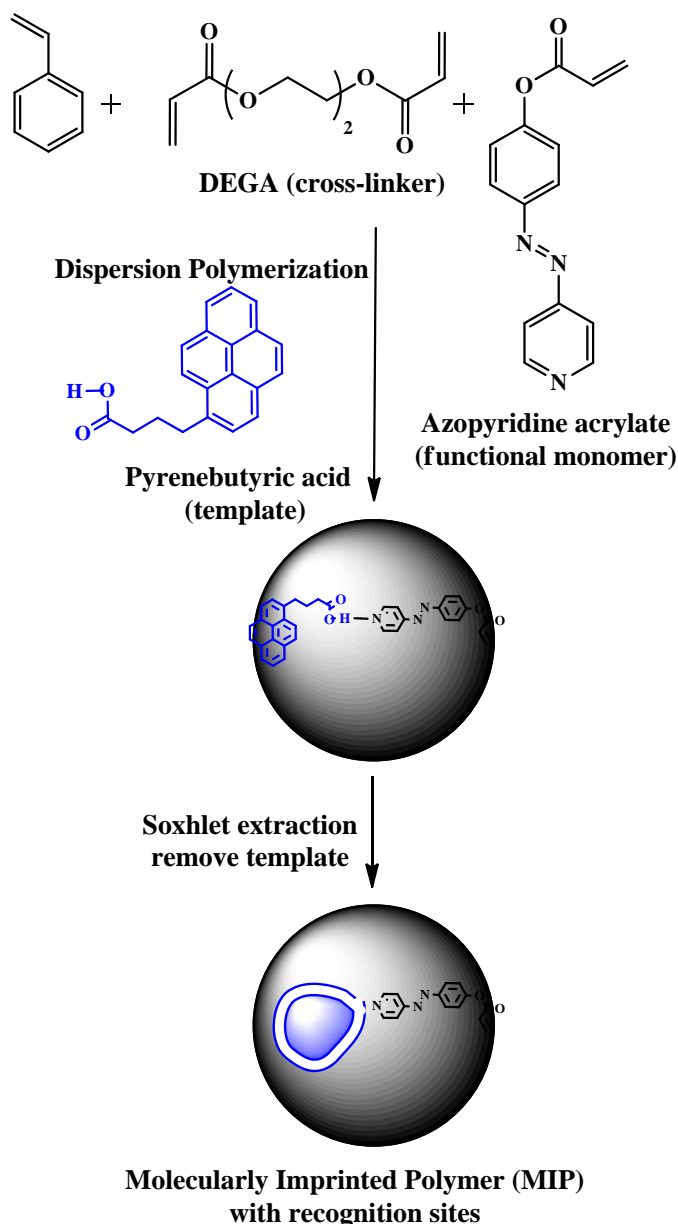


polymerization is given in experimental section and the **table 5.1** gives the contents for the same.

**Table 5.1: Dispersion Polymerization contents**

Component	Material	Amount (gm)	
		1 <sup>st</sup> Stage	2 <sup>nd</sup> Stage
Monomer	Styrene	1.89	1.89
Complex	Azopy-Py	-	0.030
Cross-linker	DEGA	No	0.18
Medium	Ethanol	7.4	7.4
Stabilizer	PVP (Mw-360,000)	0.25	No
Costabilizer	Triton X-100	0.080	No
Initiator	AIBN	0.060	No
Reaction time	8h	-	
Rotation Speed	120 rpm	-	-

This two stage strategy for the introduction of reagents avoids destabilization of the polymerization and also helps control the particle size of the formed polymer.<sup>39-40</sup> **Scheme-5.3** shows the procedure adopted for synthesis of the **MIP-Py**. The polymerization was completed in eight hours following which the polymer was centrifuged and washed repeatedly with methanol. The polymers were subjected to soxhlet extraction in acetonitrile solvent to remove the non-covalently bound template pyrenebutyric acid. The polymer was finally dried under vacuum and stored. The molecularly imprinted polymer using pyrenebutyric acid as template was named **MIP-Py**. A non imprint polymer (**NIP**) was also developed as a control polymer following identical polymerization procedure except for the absence of the template pyrenebutyric acid.



**Scheme 5.3:** Schematic representation for the development of MIP-Py.

#### 5.4.2. Thermal properties and microscopic characterization of polymers

The thermal stability of the cross-linked polymers was determined by thermogravimetric analysis carried out under nitrogen atmosphere where the 5 wt% loss was observed. The TGA plot is given in the **figure 5.3**.

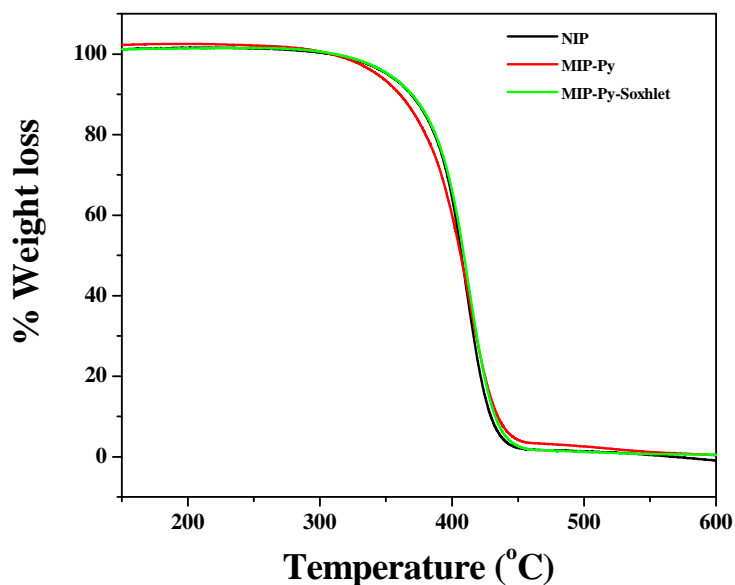


**Figure 5.3:** Thermogravimetric Analysis (TGA) of **PS-Azopy** based **NIP**, **MIP-Py** and **MIP-Py-soxhlet** samples.

The polymers (MIPs and NIP) were subjected to particle size and morphology analysis using Scanning Electron Microscope (SEM) (polymer powder dispersed in ethanol and drop cast on silicon wafers).

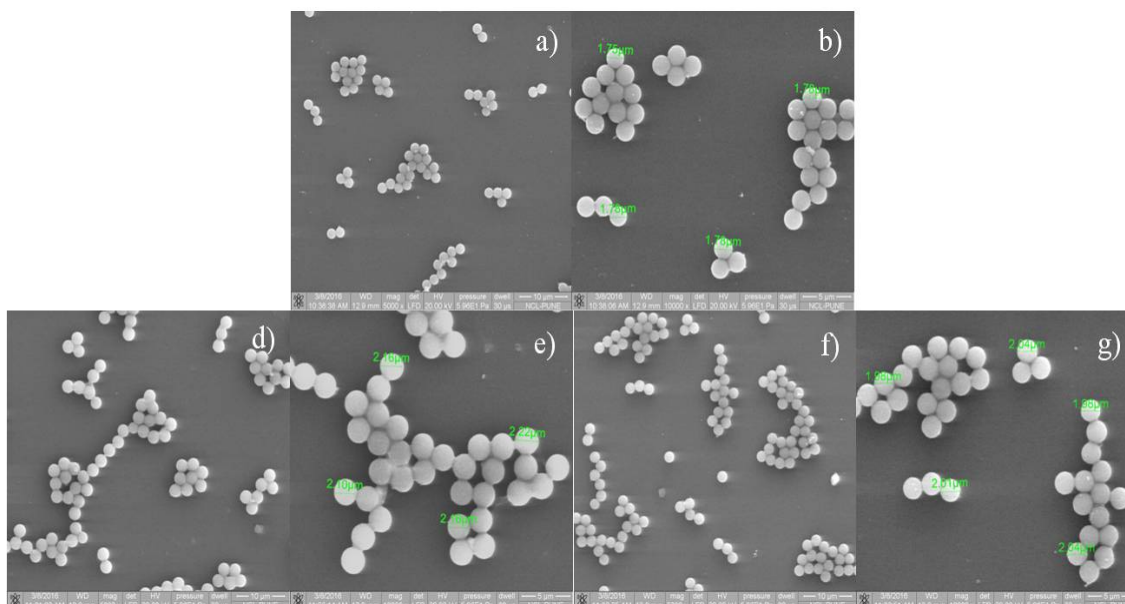


**Figure 5.4:** SEM image of **PS-Azopy** based **NIP** (a, b), **MIP-Py** (before soxhlet-c, d and after soxhlet-e, f) drop cast on silicon wafer (1 mg/ 2 ml ethanol dispersion).

**Figure 5.4** shows the SEM images for **PS-Azopy-NIP** and **MIP-Py** before and after soxhlet extraction. The images demonstrated the nearly monodisperse nature of the particles with average particle size in the range of 2 to 2.2  $\mu\text{m}$  with uniform spherical shape.

### 5.4.3 Photophysical characterization

The functional monomer **Azopy** has the typical absorption features of the azobenzene with broad absorption maxima at 360 nm corresponding to the  $\pi$ - $\pi^*$  transition of the trans azobenzene and another peak  $\sim$  450 nm corresponding to the  $n$ - $\pi^*$  transition.<sup>41</sup> **Figure 5.5** compiles the normalized absorption spectra of the functional monomer and template molecules recorded in acetonitrile.

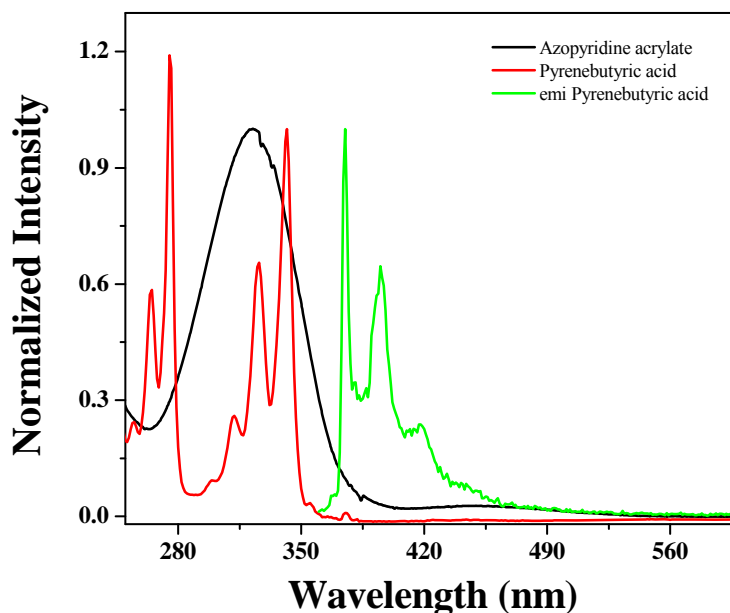


**Figure 5.5:** Normalized absorption and Emission spectra of Azopyridine acrylate (**Azopy**) and Pyrenebutyric acid (**Py**) in Acetonitrile. ( $\lambda_{\text{ex}} = 350$  nm for **Py**).

Pyrenebutyric acid (**Py**) exhibited the typical absorption bands of pyrene with vibronic fine structures in the 310 – 340 nm range.<sup>36</sup> The same figure also compares the emission from **Py** upon excitation at 350 nm, which showed the typical ‘monomeric’ emission band of pyrene in the range 375 – 420 nm. It was not possible to record the absorption spectra of the cross-linked MIP/NIP polymers. However emission was recorded for suspension of the polymer beads in acetonitrile.

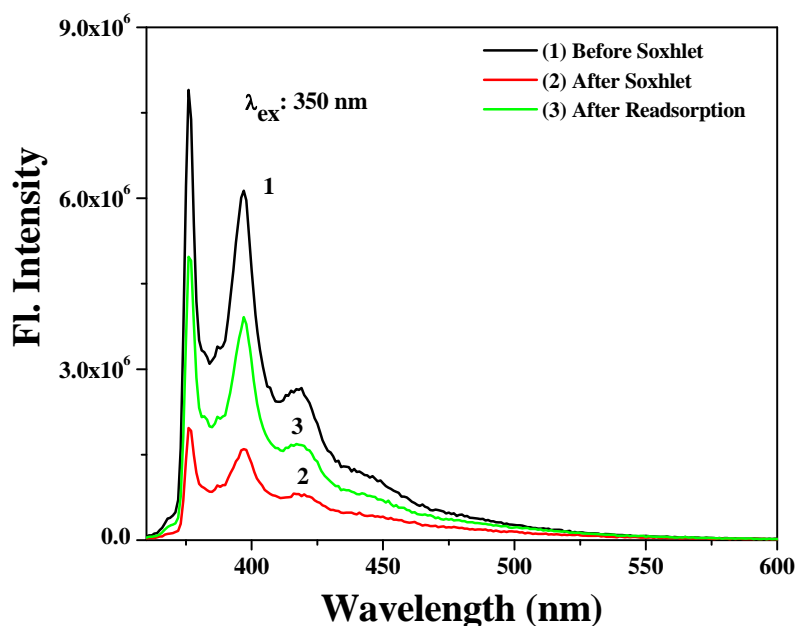


**Figure 5.6:** Comparative plot for emission spectra of **MIP-Py** from acetonitrile suspension before and after soxhlet extraction followed by readsorption (**Py**:  $\lambda_{\text{ex}} = 350 \text{ nm}$ ).

**Figure 5.6** shows the emission spectra of acetonitrile suspensions of **MIP-Py** before (**plot no. 1**) and after (**plot no. 2**) soxhlet extraction in acetonitrile. The emission of **MIP-Py** was similar to the emission of the template molecule pyrenebutyric acid (**Py**). In MIPs soxhlet extraction in acetonitrile did not completely remove the templated **Py** molecules. Residual emission from pyrene (22.6 %) could be observed in the **MIPs (plot no: 2)** after soxhlet extraction in acetonitrile continuously for three days. Excitation spectra could be collected for the polymer suspension in acetonitrile from which the signature absorption characteristics of the template molecule could be obtained which is given in **Figure 5.7**. The excitation spectra also confirmed the emission to be arising from **Py**. Thus, fluorescence is a sensitive method which can give information regarding very low concentrations of template molecule still retained within the scaffold of the **MIPs**. The usually reported techniques of characterizing **MIPs** in the literature namely, Surface Enhanced Raman Detection (SER), IR, gravimetric methods etc<sup>24</sup> would not have been able to report the presence of very low concentrations of template molecules remaining trapped inside the **MIPs**.

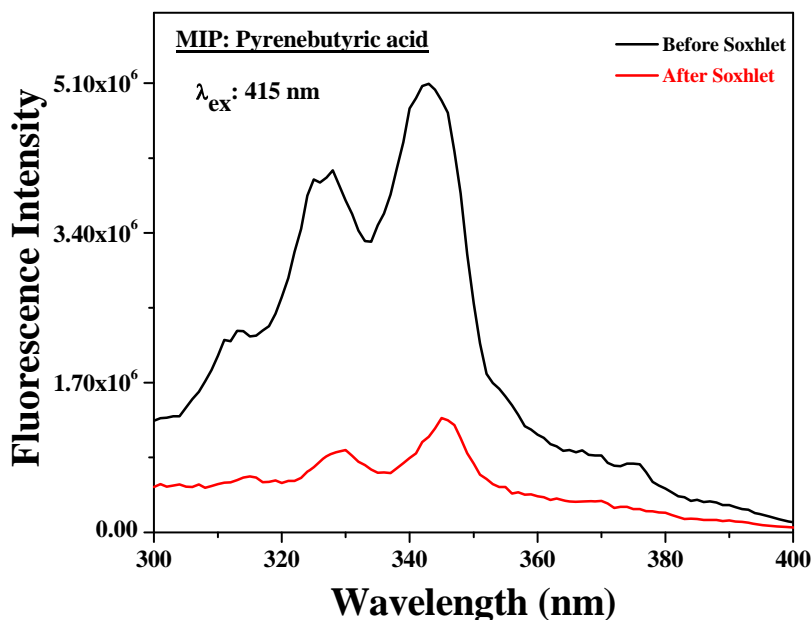


**Figure 5.7:** Excitation spectra of **MIP-Py** from acetonitrile suspension before and after soxhlet extraction ( $\lambda_{\text{ex}} = 415$  nm for pyrenebutyric acid).

The **MIP** (with the residual template molecules) were used for rebinding studies by immersing in pyrenebutyric acid solutions in acetonitrile and stirring in the dark for six hours to allow constant equilibrium between **MIP** and template. A similar procedure was carried out with the **NIP** by incubating the **NIP** with pyrenebutyric acid (**NIP-Py**) separately. After equilibrating in the template molecule solution for six hours, the **MIPs** and **NIPs** were collected by centrifuging followed by washing with acetonitrile to remove the unbound template molecules. **Figure 5.6** shows the increase in emission from the **MIP-Py** after the rebinding studies. A 57 % increase (**plot no: 2 to no: 3**) in the emission of **Py** was observed for **MIP-Py**. The emission from reabsorbed **MIP** (**plot no:3** in **figure 5.6**) is replotted with the emission from the corresponding **NIP-Py** in **figure 5.8** to compare the emission from **MIP-Py** with **NIP-Py** for each of the template molecules. From **figure 5.8** it is very clear that the intensity of emission was much higher in **MIP-Py** compared to the respective **NIP-Py**. Comparing the area of emission, the increase was ~ 93% in **MIP-Py**. In the case of the template pyrenebutyric acid, it could be seen that not only the intensity of emission, but the nature of emission also was different in the **MIP-Py** and **NIP-Py**.

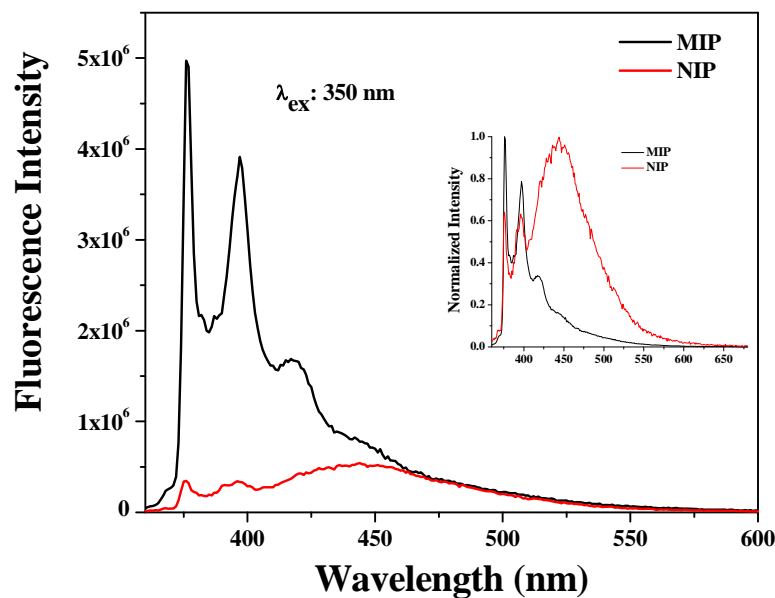


**Figure 5.8:** Comparative plot for emission spectra of **MIP-Py** and **NIP-Py** from acetonitrile suspension after readsorption of pyrenebutyric acid (**Py**:  $\lambda_{\text{ex}} = 350$  nm).

The inset in **figure 5.8** compares the normalized emission from **MIP-Py** and **NIP-Py**. The emission from **NIP-Py** had sharp peaks at 375 nm and 396 nm in addition to a broad emission centered at 440 nm, which is characteristic of pyrene excimeric emission from constrained environments. The typical pyrene excimeric emission is in the range 480 nm, whereas when the pyrene moieties find themselves in a constrained environment as in a film or adsorbed on surfaces, they are unable to attain an energy minimum sandwich configuration and are known to emit in the 440 nm range.<sup>42-43</sup>

Another experiment was conducted to evaluate the selectivity of the cavity in the **MIP-Py** towards the respective template molecule. After Soxhlet, the **MIP-Py** were incubated in a mixture of 1 mole each of **Py** and rhodamine B (**RhB**) in acetonitrile. The **NIP** also was similarly immersed in a mixture of **Py** and **RhB** and allowed to equilibrate for six hours. Finally, the **MIP-Py+RhB** and **NIP-Py+RhB** were collected by centrifuging followed by washing with acetonitrile to remove the unbound template molecules.

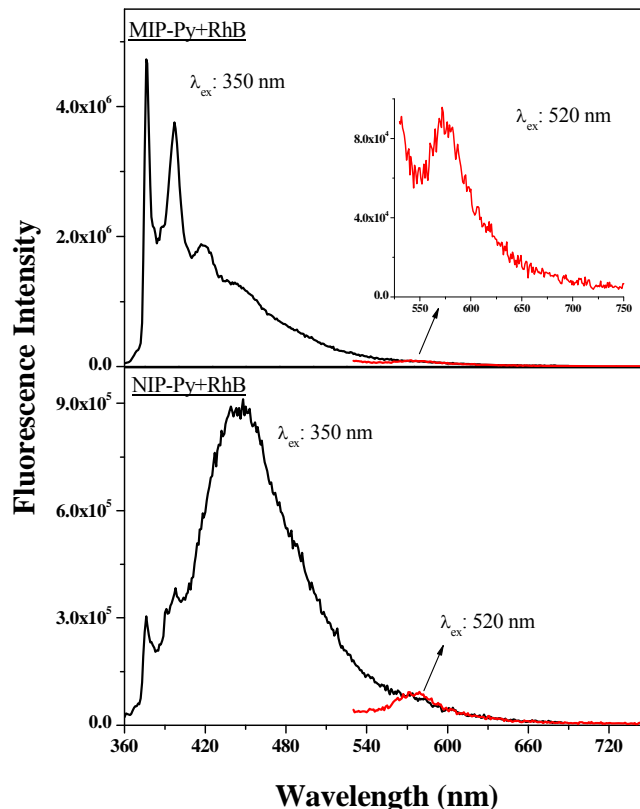


**Figure 5.9:** Comparative plot for emission spectra of **MIP-Py+RhB** (top) and **NIP-Py+RhB** (bottom) from acetonitrile suspension after readsorption from a mixture of pyrenebutyric acid and rhodamine B (**Py**:  $\lambda_{\text{ex}} = 350 \text{ nm}$ ; **RhB**:  $\lambda_{\text{ex}} = 520 \text{ nm}$ ).

**Figure 5.9** shows the comparative plot for emission spectra of **MIP-Py+RhB** (top) and **NIP-Py+RhB** (bottom) from acetonitrile suspension after readsorption from a mixture of pyrenebutyric acid (**Py**:  $\lambda_{\text{ex}} = 350 \text{ nm}$ ) and rhodamine B (**RhB**:  $\lambda_{\text{ex}} = 520 \text{ nm}$ ). **MIP-Py+RhB** showed the monomeric pyrene emission when it was excited at the pyrene absorption wavelength of 350 nm (**figure 5.9-top**). On the other hand, upon excitation at the pyrene absorption wavelength of 350 nm, the rhodamine emission at 520 nm was also observed. Direct excitation at the rhodamine absorption wavelength of 520 nm produced very weak rhodamine emission. In order to understand if the rhodamine emission observed upon exciting at the pyrene wavelength was a result of FRET induced energy transfer process, **RhB** solution in acetonitrile was excited at 350 nm which is shown in corresponding **figure 5.10**.



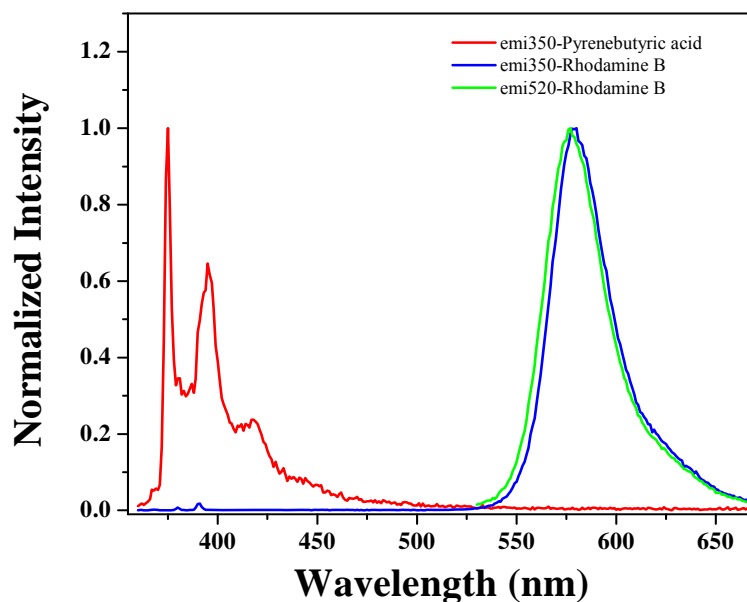


**Figure 5.10:** Emission spectra of Pyrenebutyric acid and Rhodamine B in acetonitrile ( $\lambda_{\text{ex}} = 350$  nm for **Py** and  $\lambda_{\text{ex}} = 520$  nm for **RhB**).

Intense rhodamine emission was observed upon exciting at 350 nm clearly demonstrating that selective excitation of pyrene was not possible at 350 nm and that rhodamine also could get excited since it had reasonable absorption in the 350 nm range. Therefore, the observation of rhodamine emission from **MIP-Py+RhB** upon excitation at 350 nm could not be established as arising from FRET induced energy transfer process. **Figure 5.9** (bottom) shows the emission from **NIP** after reabsorption from a mixture of both template (**Py**) and nontemplate (**RhB**) molecules. It showed again the typical pyrene excimeric emission, with almost quenched monomer emission along with very faint rhodamine emission. The intensity of pyrenebutyric acid emission was much low compared to the **MIP-Py**.

From these set of experiments the following observations could be summarized:

- The different nature of pyrene emission from **MIP** (only monomeric) and **NIP** (quenched monomeric emission and intense excimeric emission at 440 nm), indicated different environment experienced by **Py**. Monomeric emission suggested isolated pyrene moieties while excimeric emission indicated pyrene units which were close enough to interact with each other. The **NIP** does not have any cavity and therefore the mode of interaction could only be via interaction with **Azopy** moieties on the

- surface of the spherical bead. The pyrene adsorbed on the surface of the **NIP** are able to interact with each other and exhibit excimeric emission typical of pyrene emission in a constrained environment.
- b) When **MIP-Py** readsorbed **Py** and **RhB** from their mixture, the pyrene moieties were taken up inside the cavities, which were selective for them and they exhibited isolated monomeric emission. Although some amount of rhodamine emission was observed upon excitation at 520 nm, it could arise from rhodamine which were adsorbed on the surface.
  - c) This would lead to another question as to the absence of pyrene excimeric emission in **MIP-Py** arising from pyrene that could also be located on the surface. Although most of the **Py** would go into the cavities, some might be present on the surface also, which should result in constrained excimeric emission. One possible reason for the lack of a clear excimeric emission in this case could be the high intensity of the monomeric emission which could mask any small excimeric emission that could be present.

#### 5.4.4 Fluorescence microscopic characterization

An attempt was made to visualize the fluorophore in the polymer beads using fluorescence microscopy imaging. **Figure 5.11** compares the fluorescence microscopy images of **NIP** and **MIP-Py** after incubation in the mixture of **Py** and **RhB**. The images on the extreme left i.e (**a, d**) shows the blue spheres using DAPI filter highlighting the pyrene region, whereas the same upon using RFP filter highlights the red spheres (middle images; **b, e**) indicating presence of **RhB**. The fluorophores are clearly located only on the polymer spheres since the background in the images are dark. The images on the extreme right (**c, f**) corresponds to merged images where the blue and red have combined to give pink spheres indicating that the location of the red of **RhB** was same as the blue of pyrene. The images in **figure 6** were in confirmation with the observation from the photophysical studies. The top image (**a-c**) showed the relatively sparse emitting beads of **NIP** compared to the more dense spread of emitting beads in the **MIP-Py** (lower images). Photophysical data from **MIP-Py** had indicated intense monomeric pyrene emission and very less emission from Rhodamine. The bottom images (**d-f**) supported this fact, with almost no red emission visible in image-e.

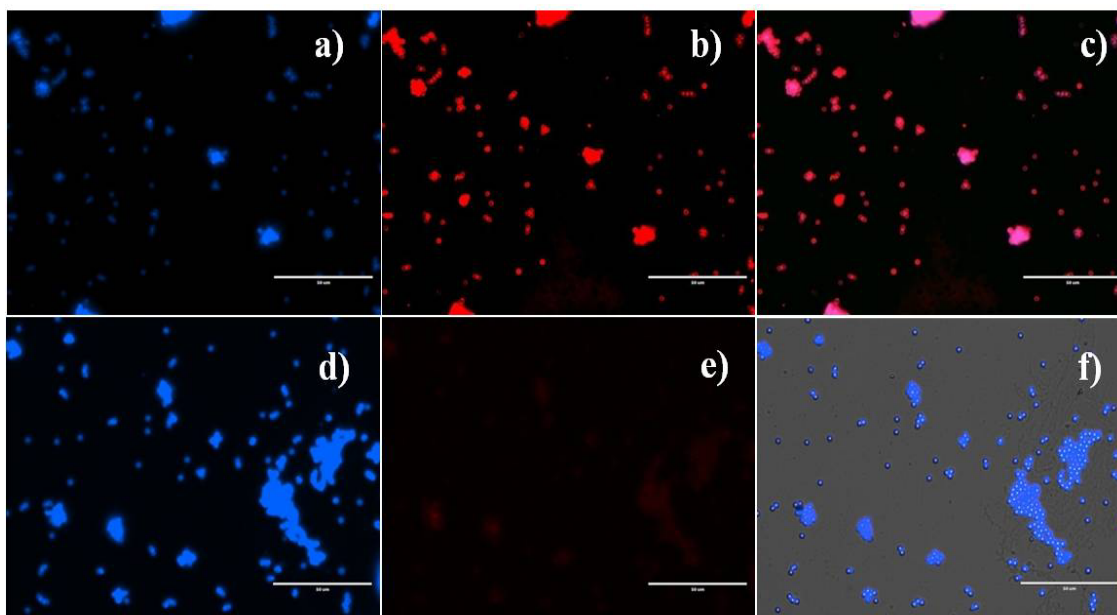


**Figure 5.11:** Fluorescence optical microscopy images of **NIP (a-c)** and **MIP-Py (d-f)** (after incubation in a mixture of pyrenebutyric acid and rhodamine B. (**a, d**) pyrene emission (blue) observed using DAPI filters, (**b, e**) rhodamine B emission (red) observed using RFP filters and (**c, f**) merged image (purple and blue) indicating the location of the rhodamine and pyrene.

It must be mentioned here that it was not possible to distinguish the monomeric and excimeric emission of pyrene using the fluorescence microscope imaging. Moreover, the PS backbone also exhibited blue emission as shown in the **figure 5.12a** and **b**, where the fluorescence microscopic image as well as fluorescence emission from neat **NIP** (no fluorophore present) is shown. However, the red emission from rhodamine B was not obstructed by any such interference and hence it could be used to visualize the differences in template binding ability of the **MIP** as well as the **NIP**.

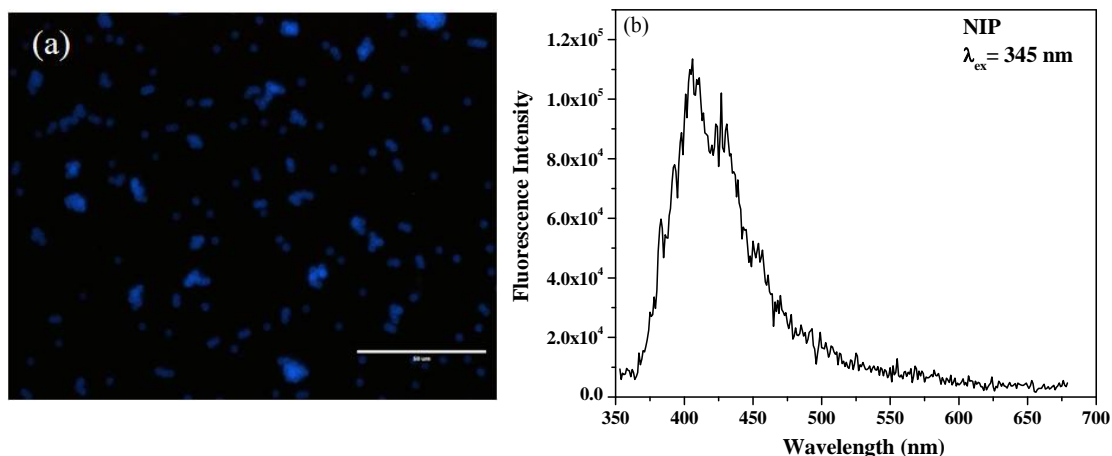


**Figure 5.12:** Fluorescence optical microscopy images of neat **NIP** observed using DAPI filter. The blue emission is from Polystyrene. Right side plot shows the emission from neat **NIP** in the range 350 – 450 nm upon excitation at 345 nm.

### 5.5 Conclusion

In summary, functional cross-linked polystyrene microbeads were developed by dispersion polymerization as fluorescent **MIPs** with specific recognition cavities. The synthesized **MIP** exhibited blue fluorescence for Pyrenebutyric acid (**Py**) as template molecules. Even trace amounts of fluorescent template molecule remaining trapped in the cross-linked **MIP** polymer matrix could be sensitively detected using fluorescence spectroscopy. Using pyrene as the fluorescent template molecule, the environment of the adsorbed molecule on the **MIP** could be differentiated from that on the **NIP**. In the absence of a cavity, the template molecules were adsorbed in small amounts on the surface of **NIP**, which was very clearly established by the excimeric emission coming from pyrene in the 440 nm range. The presence of the excimeric emission indicated close proximity of pyrene molecules, while its peak value at 440 nm confirmed its surface attachment. Thus, the fluorescence signals like the shape, intensity and peak value of emission could be used as handles to get insight into the binding sites on molecularly imprinted polymers.

## 5.6 Reference

- (1) Wattanakit, C.; Côme, Y. B.; Lapeyre, V.; Bopp, P. A.; Heim, M.; Yadnum, S.; Nokbin, S.; Warakulwit, C.; Limtrakul, J.; Kuhn, A. *Nat. Commun.* **2014**, *5*, 3325.
- (2) Chen, L.; Xu, S.; Li, J. *Chem. Soc. Rev.* **2011**, *40*, 2922–2942.
- (3) Shen, X.; Xu, C.; Ye, L. *Ind. Eng. Chem. Res.* **2013**, *52*, 13890–13899.
- (4) Haginaka, J. *J. Chromatogr. B* **2008**, *866*, 3–13.
- (5) Chen, L.; Wang, X.; Lu, W.; Wu, X.; Li, J. *Chem. Soc. Rev.* **2016**, *45*, 2137–2211.
- (6) Haupt, K.; Mosbach, K. *Chem. Rev.* **2000**, *100*, 2495–2504.
- (7) Schirhagl, R. *Anal. Chem.* **2014**, *86*, 250–261.
- (8) Ki, C. D.; Chang, J. Y. *Macromolecules* **2006**, *39*, 3415–3419.
- (9) Ge, Y.; Butler, B.; Mirza, F.; Habib-Ullah, S.; Fei, D. *Macromol. Rapid Commun.* **2013**, *34*, 903–915.
- (10) Fang, L.; Chen, S.; Guo, X.; Zhang, Y.; Zhang, H. *Langmuir* **2012**, *28*, 9767–9777.
- (11) Puoci, F.; Iemma, F.; Muzzalupo, R.; Spizzirri, U. G.; Trombino, S.; Cassano, R.; Picci, N. *Macromol. Biosci.* **2004**, *4*, 22–26.
- (12) Wulff, G. *Angew. Chem., Int. Ed. Engl.* **1995**, *34*, 1812–1832.
- (13) Benito-Peña, E.; Navarro-Villoslada, F.; Carrasco, S.; Jockusch, S.; Ottaviani, M. F.; Moreno-Bondi, M. C. *ACS Appl. Mater. Interfaces* **2015**, *7*, 10966–10976.
- (14) Kempe, H.; Kempe, M. *Anal. Chem.* **2006**, *78*, 3659–3666.
- (15) Wang, J.; Cormack, P. A. G.; Sherrington, D. C.; Khoshdel, E. *Angew. Chem. Int. Ed.* **2003**, *42*, 5336–5338.
- (16) Wackerlig, J.; Schirhagl, R. *Anal. Chem.* **2016**, *88*, 250–261.
- (17) Sonawane, S. L.; Asha, S. K. *ACS Appl. Mater. Interfaces* **2013**, *5*, 12205–12214.
- (18) Rampey, A. M.; Umpleby, R. J.; Rushton, G. T.; Iseman, J. C.; Shah, R. N.; Shimizu, K. D. *Anal. Chem.* **2004**, *76*, 1123–1133.
- (19) Haupt, K.; Linares, A. V.; Bompart, M.; Bui, B. T. S. *Top. Curr. Chem.* **2012**, *325*, 1–28.
- (20) Qin, S.; Deng, S.; Su, L.; Wang, P. *Anal. Methods* **2012**, *4*, 4278–4283.
- (21) Percival, C. J.; Stanley, S.; Galle, M.; Braithwaite, A.; Newton, M. I.; McHale, G.; Hayes, W. *Anal. Chem.* **2001**, *73*, 4225–4228.
- (22) Apodaca, D. C.; Pernites, R. B.; Ponnampati, R. R.; Del Mundo, F. R.; Advincula, R. C. *ACS Appl. Mater. Interfaces* **2011**, *3*, 191–203.

- (23) Ayankojo, A. G.; Tretjakov, A.; Reut, J.; Boroznjak, R.; Öpik, A.; Rappich, J.; Furchner, A.; Hinrichs, K.; Syritski, V. *Anal. Chem.* **2016**, *88*, 1476–1484.
- (24) Kamra, T.; Zhou, T.; Montelius, L.; Schnadt, J.; Ye, L. *Anal. Chem.* **2015**, *87*, 5056–5061.
- (25) Kantarovich, K.; Belmont, A.-S.; Haupt, K.; Bar, I.; Gheber, L. A. *Appl. Phys. Lett.* **2009**, *94*, 194103 (1–3).
- (26) Jakusch, M.; Janotta, M.; Mizaikoff, B. *Anal. Chem.* **1999**, *71*, 4786–4791.
- (27) Cserhádi, T.; Forgács, E.; Deyl, Z.; Miksik, I.; Eckhardt, A. *Biomed. Chromatogr.* **2004**, *18*, 350–359.
- (28) Siraj, N. et. al. *Anal. Chem.* **2016**, *88*, 170–202.
- (29) Sonawane, S. L.; Asha S. K. *ACS Appl. Mater. Interfaces*, **2016**, *8*, 10590–10599
- (30) Suresh, V. M.; Chatterjee, S.; Modak, R.; Tiwari, V.; Patel, A. B.; Kundu, T. K.; Maji, T. K. *J. Phys. Chem. C* **2014**, *118*, 12241–12249.
- (31) Kubo, H.; Yoshioka, N.; Takeuchi T. *Org. Lett.* **2005**, *7*, 359–362.
- (32) Liu, C.; Song, Z.; Pan, J.; Wei, X.; Gao, L.; Yan, Y.; Li, L.; Wang, J.; Chen, R.; Dai, J.; Yu, P. *J. Phys. Chem. C*, **2013**, *117*, 10445–10453.
- (33) Wan, W.; Wagner, S.; Rurack, K. *Anal. Bioanal. Chem.* **2016**, *408*, 1753–1771.
- (34) Xu, S.; Lu, H.; Li, J.; Song, X.; Wang, A.; Chen, L.; Han, S. *ACS Appl. Mater. Interfaces*, **2013**, *5*, 8146–8154.
- (35) Wan, W.; Biyikal, M.; Wagner, R.; Sellergren, B.; Rurack, K. *Angew. Chem. Int. Ed.* **2013**, *52*, 7023–7027.
- (36) Winnik, F. M. *Chem. Rev.* **1993**, *93*, 587–614.
- (37) Cui L.; Zhao, Y. *Chem. Mater.* **2004**, *16*, 2076–2082.
- (38) Fang, L.; Chen, S.; Zhang Y.; Zhang H. *J. Mater. Chem.* **2011**, *21*, 2320–2329.
- (39) Song, J. S.; Tronc, F.; Winnik, M. A. *J. Am. Chem. Soc.* **2004**, *126*, 6562–6563.
- (40) Sonawane, S. L.; Asha, S. K. *J. Phys. Chem. B* **2014**, *118*, 9467–9475.
- (41) Gong, C.; Wong, K.-L.; Lam, M. H. W. *Chem. Mater.* **2008**, *20*, 1353–1358.
- (42) Kaushlendra, K.; Deepak, V. D.; Asha, S. K. *J. Poly. Sci. Part A: Polym. Chem.* **2011**, *49*, 1678–1690.
- (43) Jang, H.-S.; Wang, Y.; Lei, Y.; Nieh, M.-P. *J. Phys. Chem. C* **2013**, *117*, 1428–1435.

**-:- Chapter 6 -:-**

---

---

*Summary and Conclusions*

---

---





The thesis entitled '**Fluorescent Polymeric Microbeads for Application as Solid State Multicolor Emitting Materials**' focuses on the design and synthesis of new solid state emitting fluorescent polymer beads by adopting dispersion polymerization method. The fluorescent dyes based on Perylenebisimide, Oligo (*p*-phenylenevinylene) and Pyrene were covalently incorporated into the PS backbone to prevent dye leakage. The appealing reason was the ability of maximum emission from very low fluorophore incorporation as larger incorporation of fluorophores like PBI and OPV are known to result in aggregation induced quenching. Thus, using this strategy upto  $\sim 5 \times 10^{-6}$  moles of the rigid fluorophores could be incorporated into PS backbone. By varying the amount of chromophores during the second stage of dispersion polymerization, tunable multicolor solid state emitting polymers with monodisperse particle size are obtained. The polymers showed good solid state quantum yield with potential applications as a white light emitting material, fluorescent security ink and sensors for nitro compound vapors. The designed fluorescent molecularly imprinted polymers showed their ability to determine the position of dye molecule in constrained environment.

A series of Polystyrene microbeads incorporating fluorophores like perylenebisimide (**PBI**) and oligo (*p*-phenylenevinylene) (**OPV**) as the cross-linker were successfully developed by two stage dispersion polymerization strategy. Dispersion polymerization was adopted as the method of choice since it was more tolerant to rigid aromatic molecules with poor solubility, and allowed their incorporation into the polymer backbone and still maintained control over the particle size distribution. The advantage of adapting the fluorophore itself as the cross-linker was to obtain the fluorescent polymer particles in one shot without the addition of two ingredients – the fluorophore and the cross-linker separately in the reaction medium and the covalent attachment of the dye to the polymer backbone. The fluorescent spherical cross-linked PS beads had an average diameter of 2-3  $\mu\text{m}$ . The PS beads incorporating PBI exhibited intense orange red emission in the solid state with quantum yield  $\phi_{\text{Powder}} = 0.25$ , while the PS incorporating OPV as the cross-linker fluorophore exhibited intense green emission very high quantum yield of  $\phi_{\text{Powder}} = 0.71$ . An added advantage of this strategy of fluorophore as cross-linker was the ability to incorporate more than one tailor-made fluorophore into the PS backbone enabling fine-tuning of the emission colors.

We have also demonstrated system having single polymer based white light and multicolor emission in the solid state. Fluorescent polystyrene microbeads in the size range of 2-3  $\mu\text{m}$  were produced by incorporating newly synthesized orange-red emitting perylenebisimide (PBITEG) and blue emitting oligo (*p*-phenylenevinylene) (OPV) as cross-linkers into the polymer backbone. Pure white light emission in the powder form with CIE coordinates (0.33, 0.32) was achieved with one of the PS samples having appropriate amounts of OPV and PBITEG (PS-PBITEG-6.25-OPV-4.28). The two-stage dispersion polymerization method along with the concept of fluorophore as cross-linker for chromophore isolation affords an easy and scalable method to produce fluorescently labeled polymer particles with controlled size from commercial polymers like PS.

The air stable, color tunable solid state emitting polystyrene microbeads was also developed in a three stage dispersion polymerization method whereby multiple fluorophores (pyrene and perylenebisimide) emitting in different wavelength could be covalently incorporated into the polymer backbone. The fluorescent beads were utilized for the detection of nitro compound vapors. The pyrene monomeric emission in the 340-500 nm region was sensitive to vapors of 4-nitrotoluene, while the emission of perylenebisimide beyond 500 nm was unaffected. The limit of detection (LOD) of pyrene emission for vapors of 4-NT was observed to be  $10^{-5}$  moles (2.7 ppm). The selectivity is attributed to the electron rich nature of pyrene, which makes it sensitive towards electron deficient nitroaromatic compounds. The easy dispersibility of the PS microbeads in ethanol also afforded fluorescent ink solution to write on various substrates like glass or paper, which were invisible under normal lighting but became visible in various color shades upon observation under a hand-held UV lamp.

Towards the end, functional cross-linked polystyrene microbeads were developed by dispersion polymerization as fluorescent MIPs with specific recognition cavities. The synthesized MIP exhibited blue fluorescence for pyrenebutyric acid as template molecules. Even trace amounts of fluorescent template molecule remaining trapped in the cross-linked MIP polymer matrix could be sensitively detected using fluorescence spectroscopy. Using pyrene as the fluorescent template molecule, the environment of the adsorbed molecule on the MIP could be differentiated from that on the NIP. In the absence of a cavity, the template molecules were adsorbed in small amounts on the

surface of NIP, which was very clearly established by the excimeric emission coming from pyrene in the 440 nm range. The presence of the excimeric emission indicated close proximity of pyrene molecules, while its peak value at 440 nm confirmed its surface attachment. Thus, the fluorescence signals like the shape, intensity and peak value of emission could be used as handles to get insight into the binding sites on molecularly imprinted polymers.

In short the thesis deals with the development of fluorescent microbeads with controlled particle size and stable intense solid state multicolor emission which finds application in material science. This is the first time that successful monomer emission (no emission from aggregate) with high quantum efficiency has been achieved from fluorophores based on PBI and OPV, which are known to undergo  $\pi$ - $\pi$  stacking interaction of their aromatic core in the solid state and even in highly concentrated form in solution resulting in quenching of their emission. The approach introduced here is expected to be a viable route towards the easy and reproducible development of tunable multicolor emitting polymer beads with good solid state quantum yield. The developed MIPs also have additional advantage of their applications in fundamental research.

**Publications in International Journals**

1. Swapnil L. Sonawane and S. K. Asha, “Highly Fluorescent Monodisperse, Cross-linked Polymer Microbeads”, 3810/DEL/2013.; US 20150183956.
2. Swapnil L. Sonawane and S. K. Asha, “Fluorescent Cross-Linked Polystyrene Perylenebisimide/Oligo (*p*-phenylenevinylene) Microbeads with Controlled Particle Size, Tunable Colors, and High Solid State Emission.” ***ACS Appl. Mater. Interfaces***, **2013**, *5*, 12205–12214.
3. Swapnil L. Sonawane and S. K. Asha “Blue, Green, and Orange-Red Emission from Polystyrene Microbeads for Solid-State White-Light and Multicolor Emission.” ***J. Phys. Chem. B***, **2014**, *118*, 9467–9475. (Highlighted as “Noteworthy Chemistry” by ACS, <http://www.acs.org/content/acs/en/noteworthy-chemistry/2014-archive/september-22.html#nc1>).
4. Swapnil L. Sonawane and S. K. Asha, “Fluorescent Polystyrene Microbeads as Invisible Security Ink and Optical Vapor Sensor for 4-Nitrotoluene.” ***ACS Appl. Mater. Interfaces***, **2016**, *8*, 10590-10599.
5. Swapnil L. Sonawane and S. K. Asha, “Tailor Made Functional Beads by Dispersion Polymerization for Application in Fluorescence Molecular Imprinting Technology.” manuscript submitted for publication

**Papers Presented in Conferences**

1. **Swapnil L. Sonawane** and Asha S. K. “Polystyrene Microbeads with Tunable Solid State Light Emission and Control Particle Size by Dispersion Polymerization.” **Warwick Polymer Conference-2016**, University of Warwick, Coventry, United Kingdom (UK) **July-2016**.

2. **Swapnil L. Sonawane** and Asha S. K. “Tunable Solid State Emitting Monodisperse Polystyrene Microbeads by Dispersion Polymerization.” Humboldt Kolleg on “**Sustainable Development: Megatrends of the 21<sup>st</sup> Century**” organized by Humboldt Academy, Pune Chapter, Goa, **Nov-2015**.

3. Swapnil L. Sonawane and Asha S. K. “Multicolor Emitting functional Polystyrene Microbeads for Sensing.” **MACRO 2015, International Symposium on Polymer Science and Technology**, at Indian Association for the Cultivation of Science, Kolkata, India, **Jan-2015**.

4. Swapnil L. Sonawane and Asha S. K. “Monodisperse Polystyrene Microbeads with Multicolor Solid State Emission.” **8<sup>th</sup> Asian Photochemistry Conference**, (8<sup>th</sup> APC-2014) IISER-TVM jointly with CSIR-NIIST, Kerala, India, **Nov-2014**.

5. Swapnil L. Sonawane and Asha S. K. “Fluorescent Polystyrene Monodisperse Microbeads with Tunable Color and High Solid State Emission.” Global Opportunities for Latest Development in Chemistry and Technology-2014 (**GOLD-CT-2014**), **International Conference on Chemistry**, North Maharashtra University, Jalgaon, Maharashtra, India, **Feb-2014**. (*Best Oral Presentation*)

6. Swapnil L. Sonawane and Asha S. K. “Fluorescent Cross-linked Polymer Particles.” 3<sup>rd</sup> FAPS Conference and MACRO 2013 (**FAPS-MACRO, 2013**), **International Conference on Polymers**, Indian Institute of Science, Bangalore, Karnataka, India, **May-2013**. (*Best Poster Presentation*)

7. Swapnil L. Sonawane and Asha S. K. “Fluorescent Cross-linked Polymer Particles by Two Stage Dispersion Polymerization.” **National Science Day**, CSIR-NCL, Pune, Maharashtra, India, **Feb-2013**.